Organocatalytic Routes To Enantiomerically Pure α- And β-Amino Acids

Inaugural-Dissertation

zur Erlangung der Doktorwürde
der
Mathematisch-Naturwissenschaftlichen Fakultät
der
Universität zu Köln

vorgelegt von
Santanu Mukherjee
aus Hooghly (Indien)

Köln 2005

Gutachter:	Prof. Dr. A. Berkessel
	Prof. Dr. H.-G. Schmalz
	Prof. Dr. B. List
Tag der mündlichen Prüfung:	20. Februar 2006

"*Study the past if you would define the future.*"

– Confucius (551 BC – 479 BC)

Dedicated to my parents

Acknowledgements

The work embodied in this thesis was carried out from July 2002 to October 2005 at the Institute for Organic Chemistry of the University of Cologne under the supervision of Prof. Dr. Albrecht Berkessel.

First of all, I would like to acknowledge Prof. Dr. Albrecht Berkessel for giving me an opportunity to carry out my Ph. D. in his group and for introducing me to the fascinating field of asymmetric catalysis. I am deeply thankful to him for his constant help, critical advises and active encouragement throughout the project work which helped me a lot in understanding the subject and tackling several problems with fruitful solutions.

I would like to thank Prof. Dr. Hans-Günther Schmalz and Prof. Dr. Benjamin List for reviewing the thesis.

I am grateful to all of my colleagues, particularly my lab mates Marc Brandenburg and Dr. Christoph Koch for providing a wonderful working atmosphere and for their help and support. I would also like to express my special thanks to Felix Cleemann, Dr. Thomas Müller and Kerstin Etzenbach-Effers for productive discussions and interesting ideas during our successful collaborative works. I am thankful to my practical students, particularly to Ilona Jurkiewicz, for sharing some of my experimental work. I also want to thank the group members of Prof. Schmalz's lab for their help with the instruments during the course of this work.

My special thanks are due to Jens Adrio, Dennis Bankmann, Felix Cleemann, Dr. Ralf Giernoth, Daniel Hüttenhein and Katrin Roland for critical reading of the manuscript and their valuable suggestions.

I would like to thank all the employees of the Institute for Organic Chemistry, particularly to Sarwar Aziz (HPLC), Ingrid Hoven, Kathrin König, Dr. Nils Schlörer, Dr. Hans Schmickler and Walentin Ten (NMR), Dr. Johann Lex and Dr. Jörg Neudörfl (X-ray), Michael Neihs and Dr. Mathias Schäfer (MS), Christof Schmitz (GC-MS, EA). My special thanks are due to Susanne Geuer, Dr. Wolfgang Klug and Monika Boyo for their help in organizational problems. I also want to thank Herbert Hartmann and his team and Dietmar Rutsch for their help with the technical problems in the laboratory.

It is my pleasure to thank my friend Sudipta Basu for the motivating discussions and moral support during my thick and thin days in Germany.

This part of my thesis would, of course, remain incomplete without expressing my sincerest appreciation to Ritika Uppal, my confidant of many years. Her support of me has been unwavering; she has been my strength when times were hard, the voice of reason when I was irrational, and the

greatest fan when I had success. I have always been able to count on her for her laughter, her sensibility, and most of all her friendship.

And finally the persons who are always there behind the screen, with their unending support and tolerance, always there when I needed them, never angry, never questioning – my parents and sister who have always wanted to see me what I am today, saying ‘thank you’ would be an insult to your efforts. I just want to say that you were there and will always be for me.

Table of Contents

1 Summary

This thesis deals with catalytic asymmetric synthesis of α- and β-amino acids using metal-free catalysts. For the synthesis of α-amino acids, existing methods were revisited using new type of catalysts whereas a new method was developed for the synthesis of β-amino acids, which involved the kinetic resolution (KR) of oxazinones.

A series of bifunctional organocatalysts (Scheme 1.1) were synthesized using *trans*-1,2-diamino-cyclohexane as the central chiral unit.

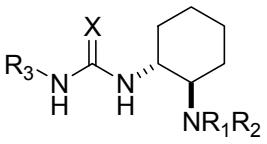

	R_1	R_2	R_3	X		R_1	R_2	R_3	X
1	Me	Me	3,5-$(CF_3)_2C_6H_3$	S	**7**	Me	Me	2,4,6-$(CH_3)_3C_6H_2$	O
2	Me	Me	3,5-$(CF_3)_2C_6H_3$	O	**8**	Me	Me	3-pyridyl	S
3	Et	Et	3,5-$(CF_3)_2C_6H_3$	O	**9**	Me	Me	*c*-hex	S
4	-$(CH_2)_4$-		3,5-$(CF_3)_2C_6H_3$	O	**10**	Me	Me	1-adamantyl	S
5	Me	Bn	3,5-$(CF_3)_2C_6H_3$	O	**12**	Me	Me	(*R*)-PhCH(CH_3)	O
6	Me	Me	3,5-$(NO_2)_2C_6H_3$	O	**13**	Me	Me	(*S*)-PhCH(CH_3)	O

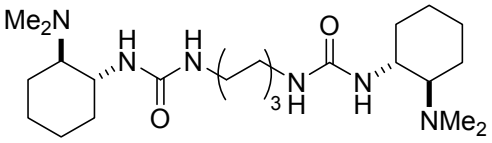

11

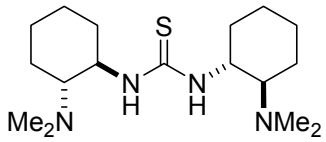

14

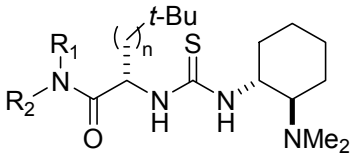

	R_1	R_2	n
15	Me	Me	0
16	Et	Et	0
17	*i*-Bu	*i*-Bu	0
18	Me	Bn	0
20	H	Bn	0
21	Me	Bn	1

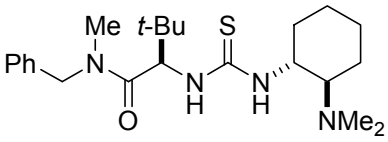

19

Scheme 1.1 Library of bifunctional organocatalysts.

This library of catalysts was screened in the ring opening of the *tert*-leucine derived azlactone *rac*-**22a** with allyl alcohol **23** (Scheme 1.2). The best results in terms of enantioselectivity were obtained with catalyst **18** containing a second element of chirality.

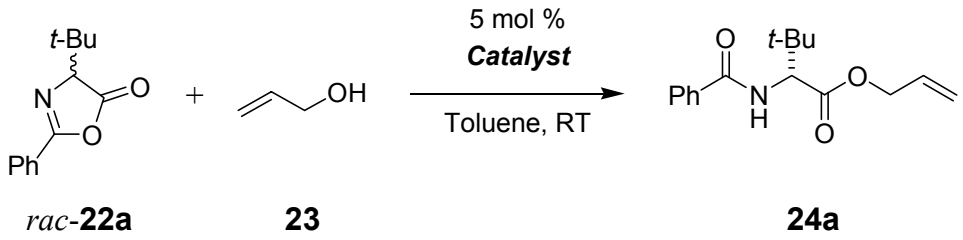

rac-**22a** **23** **24a**

Scheme 1.2 Alcoholytic DKR of the *tert*-leucine derived azlactone *rac*-**22a**.

The best catalyst **18** was applied for the DKR of a broad range of azlactones **22a**-**h** derived both from natural and non-natural α-amino acids (Scheme 1.3).

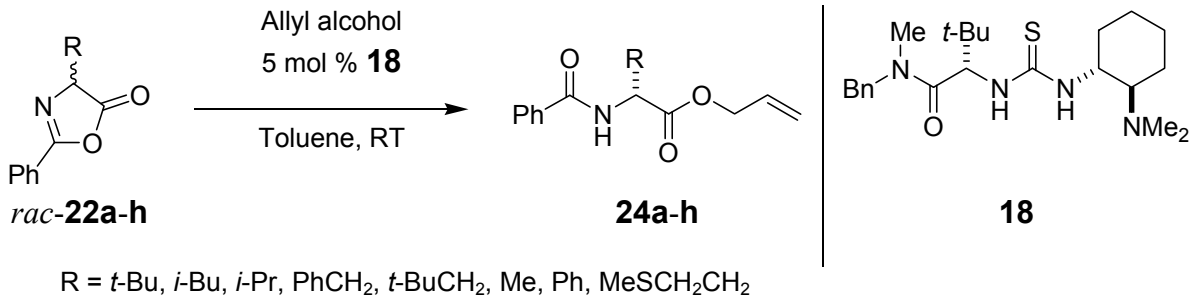

rac-**22a**-**h** **24a**-**h** **18**

R = *t*-Bu, *i*-Bu, *i*-Pr, $PhCH_2$, *t*-$BuCH_2$, Me, Ph, $MeSCH_2CH_2$

Scheme 1.3 Substrate scope for the DKR of azlactones with **18**.

Using 5 mol % of **18**, the (*R*)-*N*-benzoyl α-amino acid allyl esters **24a**-**h** were obtained in high yields (up to 94 %) and with excellent enantioselectivities (up to 95 % ee) in most cases. The level of enantioselectivity produced by catalyst **18** is the highest ever achieved in the chemically catalyzed DKR of azlactones.

Kinetic and NMR-studies were also carried out to shed light on the mechanism of this DKR process. The involvement of one catalyst molecule in the catalytic cycle and the type of substrate-catalyst interaction were evidenced from these studies.

The catalyst **18** was then applied for the kinetic resolution (KR) of oxazinones **25** (Scheme 1.4), the β-amino acid counterparts of the azlactones **22**. A series of oxazinones **25a**-**f** derived from β-substituted β-amino acids with aromatic and aliphatic substituents were subjected to ring opening with allyl alcohol **23** (Scheme 1.4).

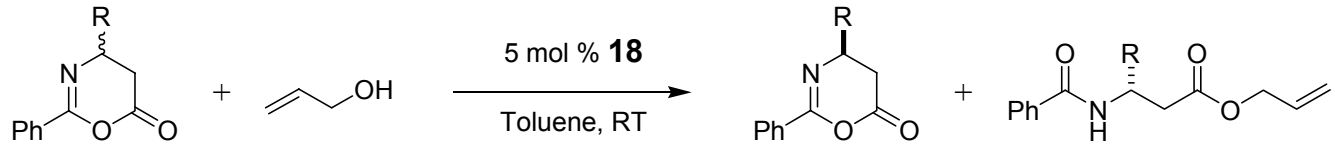

rac-**25a**-**f** **23** (*R*)-**25a**-**f** (*S*)-**26a**-**f**

R = Ph, *p*-ClC_6H_4, *m*-$NO_2C_6H_4$, *p*-$OMeC_6H_4$, *t*-Bu, *i*-Pr

Scheme 1.4 Substrate scope for the KR of oxazinones with **18**.

All oxazinones were resolved with high degrees of enantioselectivity. In the presence of 5 mol % of catalyst **18**, the oxazinones (*R*)-**25a**-**f** were generally recovered with excellent enantiomeric excesses (>97 % ee) whereas the esters (*S*)-**26a**-**f** were still produced with 80-90 % ee. This is the first example of catalytic alcoholytic ring opening of oxazinones by kinetic resolution.

Besides the DKR process described above, another method, namely the hydrocyanation of aldimines **27** (Scheme 1.5) was adopted for the asymmetric synthesis of α-amino acids.

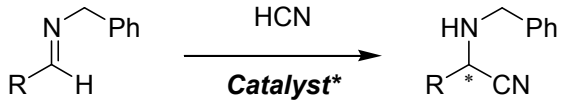

27 **28**

Scheme 1.5 Asymmetric hydrocyanation of aldimines.

The catalysts employed for this reaction were the chiral oxazaborolidines **29** and their protonated counterparts, oxazaborolidinium cations **30** (Scheme 1.6).

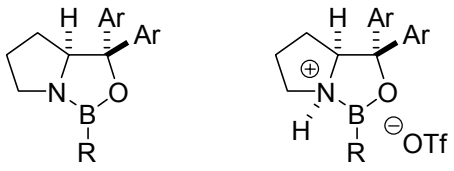

29 **30**

29a/**30a**: Ar = Ph, R = Me

29b/**30b**: Ar = Ph, R = Ph

29c/**30c**: Ar = *m*-Xyl, R = *o*-Tol

Scheme 1.6 Oxazaborolidines and oxazaborolidinium cations.

Screening of the catalysts **29a**-**c** as well as **30a**-**c** for the hydrocyanation of the benzaldehyde derived imine **27a** (R = Ph, Scheme 1.5) proved **29a** and **30a** to be the most practical catalysts (among those in Scheme 1.6) for this reaction.

A series of imines **27a**-**f** derived from aromatic aldehydes and pivalaldehyde were subjected to hydrocyanation in the presence of **29a** or **30a** (Scheme 1.7).

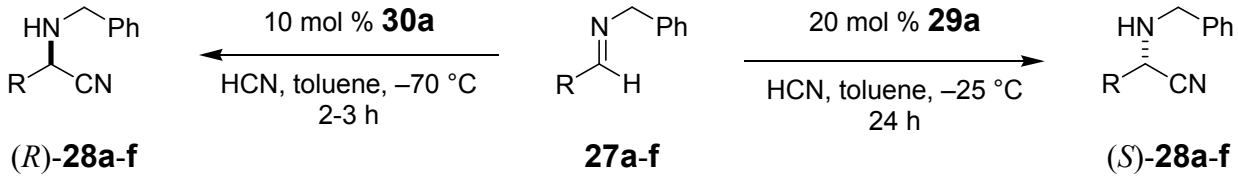

(*R*)-**28a**-**f** **27a**-**f** (*S*)-**28a**-**f**

R = Ph, *o*-BrC_6H_4, *m*-BrC_6H_4, 2-naphthyl, *p*-$OMeC_6H_4$, *t*-Bu

Scheme 1.7 Substrate scope for the asymmetric hydrocyanation of imines with **29a** or **30a**.

Although the enantioselectivities of the product *α*-amino nitriles **28a**-**f** were only moderate in both cases (up to 71 % ee in the case of **29a** and up to 42 % ee in the case of **30a**), products with opposite sense of stereoinduction were obtained upon protonation of the catalyst. This is the first successful application of neutral and cationic oxazaborolidine for the asymmetric hydrocyanation of imines. Moreover, to the best of my knowledge, this is the first example of a protonation-induced switch of the sense of stereoinduction.

In addition to the synthesis of enantioenriched *α*- and *β*-amino acids, a new modular tridentate ligand system **31** (Scheme 1.8) was developed and three ligands **31a**-**c** were synthesized following an ex-chiral pool approach.

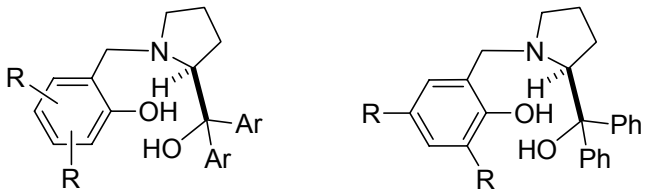

31 **31a**: R = *t*-Bu
31b: R = I
31c: R = Br

Scheme 1.8 The new tridentate ligand system **31** and ligands synthesized.

To demonstrate the potential of this new ligand system, an aluminium complex **32** (proposed structure) of the ligand **31a** was prepared and applied for hydrocyanation of benzaldehyde **33** (Scheme 1.9).

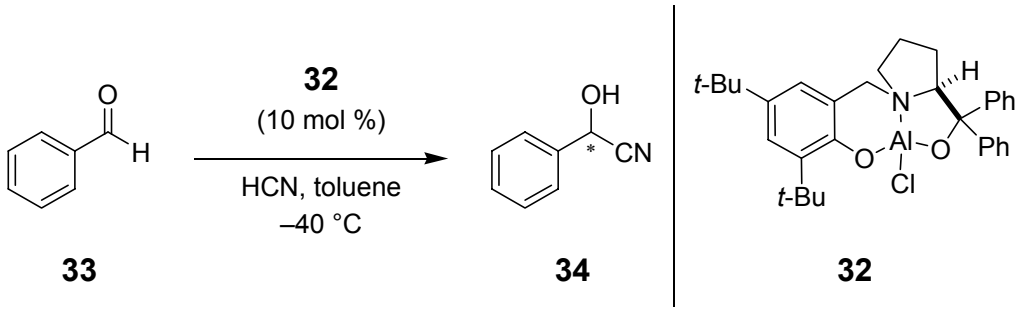

Scheme 1.9 Asymmetric hydrocyanation of benzaldehyde catalyzed by the proposed aluminium complex **32**.

The cyanohydrin **34** was obtained only in moderate enantiomeric purity of 50 % ee. Nevertheless, this reaction showed the potential of this modular ligand system.

2 Introduction

"If a definitive history of twentieth century science is ever written, one of the highlights may well be a chapter on the chemical synthesis of complex molecules, especially the total synthesis of naturally occurring substances." – E. J. Corey.[1]

Many naturally occurring substances are optically active due to the tendency of living organisms to produce only a single enantiomer of a given molecule. The asymmetry of these molecules arises from the inherent chirality of the enzymes that are responsible for their production. Besides innumerable natural products, there are thousands of synthetic compounds whose physical and chemical properties are characteristic of the spatial orientation of the atoms and groups within the molecule.[2] Although the apparent physical differences between two enantiomers may seem small, the spatial orientation of a single functional group/residue drastically affects the properties of the compounds. This has strong implications for the human body. The difference in our olfactory response to either one of the enantiomers can be illustrated by the classic example of the enantiomeric forms of the terpene carvone: (*R*)-(–)-carvone **35** has the odor of spearmint, whereas (*S*)-(+)-carvone *ent*-**35** smells like caraway (Scheme 2.1).[3]

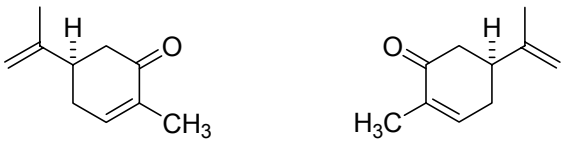

(*R*)-(–)-Carvone **35** (*S*)-(+)-Carvone *ent*-**35**

Scheme 2.1 The enantiomers of the natural compound carvone.

Similarly, different stereoisomers of a given biomolecule can exhibit dramatically different biological activities. This difference is demonstrated by the tragic administration of the drug thalidomide **36** (Scheme 2.2) to pregnant women in the 1960s.[4] Although, the (*R*)-thalidomide **36** has desirable sedative properties, its (*S*)-enantiomer *ent*-**36** is teratogenic.[5] This fact along with the *in vivo* racemization of the (*R*)-enantiomer[6] resulted in a high incidence of fetal deaths, neonatal deaths, and congenital malformations.

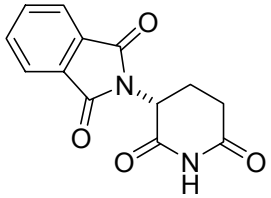

(*R*)-(+)-Thalidomide, **36**

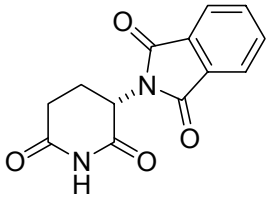

(*S*)-(–)-Thalidomide, *ent*-**36**

Scheme 2.2 The enantiomers of the drug thalidomide **36** and *ent*-**36**.

These examples are among literally hundreds of cases where biological systems, whether in plant, animal, or insect domain, react differently to the enantiomeric forms of a certain molecule. It is thus highly desirable, if not mandatory, to prepare molecules in enantiomerically pure form for meaningful studies of their chemical and biological properties. Besides the ex-chiral pool synthesis[7] from the nature's collection of chiral compounds, there are two general methods for obtaining enantiomerically homogeneous compounds: they may either be synthesized in racemic form and resolved by mechanical or chemical means into their optical antipodes, or the synthesis may be performed in an enantioselective manner so as to produce chirally enriched compounds.

The separation of enantiomers was achieved for the first time by mechanical resolution in 1848 when *Louis Pasteur* separated the crystals of the two optical isomers of sodium ammonium tartrate. Although this method itself is not generally applicable, the idea of selective crystallization of one enantiomer by diastereomeric salt formation is still quite popular for the large scale preparation of enantiomerically pure acids or amines. Other methods of resolution involve the formation of covalent bonds between the racemic substrate and an enantiomerically pure compound. The resulting diastereomeric products can be separated, in most cases, by chromatographic techniques and the desired enantiomer can be regenerated from the appropriate diastereomer by chemical manipulations. The separation of enantiomers has also been achieved up to gram scale by more sophisticated chiral chromatographic techniques. In addition to several limitations associated with each of the above methods, they suffer from lack of elegance.

Furthermore, the number of stereoisomers increases by a factor of 2^n with the introduction of additional chiral centers. Consequently, in the cases of molecules with more than two chiral centers, the separation of one enantiomer from the mixture by resolution techniques is impractical, if not impossible to achieve. The solution to this problem is asymmetric synthesis.

Within the domain of asymmetric synthesis, catalysis holds a special appeal for both the practitioner and the user alike. The ability to produce large quantities of desired, enantiomerically pure compounds from simple building blocks and relatively small quantities of enantioenriched catalysts has tremendous practical implications.[8] Until quite recently, the field of asymmetric catalysis was

dominated mainly by two types of catalysts – transition metal complexes and enzymes. For the synthetic chemists, it is very important to have reagents and catalysts with predictable behavior when planning new syntheses. The transition metal catalysts not only effect a wide range of transformations with useful level of enantioselectivity, but often do so with high predictability.[7] The contribution of transition-metal catalysis in organic chemistry is evidenced by the fact that in 2001 the Nobel Prize in Chemistry was awarded to *K. Barry Sharpless* "for his work on chirally catalyzed oxidation reactions", and to *William R. Knowles* and *Ryoji Noyori* "for their work on chirally catalyzed hydrogenation reactions". With a few important exceptions (such as certain lipases), such generality is highly unusual with enzymes.[9] The past few years have witnessed a significant new movement in organic synthesis: the use of small, purely organic compounds as catalysts for an ever-widening range of asymmetric transformations.[10-13] The term *organocatalysis* has been aptly coined for this new approach, which is an alternative to the use of traditional metal-ligand complexes and biocatalytic enzymes that have previously been developed. Despite the rather recent introduction of this kind of catalysts to synthetic organic chemistry, organocatalytic reactions look back on a venerable history.[12] In fact, in the early days of asymmetric catalysis, some of the very first asymmetric catalysts were purely organic molecules.[11] As early as in 1912, *Bredig* et al. reported a modestly enantioselective alkaloid-catalyzed cyanohydrin synthesis.[14] The real breakthrough in the area of organocatalysis came in 1970s when *Hajos* et al. and *Wiechert* et al. reported a highly catalytic enantioselective intramolecular aldol reaction using the simple amino

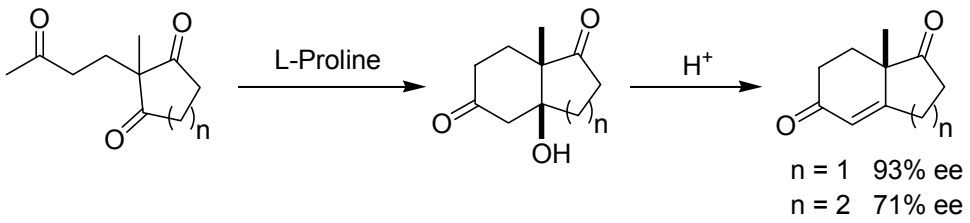

Scheme 2.3 The *Hajos-Parrish-Eder-Sauer-Wiechert* reaction.

acid L-proline as the catalyst (Scheme 2.3).[15] Recently, *List* et al. promoted this reaction and used L-proline for intermolecular aldol reaction of ketones to various aldehydes.[13, 16]

The growing interest in the field of asymmetric organocatalysis is evidenced by the increasing number of publications appearing everyday besides an already published book[12] and several reviews.[10, 11, 13]

3 Background

3.1 Asymmetric Organocatalysis

Organocatalysis is the process of acceleration of a chemical reaction with an organic compound that does not contain a metal atom in its active center.[10, 12, 13] This type of catalysis is complementary with the metal-complex mediated, and also, with biocatalytic transformations. Preparative advantages of organocatalysts are notable: they are readily available from simple chiral feedstocks. Usually the organocatalytic reactions can be performed under an aerobic atmosphere, with wet solvents and in most cases protection of functional groups is not required.[12]

An important class of organocatalysts that were known even before the term *organocatalysis* was introduced is the phase transfer catalyst.[17] Even asymmetric version of the phase-transfer catalysts[12] has been quite popular ever since their introduction in 1976.[18] The field of asymmetric organocatalysis, during the first few years after it acquired the name, was dominated by covalent catalysis involving enamine or iminium ion intermediates (Scheme 3.1). Although L-proline **37** was

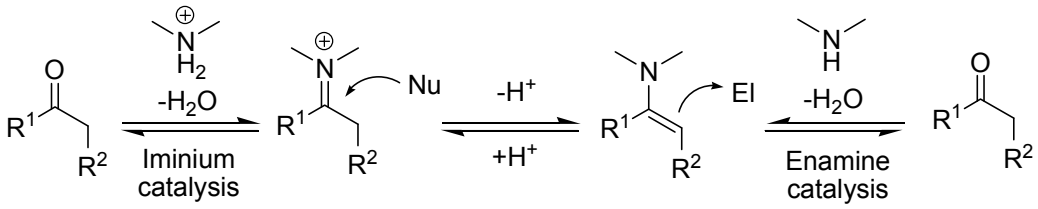

Scheme 3.1 Activation of a carbonyl group by the formation of iminium ion or enamine intermediates.

initially used for this type of catalysis, several proline derivatives and other chiral secondary amines were eventually developed (Scheme 3.2).[12] The enamine and iminium ion catalysis were applied

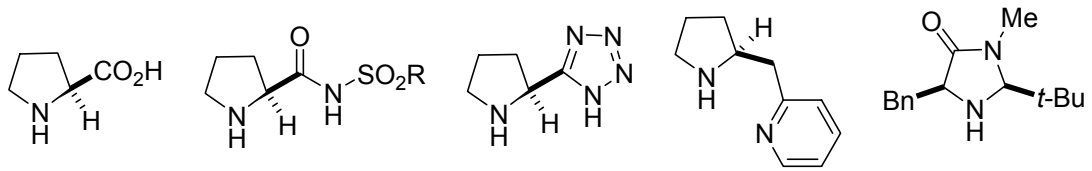

37

Scheme 3.2 L-Proline **37** and some other secondary amine organocatalysts.

for a wide range of asymmetric transformations and even for the synthesis of carbohydrates[19] and other complex natural products.[20] Very recently *MacMillan* and co-workers introduced a cascade enamine-iminium ion catalysis concept,[21] which clearly demonstrates the potential of this type of covalent catalysis.

If the covalent catalysis *via* enamine and iminium ion intermediates is one of the most widely studied areas of asymmetric organocatalysis, the least studied area must be the chiral proton catalysis.[22] This strategy was reported a year ago by *Johnston* and co-workers.[23] In this approach, a chiral catalyst is generated by coordinating a proton, which stems from the strong *Brønsted* acid TfOH, to a chiral C_2-symmetric diamine. The resulting salt **38** is an excellent catalyst for the asymmetric aza-*Henry* reaction and affords the corresponding products in good yields with up to 95 % ee (Scheme 3.3).[23]

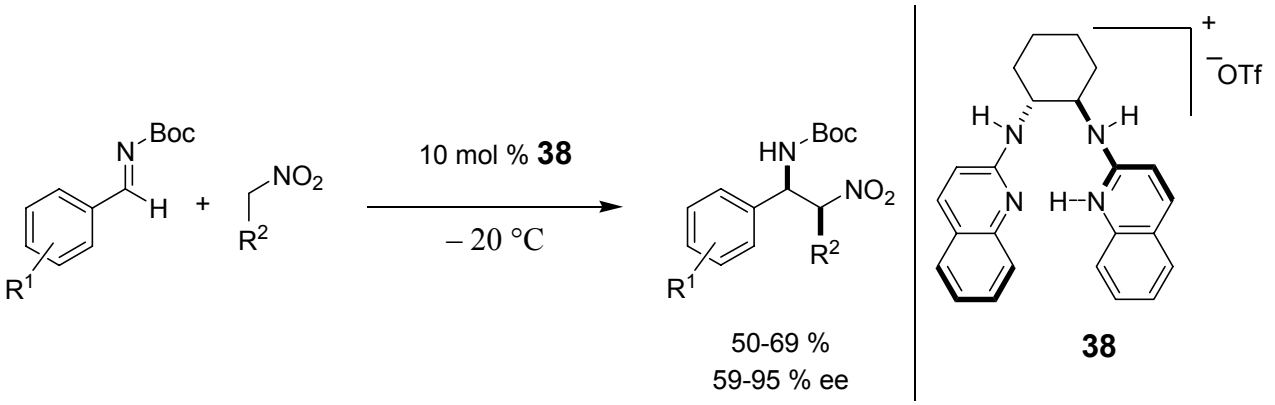

Scheme 3.3 *Johnston*'s chiral proton catalyst **38** in asymmetric aza-*Henry* reaction.[23]

Another and even more promising chiral proton catalyst, a chiral phosphoric acid **39** (Scheme 3.4) was developed in the same year by *Terada* et al. for asymmetric *Mannich* reaction,[24]

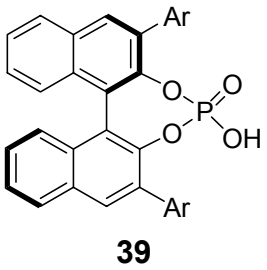

Scheme 3.4 The chiral proton catalyst **39** of *Terada*.[24-26]

aza-*Friedel-Crafts* alkylation of furan[25] and direct alkylation of α-diazoester.[26] Quite recently *Rueping* and co-workers applied this catalyst for the enantioselective transfer hydrogenation of ketimines.[27]

An intermediate concept between the covalent enamine/iminium ion catalysis and chiral proton catalysis is the activation of substrates by hydrogen bonding.[28, 29] Hydrogen bonding activation by diols were first demonstrated by *Hine*[30] and *Kelly*[31] for the activation of epoxides and carbonyls, respectively; whereas *Etter* and co-workers[32] discovered the potential of ureas to form cocrystals with a variety of H-bond acceptors, including carbonyl compounds. This property of urea was explored by *Curran*[33] and *Schreiner*[34] for promoting chemical transformations using urea or thiourea as the catalysts.

An important contribution in the arena of chiral diol-catalyzed asymmetric transformation was made by *Rawal* and co-workers.[35] They developed a highly enantioselective hetero-*Diels-Alder* (HDA) reaction catalyzed by a TADDOL derivative **40** (Scheme 3.5). In the presence of 10 mol % of **40**, the HDA products were obtained in good yields and with excellent enantioselectivities.

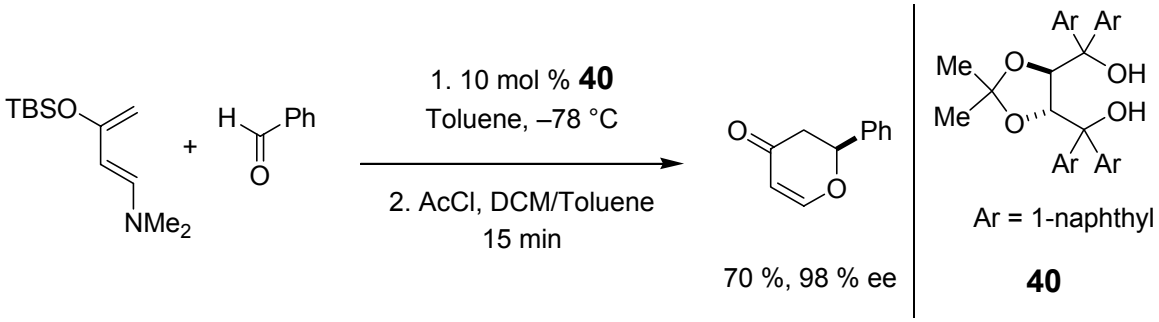

Scheme 3.5 Asymmetric hetero-*Diels-Alder* reaction from *Rawal* et al.[35]

The most remarkable advances in the domain of urea and thiourea catalysts were made by the *Jacobsen* group.[36-42] They identified and optimized a series of (thio)urea-containing catalysts (e.g. **41**, Scheme 3.6) for a wide range of nucelophilic addition to imines. These catalysts represent the

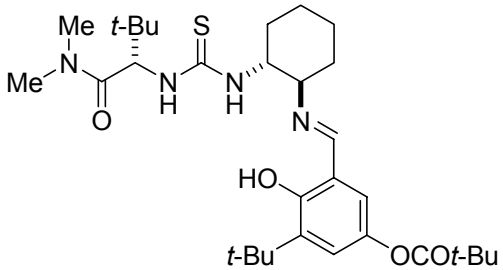

Scheme 3.6 An example of *Jacobsen*'s thiourea-containing catalysts.

most enantioselective double-hydrogen-bonding catalysts discovered so far. A representative example of the application of these catalysts is the enantioselective hydrophosphonylation of imines

(Scheme 3.7).[42] In the presence of 10 mol % of **41**, α-amino phosphonates were obtained in high yields and excellent enantioselectivities in most cases.

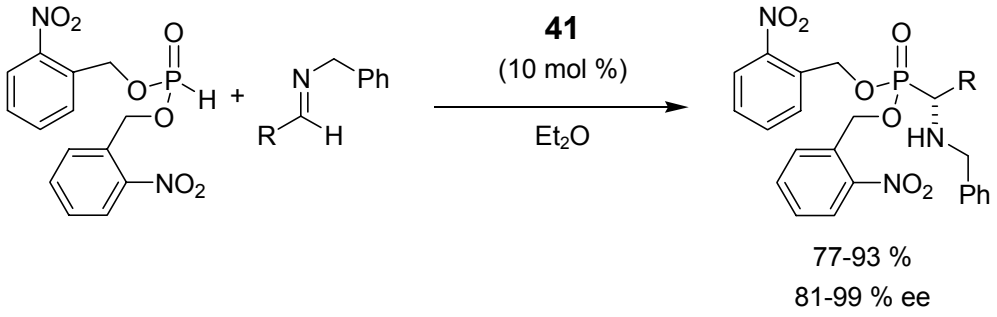

Scheme 3.7 Enantioselective hydrophosphonylation of imines from *Jacobsen* et al.[42]

3.2 Bifunctional asymmetric catalysis

Despite tremendous progress in the field of asymmetric catalysis,[7, 43] the development of new enantioselective catalysts continues to be an important topic in the field of organic chemistry. At the same time there has been ongoing interest for the discovery of new catalyst concepts. From the catalyst design to the synthesis of complex molecular architecture, the chemists have always been inspired by nature. Nature is an uncontested master for promoting chemical transformations in most efficient, selective and atom-economical fashion. The selectivities (in every sense) achieved by nature's catalyst, namely the enzymes, can barely be matched by their synthetic counterparts. The efficiencies and more importantly selectivities achieved by the enzymes in most, if not all, cases can be attributed to the synergistic cooperation between different functionalities at the active site (Scheme 3.8). On the other hand, most of the synthetic asymmetric catalysts rely on the activation

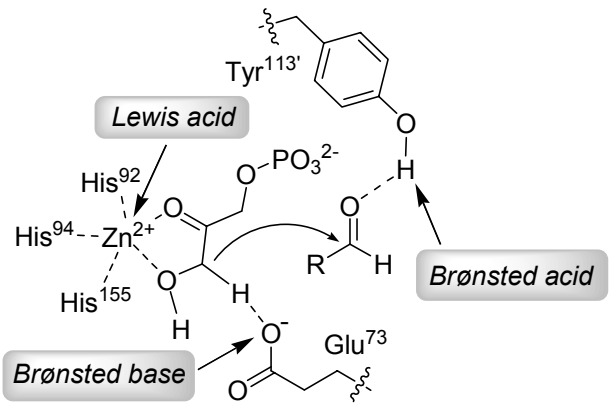

Scheme 3.8 Proposed multifunctional mode of action at the active site of class-II aldolase.

of only one of the substrates in an intermolecular reaction. Chemists were also inspired by nature's approach of controlling reactivity and a new catalytic concept evolved: the so called multifunctional catalysis. A relevant and even more popular version of multifunctional catalysis is bifunctional catalysis, particularly in the domain of asymmetric catalysis.[44] Bifunctional catalysts can drastically improve the efficiency of asymmetric processes with respect to enantioselectivity and/or conversion rate owing to the attachment of both electrophilic as well as nucleophilic substrates to the chiral catalyst in the transition-state (Scheme 3.9). Such a coordination of both substrates within an asymmetric space would lead to a stronger stereodiscrimination and should result in a highly enantioselective process. The main concern for such two-center catalysts is the choice of suitable

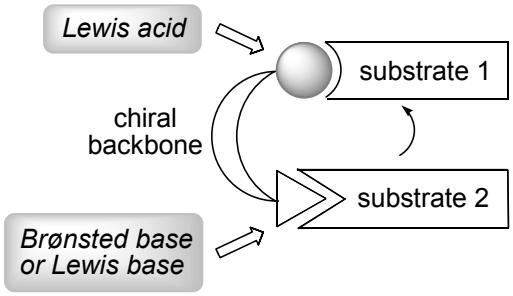

Scheme 3.9 General concept of bifunctional asymmetric catalysis.

Lewis acid and *Lewis* base/*Brønsted* base partners. In addition, the prevention of internal coordination between the acid-base pair is one of the main challenges for such systems. The latter issue is often overcome by integrating the two functionalities in an appropriate chiral environment. Important contributions in the field of bifunctional asymmetric catalysis have been made by *Corey* et al. in oxazaborolidine catalyzed asymmetric reduction of ketones (Scheme 3.10a) [45] and by *Noyori* et al. in the Zn-complex catalyzed asymmetric aldehyde alkylation reaction (Scheme 3.10b).[46] These catalysts, however, utilize heteroatoms directly conjugated to the *Lewis* acid as a *Lewis* base (Scheme 3.10).

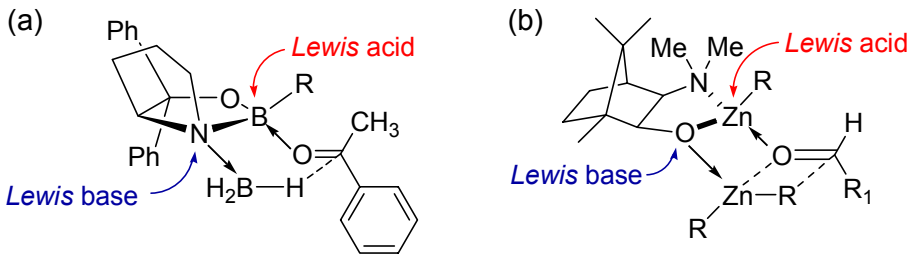

Scheme 3.10 Concepts of *Lewis* acid-*Lewis* base bifunctional asymmetric catalyst from (a) *Corey* and (b) *Noyori*.

The *Shibasaki* group recently reported a chiral *Lewis* acid-*Lewis* base bifunctional catalyst for the asymmetric cyanosilylation of aldehydes. *Lewis* acidic aluminium and *Lewis* basic phosphine oxide are elegantly embedded in the chiral 1,1′-binaphthyl backbone to form this highly efficient bifunctional catalyst **42** (Scheme 3.11a).[47] The internal complexation of phosphine oxide with aluminium is avoided by applying a linker of appropriate length between the two functionalities. In addition to the phosphine oxide already present in the catalyst, a substoichiometric phosphine oxide was used as an additive. In the working model proposed by the authors for the catalytic cycle, this external phosphine oxide would produce a trigonal bipyramidal aluminium complex by coordinating to the aluminium (Scheme 3.11b). This geometry would allow the aldehyde to position itself at the apical site close to the internal phosphine oxide. TMSCN could then be activated by

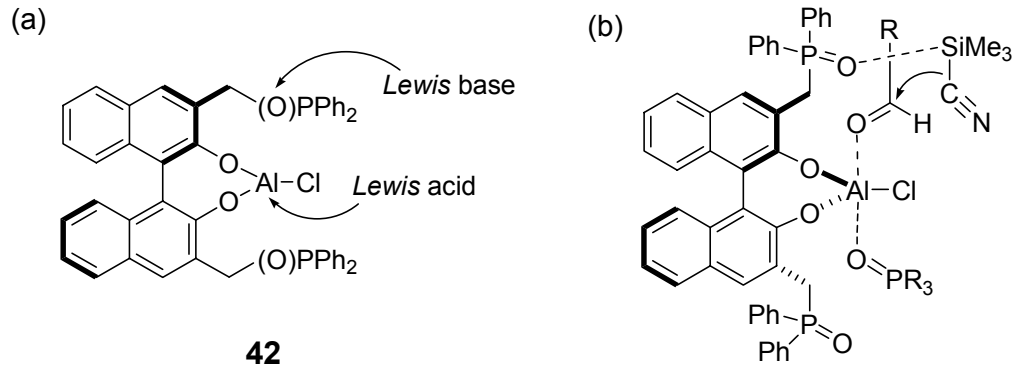

Scheme 3.11 (a) *Shibasaki*'s bifunctional catalyst and (b) its proposed dual activation in the cyanosilylation of aldehydes.[47]

interacting with the internal phosphine oxide for the transfer of cyanide to the aldehyde to afford the cyanohydrin with the observed stereochemistry (*S*).[47]

Building on the work of *Shibasaki* and co-workers, *Nájera*, *Saá* and co-workers designed a very similar bifunctional catalyst in which the *Lewis* basic phosphine oxide moiety was replaced by a *Brønsted* basic tertiary amine.[48] This catalyst was applied for the same reaction and similar level of enantioselectivity was achieved.

In the field of organocatalysis, significant developments have also been made with respect to the design and discovery of new asymmetric bifunctional catalysts.[12] *Corey* and *Grogan* reported a C_2-symmetric chiral bicyclic guanidine **43** (Scheme 3.12) for the asymmetric hydrocyanation of *N*-benzhydryl imines (for details, see page 31).[49] The authors proposed a bifunctional mode of action for this catalyst (Scheme 3.12). Protonation of the catalyst **43** with HCN generates a guanidinium cyanide complex which can serve as the hydrogen bond donor to the aldimine forming

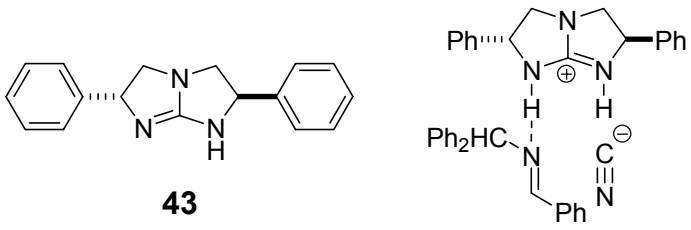

Scheme 3.12 *Corey*'s chiral bicyclic guanidine **43** and its proposed bifunctional mode of action.[49]

the termolecular pretransition-state assembly. The attack by cyanide ion within the ion pair on the hydrogen-bond-activated aldimines affords the hydrocyanation product.[49]

An excellent example of diol based asymmetric bifunctional catalyst was demonstrated by *Sasai* and co-workers for the enantioselective aza-*Morita-Baylis-Hillman* reaction (Scheme 3.13).[50] In

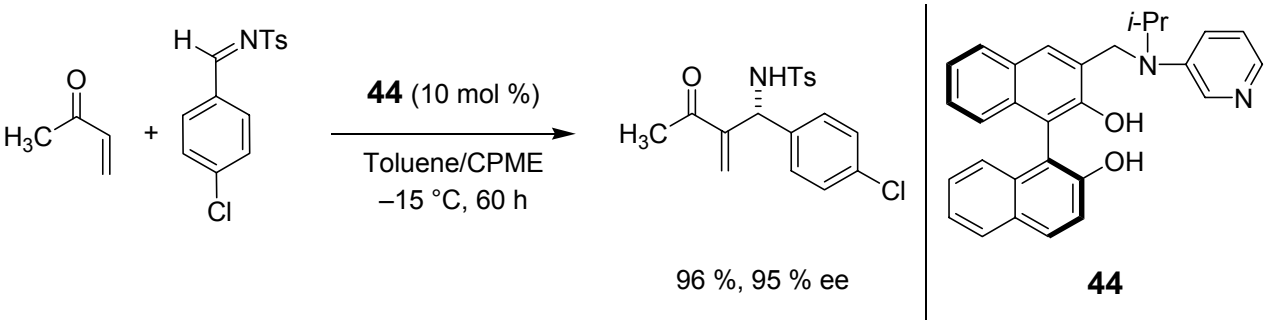

Scheme 3.13 Diol-based bifunctional catalyst **44** for the enantioselective aza-*Morita-Baylis-Hillman* reaction.[50]

this catalyst **44**, a quasi-*Lewis* acidic diol and a *Brønsted* basic 3-aminopyridine-derivative were integrated on a chiral binaphthyl backbone. The authors showed that a combination of 3-DMAP and (*S*)-BINOL afford the racemic product only in low yield. This illustrates the importance of having two functionalities in the same molecule.

Takemoto et al. developed a thiourea-based bifunctional organocatalyst for the enantioselective *Michael* addition of malonates to nitroolefins (Scheme 3.14).[51-53] This catalyst **1** is an elegant combination of the quasi-*Lewis* acidic thiourea and a *Brønsted* basic tertiary amine. These two

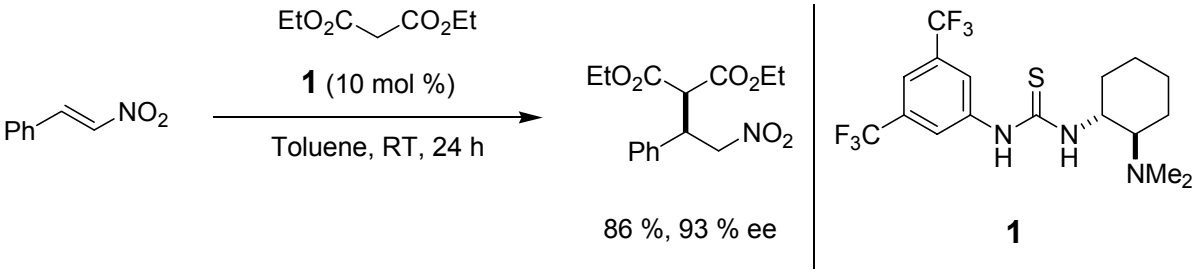

Scheme 3.14 Asymmetric *Michael* addition of malonates to nitoolefins by **1**.[51]

functionalities are combined in a single chiral environment to generate this highly efficient catalyst that promotes the *Michael* addition to afford the products with high enantioselectivities.[51] The authors also investigated the mechanism of this reaction and proposed a bifunctional mode of activation of both the substrates by the catalyst **1** (Scheme 3.15).

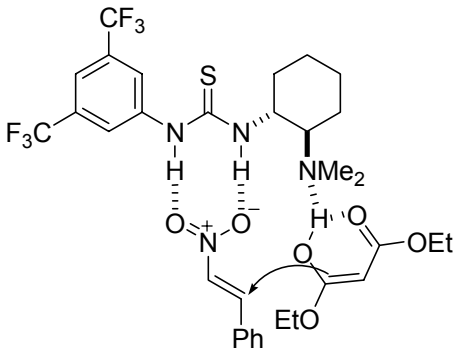

Scheme 3.15 Transition state model for the *Michael* addition of malonates to nitroolefins by **1**.[53]

After the report of *Takemoto* et al.,[51] several groups applied[54-56] the catalyst **1** and developed[56-58] a number of (thio)urea-tertiary amine bifunctional organocatalysts (Scheme 3.16) for a wide array of asymmetric transformations with good results in most cases.

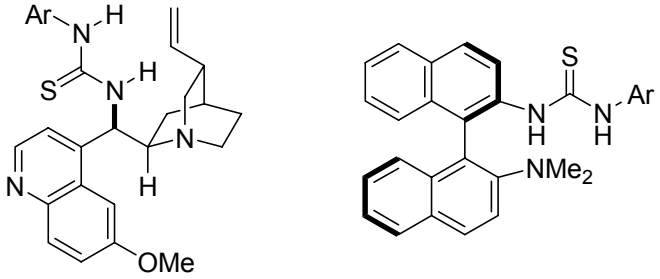

Scheme 3.16 Examples of *Takemoto*-type bifunctional organocatalysts [Ar = 3,5-$(CF_3)_2C_6H_3$].

3.3 Kinetic and dynamic kinetic resolution

The goal of asymmetric synthesis is to prepare stereochemically-enriched compounds in the most efficient and practical manner possible. At the same time, it is important to accomplish the synthesis in a way to achieve highest "atom economy".[59] Driven by the demand to enhance the economic balance of chemical processes, there has been an increased interest in the transformation of racemates into a single stereoisomeric product without the occurrence of an undesired isomer. Despite numerous efforts to transform an unwanted isomer into the desired final product, for

example by re-racemization or *via* independent enantio-convergent synthesis, processes based on the separate use of two enantiomers are far from being economically optimal and certainly lack elegance. Even today, the resolution of racemates is still one of the major methods for the production of enantiopure compounds on an industrial scale.[8, 60] Although numerous methods exist which are highly efficient in terms of enantio-discrimination, the maximum theoretical yield of 50 % for each enantiomer sets a low ceiling on the productivity of such processes. In order to overcome this limitation, considerable effort has been devoted to create processes which afford the product with the same high enantiomeric purity, but in significantly improved chemical yield. A number of strategies have been developed during the past few years to allow the conversion of both enantiomers from a racemate into a single stereoisomer in a concurrent and non-sequential fashion.[61] One of these strategies, the so-called kinetic resolution (KR) is based on the difference of reaction rates (k_R, k_S) of substrate enantiomers (S_R, S_S) during the transformation to product enantiomers P_R and P_S by a chiral catalyst *via* diastereomeric transition state (Scheme 3.17).[62] Due

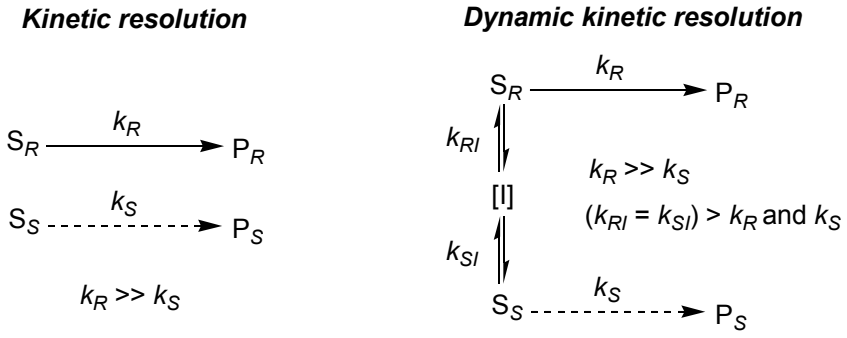

Scheme 3.17 Principles of kinetic and dynamic kinetic resolution.

to the fact that two enantiomeric species react simultaneously at different rates (in preferably irreversible manner), the relative concentrations of S_R/S_S and P_R/P_S change as the reaction proceeds and, as a consequence, the enantiomeric composition of S and P becomes a function of the conversion. Recovery of the formed product P_R and the unreacted substrate enantiomer S_S in non-racemic form constitutes a kinetic resolution. The efficiency of KR is often expressed by the selectivity factor s or k_{rel}: $s = k_R/k_S$. Although the maximum theoretical yield based on racemic starting material is only 50 %, the most attractive aspect of KR from the point of view of preparative synthesis is that unreacted substrate can be recovered in high ee, simply by carrying the reaction to high enough conversion, even if s (or k_{rel}) is not very high.

A significant breakthrough to overcome the 50 % yield barrier in KR was achieved by the development of dynamic kinetic resolution (DKR). The latter combines the resolution step with an *in situ* racemization of the substrate enantiomers S_R and S_S *via* an achiral or prochiral

intermediate/transition state (Scheme 3.17). As a consequence, as the faster reacting enantiomer (S_R) is depleted during the enantioselective reaction, the equilibrium of S_R/S_S is constantly re-adjusted by racemization of the slow reacting counterpart S_S. To indicate the non-static character of this process, the term "dynamic kinetic resolution" has been coined. It is conceivable that the kinetic balance of the two concurring reactions is of crucial importance for the success of a DKR. As a rule of thumb, the racemization of the substrate should occur at an equal or higher rate than the catalytic asymmetric reaction (see Scheme 3.17).

3.4 The routes to enantiomerically pure *α*-amino acids

α-Amino-carboxylic-acids, commonly known as *α*-amino acids, are one of the five major classes of natural products that exhibit diverse biological functions. They are fundamental constituents of proteins and act as mediators for nitrogen metabolism, providing the raw materials for the production of many primary and secondary metabolites. Historically, the amino acids have been subdivided into the 20 proteinogenic and the non-proteinogenic representatives. Besides their numerous applications for natural processes, enantiomerically pure *α*-amino acids are extremely valuable chemicals in their own right. Both proteinogenic and non-proteinogenic *α*-amino acids find wide application for the synthesis of a wealth of enantiomerically pure pharmaceuticals (Scheme 3.18).[63] In this context, the structure of the extremely potent antibiotic vancomycin **45**

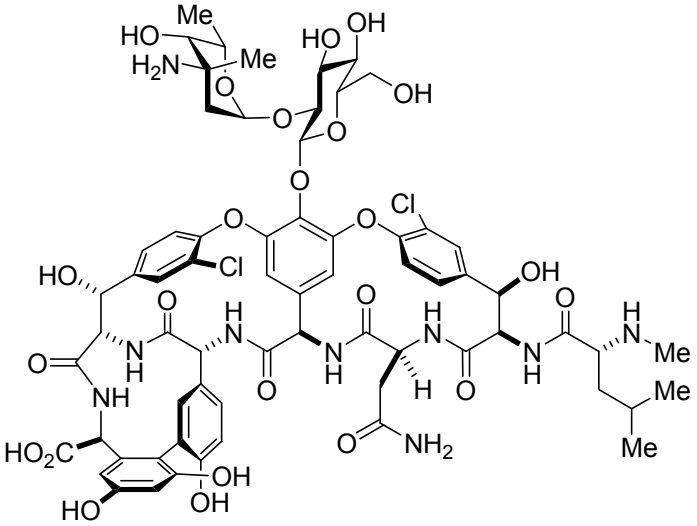

Vancomycin, **45**

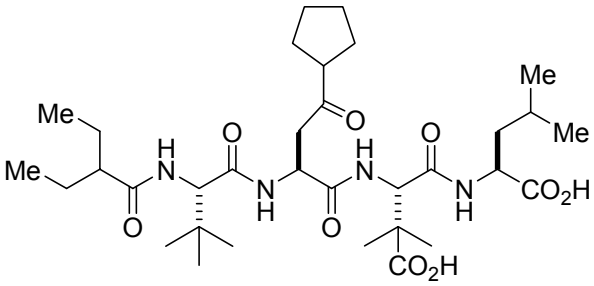

Biomega, **46**

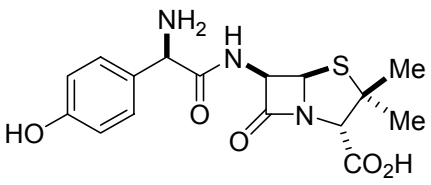

Amoxicillin, **47**

Scheme 3.18 *α*-Amino acid containing pharmaceuticals.

is particularly noteworthy because of the presence of a wide array of nonnatural *α*-amino acids. Alongside the non-natural *α*-amino acids, there is a growing interest for natural or non-natural D-amino acids. D-Amino acids are significant as components of antibiotics, pharmaceuticals, or pesticides that are often more active and also more stable compared to their L-containing analogs.[63] D-Amino acid-containing pharmaceuticals for example, are more stable than L-analogs against decomposition in liver, kidney and bloodstream. Furthermore, *α*-amino acids are extensively used as chiral starting materials, auxiliaries, organocatalysts and also ligands for transition-metal catalysts in modern organic synthesis.[64, 65] The ever-increasing interest for various *α*-amino acids has prompted the development of new methodologies and strategies for their asymmetric synthesis.
There are two general approaches for obtaining enantiomerically pure α-amino acids (as to the preparation of any enantiomerically pure compounds): (i) synthesis in racemic form, followed by separation of the product enantiomers, and (ii) asymmetric synthesis, preferably by catalytic methods.

3.4.1 Resolution of racemic *α*-amino acids

3.4.1.1 Dynamic kinetic resolution of hydantoins

The compound imidazolidine-2,4-dione or hydantoin was discovered by *von Baeyer* in 1861 by reduction or hydrogenation of allantoin, a cyclic amide naturally occurring in many plants.[66] A wide spectrum of various 5-mono and 5,5′-disubstituted hydantoin derivatives of industrial and pharmaceutical interest is described in the literature.[9] Among them, 5-monosubstituted hydantoins may be regarded as cyclic ureides of *α*-amino acids. They are important precursors, in the industrial production of optically pure *α*-amino acids (Scheme 3.19). Various enzymes, so called hydantoinases, facilitate the hydrolysis of the hydantoin ring system as an initial reaction step. The hydantoinases generally have different substrate specificities and in general are selective in hydrolyzing D- or L-hydantoins to the corresponding D- or L-*N*-carbamoyl amino acids (or hydantoic acid). The hydantoins are often applied in combination with the highly stereoselective enzyme *N*-carbamoyl amino acid amidohydrolases (mostly known as *N*-carbamoylases), which catalyze the further hydrolysis of the hydantoic acids to the free aminoacids in an irreversible reaction. 5-Monosubstituted hydantoins racemize through keto-enol tautomerism above pH 8, owing to their acidic hydrogen in 5-position. However, the rate constant of racemization strongly depends on the residue in 5-position ($\tau_{1/2}$: phenylhydantoin 0.3 h, benzylhydantoin 5 h and

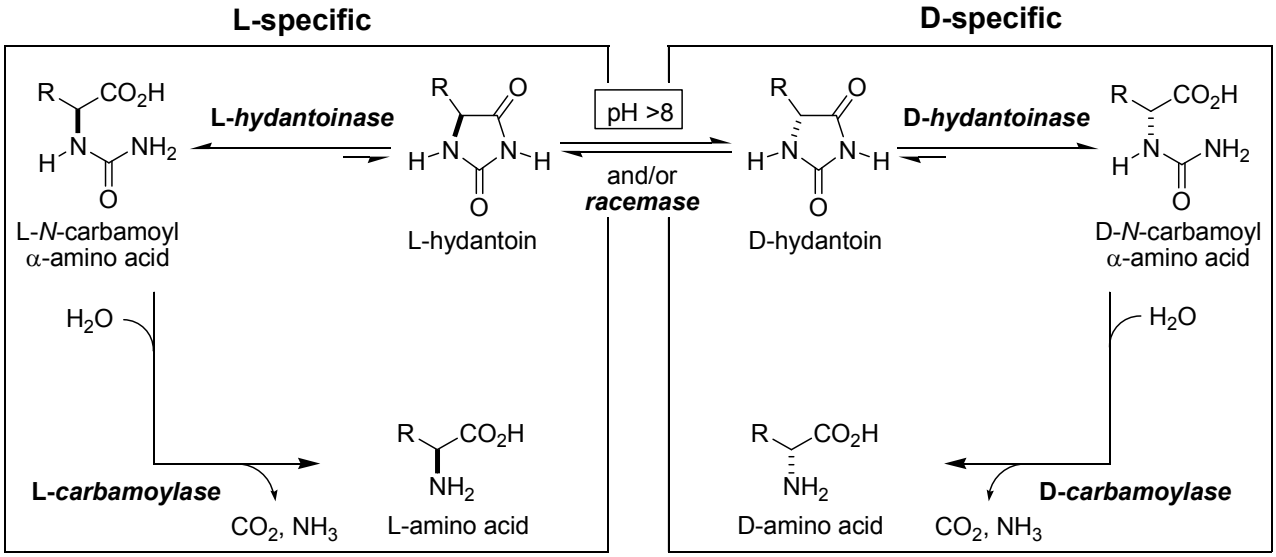

Scheme 3.19 The "hydantoinase-process" for the production of D- and L-amino acids.

isopropylhydantoin 56 h).[63] Thus, in some cases, a third enzyme called hydantoin-racemase is involved. Together, these three enzymes accomplish the total conversion of racemic 5-monosubstituted hydantoin derivatives into the corresponding enantiomerically pure D- or L-α-amino acids. This cascade of reactions, whether located in whole cells or carried out using isolated enzymes is called the "hydantoinase-process" (Scheme 3.19).[9]

3.4.1.2 Dynamic kinetic resolution of azlactones

Oxazol-5(4*H*)-ones, commonly known as azlactones (**A** or *ent*-**A** in Scheme 3.20), constitute a readily available class of highly versatile intermediates for the synthesis of α-amino acids and peptides, for they undergo facile ring opening with various nucleophiles to produce α-amino acid

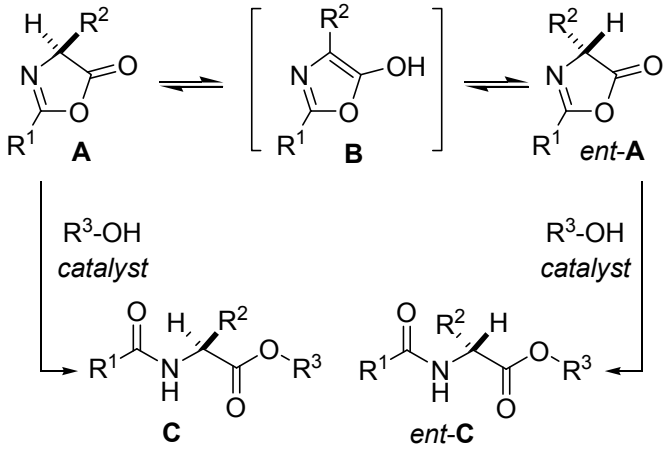

Scheme 3.20 Basis for the dynamic kinetic resolution of azlactones.

derivatives. They are easily prepared from glycine azlactone (R^2 = H in Scheme 3.20) by the *Erlenmeyer* azlactone synthesis or from *α*-amino acids by *N*-acylation followed by cyclodehydration in the presence of a condensation agent (e.g. acetic anhydride).[67] Owing to the relatively high acidity of the C-4 proton (pKa ~ 8.9)[68] and aromatic character of the intermediate enol form (**B** in Scheme 3.20), azlactones racemize under very mild conditions, even in the absence of external base.[69] These properties of azlactones made them excellent substrates for enantioselective ring-opening under the condition of a dynamic kinetic resolution (see Scheme 3.17 on page 17). The alcoholytic ring opening of azlactones leads to *N*-acyl *α*-amino acid esters (such as **C** or *ent*-**C**; Scheme 3.20), the *N*,*C*-doubly protected *α*-amino acid derivative.

Proteases[70] and lipases[71] have been used for the rather efficient enzymatic DKR of azlactones. But only a few examples of chemically catalyzed DKR of azlactones appear to exist. As reported by *Seebach* et al., arylalanine-derived azlactones (R^2 = CH_2Ar in Scheme 3.20) could be resolved using titanium-taddolates **48** (Scheme 3.21) in good yields with moderate ee.[72] In this approach, **48** was used in stoichiometric quantities, or at 0.7 eq. loading in the presence of 0.5 eq. of Al(O*i*-Pr)$_3$. Enantiomeric excesses up to 72 % was obtained with 74 % yield of the product ester within 5 to 10 days.

Hua and co-workers used the cyclic dipeptide *cyclo*-[(*S*)-His-(*S*)-Phe] **49** (Scheme 3.21) as an organocatalyst for the alcoholic DKR of the phenylalanine-derived azlactone (R^2 = CH_2Ar in Scheme 3.20).[73] However, the enantiomeric excess achieved in this case was only up to 39 % with

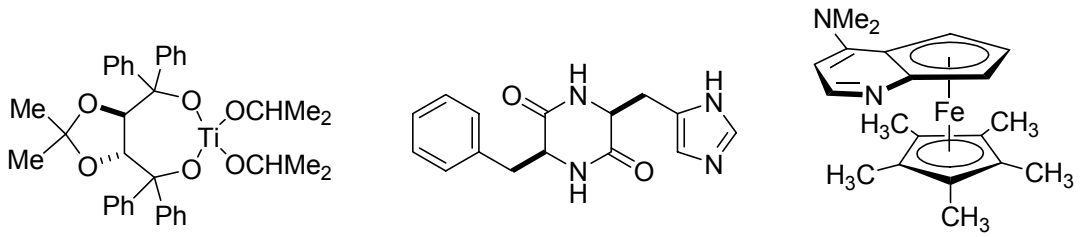

48 **49** **50**

Seebach 1997 *Hua* 1999 *Fu* 1998

Scheme 3.21 Non-enzymatic reagents and catalysts for the dynamic kinetic resolution of azlactones.

a conversion of ca. 30 % after 15 days. All these methods described above suffer either from narrow substrate scope or very long reaction times (ranging from days to weeks), or both.

Fu et al. showed that the DKR of azlactones can also be effected by alcoholysis in the presence of the planar-chiral DMAP-derivative **50** (Scheme 3.21) as catalyst.[74] For example, using 5 mol % of **50** and methanol as the nucleophile, enantiomeric excesses of 44-61 % were achieved in the DKR

of a number of azlactones. In the case of the alanine-derived azlactone ($R^2 = CH_3$ in Scheme 3.20), 78 % ee were observed with 2-propanol as the nucleophile ($R^3 = i$-Pr in Scheme 3.20), albeit at the expense of a relatively low reaction rate.[74]

3.4.2 Enantioselective synthesis of *α*-amino acids

Several different (catalytic) asymmetric approaches to *α*-amino acids are reported in the literature.[75, 76] Most of them, if not all, involve enantioselective carbon-carbon, carbon-nitrogen and carbon-hydrogen bond formation as the key step (path a-d; Scheme 3.22).

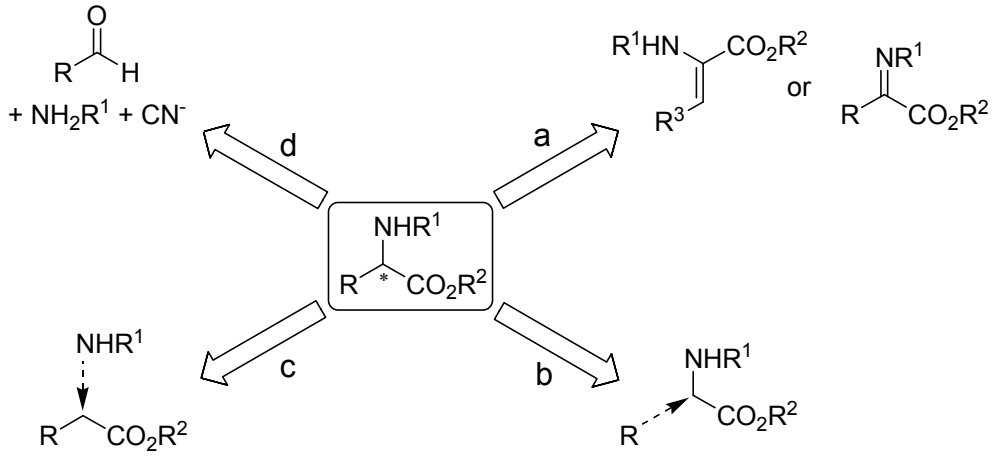

Scheme 3.22 Catalytic asymmetric route to *α*-amino acids.

3.4.2.1 Asymmetric hydrogenation of *α,β*-didehydroamino acid derivatives

Asymmetric hydrogenation of *α,β*-didehydroamino acid derivatives has emerged as one of the most practicable and cost effective routes to a diverse array of both D- and L-natural and unnatural *α*-amino acids.[77] The historical importance of this reaction lies in the fact that the desire to develop practical routes to enantiomerically pure *α*-amino acid derivatives provided the initial inspiration for the advent of catalytic asymmetric hydrogenation reactions more than 30 years ago. The original objective was to identify a catalyst that would allow the enantioselective addition of hydrogen across the C=C double bond of an *α*-enamide substrate **51** (Scheme 3.23). The inaugural studies culminated in Monsanto's commercial production of L-DOPA.[78] Shortly before the beginning of this study, *Wilkinson* established the feasibility of homogeneous hydrogenation of alkenes with

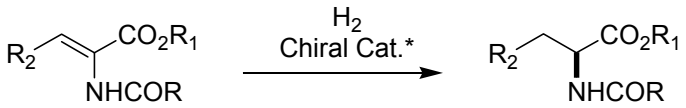

51 **52**

Scheme 3.23 Asymmetric hydrogenation of α,β-didehydroamino acid derivatives.

$RhCl(PPh_3)_3$ as the catalyst precursor.[79] The most obvious approach was to replace PPh_3 with chiral phosphine ligands. Although the initial studies were based on using chiral monophosphine (with the chiral centre on the phosphorous atom) as the ligand,[80] soon the importance of chelating diphosphines was realized.[81] Some of these chiral bis(phosphines) ligands are shown in Scheme 3.24. Like several phosphine ligands, a wide range of catalysts also have been examined for this process. In general, the most efficacious catalysts for α-enamide hydrogenations have been those derived from rhodium complexes bearing chiral C_2-symmetric diphosphine ligands. In particular, cationic rhodium complexes of the type $[(diene)Rh(diphosphine)]^+X^-$ (diene = 1,5-cyclooctadiene or norbornadiene, diphoshphine = chiral diphosphine , X = non-coordinating anions like BF_4, SbF_4, OTf, etc.) have proven to be the most efficient and highly enantioselective catalyst precursors

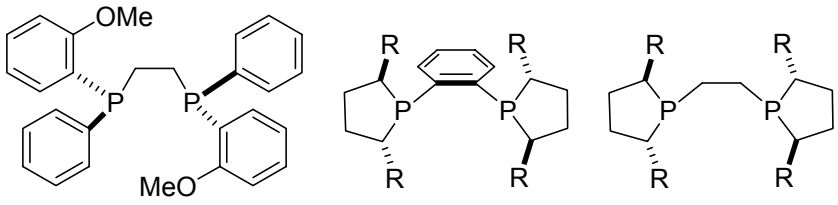

DiPAMP **53** DuPHOS **54** BPE **55**

Scheme 3.24 Selected examples of chiral bis(phosphines) ligands used for Rh-catalyzed asymmetric hydrogenation.

discovered to date for α-enamide hydrogenations. An important fact about this reaction is that high enantioselectivities have been restricted primarily to *Z*-α-enamide substrates. The *E*-α-enamide isomer often is reduced with significantly lower enantioselectivity, and occasionally with opposite sense of stereoinduction. Although DiPAMP **53** appeared to be the most frequently used ligand and also performs satisfactorily in most cases, more recent studies showed that BPE (**55**) and particularly DuPHOS (**54**) are superior to all the other ligands for rhodium catalyzed asymmetric hydrogenation of enamides. Rhodium catalysts derived from the Me-DuPHOS (**54**, R = Me) and Et-DuPHOS (**54**, R = Et) ligands have been shown to be uniquely capable of providing high enantioselectivities in the hydrogenation of α-enamides **51** (Scheme 3.23 on page 23) bearing a wide array of both β-aryl and β-alkyl substituents. For example, *N*-acetyl-α-enamides **51** (R = CH_3,

Scheme 3.23) bearing an unprecendented range of *β*-substituents may be hydrogenated with the cationic (*R*,*R*)-Et-DuPHOS-Rh catalyst to furnish unnatural D-*α*-amino acid derivatives with enantioselectivities routinely >98 % ee.[82] These cationic DuPHOS-Rh catalysts are extremely efficient; substrate-to-catalyst ratios as high as 50000:1 have been demonstrated in *α*-enamide hydrogenations. In many cases both *E*- and *Z*-*α*-enamide isomers may be hydrogenated with high enantioselectivity, and both geometric isomers afford products of the same absolute configuration. The potential of these catalysts to hydrogenate both *E*- and *Z*-isomers provides the possibility to extend the substrate scope to the *β*,*β*-disubstituted *α*-enamides **56** (Scheme 3.25). In fact, the DuPHOS-Rh and BPE-Rh catalysts are singular in their ability to hydrogenate *β*,*β*-disubstituted *α*-enamides with high enantioselectivity: they allow the production of an expansive array of novel

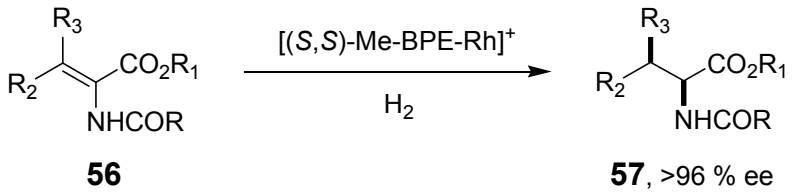

56 **57**, >96 % ee

Scheme 3.25 Asymmetric hydrogenation of *β*,*β*-disubstituted *α*-enamides.

β-branched *α*-amino acid derivatives **57** with enantioselectivities >96 % ee (Scheme 3.25).[83] Also, with two different *β*-substituents, two contiguous stereogenic centers are created simultaneously upon hydrogenation.

Recent studies have also revealed that hydrogenation of *α*-enamides possessing more easily removed *N*-protecting groups, such as *N*-Cbz or *N*-Boc can be accomplished by DuPHOS-Rh catalysts. Enantioselectivities comparable to *N*-acetyl-*α*-enamides have been achieved with a wide range of *N*-Cbz and *N*-Boc *α*-enamides.[82, 84]

3.4.2.2 Asymmetric alkylation of glycine derivatives

The use of benzophenone imines of glycine esters **58** as substrates in enantioselective organocatalytic alkylation has emerged as an excellent method for the preparation of a wide range of optically active *α*-amino acids with high enantioselectivity (Scheme 3.26).[85] The application of chiral phase-transfer catalysts (PTC) to the asymmetric alkylation of glycine imine *tert*-butyl ester **58** (R = *t*-Bu in Scheme 3.26) was first reported by the group of *O'Donnell* in 1989.[86] In the presence of 10 mol % of the cinchona-alkaloid-derived PTC **60** (Scheme 3.27), the desired products

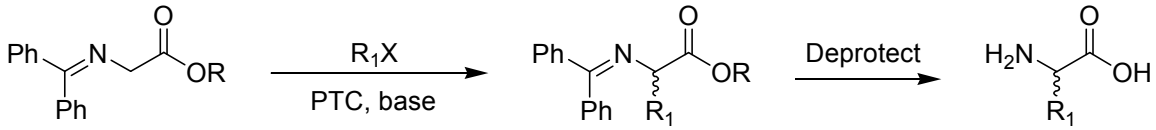

58 **59**

Scheme 3.26 Alkylation of glycine derivative for the preparation of α-amino acids.

of type **59** (R = *t*-Bu; Scheme 3.26) were obtained in good chemical yields (up to 82 %) and enantioselectivities up to 66 % ee.[86] Few years later, the same group made a remarkable improvement in the enantioselectivity by using modified alkaloid catalyst with an *O*-allyl substituent.[87] Applying the new *O*-allylated PTC **61** (Scheme 3.27) in the alkylation reaction led to enantioselectivities up to 81 % ee.[87] A further major enhancement in the enantioselectivity with a "jump" of ee values to the range >90 % was achieved simultaneously in 1997 by the *Lygo*[88] and *Corey*[89] group. They replaced the *N*-benzyl group of the *O'Donnell* catalyst with a 9-anthracenylmethyl group. The resulting PTCs **62** (Scheme 3.27) with either free or allylated OH group revealed their high catalytic potential with excellent enantioselectivities of up to 99.5 % ee

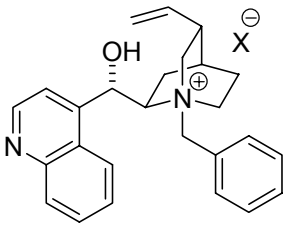

60

O'Donnell 1989

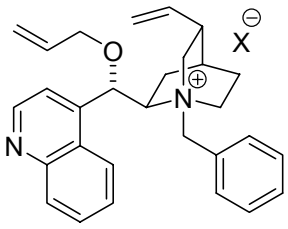

61

O'Donnell 1994

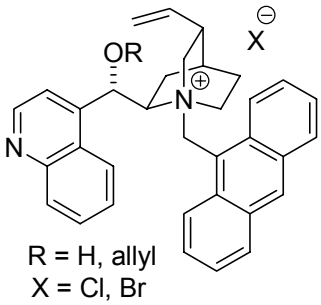

62

Lygo & *Corey* 1997

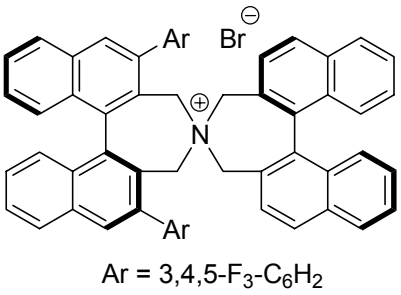

63

Maruoka 1999

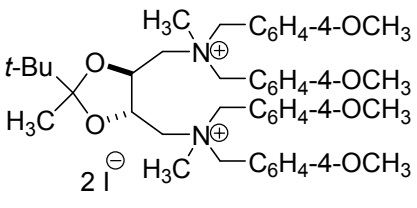

64

Shibasaki 2002

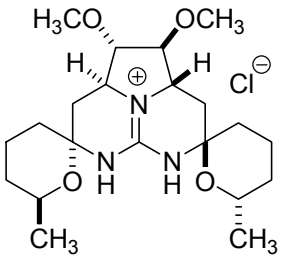

65

Nagasawa 2002

Scheme 3.27 Selected phase transfer catalysts for the asymmetric alkylation of glycine derivatives.

with both activated and non-activated alkyl halides as alkylating agents.[88, 89] Towards the end of the last century, *Maruoka* and co-workers developed a completely new type of robust and structurally rigid, C_2-symmetric, 1,1′-binaphthyl-derived chiral spiro ammonium salts for asymmetric alkylation of glycine imine *tert*-butyl ester **58**.[90, 91] In presence of only 0.2–1.0 mol % of the PTC **63** (Scheme 3.27), high yields of up to 98 % and excellent enantioselectivities, often 99 %, were obtained for the product **59** within very short reaction times (0.5 to 10 h).[90] Despite these tremendous advantages along with their modular structure for substrate-specific optimization, these catalysts suffer from the serious drawback for large scale applications due to their rather long synthetic route and expensive starting materials (they are not derived from the chiral pool). *Shibasaki* et al. reported a tartrate-derived two-centered C_2-symmetric phase-transfer catalyst **64** (Scheme 3.27) for the alkylation of **58** (R = *t*-Bu in Scheme 3.26) with active alkyl halides.[92] Using 10 mol % of this catalyst under optimum reaction conditions, high yields (up to 92 %) and enantioselectivities (up to 93 %) were obtained for a broad range of substrates.[92] The *Nagasawa* group introduced a chiral C_2-symmetric pentacyclic guanidinium cation **65** (Scheme 3.27) for the asymmetric alkylation of **58** (R = *t*-Bu in Scheme 3.26) with activated alkyl halides.[93] Applying 30 mol % of **65** as the catalyst, alkylated products were formed with moderate to good yields (61-85 %) and good enantioselectivities (76-90 %).[93]

Although this methodology is quite useful for the asymmetric synthesis of a wide range of aliphatic α-amino acids, it is not possible to synthesize aromatic α-amino acids by this technique.

3.4.2.3 Asymmetric hydrocyanation of imines

The addition of hydrogen cyanide to the *in situ* generated imines, the *Strecker* reaction, constitutes the oldest and most direct method for the synthesis of α-amino acids (Scheme 3.28a).[94] The versatility of this method stems from its simplicity and economical *via*bility for the production of

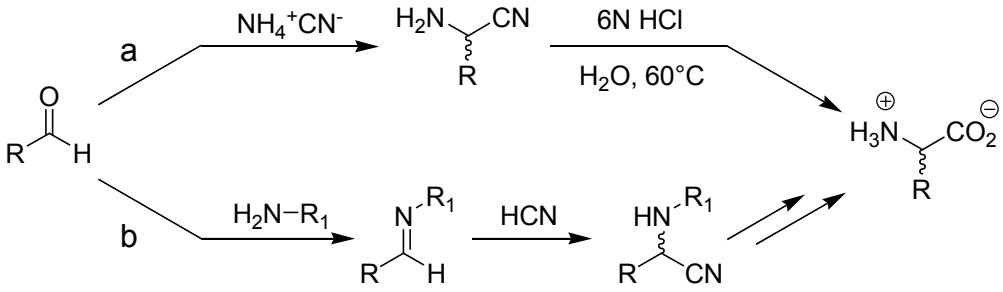

Scheme 3.28 The (a) original *Strecker* synthesis of α-amino acids and (b) its modified version.

α-amino acids both on lab scale as well as on technical scale. When using amines instead of ammonia, the pre-formation of imines, followed by hydrocyanation instead of the original one-pot synthesis represents a popular and widely used alternative route (Scheme 3.28b). The biggest advantage of this method is that, in principle, any α-amino acid can be synthesized *via* this route. Despite these practical advantages, this method suffers from the obvious limitation that the products obtained in this reaction are racemic. Consequently, an enantioselective version of the process, which could lead to the practical production of a wide range of α-amino acids, has been of great interest.

Significant progress has been made in the development of stereoselective versions of this reaction using imines bearing covalently attached chiral auxiliaries. This method entails substitution of ammonia with optically active amines, thereby providing some asymmetric induction, resulting in

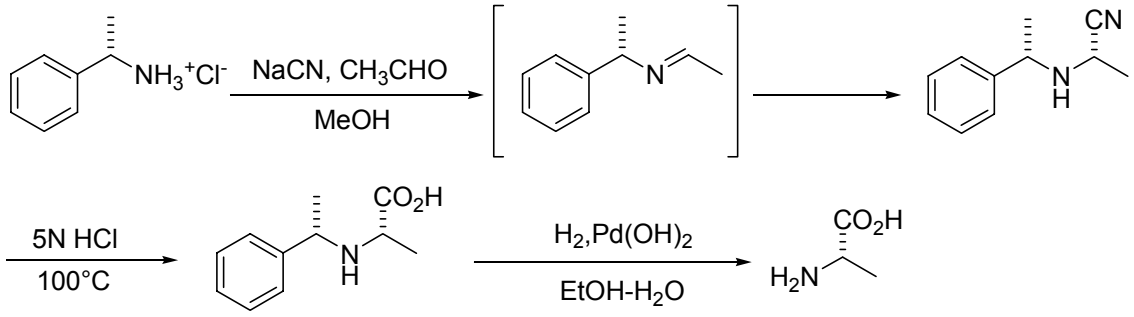

Scheme 3.29 *Harada*'s asymmetric synthesis of L-alanine by using a chiral auxiliary.[95]

diastereoselective addition of HCN to the imine. Particularly noteworthy in this field is the pioneering work of *Harada* in 1963: (–)-α-methylbenzylamine was used as the chiral auxiliary for the synthesis of L-alanine in 95 % ee (Scheme 3.29).[95] Although the auxiliary-based methods afford quite high enantioselectivities, the cost of using stoichiometric amounts of unrecoverable chiral auxiliaries prevents the adoption of these methods for the large-scale synthesis of α-amino acids. Practical substitutes for the chiral auxiliaries are chiral catalysts.[96, 97]

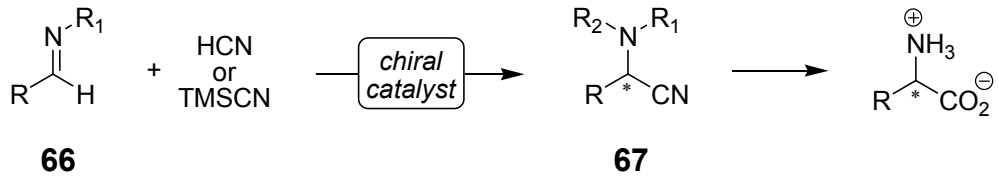

66 **67**

Scheme 3.30 Catalytic enantioselective cyanation of imines.

The progress of catalytic asymmetric hydrocyanation of imines took place mainly during the last decade.[96, 97] Most of the catalytic asymmetric syntheses of α-amino acids by this route are based on the use of preformed imines **66** and the subsequent nucleophilic addition of HCN or TMSCN in the presence of a chiral catalyst (Scheme 3.30). The enantioselective catalysts for the imine cyanation can be broadly divided into two major classes: catalysts containing *Lewis* acidic metal ion in their active site[96, 97] and metal-free catalysts or organocatalysts.[12, 96, 97]

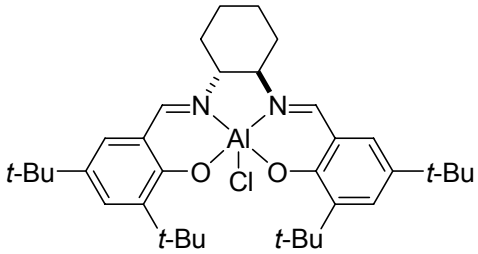

68

Jacobsen 1998

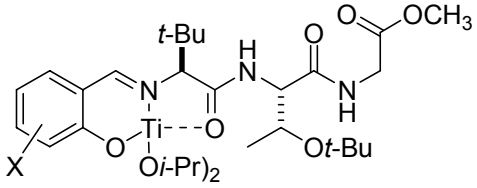

69

Hoveyda 1999

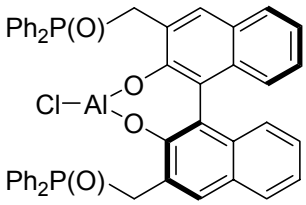

42

Shibasaki 2000

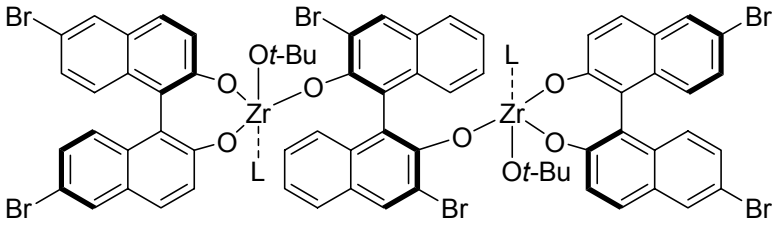

70

Kobayashi 2000

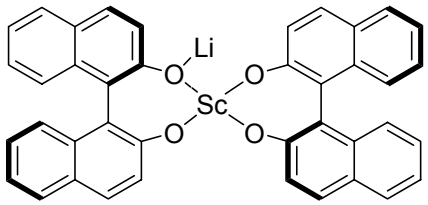

71

Vallée 2001

Scheme 3.31 Chiral metal catalysts for the asymmetric hydrocyanation of imines.

In recent years, several groups contributed to the development of successful metal catalysts for the catalytic asymmetric *Strecker* reaction. As a result, a number of chiral *Lewis* acid catalysts containing various metals (e.g. aluminium, titanium, zirconium, lanthanoid etc.) have emerged during the last few years (Scheme 3.31). It is noteworthy that each catalyst requires the use of a specific *N*-substituent (R_1 in Scheme 3.30) for obtaining good results. Thus, the preferred type of *N*-substituent depends on the type of applied catalyst.[97]

Jacobsen et al. reported the first example of a metal-catalyzed enantioselective addition of hydrogen cyanide to imines **66** (R_1 = allyl, Scheme 3.30) using a chiral Al(III)-salen complex **68** (Scheme 3.31).[98] A variety of *N*-allylimines was evaluated in the reaction catalyzed by 5 mol % of **68** at –70 °C over 15 h to give product **67**, which were isolated as trifluoroacetamides (R_1 = allyl, R_2 = CF_3CO; Scheme 3.30) in good yields (69-99 %) and moderate to excellent enantioselectivities

(37-95 % ee). Substituted arylimines **67** (R = Ar, Scheme 3.30) were the best substrates (79-95 % ee), while alkyl-substituted imines afforded products with considerably lower ee values (37-57 % ee).[98]

A year later, *Snapper*, *Hoveyda* and co-workers employed the Ti-complex **69** (Scheme 3.31) of a modular *Schiff* base ligand for the enantioselective *Strecker* reaction of aromatic *N*-benzhydrylimines **66** (R_1 = $CHPh_2$, Scheme 3.30) to give the addition product **67** (R_1 = $CHPh_2$, R_2 = H).[99, 100] Good to excellent enantioselectivities (85 to >99 % ee) were obtained in the presence of 5-10 mol % of **69** at 4 °C using TMSCN as the cyanide source. It was found that catalyst turnover was facilitated significantly in the presence of *i*-PrOH as an additive. Albeit most of the substrates studied are arylimines, the authors showed that alkyl imines can also be used and the products with same level of enantioselectivity as aryl substrate were achieved.[99] The aminonitriles **67** (R_1 = $CHPh_2$, R_2 = H, Scheme 3.30) are stable and can be readily converted to the corresponding amino acids with 6N HCl by concomitant cyanide hydrolysis and amine deprotection.[99]

The *Shibasaki* group disclosed a general asymmetric *Strecker*-type reaction that was controlled by bifunctional *Lewis* acid–*Lewis* base catalyst **42** (Scheme 3.31).[101] A variety of aromatic, aliphatic, heterocyclic, and *α*,*β*-unsaturated *N*-fluorenylimines underwent catalytic asymmetric trimethylsilylcyanation with 9 mol % of the binaphthol catalyst **42** at –40 °C to give *α*-aminonitriles in good to excellent yields (80-97 %) and enantioselectivities (72-95 % ee). The *α*-aminonitriles could then be converted into *α*-amino acids in several steps.The addition of phenol was found to have a beneficial effect on the reaction rates. The origin of high selectivity is believed to be attributed to the simultaneous activation of imines and TMSCN by the *Lewis* acidic Al(III) and the *Lewis* basic oxygen atom of the phosphane oxide, respectively.[101]

Kobayashi et al. developed the chiral zirconium binuclear catalyst **70** (Scheme 3.31) for the asymmetric synthesis of *α*-aminonitriles from aldimines with tributyltin cyanide (Bu_3SnCN).[102] An *o*-hydroxyphenyl group as an *N*-substituent (R_1, Scheme 3.30) was found to be beneficial for high asymmetric induction. Various aromatic, aliphatic, and heterocyclic aldimines were employed as substrate in this reaction; high levels of enantioselectivities (up to 91 % ee) were observed with these substrates. The most attractive aspect of *Kobayashi* catalyst **70** is that the catalytic asymmetric *Strecker* amino acid synthesis starting from achiral aldehydes, amines (R_2 = H, CH_3) and hydrogen cyanide has been achieved with this catalyst (Scheme 3.32).[102] It is interesting to note that 150 years after the discovery of the *Strecker* reaction, a truly efficient three-component asymmetric version has been accomplished. While the use of tributyltin cyanide is suitable for

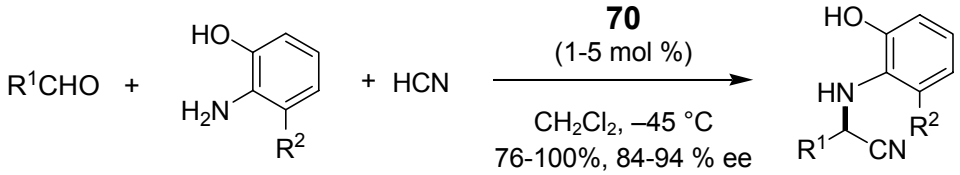

Scheme 3.32 *Kobayashi*'s three-component *Strecker* synthesis with chiral Zr-binuclear catalyst **70**.[102]

laboratory-scale experiments, industrial applications are expected for a more benign three-component catalytic asymmetric *Strecker* process using hydrogen cyanide.

The *Vallée* group reported the addition of TMSCN to aromatic and aliphatic aldehyde-derived *N*-benzyl aldimines **66** (R = alkyl/aryl, R_1 = $PhCH_2$; Scheme 3.30 on page 27) using heterobimetallic scandium complex **71** (Scheme 3.31).[103] In the presence of 10 mol % of **71**, high yields of 80 % and enantioselectivities of 91 % ee were obtained with *N*-benzyl benzaldimine after only 3 h reaction time.

In addition to these metal-catalyzed asymmetric cyanations, several versions of this process based on the use of organocatalysts have been developed so far.[12, 97] Interestingly, completely different types of organic molecules were found to possess the ability to catalyze this reaction (Scheme 3.30 on page 27).

In 1998 *Jacobsen* and co-workers identified a new type of organocatalyst *via* parallel library synthesis and screening of resin-bound derivatives.[36] This highly modular *Schiff* base-(thio)urea organocatalyst (Scheme 3.33) was optimized through iterative structural modification of various components.[37, 39, 40] As low as 1 mol% of the optimum catalyst **41** was found to effect asymmetric hydrocyanation of a wide range of aromatic, aliphatic *N*-allyl (also *N*-benzyl) aldimines and cyclic imines with excellent yields (up to 99 %) and enantioselectivities (up to >99 % ee) of the product **72** (Scheme 3.33).[37] The key elements responsible for the high enantioselectivity were the

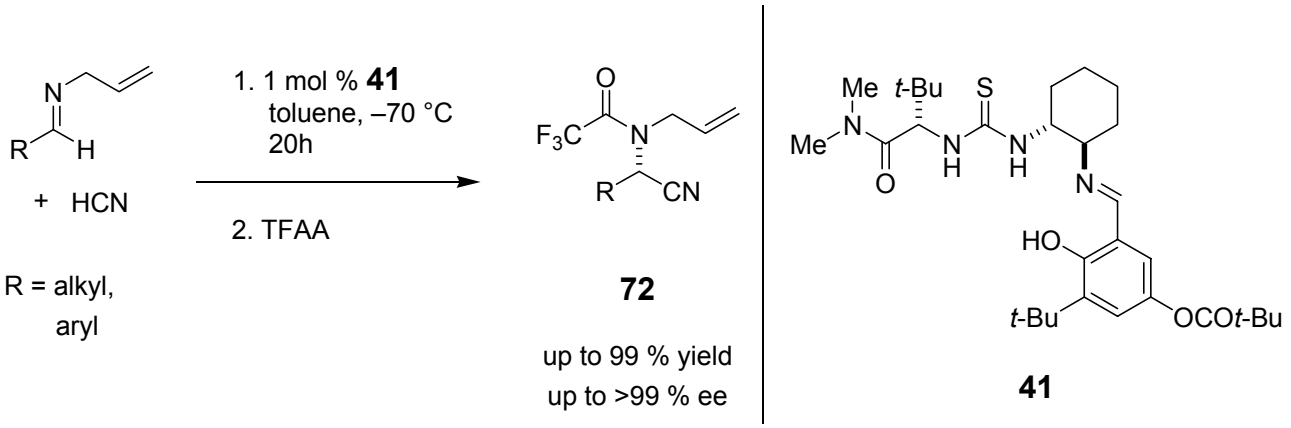

Scheme 3.33 *Jacobsen*'s organocatalytic asymmetric hydrocyanation of imines.

presence of bulky *tert*-butyl substituents at both the amino acid position and at the 3-position of the salicylimine moiety. The authors also demonstrated the practical potential of the resin-bound catalyst for the hydrocyanation of pivalaldimine (R = *t*-Bu). The resin-bound catalyst allowed purification of the product by simple filtration and solvent removal, and the catalyst could be reused indefinitely without loss of either activity or enantioselectivity.[37] They also investigated the mechanism of this hydrocyanation reaction. It is believed that the imine was activated by the reversible binding of its *Z*-isomer to the catalyst through bifurcated hydrogen bonding from the thiourea *NH*s and addition of HCN takes place over the diaminocyclohexane portion of the catalyst.[39]

The *Corey* group reported a C_2-symmetric bicyclic guanidine as a bifunctional catalyst for the addition of HCN to achiral *N*-benzhydryl imines (Scheme 3.34).[49] In the presence of 10 mol% of **43**, aromatic and aliphatic *N*-benzhydryl imines undergoes hydrocyanation to afford *N*-benzhydryl-*α*-amino nitriles with high yields (88-99 %) and high enantioselectivities (up to 86 % ee). It turned out that the choice of the *N*-substituent is of importance. In contrast to the high

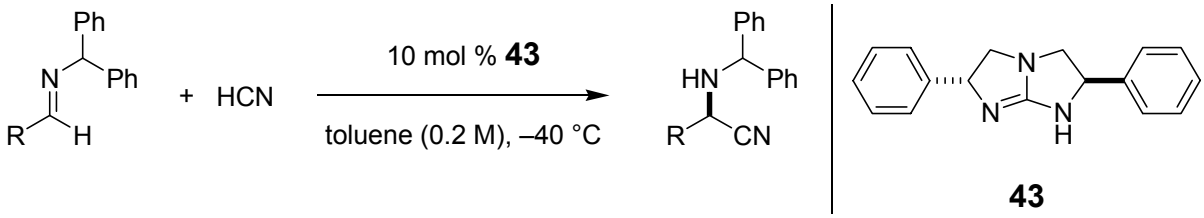

Scheme 3.34 *Corey*'s asymmetric hydrocyanation of imines with the chiral guanidine catalyst.

enantioselectivities achieved with imines bearing *N*-benzhydryl substituent, remarkably lower ees (0-25 % ee) were observed with other *N*-substituents like *N*-benzyl or *N*-(9-fluorenyl). It is noteworthy that when aliphatic imines were used, the product was obtained with opposite selectivity (*S*-enantiomer major) compared to the aromatic imines (*R*-enantiomer major). The effect has been mechanistically explained by the *Corey* group.[49] The hydrogen atom (attached to the nitrogen of the guanidine) is essential for catalytic activity. From the viewpoint of practical application, this catalyst system is interesting because the catalyst **43** can be recovered for reuse in 80-90 % yield by extraction with oxalic acid.

Whereas these two organocatalysts activate the substrate imines *via* hydrogen bonding from the *NH*s, organic molecules without any NH bond, appear to be able to catalyze the cyanation of imines. *Feng* and *Jiang* found that in the presence of chiral *N*-oxides **73** (Scheme 3.35), the reaction of several types of aldimines and TMSCN furnished the desired *α*-amino nitrile in yields of

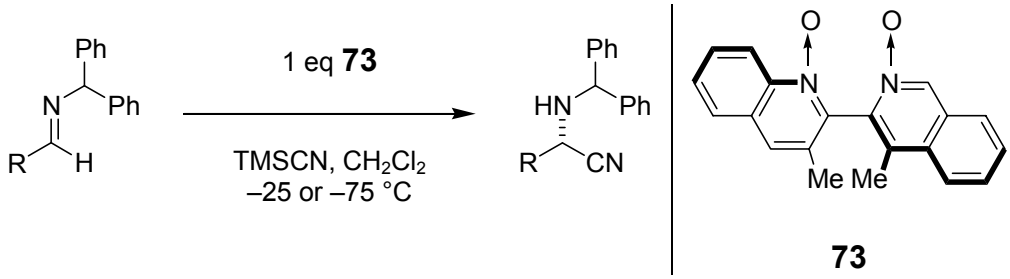

Scheme 3.35 *Feng*'s asymmetric cyanosilylation mediated by chiral *N*-oxides.

up to 95 %, and with enantioselectivities in the range of 37-73 % ee.[104] However, stoichiometric amount of the chiral *N*-oxide **73** is required. Besides the use of a stoichiometric amount of *N*-oxide and medium enantioselectivities, another drawback is the use of TMSCN as the cyanide source from both atom-economical and industrial considerations.

Recently, *Corey* et al. reported another type of catalyst, namely a chiral ammonium salt **74** (Scheme 3.36) that possesses an activating site and a binding pocket for *N*-allyl aldimines as substrate.[105] In the presence of 10 mol % of **74**, hydrocyanation occurs smoothly with a series of *N*-allyl aromatic

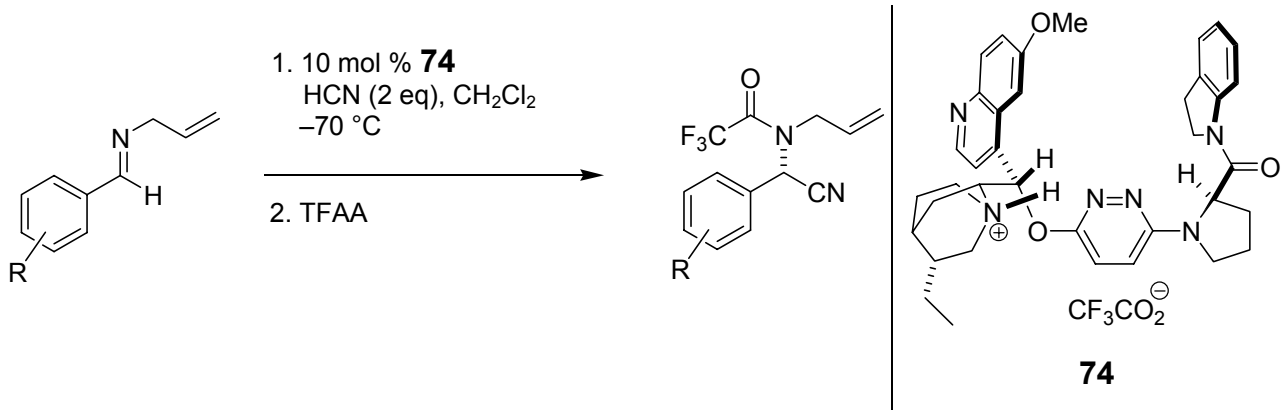

Scheme 3.36 *Corey*'s asymmetric hydrocyanation of imines with chiral ammonium salt.

aldimines at –70 °C to give the corresponding (*S*)-*α*-amino nitrile in excellent yields (86-98 %) and good to excellent enantioselectivities (79 to >99 % ee). Like in the case of C_2-symmetric guanidine catalyst **43** (Scheme 3.34), here also the choice of the *N*-substituent is important as the *N*-benzyl or *N*-benzhydryl aldimines afforded products with lower ees.[105] Dichloromethane was the preferred solvent over toluene, presumably due to the ability of toluene to compete with the aldimine substrate for the U-shaped binding pocket. An interesting aspect of this process is that the catalyst **74** can be recovered with ca. 90 % efficiency by chromatographic purification. The main disadvantage of this method is the limited substrate scope, i.e. only aromatic aldimines can be used as the substrates.

3.4.2.4 Miscellaneous examples of *α*-amino acid synthesis

Johannsen[106] and *Jørgensen*[107] group independently applied the combination of $CuPF_6$ and (*R*)-tol-BINAP in the addition reaction of imino esters **75** to electron-rich aromatic compounds (Scheme 3.37). The reaction led to protected optically active *α*-aryl *α*-amino acid esters **76** generally in good to high yields, high regioselectivities and enantioselectivities (up to 98 % ee). The limitation with this addition reaction is, however, the restriction to electron-rich aromatic compounds.

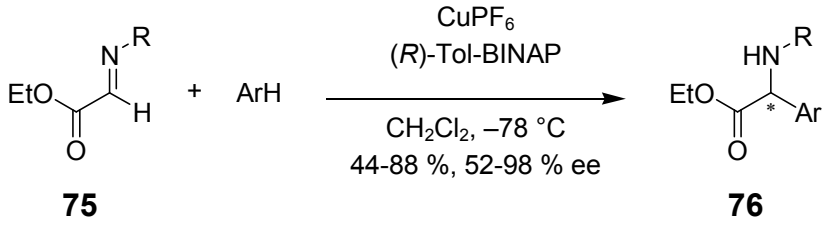

Scheme 3.37 The catalytic asymmetric arylation of *α*-imino esters.[106, 107]

List and co-workers established a practical synthesis of *α*-amino acids via a proline-catalyzed *α*-amination of aldehydes with dibenzyl diazodicarboxylate **I** (Scheme 3.38).[108] A simple oxidation of the aldehyde intermediates **II** gave the chiral non-racemic *α*-hydrazino carboxylic acids **III**. Reductive N–N bond cleavage and simultaneous protecting group removal provides unprotected *α*-amino acids **IV** with moderate yields and high ees.[108]

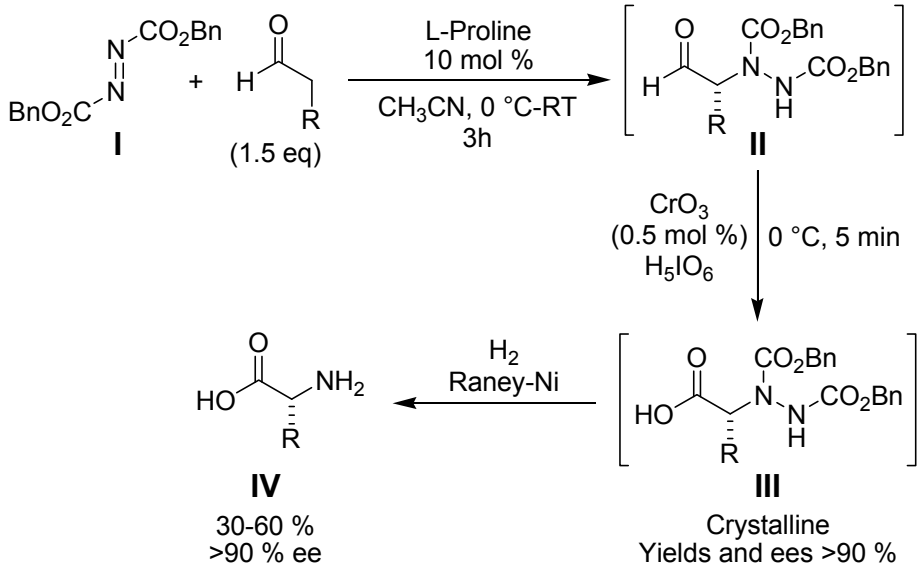

Scheme 3.38 Direct catalytic asymmetric *α*-amination in the synthesis of *α*-amino acids.[108]

3.5 The Routes to enantiomerically pure *β*-amino acids

In contrast to proteinogenic *α*-amino acids which are constituents of all enzymes which control the metabolism in living organisms and are thus an essential prerequisite for life, most *β*-amino acids only occur as constituents of distinct natural products, such as peptides, cyclopeptides, depsipeptides, glycopeptides, alkakoids, or terpenoids.[109] Apparently, bacteria, cyanobacteria, fungi, and plants often incorporate *β*-amino acids into secondary metabolites that serve as tools to secure their survival in competition with other organisms. Therefore, these compounds are frequently characterized by potent biological and physiological activities that are often crucially based on their *β*-amino acid substructures. As a consequence, enantiomerically pure *β*-amino acids are of considerable importance because they are crucial components of medicinally useful molecules such as the anti-cancer natural product taxol **77** or the potent anti-tumor depsipeptide cryptophycin **78** (Scheme 3.39).[110]

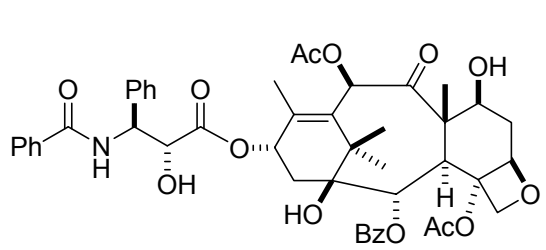

Taxol, **77**

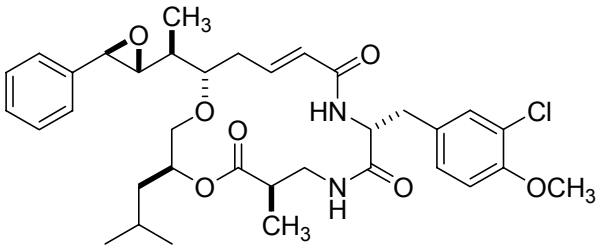

Cryptophycin, **78**

Scheme 3.39 *β*-Amino acid containing pharmaceuticals.

Moreover, the incorporation of *β*-amino acids into peptides instead of *α*-amino acids increases their stability against degradation by mammalian peptidases.[111] This enhanced stability is caused by a lack of enzymes which allow cleavage of peptidic bonds between *α*-amino acids and *β*-amino acids.[112] Therefore, *β*-amino acids are an important tool in the development of peptide-like drugs capable of withstanding hydrolytic degradation for prolonged period of time.[111] Furthermore, *β*-amino acids are synthetic precursors of *β*-lactams, which are potentially biologically active and of current interest.[113]

The simplest *β*-amino acid is *β*-aminopropionic acid which is also called *β*-alanine. Although this is not a proteinogenic amino acid, it is an essential component of many relevant, biologically active compounds, such as vitamin B_3/pantothenic acid (Scheme 3.40).

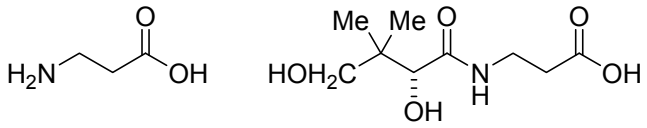

β-Alanine (*R*)-(+)-Pantothenic acid

Scheme 3.40 The simplest *β*-amino acid and vitamin B_3.

There are three general types of open-chain chiral *β*-amino acids, depending on whether the substituents are at the carbon next to the carboxyl group (*α*-substituted), the carbon next to the amino group (*β*-substituted), or at both positions (*α*,*β*-disubstituted) (Scheme 3.41).

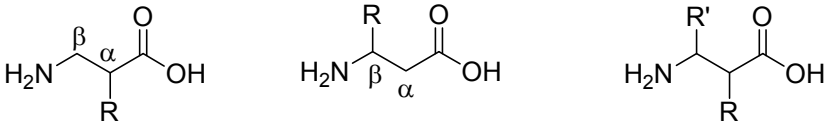

α-substituted *β*-substituted *α*,*β*-disubstituted

Scheme 3.41 The classification of *β*-amino acids.

There is no single "best" approach towards enantiomerically pure *β*-amino acids. Each method itself possesses its own advantages and limitations. Nevertheless, likewise *α*-amino acids (see section 3.4 on page 18), there are two general ways for obtaining enantiomerically pure *β*-amino acids[76, 110, 114, 115]: (i) resolution of racemic mixture, and (ii) asymmetric synthesis.

3.5.1 Resolution of racemic *β*-amino acids

3.5.1.1 Classical resolution of *β*-amino acids

A traditional method to resolve a carboxylic acid is to transform its racemic mixture into diastereomeric salts *via* complexation with a chiral base. Ephedrine is among the most commonly used chiral bases in this process, as it is readily available and inexpensive. Upon treatment of racemic *N*-protected *β*-amino acids with (–)-ephedrine two diastereomeric salts will be produced (Scheme 3.42) which can then be separated by fractional crystallization. After separation, the resulting diastereomerically pure salt can be easily converted back to the free acids while the chiral base can be recovered and reused. However, multistep fractional recrystallization is often required, and therefore the sequence is long and tedious. Following this methodology, a few *β*-substituted *β*-amino acids and carbocyclic *β*-amino acids were resolved in enantiopure form.[116]

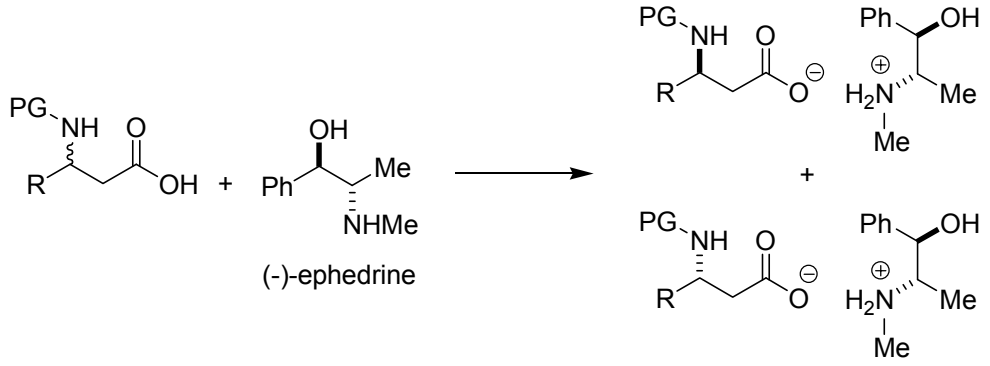

Scheme 3.42 Resolution of *β*-amino acids using a chiral base.

Alternatively, racemic amines can be transformed into diastereomeric salts with a chiral acid. *β*-Amino esters were resolved through diastereomeric salt formation between the amino group and a chiral acid, such as tartaric acid, mandelic acid or camphorsulfonic acid.[117]

3.5.1.2 Enzymatic resolution of *β*-amino acids

Despite the prominent role of the enzymatic resolution of racemates in the production of *α*-amino acids, far fewer results on its application for the preparation of enantiopure *β*-amino acids appear to exist. Indeed, a disadvantage of the enzymatic method is often the narrow tolerance of the substrate; thus the different position of the chiral center, usually *α* to the carbonyl group, can be a reason why the more popular methods for the enzymatic separation of *α*-amino acid derivatives fail when applied to the *β*-amino acid derivatives.

Most of the resolution methods reported[118] so far involve either the selective acylation of the amine group of the racemic *β*-amino acids with some acylating agents (Scheme 3.43a), selective hydrolytic de-acylation of racemic *N*-acyl *β*-amino acids (Scheme 3.43b), or selective hydrolysis of the ester (Scheme 3.43c) under the condition of kinetic resolution in the presence of enzymes. Several different enzymes are employed for these purposes but only few of them, namely various lipases (e.g. CAL-A, CAL-B), acylases (penicillin G acylase or PGA) or amidases are found to effect the acylation or hydrolysis reactions with high selectivities. Although in some cases the enantioselectivities obtained are as high as >99 % ee and the enzymatic approach is the method of choice to prepare enantiomers of the corresponding *β*-amino acids, the major disadvantage of these biocatalytic procedures is the limit of 50 % theoretical yield for the resolution process. Moreover, these enzymes are highly substrate specific and thus restrict their application to differently substituted *β*-amino acids.

(a) *Acylation strategy for resolution*

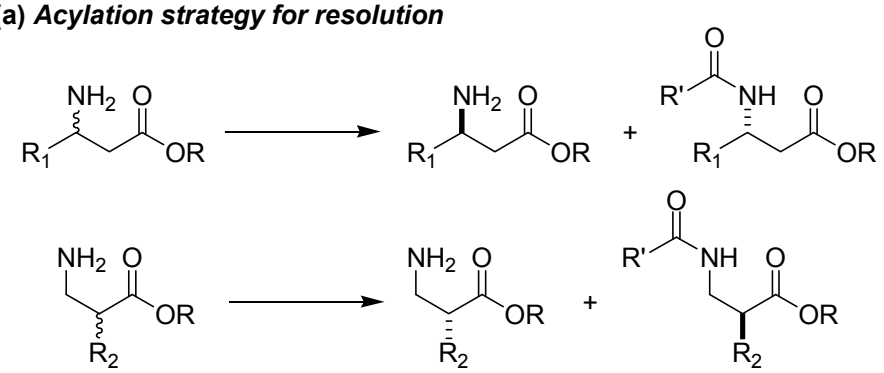

(b) *De-acylation strategy for resolution*

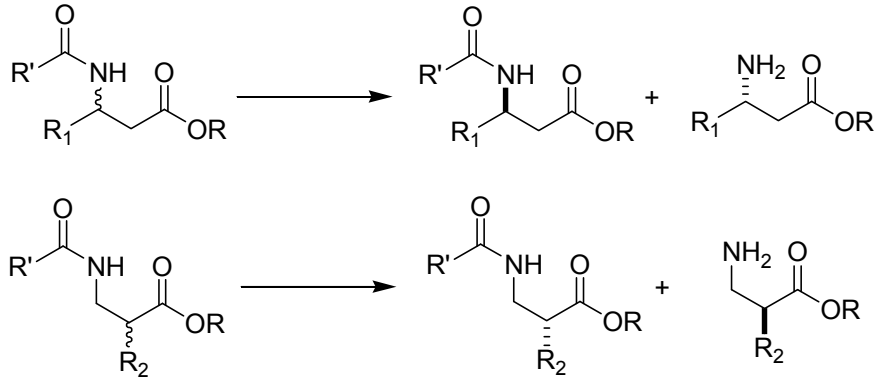

(c) *Ester hydrolysis strategy for resolution*

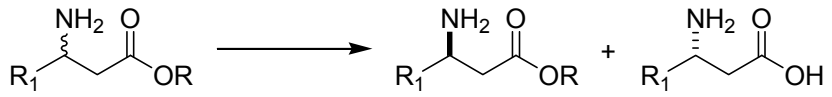

Scheme 3.43 Strategies for the enzymatic resolution of *β*-amino acids.

3.5.2 Enantioselective synthesis of *β*-amino acids

Enantioselective synthesis of *β*-amino acids can be broadly classified into three categories: (i) the chiral pool approach, (ii) the auxiliary-based approach, which can be more appropriately called diastereoselective synthesis and (ii) the catalytic asymmetric synthesis.

3.5.2.1 The chiral pool approach

α-Amino acids are ideal chiral pool compounds for the preparation of *β*-amino acids. This is due not only to the fact that a plethora of methods for their synthesis is available[75] but also to the stereogenic center present in these compounds that, on utilization of suitable methods, is retained

without significant racemization in the homologated *β*-amino acids.[110] Direct homologation of *α*-amino acids to prepare *β*-amino acids following the *Arndt-Eistert* procedure has found many applications in small molecule as well as natural product synthesis.[115] In this approach (Scheme 3.44), the *N*-protected *α*-amino acids **I** were converted to the mixed anhydrides using $Et_3N/ClCO_2Et$, followed by addition of diazomethane to afford the diazoketones **II** with good yield

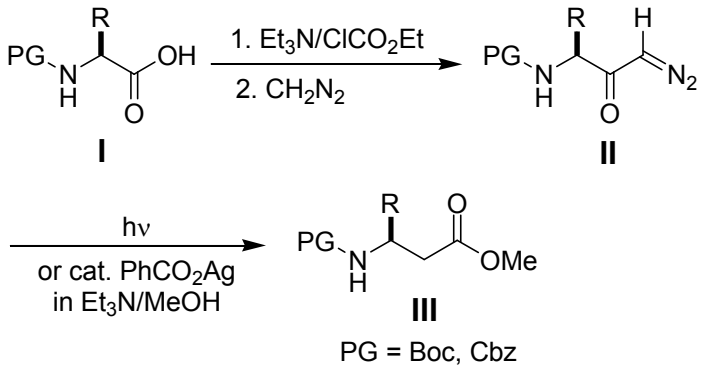

Scheme 3.44 *Arndt-Eistert* homologation of *α*-amino acids for the synthesis of *β*-substituted *β*-amino acid derivatives.

and in enantiomerically pure form. *Wolff* rearrangement of diazoketones to the *β*-substituted *β*-amino acid derivatives (here ester **III**) was most conveniently achieved with catalytic amounts of silver cations, although photochemical or thermal conditions can be employed similarly.[110]

Photo induced *Wolff* rearrangement was applied in the homologation to *α,β*-disubstituted *β*-amino acid derivatives.[119] In this approach (Scheme 3.45), the diazoketones **II** was converted to the *α*-alkyl diazoketones **IV** with alkyl halides. Photo-*Wolff* rearrangement of **IV** generates *α,β*-disubstituted *β*-amino acid derivatives **V** in good yield (up to 77 %) favoring the *anti* products.

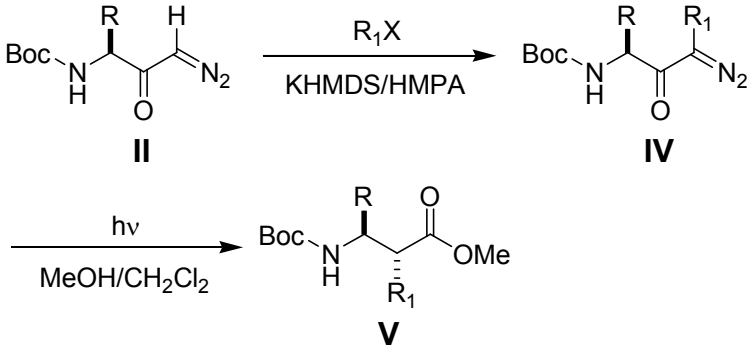

Scheme 3.45 Homologation strategy for the synthesis of *α,β*-disubstituted *β* amino acid derivatives.[119]

While the *Arndt-Eistert* protocol works very well for the preparation of enantiomerically pure *β*-substituted as well as *α,β*-disubstituted *β*-amino acid derivatives, it is not suitable for large scale

synthesis due to the high cost of the silver catalyst and difficult handling of the hazardous reagent CH_2N_2. *Longobardo* and co-workers have reported a new way to synthesize *β*-amino acids *via* reduction of *N*-protected *α*-amino acids, followed by conversion of the corresponding *β*-amino alcohols to *β*-amino iodides and then to *β*-amino cyanides (Scheme 3.46).[120]

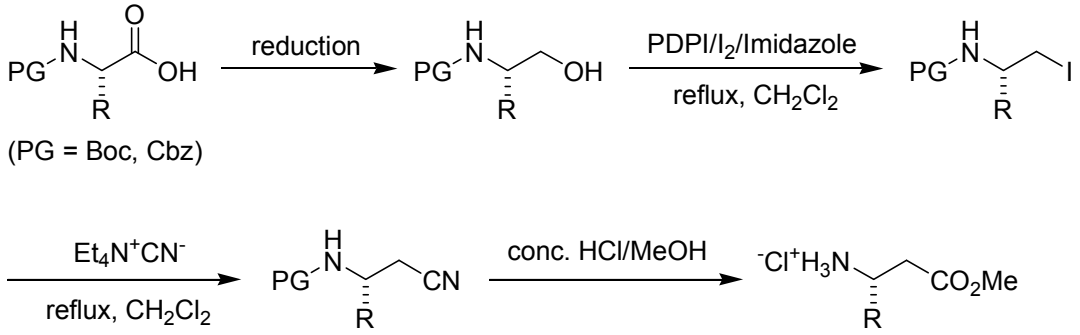

Scheme 3.46 Alternative homologation strategy for the synthesis of *β*-substituted *β*-amino acid derivatives.[120]

The key step of this transformation was to generate the iodide in high yields and without racemization using polystyryl diphenylphosphine-iodide (PDPI) complex.[120]

Besides the homologation approaches described above, there are other strategies known for the synthesis of enantiopure *β*-amino acids using asparagine and aspartic acid as chiral pool compounds.[115]

3.5.2.2 The auxiliary-based approach

Analogous to the *α*-amino acids (section 3.4.2.3, page 26), enantioselective synthesis of *β*-amino acids has also been achieved by addition to imines containing a chiral auxiliary. The chiral imines used in this case were *tert*-butylsulfinyl imines **79**, derived from chiral *tert*-butylsulfinamide **80** (Scheme 3.47).[121] Addition of Ti(O*i*-Pr)$_3$ ester enolates to *tert*-butylsulfinyl imines **79** provides

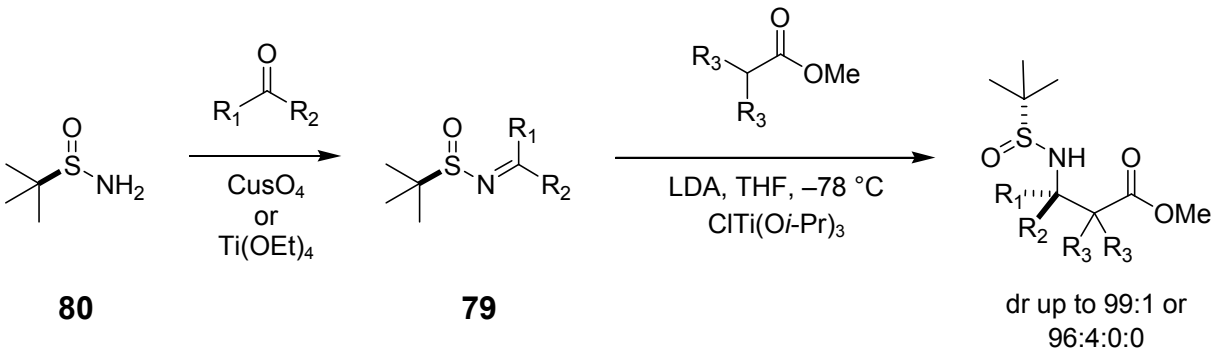

Scheme 3.47 Synthesis of *N*-*tert*-butylsulfinyl protected *β*-amino esters.[122, 123]

N-tert-butylsulfinyl protected *β*-substituted, *α*,*β*-disubstituted, *α*,*β*,*β*- and *α*,*α*,*β*-trisubstituted, and *α*,*α*,*β*,*β*-tetrasubstituted *β*-amino acid derivatives in high yields and with high diastereoselectivities (Scheme 3.47).[122, 123]

The *N-tert*-butylsulfinyl protecting group is cleaved using HCl in MeOH to afford *β*-amino esters (Scheme 3.48).[123] For *β*-substituted amino esters, the methyl ester is saponified using LiOH in MeOH and H_2O without any deprotection of the *N*-sulfinyl-protected amine (Scheme 3.48).[123]

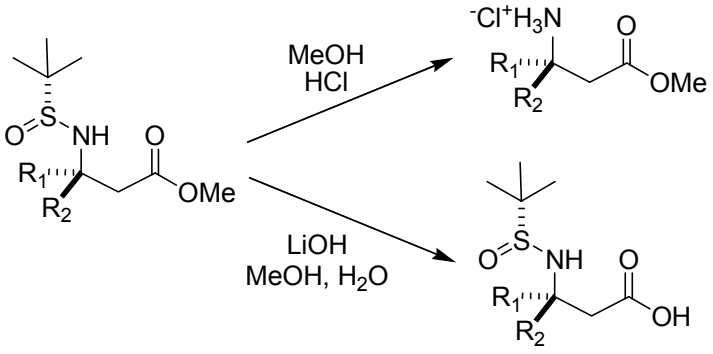

Scheme 3.48 Chemoselective cleavage of protecting groups of *N*-sulfinyl-protected *β*-amino esters.[124]

Like any auxiliary-based synthesis, this approach also suffers from the limitation of the consumption of stoichiometric amounts of unrecoverable chiral auxiliaries. However, in this particular case this drawback is at least partially counterbalanced by easy accessibility of the chiral auxiliary **80**.[124]

3.5.2.3 The catalytic asymmetric synthesis

As with *α*-amino acids, all catalytic asymmetric syntheses of *β*-amino acids involve C–H, C–C or C–N bond formation as the key step.[110]

Enantioselective hydrogenation of prochiral *β*-(acylamino)acrylates **81** under the influence of a chiral catalyst offer one of the most efficient routes for the large scale preparation of enantiopure *β*-substituted *β*-amino acids (Scheme 3.49).[125] A large number of catalysts based on Ru or mainly

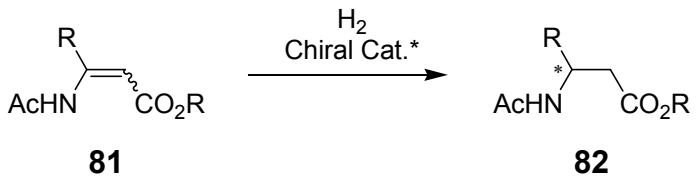

Scheme 3.49 Asymmetric hydrogenation of *β*-(acylamino)acrylates **81**.

Rh and chiral phosphine ligands were applied for this reaction with varying results.[125] Like for the hydrogenation route to the *α*-amino acids, here also a major concern was the double bond configuration of the substrates as the enantioselectivities of the products obtained vary with *E*- or *Z*-configuration of the double bond depending on the catalyst employed. There is no single choice of catalyst that is suitable for every substrate, though Rh-complexes were found to be superior compared to the Ru-complexes.[125]

As for the *α*-amino acids, Rh-complex of Me-DuPHOS (**54**, R = Me, Scheme 3.50) of type [(diene)Rh(diphosphine)]OTf was also found to be quite efficient for the hydrogenation of

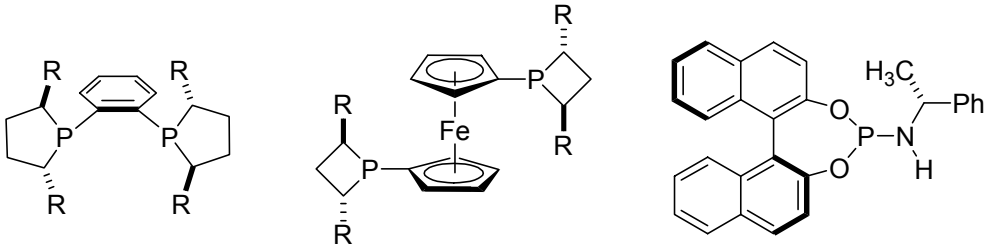

DuPHOS **54** Ferrotane **83** (*S*,*R*)-**84**

Scheme 3.50 Chiral phoshphine ligands for Rh-catalyzed asymmetric hydrogenation of *β*-(acylamino)acrylates.

E-*β*-(acylamino)acrylates with aliphatic substituents, afforded *β*-alkyl substituted *β*-amino acid derivatives with up to >99 % ee.[126] On the other hand, for the synthesis of *β*-aryl substituted *β*-amino acid derivatives, Rh-complex of Et-Ferrotane (**83**, R = Et, Scheme 3.50) of type [Rh-Et-Ferrotane$(CH_3OH)_2$]BF_4 turned out to be highly effective.[127] A range of *E*-*β*-aryl-substituted *β*-(acylamino)acrylates containing both electron-donating as well as electron-withdrawing substituents were hydrogenated in the presence of 1 mol % of the Et-Ferrotane-Rh complex to generate the desired products with enantioselectivities between 98 and >99 % ee.

Although the field of asymmetric hydrogenation has been dominated by bidentate phosphine ligands, high enantioselectivities could also be achieved using monodentate phosphine ligands. *Feringa* et al. recently reported the use of monodentate phosphoramidite (*S*,*R*)-**84** (Scheme 3.50) for the asymmetric hydrogenation of *Z*-*β*-substituted *β*-(acylamino)acrylates.[128] Fairly high enantioselectivities (92-94 % ee) were obtained for alkyl and some aryl substituted *β*-(acylamino)acrylates.

Enantioselective C–C bond formation reaction was applied by several groups for the synthesis of *β*-amino acids.[76, 110] Most of these approaches involve asymmetric *Mannich*-type reactions as the C–C bond formation step. *Kobayashi* and co-workers reported the first example of catalytic

enantioselective *Mannich*-type reactions of aldimines **85** with silyl enolates **86** using a Zr(IV)-based chiral *Lewis* acid catalyst **87** (Scheme 3.51).[129] This reaction afforded optically active *β*-amino acid derivatives **88** in high yields (70-100 %) and enantioselectivities (83-98 % ee).

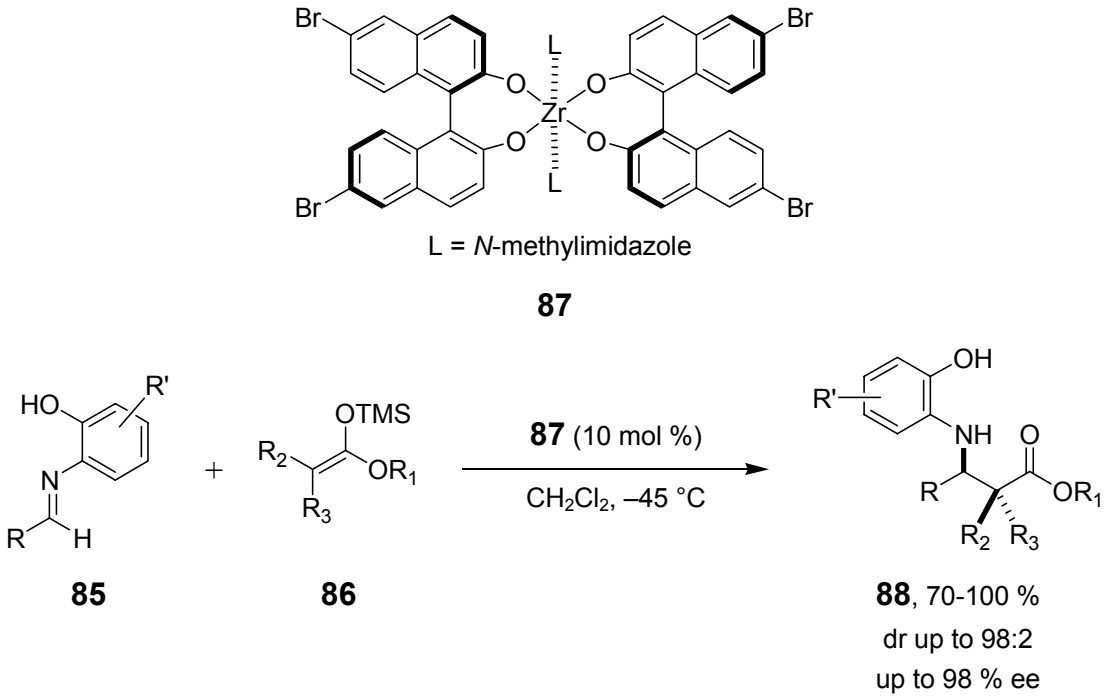

Scheme 3.51 *Kobayashi*'s catalytic asymmetric *Mannich*-type reaction for the synthesis of *β*-amino acid derivatives.[129]

The key elements responsible for the high yields, selectivities, and the catalyst turnover were the presence of *N*-substituted hydroxyphenyl moiety at the aldimine groups and the electron-withdrawing groups at the 6,6′-positions of the catalyst **87**. Both *syn*- and *anti*-products were obtained depending on the *O*-substitutents (R_1) of the silyl enolates **86** with selectivities up to 98:2.[130] In the reactions with aliphatic aldimines, high enantioselectivities were obtained using imine **85** prepared from the aldehydes and 2-amino-3-methylphenol (R′ = 3-Me).[129] This method is only suitable for the synthesis of *α*,*β*-disubstituted *β*-amino acid derivatives.

In 2002 *Jacobsen* et al. reported a highly efficient organocatalytic route to *N*-Boc protected *β*-substituted *β*-amino acids *via* the *Mannich*-type reaction using the thiourea catalyst **89** (Scheme 3.52).[41] Aldimines derived from aromatic aldehydes gave products in high yields and with high enantiomeric excesses. This method is particularly suited for the highly enantioselective synthesis of thienyl-, furyl-, pyridyl- and quinolinyl-substituted *β*-amino acid derivatives.

In addition to the two methods described above there are several other, particularly organocatalytic[131] methods for the synthesis of *β*-amino acids *via* enantioselective *Mannich*-type reactions.

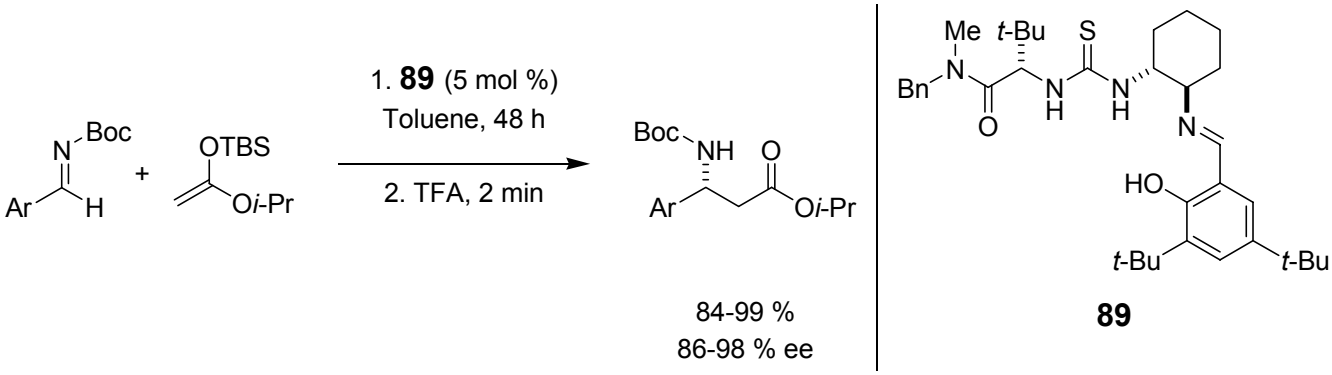

Scheme 3.52 *Jacobsen*'s organocatalytic asymmetric *Mannich*-type reaction for *β*-amino acid synthesis.[41]

Jacobsen group also developed a method for the synthesis of *α*-substituted *β*-amino acid derivatives *via* Al(III)(salen)Cl **68** catalyzed conjugate addition of cyanide to the *α*,*β*-unsaturated imides **90** (Scheme 3.53).[132] The hydrocyanation adducts **91** were obtain in high yields and with very high

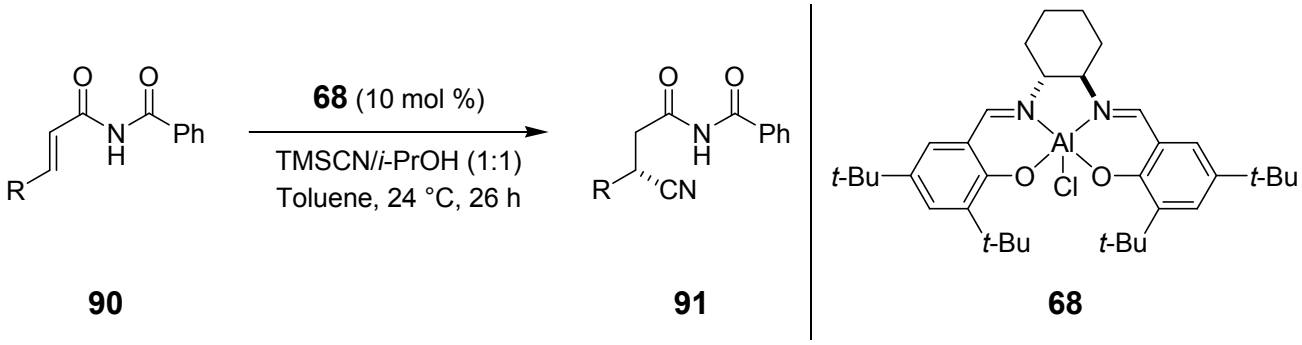

Scheme 3.53 Enantioselective conjugate addition of cyanide to *α*,*β*-unsaturated imide.[132]

enantioselectivities. Conversion of **91** to the corresponding acid followed by *Curtius* rearrangement yielded Boc-protected cyanoamid which was subsequently hydrolyzed to afford Boc-protected *α*-substituted *β*-amino acid in excellent yield with only a very small degree of racemization (Scheme 3.54).[132] One limitation of this method is that this is applicable for the synthesis of *β*-amino acids with only aliphatic *α*-substituents.

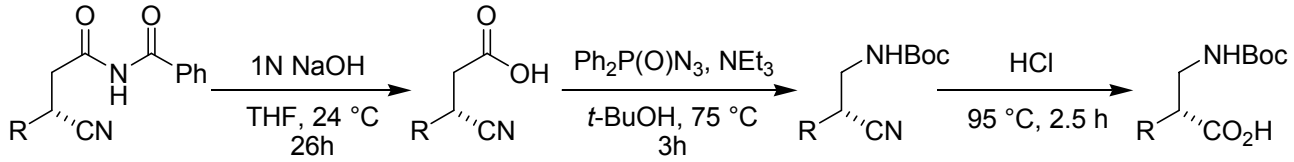

Scheme 3.54 Conversion of into **91** *α*-substituted *β*-amino acid.[132]

Catalytic enantioselective conjugate addition of an ammonia equivalent to *α*,*β*-unsaturated carboxylic acid derivatives represents another attractive and versatile method for the synthesis of

enantiopure *β*-amino acids.[110] *Myers* and *Jacobsen* have developed an Al(III)(salen)Me complex **92** catalyzed addition of hydrazoic acid (HN_3) to a range of *α,β*-unsaturated imides **90** (Scheme 3.55).[133] In the presence of 5 mol % of **92**, the imides **90** were converted to the azide adducts **93**

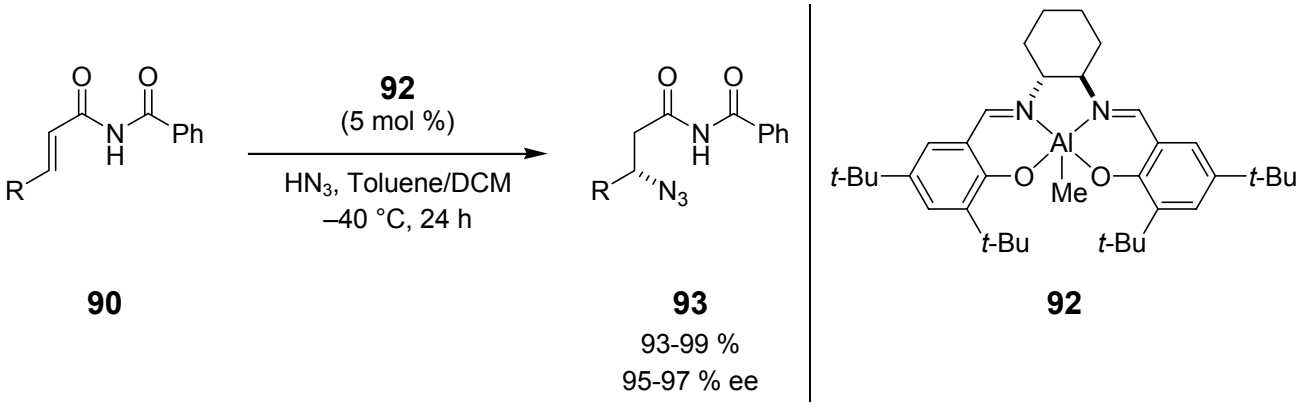

Scheme 3.55 Enantioselective conjugate addition of hydrazoic acid to *α,β*-unsaturated imide.[133]

in high yields (93-99 %) and with excellent enantioselectivities (95-97 % ee). Products **93** can be converted to the desired *β*-substituted *β*-amino acids in two simple steps; reduction of azide in the presence of Boc_2O afforded an intermediate carbamate which can be hydrolyzed using NaOH to afford the Boc-protected amino acid in high yield.[133] However, this method is restricted only to the aliphatic substituents; only moderate ee was obtained for substrate with aromatic substituent.

Miller and co-workers also reported an organocatalytic conjugate addition of azide to imides using a peptide based catalyst to produce *β*-amino acid derivatives with up to 92 % ee.[134]

Besides azide, amines have also been used as the ammonia equivalent for conjugate addition to the *α,β*-unsaturated acid derivatives. The *Sibi* group developed a magnesium-based chiral *Lewis* acid catalyzed addition of *O*-benzylhydroxylamine to 3,5-dimethylpyrazole-derived enoate **94** (Scheme 3.56).[135] In the presence of 30 mol % of $MgBr_2$ and the bisoxazoline **95**, *β*-amino acid derivatives **96** were obtained in good yields and with high enantioselectivities.

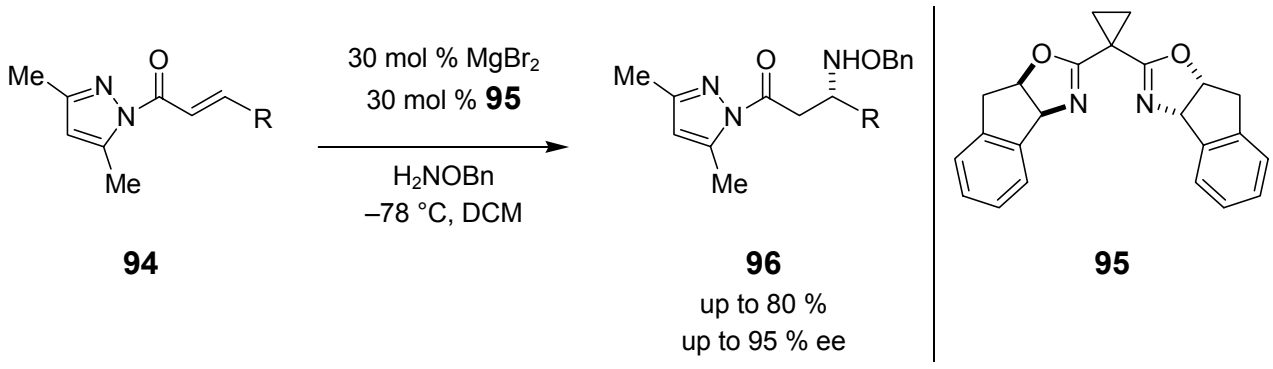

Scheme 3.56 *Sibi*'s enantioselective conjugate addition of $BnONH_2$.[135]

4 Concept

4.1 Synthesis of new bifunctional organocatalysts for the DKR of azlactones and KR of oxazinones

The goal of this work was to develop metal-free catalysts for the dynamic kinetic resolution (DKR) of azlactones **A** and kinetic resolution (KR) of oxazinones **C** (Scheme 4.1). The alcoholytic ring opening of azlactones **A** (or *ent*-**A**) in the presence of an suitable chiral catalyst would generate *N*-acyl-*α*-amino acid esters **B** (see section 3.4.1.2 on page 20), an *N*,*C*-doubly protected *α*-amino acid derivative (Scheme 4.1a). Formal insertion of a methylene group between the carbonyl group and the *α*-C-atom of the azlactone shifts the nitrogen atom to the *β*-position. The resulting compounds are known as 4,5-dihydro-1,3-oxazin-6-ones **C** which, in contrast to azlactones, are

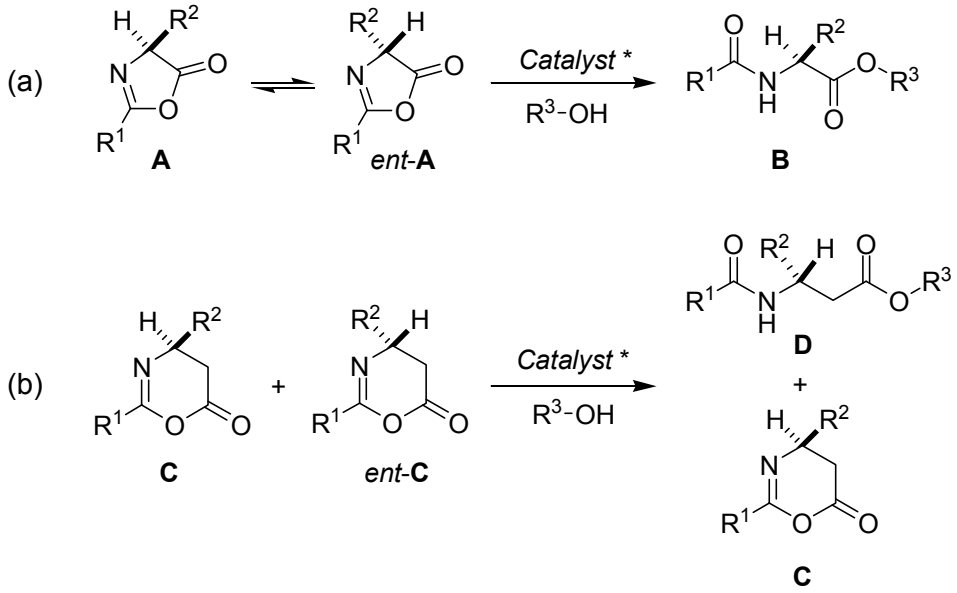

Scheme 4.1 General concept for (a) the DKR of azlactones and (b) KR of oxazinones.

configurationally stable. The alcoholytic ring opening of these oxazinones in the presence of an appropriate chiral catalyst would lead to kinetic resolution: one enantiomer of the oxazinones (e.g. *ent*-**C**) would be converted to the corresponding *N*-acyl-*β*-amino acid ester **D** whereas the other (e.g. **C**) would remain unaffected.

From the work of *Jacobsen*[39] and *Takemoto,*[53] it was known that urea and thiourea can activate imines or nitroolefins towards nucleophilic attack by bifurcated hydrogen bonding from both NHs

of the (thio)urea moiety. The activation of carbonyls in the similar way was also demonstrated by *Curran*[33] and *Schreiner*.[28, 34] The idea behind this work was to exploit this ability of quasi-*Lewis* acidic urea and thiourea for the activation of azlactones and oxazinones towards nucleophilic (alcohol) attack. Alcohols can also be activated by coordinating to a *Brønsted* base such as tertiary amines. It was reasoned that pre-organization of these two functionalities (urea or thiourea and

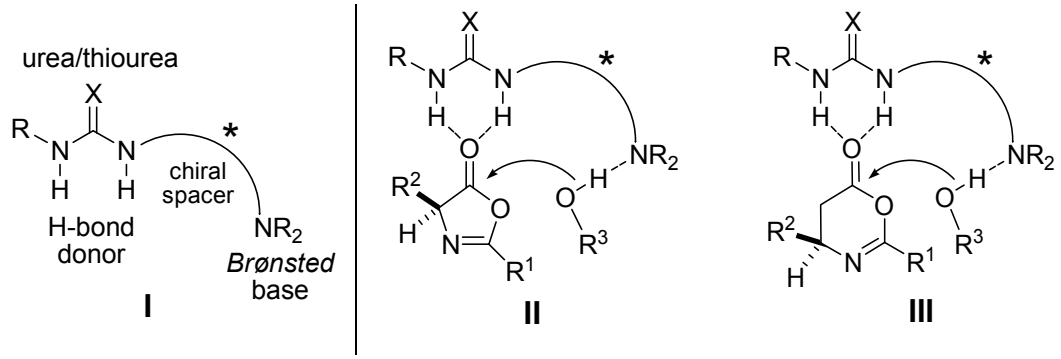

Scheme 4.2 The catalyst concept (**I**) and the bifunctional mode of activation for the DKR of azlactones (**II**) and the KR of oxazinones (**III**).

the tertiary amine) within a single molecule with an appropriate chiral environment would be efficient to activate the substrate (azlactone in case of DKR; oxazinone in case of KR) and the alcohol simultaneously (Scheme 4.2). Stereodiscrimination was also expected due to the presence of these supramolecular aggregates (**II** and **III**) in a chiral environment.

An excellent example of this bifunctional (thio)urea-tertiary amine type organocatalyst is the catalyst **1** (Scheme 4.3) recently reported by *Takemoto* et al.[51-53, 55, 136] This catalyst is a

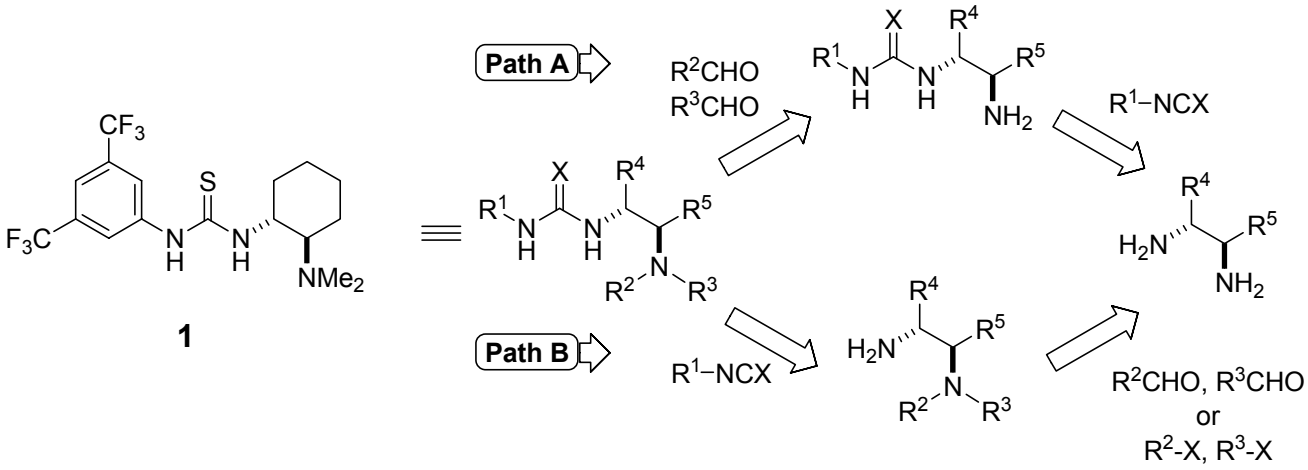

Scheme 4.3 Possible mode of variation and retrosynthesis of the bifunctional organocatalyst **1**.

combination of the quasi-*Lewis* acidic thiourea and a *Brønsted* basic tertiary amine. Both the functionalities are elegantly incorporated in chiral *trans*-1,2-diaminocyclohexane moiety. The biggest advantage of this catalyst is its highly modular structure and the ease with which the modifications can be made. Also, the non-C_2-symmetric structure of the catalyst is beneficial for diversification as changing any part of the structure would lead to a new compound. The (thio)urea group may be introduced in one step from the amine by reacting with iso(thio)cyanate, whereas the substituents on the tertiary nitrogen may be incorporated either by (S_N2) alkylation with alkyl halides or by reductive alkylation, employing aldehydes in the presence of a reducing agent. Again, these two functionalities can be introduced in different orders (path A and B, Scheme 4.3). The selective mono-(thio)urea formation from the diamine followed by alkylation (path A) provides a shorter route to the catalyst (as the monoprotection of the diamine is not needed prior to alkylation as in path B). However, the scope of this pathway is rather limited because the alkyl groups on nitrogen can only be introduced by reductive alkylation; the S_N2 alkylation may also lead to alkylation at the (thio)urea nitrogens. Path B is more general and may also be used for other diamines besides 1,2-diamines. A second element of chirality may also be introduced on the (thio)urea (with chiral R^1).

4.2 Oxazaborolidine catalyzed asymmetric hydrocyanation of imines

A second aim of this work was to develop a new (preferably metal-free) catalytic concept for the asymmetric hydrocyanation of imines, in particular aldimines. The hydrocyanation of aldimines **E** catalyzed by appropriate chiral catalysts would generate enantiomerically enriched α-amino nitriles **F**, important precursor for the synthesis of α-amino acids **G** (Scheme 4.4). Despite the myriad of

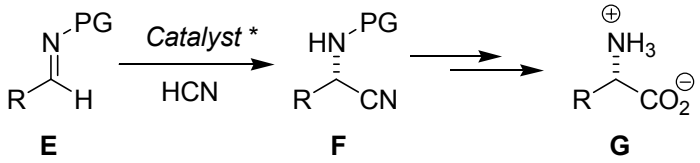

Scheme 4.4 Asymmetric hydrocyanation of imines.

catalysts that already exist for the asymmetric imine hydrocyanation (see section 3.4.2.3, page 26), there is barely a single choice of method that is applicable to every imine.

Chiral oxazaborolidines **29** (Scheme 4.6) are an important class of compounds that are known for catalyzing the highly enantioselective reduction of prochiral ketones (Scheme 4.5).[45] The most

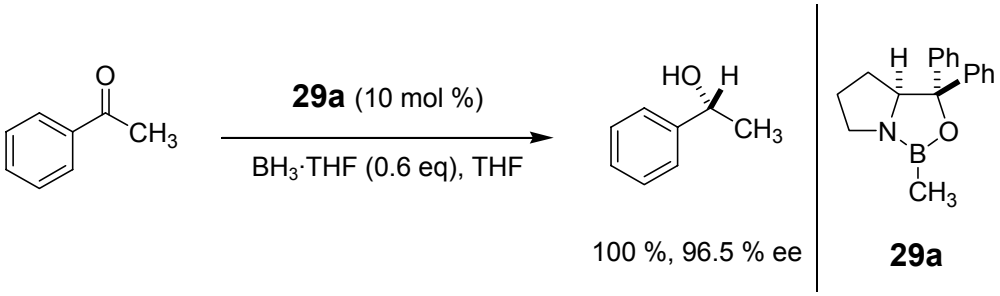

Scheme 4.5 Enantioselective reduction of ketone with oxazaborolidine **29a**.

interesting aspect of these catalysts is the extraordinary predictability of the product configuration. The *Corey* group investigated the mechanism of this widely popular methodology in detail[45] and proposed a bifunctional mode of activation for both the carbonyl compound and the reducing agent borane (Scheme 4.6a). In this pre-transition state assembly, the coordination of the electrophilic BH_3 to the nitrogen atom of **29** serves to activate BH_3 as a hydride donor and also to increase the *Lewis* acidity of the endocyclic boron atom. The strongly *Lewis* acidic boron atom then readily binds to the carbonyl oxygen at the more sterically accessible electron lone pair

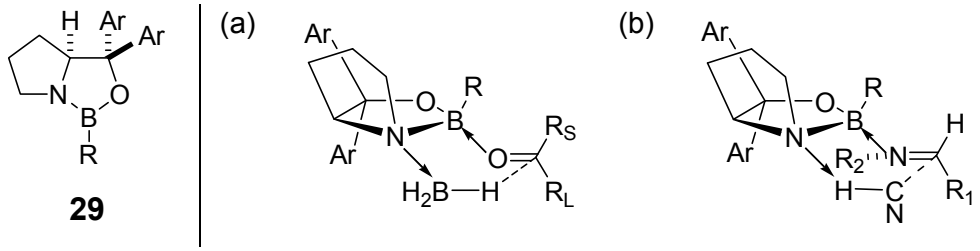

Scheme 4.6 Chiral oxazaborolidine **29** and the proposed pre-transition state assembly for (a) the reduction of ketones and (b) the hydrocyanation of imines.

and activates the carbonyl carbon towards hydride attack. A similar bifunctional mode of activation was envisaged for the HCN addition to imines: the nucleophilicity of HCN would be enhanced by binding to the oxazaborolidine nitrogen whereas the coordination of the imine nitrogen to the boron atom would increase the electrophilicity of imine carbon for cyanide attack (Scheme 4.6b). The face-selective cyanide attack *via* a six-membered transition state was expected to form the desired *α*-amino nitrile with high enantiomeric purity.

Recently *Corey* et al. also showed that protonation of oxazaborolidine **29** generates a potent cationic *Lewis* acid. This oxazaborolidinium cation **30** (Scheme 4.7) can be used as very active catalyst for highly enantioselective *Diels-Alder* and other cycloaddition reactions (both intra- and intermolecular),[137-139] and particularly for the cyanosilylation of aldehydes and ketones.[140, 141] A mechanistic model has been proposed for the cyanosilylation reactions (Scheme 4.7).[140]

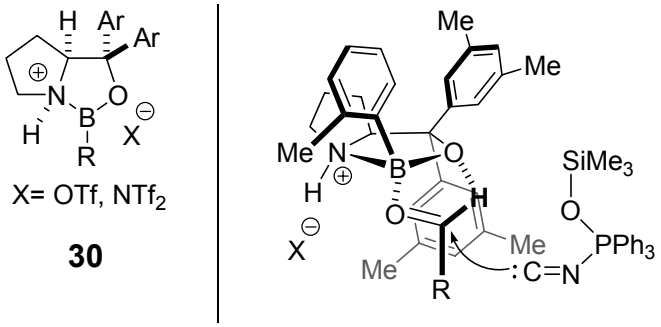

Scheme 4.7 Chiral oxazaborolidinium cations **30** and the proposed transition state for the cyanosilylation reactions.[140]

A similar mode of action was expected for the hydrocyanation of imines and therefore oxazaborolidinium cations **30** may also be used as catalysts for this reaction.

A major advantage of using **29** or **30** is their modular structure: both aryl groups and substituent on the boron atom can be easily modified. A structural optimization can be carried out to find the best catalyst. Some oxazaborolidines (e.g. Ar = Ph, R = Me) are even commercially available. Others can be prepared easily in a one step procedure by cyclodehydration of *α*,*α*-diaryl prolinols **97** and

boronic acids **98**. Diaryl prolinols **97** can in turn be synthesized from the readily available and inexpensive chiral pool compound L-proline **37** (Scheme 4.8).

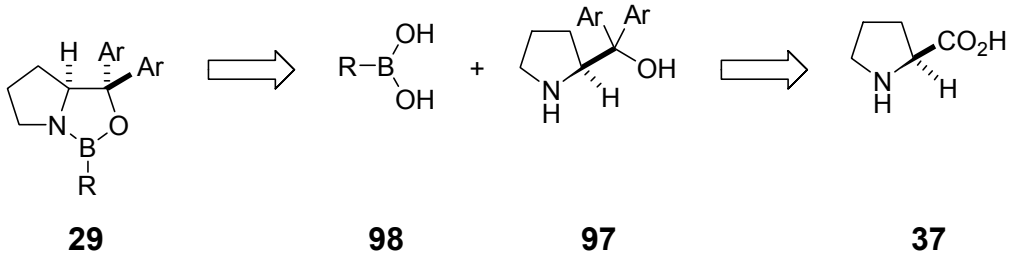

29 **98** **97** **37**

Scheme 4.8 Retrosynthetic analysis of oxazaborolidines **29**.

4.3 Development of a new ligand system for the metal-catalyzed asymmetric transformations

The third goal of this work was to develop an easy-to-synthesize and modular chiral ligand system that can coordinate to a *Lewis* acidic metal ion with the resulting complex being able to catalyze asymmetric transformations efficiently. Since the beginning of metal-complex catalyzed asymmetric transformations, numerous chiral ligands have been developed.[7, 65] One of the most widely applicable chiral ligands for *Lewis* acidic metal ions is the salen ligands **99** (Scheme 4.9).[142] Chiral metal(salen) complexes have been applied for a wide array of different asymmetric

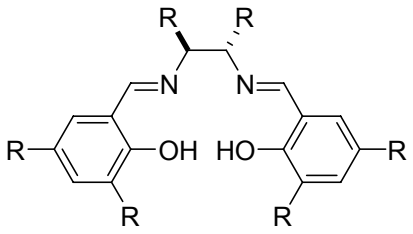

99

Scheme 4.9 Chiral salen ligands **99**.

transformations.[143] The popularity of these ligands is due to their easy accessibility, modular structure and because of the high levels of enantioselectivity often achieved with the metal complexes. These advantages of the salen ligands promoted the metal(salen) complexes to the level of privileged catalysts.[144]

It was envisaged that disruption of the C_2-symmetry of salen ligands would enhance their modularity to a great extent. A tridentate ligand system **31** containing an achiral salicylaldehyde derivative and an element of chirality would be of high stability and modularity (Scheme 4.10).

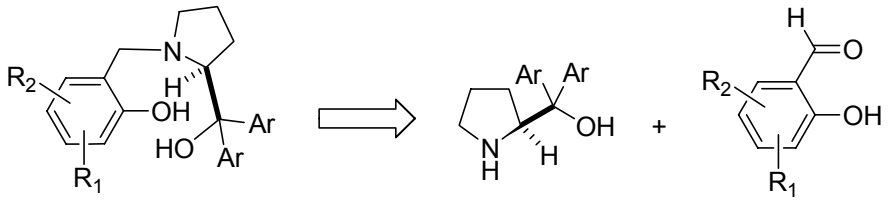

31 **97** **100**

Scheme 4.10 Retrosynthetic analysis of the tridentate ligand system **31**.

Besides modularity (through R_1, R_2 and Ar), the biggest advantage of this ligand system is the ease of synthesis. Such ligands may be synthesized in a single-step from *α*,*α*-diaryl prolinols **97** and salicylaldehyde derivatives **100** by C–N bond formation *via* reductive amination (Scheme 4.10). Several salicylaldehyde derivatives are commercially available or can be prepared from phenol. On the other hand, the *α*,*α*-diaryl prolinols **97** are ex-chiral pool compounds (see Scheme 4.8, page 50) and some of them are commercially available.

A similar but C_2-symmetric ligand system containing two such elements of chirality (Scheme 4.11) has been developed by *Trost* et al. for metal catalyzed asymmetric transformations.[145]

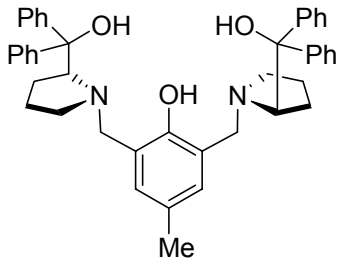

Scheme 4.11 *Trost*'s C_2-symmetric ligand system for metal catalyzed asymmetric transformations.

5 Results

5.1 Synthesis of bifunctional organocatalysts

5.1.1 Synthesis of the parent catalysts

The thiourea-tertiary amine catalyst **1** and its urea analog **2** can be synthesized in one step from the amine **101** (Scheme 5.1).

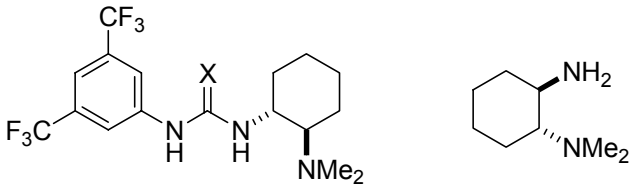

1, X = S
2, X = O

101

Scheme 5.1 The parent catalysts **1** and **2**, and their immediate precursor **101**.

The main challenge was to synthesize the unsymmetrically substituted amine **101**. This was accomplished by a monoprotection → dimethylation → deprotection sequence from the commercially available enantiomerically pure *trans*-1,2-diaminocyclohexane **102**.

The monoprotection of the diamine **102** as phthalimide was carried out following the literature procedure by *Gawronski* et al.[146] Condensation of **102** with phthalic anhydride **103** in the presence of anhydrous *p*-toluene sulfonic acid afforded the salt **104**, which can easily be deprotonated to generate the free monoprotected amine **105** (Scheme 5.2). The monoprotected diamine **105** was obtained in high yield (>90 %) over the two steps.

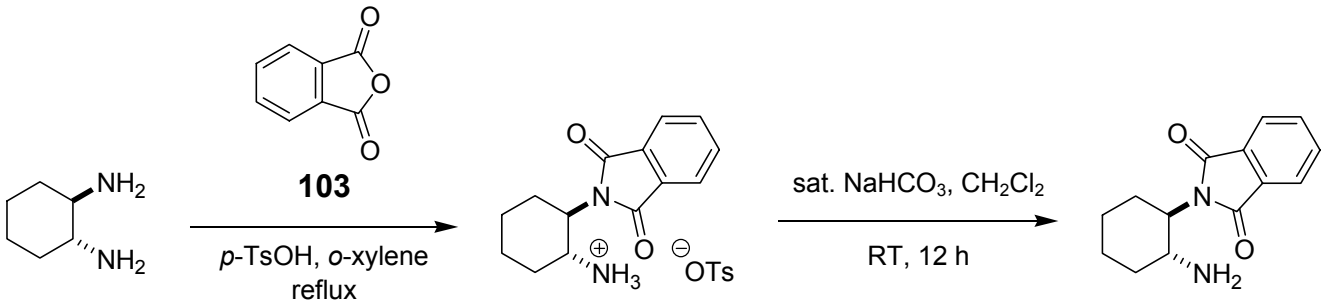

102

104, 97 %

105, 93 %

Scheme 5.2 Monoprotection of the diamine **102** as phthalimide.[146]

The dimethylation of the monoprotected diamine **105** was then achieved by reductive methylation which can be performed under two different conditions (Scheme 5.3).[146, 147] Under conditions 1,[146] the amine was refluxed with formaldehyde and formic acid whereas in conditions 2,[147] the reaction was carried out at room temperature using sodium cyanoborohydride ($NaBH_3CN$) as the hydride source. The latter method was found to be superior over the first one in terms of reaction condition, yield and the purity of the product obtained.

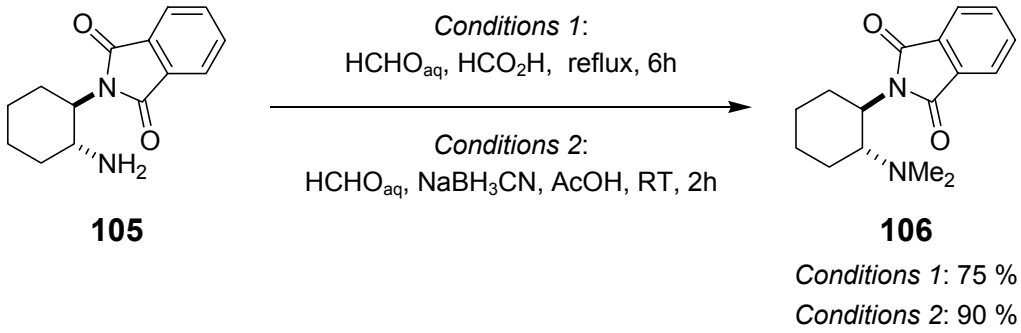

Scheme 5.3 Dimethylation of the monoprotected diamine **105**.[146, 147]

Deprotection of the phthalimide group of **106** was accomplished with hydrazine monohydrate using a modified literature procedure (Scheme 5.4).[146] The immediate precursor of the target catalysts **101** was obtained in good yield.

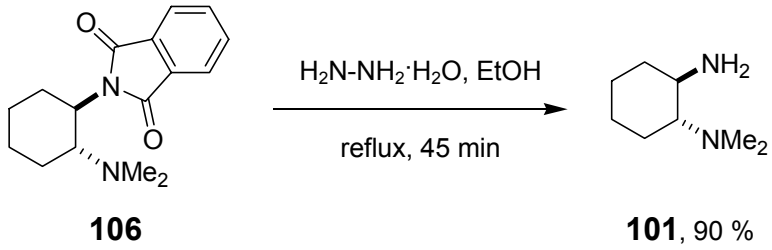

Scheme 5.4 Deprotection of the phthalimide group of **106**.[146]

With the unsymmetrically substituted amine **101** in hand, the desired thiourea-tertiary amine catalysts **1** and its urea analog **2** were synthesized by condensation with the commercially available 3,5-bis(trifluoromethyl)phenyl isothiocyanate **107** and the corresponding isocyanate **108**, respectively (Scheme 5.5). Both the thiourea **1** and urea **2** were obtained in good yields.

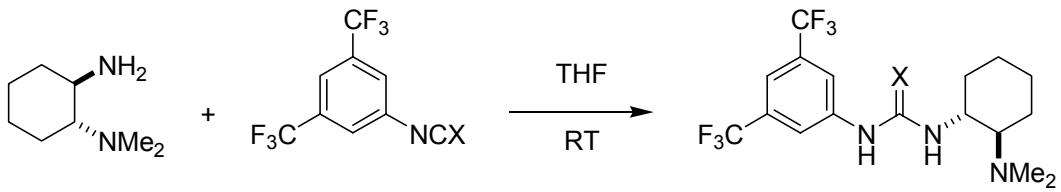

101 **107**, X = S **1**, X = S, 84 %

108, X = O **2**, X = O, 87 %

Scheme 5.5 Synthesis of the catalysts **1** and **2**.

The urea-derivative **2** was crystallized from chloroform to obtain crystals suitable for X-ray diffraction. The X-ray structure was determined (Figure 5.1).

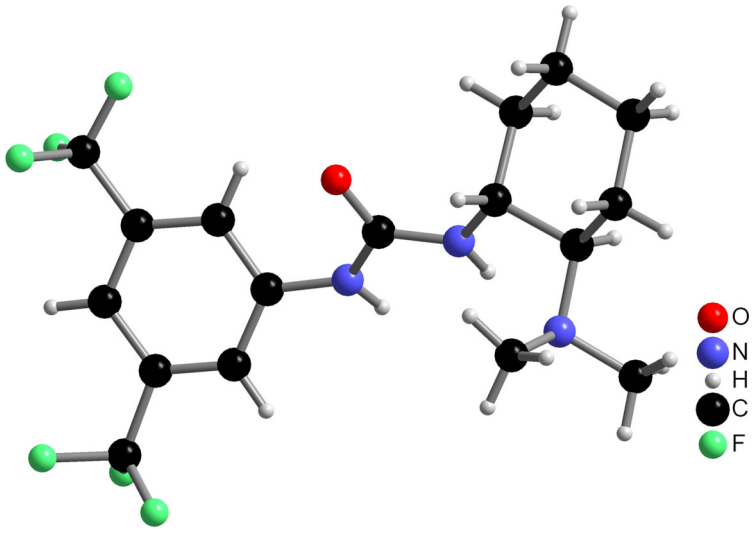

Figure 5.1 X-ray structure of 1-{3,5-bis(trifluoromethyl)phenyl}-3-{(1*R*,2*R*)-2-(dimethylamino)cyclohexyl}urea **2**.

5.1.2 Variation of the tertiary amine part of the catalyst

To replace the methyl groups at the tertiary amine of the parent catalyst with ethyl residues, the monoprotected diamine **105** was diethylated by refluxing with ethyl iodide to obtain the diethyl derivative **109** in almost quantitative yield (Scheme 5.6).

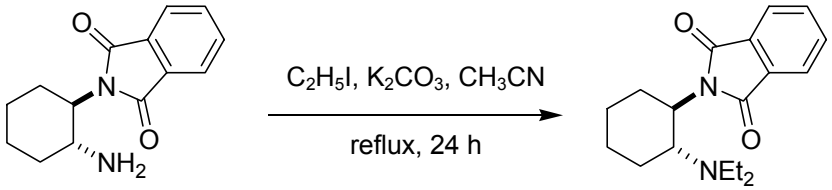

105 **109**, 99 %

Scheme 5.6 Diethylation of the monoprotected diamine **105** with ethyl iodide.

Similarly, when 1,4-diiodobutane **110** was used as the alkylating agent, the pyrrolidine derivative **111** was obtained in almost quantitative yield (Scheme 5.7).

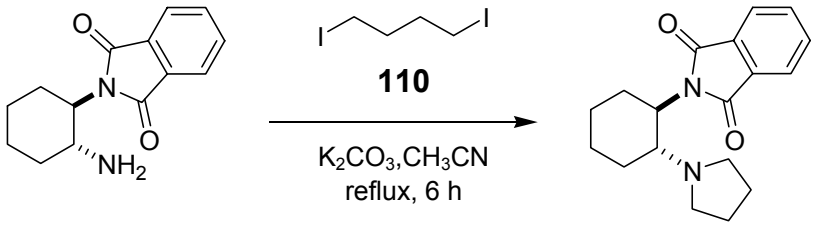

105 **111**, 99 %

Scheme 5.7 Synthesis of the pyrrolidine derivative **111**.

Whereas in the two above cases two identical substituents were introduced on nitrogen *via* S_N2 alkylation, the reductive alkylation protocol was followed to introduce different substituents. Thus, to prepare the methyl-benzyl-derivative **112**, phthalimide protected diamine **105** was first reacted with benzaldehyde **33** to obtain the imine **113** in very high yield. The imine **113**, without any further purification, was then applied as the substrate for the reductive methylation reaction with $NaBH_3CN$ to obtain the desired heterodialkyl substituted product **112** in pure form and excellent yield (Scheme 5.8).

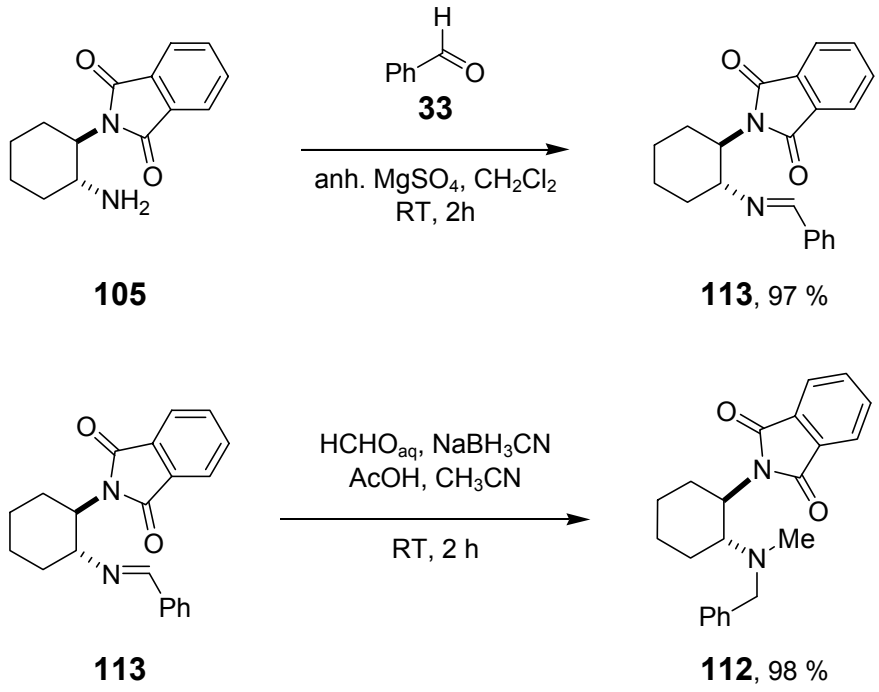

Scheme 5.8 Synthesis of the methyl-benzyl substituted amine **112**.

The phthalimide groups of these dialkyl-substituted compounds were cleaved under the same conditions as for **106** with hydrazine monohydrate in ethanolic solution to obtain the free amines **114**-**116** (Scheme 5.9).

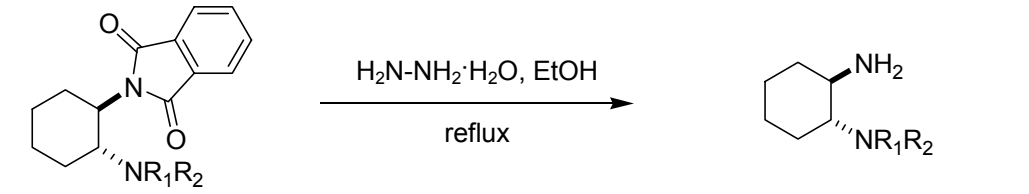

109, $R_1 = R_2 = Et$
111, $R_1 = R_2 = -(CH_2)_4-$
112, $R_1 = Me$, $R_2 = Bn$

114, $R_1 = R_2 = Et$, 95 %
115, $R_1 = R_2 = -(CH_2)_4-$, 89 %
116, $R_1 = Me$, $R_2 = Bn$, 97 %

Scheme 5.9 Hydrazinolytic cleavage of the phthalimide groups of **109**, **111** and **112**.

These free amines **114**-**116** were then reacted with 3,5-bis(trifluoromethyl)phenyl isocyanate **108** to obtain the corresponding urea catalysts **3**-**5**, respectively in moderate to good yields (Scheme 5.10).

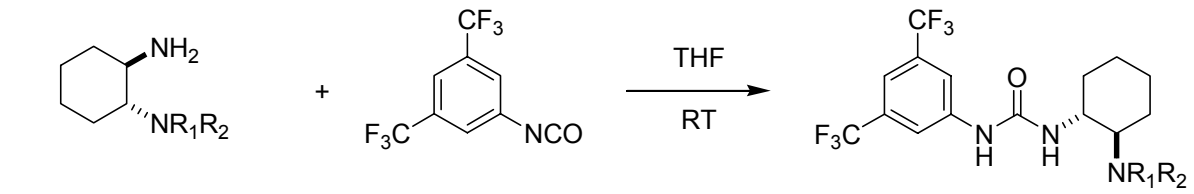

114, $R_1 = R_2 = Et$ **108** **3**, $R_1 = R_2 = Et$, 71 %

115, $R_1 = R_2 = -(CH_2)_4-$ **4**, $R_1 = R_2 = -(CH_2)_4-$, 71 %

116, $R_1 = Me$, $R_2 = Bn$ **5**, $R_1 = Me$, $R_2 = Bn$, 87 %

Scheme 5.10 Synthesis of the urea catalysts.

The urea derivative of the *N*,*N*-heterodialkyl amine **5** was crystallized from ethanol to obtain X-ray diffraction quality crystals (Figure 5.2). The crystal structure contains one ethanol molecule in the unit cell.

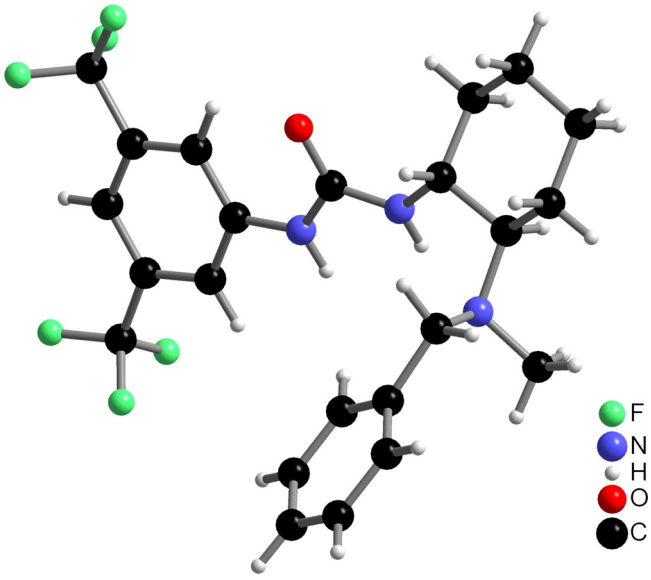

Figure 5.2 X-ray structure of 1-{3,5-bis(trifluoromethyl)phenyl}-3-{(1*R*,2*R*)-2-(*N*-benzyl-*N*-methylamino)cyclohexyl}urea **5**.

5.1.3 Variation of the (thio)urea substituents of the catalyst

After varying the substituents on the tertiary amine, the next site for diversification was the substituent on the (thio)urea nitrogen. For this study, the substituent on the (thio)urea nitrogen was varied, keeping the tertiary amine part fixed to *N*,*N*-dimethyl derivative.

5.1.3.1 Synthesis of catalysts containing aromatic substituents

First, the 3,5-bis(trifluoromethyl)phenyl group of the catalyst **2** was replaced with another electron withdrawing aromatic group, 3,5-dinitrophenyl, to yield a new bifunctional catalyst **6**. It was synthesized in good yield in a single-step procedure from the *N*,*N*-dimethyl amine **101** by reaction with commercially available 3,5-dinitrophenyl isocyanate **117** (Scheme 5.11).

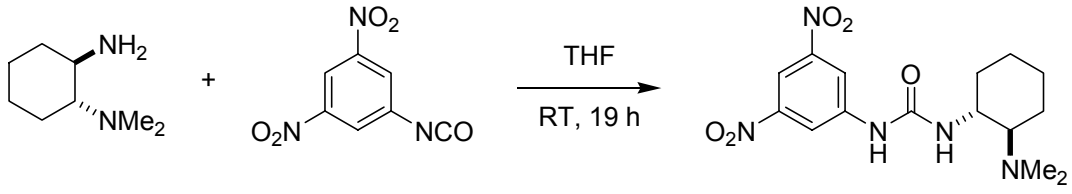

101 **117** **6**, 80 %

Scheme 5.11 Synthesis of the 3,5-dinitrophenyl substituted urea **6**.

The urea-derivative **6** was crystallized from a methanol-water mixture to obtain X-ray diffraction quality crystals (Figure 5.3). The crystal structure contains one water molecule in the unit cell.

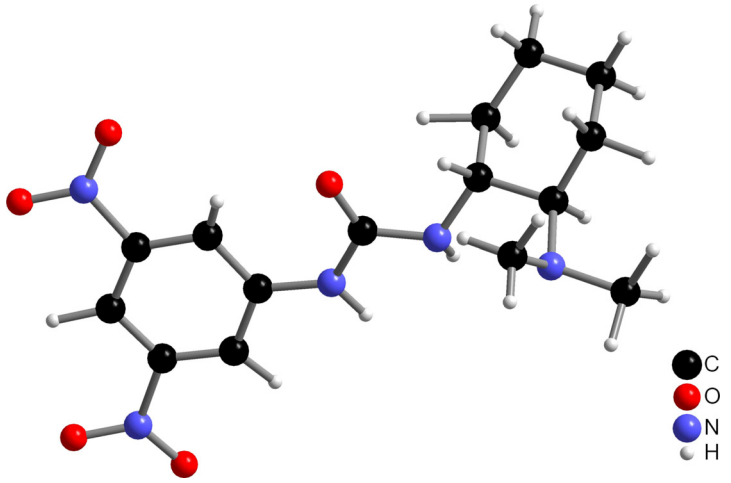

Figure 5.3 X-ray structure of 1-(3,5-dinitrophenyl)-3-{(1*R*,2*R*)-2-(dimethylamino)cyclohexyl}urea **6**.

Electron rich aromatic groups were also introduced on the urea nitrogen atom of the catalyst. The amine **101** was reacted with mesitylisocyanate **118** to obtain the urea-derivative **7** in moderate yield (Scheme 5.12).

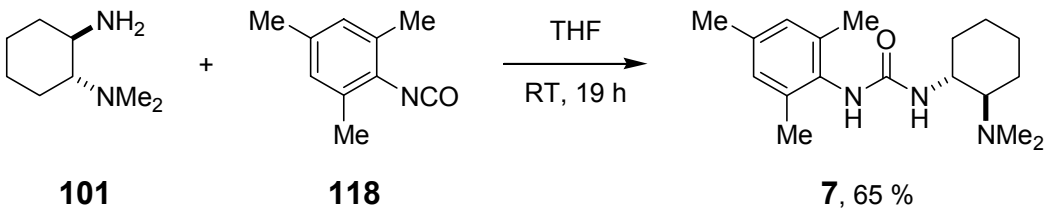

101 **118** **7**, 65 %

Scheme 5.12 Synthesis of the mesityl substituted urea **7**.

Crystallization from ethanol afforded X-ray diffraction quality crystals of this urea-derivative **7** (Figure 5.4).

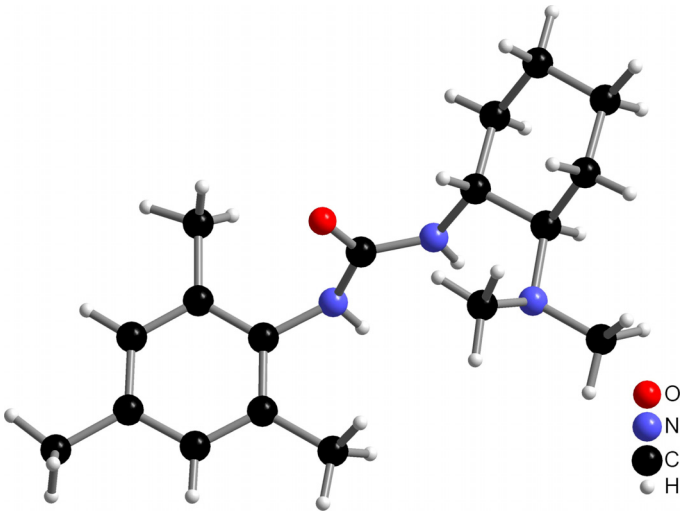

Figure 5.4 X-ray structure of 1-{(1*R*,2*R*)-2-(dimethylamino)cyclohexyl}-3-mesitylurea **7**.

Similarly, reaction of **101** with 3-pyridyl isothiocyanate **119** afforded the electron-rich aromatic heterocycle substituted thiourea **8** in 71 % yield (Scheme 5.13). This thiourea derivative contains, in addition to the tertiary amine, a second *Brønsted* basic functionality.

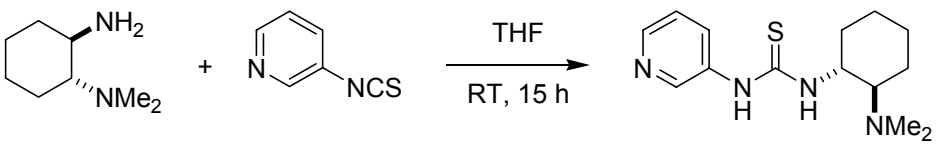

101 **119** **8**, 71 %

Scheme 5.13 Synthesis of 3-pyridyl substituted thiourea **8**.

5.1.3.2 Synthesis of catalysts containing aliphatic substituents

The aromatic moiety of the parent catalysts **1** and **2** was then replaced by aliphatic substituents. The cyclohexyl substituted bifunctional organocatalyst **9** was prepared by reacting the amine **101** with commercially available cyclohexyl isothiocyanate **120** in moderate yield (Scheme 5.14).

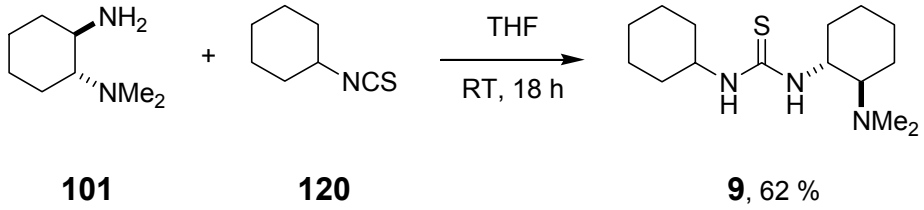

101 **120** **9**, 62 %

Scheme 5.14 Synthesis of the cyclohexyl substituted thiourea catalyst **9**.

To increase the steric bulk at this part of the molecule, the cyclohexyl group was exchanged with a bulkier 1-adamantyl group. This thiourea **10** was synthesized from 1-adamantyl isothiocyanate **121** in 78 % yield (Scheme 5.15).

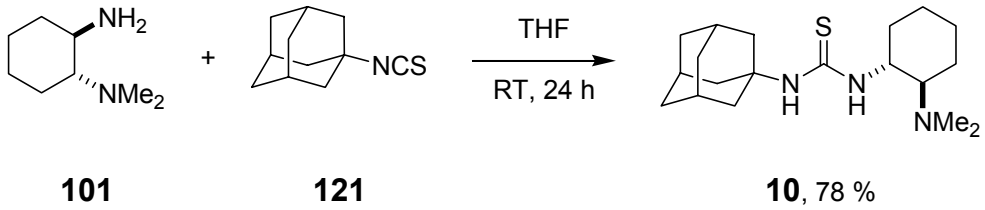

101 **121** **10**, 78 %

Scheme 5.15 Synthesis of the 1-adamantyl substituted thiourea **9**.

To check the effect of double bifunctionality in a single molecule, a catalyst containing two quasi-*Lewis* acidic urea moieties as well as two *Brønsted* basic tertiary amines was designed. A linear 1,6-hexyl chain was used as the spacer between two bifunctional units. The new compound **11** was synthesized in one step from 1,6-diisocyanatohexane **122** in good yield (Scheme 5.16).

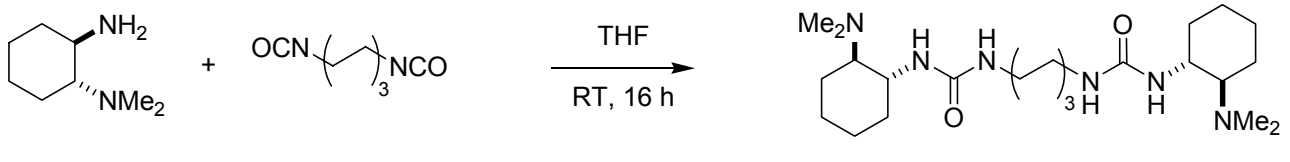

101 **122** **11**, 79 %

Scheme 5.16 Synthesis of the catalyst **11** with double bifunctionality.

5.1.3.3 Synthesis of catalysts containing a second element of chirality

A series of bifunctional organocatalysts containing an additional element of chirality besides the chiral diamine (second-generation catalysts) were synthesized either from the commercially available isocyantes, or from the isothiocyantes derived from the readily available starting materials. First, the commercially available enantiomers of 1-phenylethyl isocyanate **123** and *ent*-**123** were used as the second source of chirality (Table 5.1). The diastereomeric urea catalysts **12** and **13** were obtained in rather good yields.

Table 5.1 Synthesis of bifunctional catalysts containing additional chiral centers.

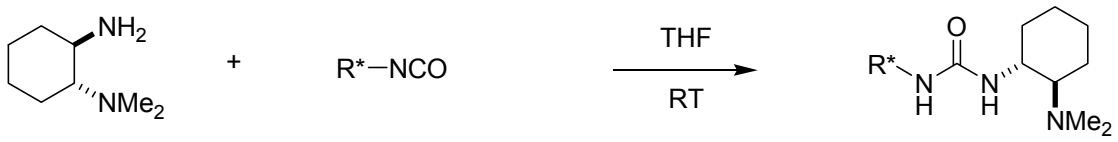

101

Isocyanate	Urea	Yield
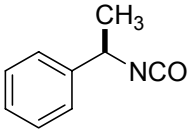	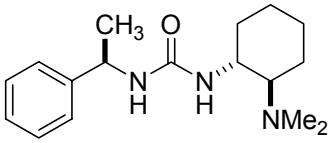	70 %
123	**12**	
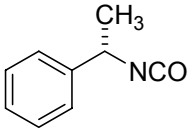	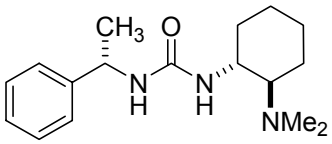	75 %
ent-**123**	**13**	

Both of these compounds were crystallized from chloroform to obtain crystals suitable for X-ray diffraction. The X-ray structures of these two bifunctional organocatalysts (**12** and **13**) were determined (Figure 5.5).

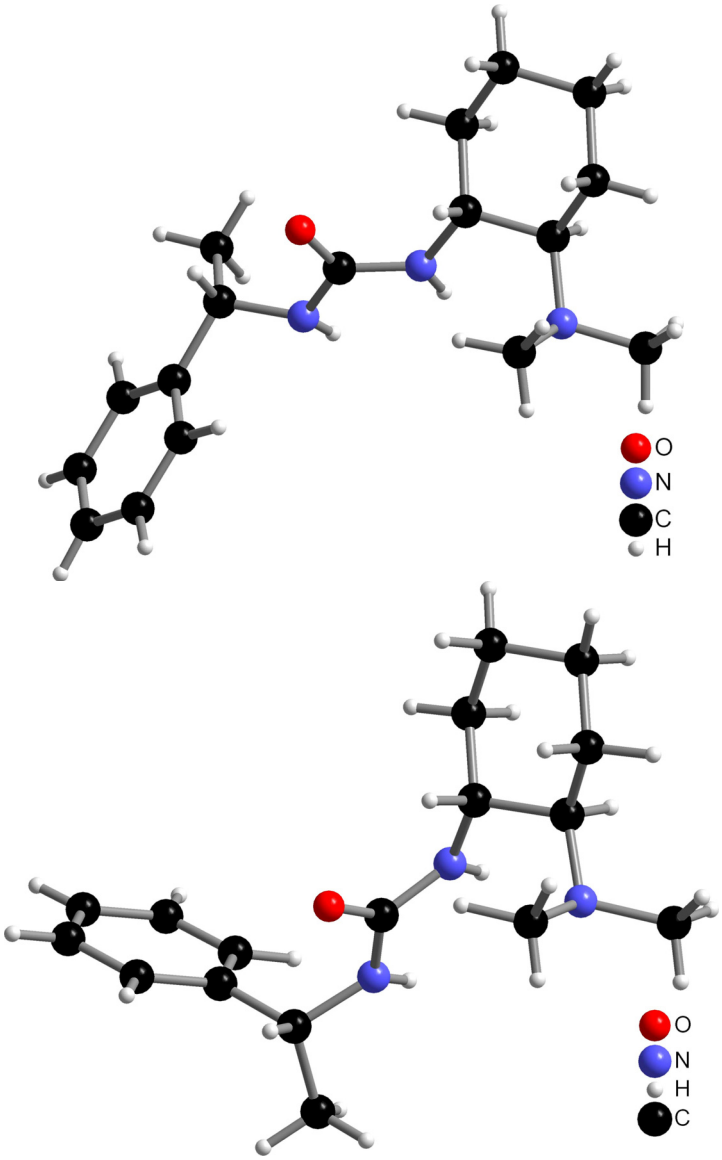

Figure 5.5 X-ray structure of the diastereomeric catalysts **12** (top) and **13** (bottom).

A C_2-symmetric thiourea-tertiary amine catalyst **14** containing two *N*,*N*-dimethyl-1,2-diaminocyclohexane **101** moieties was also synthesized. First, **101** was converted into the corresponding isothiocyanate **124** with thiophosgene. This isothiocyanate **124**, without any further purification, was condensed with a second molecule of **101** to obtain the desired C_2-symmetric catalyst **14** in acceptable 60 % yield over the two steps (Scheme 5.17).

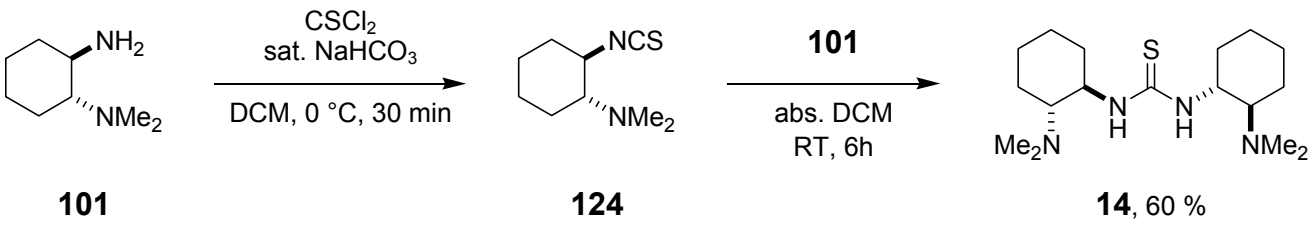

101 **124** **14**, 60 %

Scheme 5.17 Synthesis of the C_2-symmetric catalyst **14**.

A number of chiral isocyanates and isothiocyanates are commercially available which can be reacted with the amine **101** to obtain various bifunctional catalysts containing a second element of chirality. However, it was envisaged that an iso(thio)cyanate of modular nature would be very useful for diversification of the catalysts structure. Like the amine, the iso(thio)cyanate can also be modified easily at any desired part to find the best catalyst structure. The *Jacobsen* group developed a series (thio)urea-catalysts which were synthesized from α-amino acid derived iso(thio)cyanates.[36] These iso(thio)cyanates have two sites for modification (Scheme 5.18). There

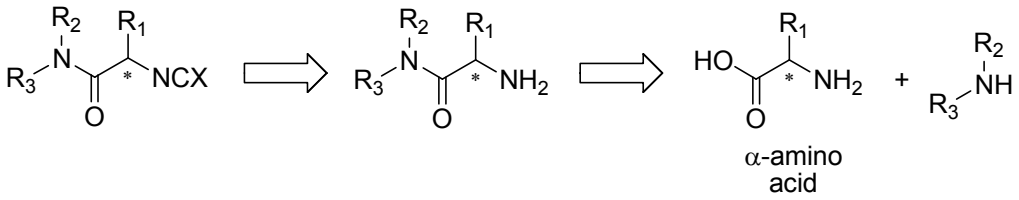

Scheme 5.18 α-Amino acid derived iso(thio)cyanates.

are 19 natural and numerous non-natural α-amino acids available for structural variation (different R_1) and the same holds for the primary and secondary amines (different R_2 and R_3). Steric bulk at the chiral center can be tuned by using different amino acids. For the present purpose, L- and D-*tert*-leucine (R_1 = *t*-Bu) and L-neopentylglycine (R_1 = *t*-BuCH_2) were used as the α-amino acid component.

The point of departure for the synthesis was the Boc-protection of the α-amino acids with Boc-anhydride **125** (Scheme 5.19), which was carried out following a literature procedure.[148] Pure Boc-protected α-amino acids were obtained in excellent yields in most cases.

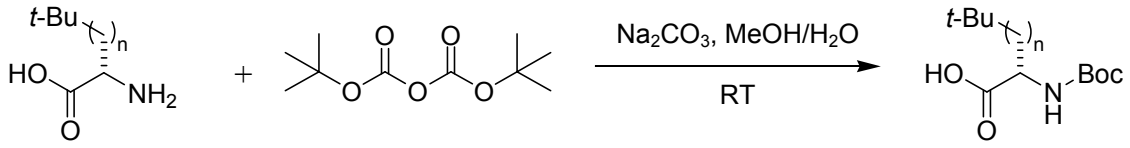

126, n = 0
ent-**126**, n = 0
127, n =1

125

128, n = 0, 91 %
ent-**128**, n = 0, 98 %
129, n = 1, 92 %

Scheme 5.19 Boc-protection of *α*-amino acids.

These *N*-Boc-*α*-amino acids were then coupled with various primary and secondary amines using *O*-benzotriazol-1-yl-*N*,*N*,*N*′,*N*′-tetramethyluronium hexafluorophosphate (HBTU) as the coupling reagent following a literature procedure (Scheme 5.20).[39] The amides **130**-**135** were obtained contaminated with tetramethyl urea in very good to excellent yields and were used in the following step without any further purification.

128, n = 0
ent-**128**, n = 0
129, n = 1

130, n = 0, R_1 = R_2 = Me, >99 %
131, n = 0, R_1 = R_2 = Et, 85 %
132, n = 0, R_1 = R_2 = *i*-Bu, >99 %
133, n = 0, R_1 = Me, R_2 = Bn, 91 %
ent-**133**, n = 0, R_1 = Me, R_2 = Bn, >99 %
134, n = 0, R_1 = H, R_2 = Bn, >99 %
135, n = 1, R_1 = Me, R_2 = Bn, >99 %

Scheme 5.20 Coupling of *N*-Boc-*α*-amino acids with amines.

The Boc-group of these amides **130**-**135** was then deprotected with trifluoroacetic acid (TFA) following a standard literature procedure[39] to afford the free primary amines **136**-**141** in quantitative yields in most cases (Scheme 5.21).

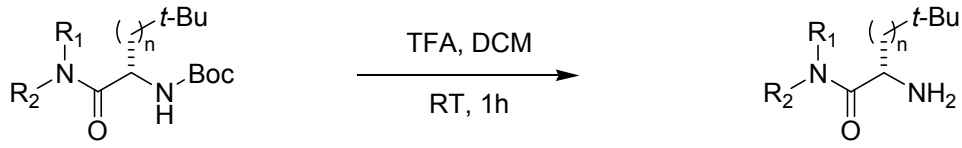

130, n = 0, R_1 = R_2 = Me
131, n = 0, R_1 = R_2 = Et
132, n = 0, R_1 = R_2 = *i*-Bu
133, n = 0, R_1 = Me, R_2 = Bn
ent-**133**, n = 0, R_1 = Me, R_2 = Bn
134, n = 0, R_1 = H, R_2 = Bn
135, n = 1, R_1 = Me, R_2 = Bn

136, n = 0, R_1 = R_2 = Me, 77 %
137, n = 0, R_1 = R_2 = Et, 99 %
138, n = 0, R_1 = R_2 = *i*-Bu, >99 %
139, n = 0, R_1 = Me, R_2 = Bn, 100 %
ent-**139**, n = 0, R_1 = Me, R_2 = Bn, >99 %
140, n = 0, R_1 = H, R_2 = Bn, 84 %
141, n = 1, R_1 = Me, R_2 = Bn, >99 %

Scheme 5.21 Boc-deprotection of the amides.

These primary amines **136**-**141** were then converted to the corresponding isothiocyanates with thiophosgene ($CSCl_2$) following a literature procedure (Scheme 5.22).[39] The isothiocyanates **142**-**147** were obtained in excellent yields and used immediately for the thiourea-formation without any further purification or characterization.

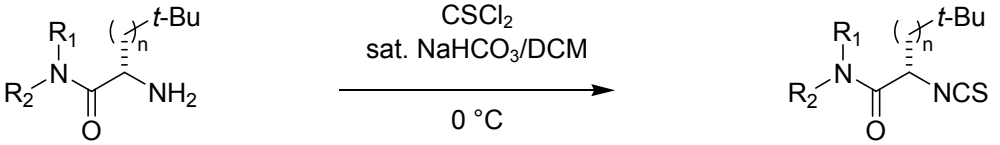

136, n = 0, R_1 = R_2 = Me
137, n = 0, R_1 = R_2 = Et
138, n = 0, R_1 = R_2 = *i*-Bu
139, n = 0, R_1 = Me, R_2 = Bn
ent-**139**, n = 0, R_1 = Me, R_2 = Bn
140, n = 0, R_1 = H, R_2 = Bn
141, n = 1, R_1 = Me, R_2 = Bn

142, n = 0, R_1 = R_2 = Me, 97 %
143, n = 0, R_1 = R_2 = Et, 97 %
144, n = 0, R_1 = R_2 = *i*-Bu, 97 %
145, n = 0, R_1 = Me, R_2 = Bn, 96 %
ent-**145**, n = 0, R_1 = Me, R_2 = Bn, 95 %
146, n = 0, R_1 = H, R_2 = Bn, 99 %
147, n = 1, R_1 = Me, R_2 = Bn, 96 %

Scheme 5.22 Preparation of isothiocyanates from the primary amines.

Reaction of the amine **101** with the isothiocyanates **142**-**147** according to the standard literature procedure afforded a series of thiourea-based bifunctional organocatalysts in moderate to good yields (Table 5.2).[39]

Table 5.2 Synthesis of thiourea-based modular bifunctional organocatalysts.

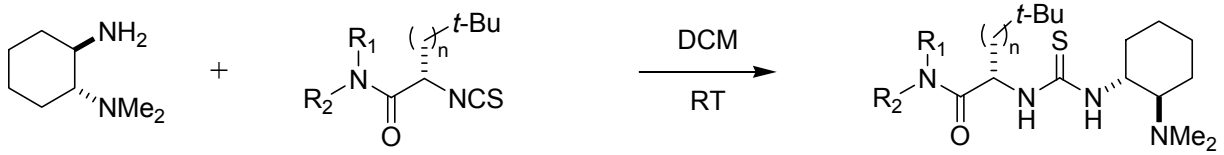

101 n = 0, 1 n = 0, 1

Isothiocyanate	Thiourea	Yield
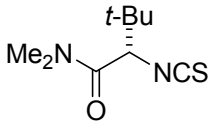 **142**	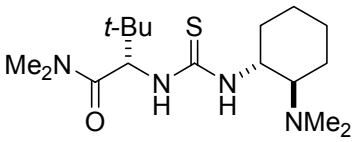 **15**	61 %
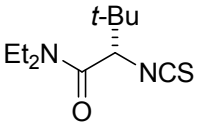 **143**	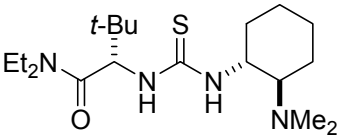 **16**	72 %
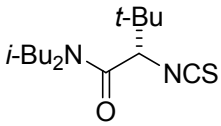 **144**	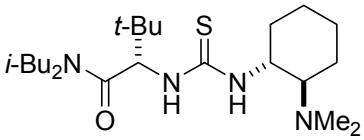 **17**	67 %
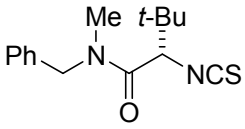 **145**	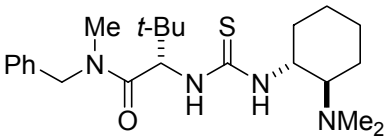 **18**	74 %
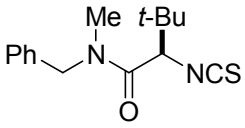 *ent*-**145**	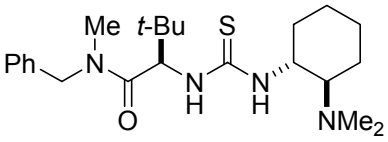 **19**	64 %
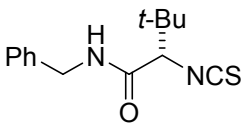 **146**	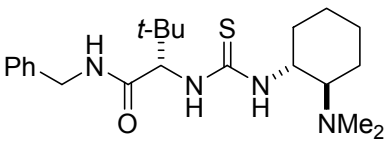 **20**	74 %

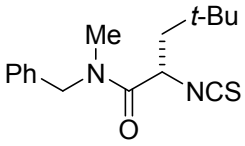

147

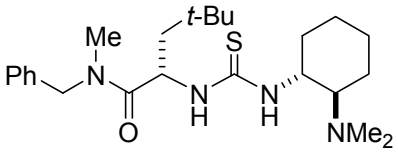

21

75 %

The thiourea-derivative **16** was crystallized from acetone to obtain X-ray diffraction quality crystals (Figure 5.6).

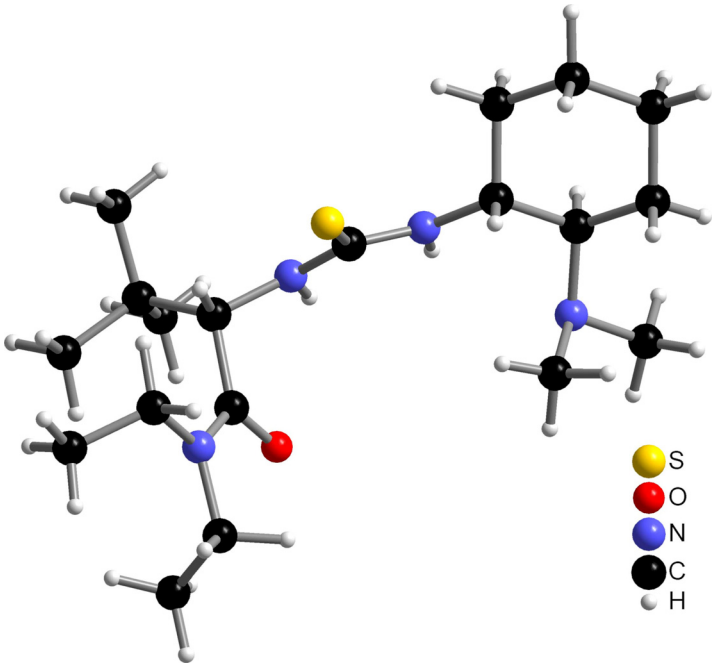

Figure 5.6 X-ray structure of the catalyst **16**.

5.1.4 Synthesis of chiral guanidine and guanidinium cation

Besides the bifunctional (thio)urea-tertiary amine organocatalysts described above, a chiral guanidine and its corresponding guanidinium cation were also synthesized. The guanidine **148** was synthesized in one-step from the amine **101** by refluxing with 1,3-dicyclohexyl carbodiimide **149** following a literature procedure (Scheme 5.23).[149] The desired guanidine was obtained in good yield.

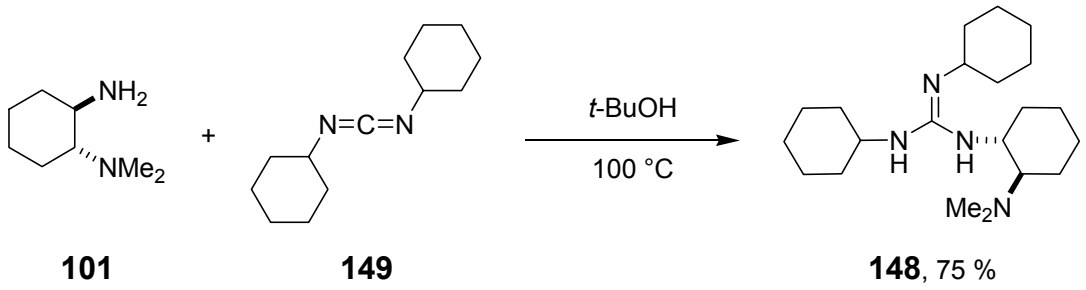

101 **149** **148**, 75 %

Scheme 5.23 Synthesis of chiral guanidine **148**.

This guanidine **148** was protonated with trifluoroacetic acid to obtain the guanidinium cation **150** in quantitative yield (Scheme 5.24).

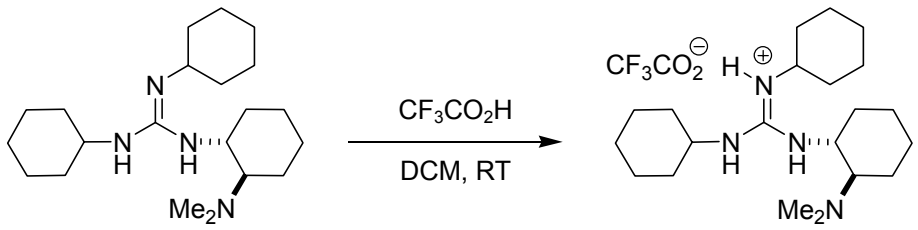

148 **150**, 100 %

Scheme 5.24 Synthesis of the guanidinium cation **150**.

5.2 Dynamic kinetic resolution of azlactones

5.2.1 Catalyst screening

The catalysis experiments were conducted by *F. Cleemann* with substrates synthesized by himself. The alcoholytic ring opening of the *tert*-leucine derived azlactone *rac*-**22a** (Scheme 5.25) was used as the test reaction for the bifunctional organocatalysts. Allyl alcohol **23** was used as the nucleophile in all screening experiments due to its superior behaviour in terms of enantioselectivity over all other alcohol nucleophiles studied.[150] Similarly, toluene was found to be the optimal solvent. Unless otherwise stated, all catalysis experiments were carried out at room temperature using 1.5 equivalents of allyl alcohol.

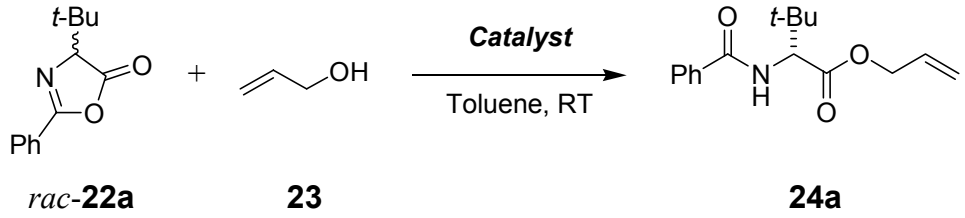

rac-**22a** **23** **24a**

Scheme 5.25 Alcoholytic DKR of *tert*-leucine derived azlactone *rac*-**22a**.

To optimize the *Brønsted* basic part of the catalyst structure, the bifunctional organocatalysts containing different substituents at the tertiary amine moiety were first screened in the aforementioned reaction (Scheme 5.25). The catalyst loadings were kept constant at 5 mol % in all cases. Conversion and enantiomeric excesses of the product ester **24a** obtained after 48 h with each of these urea-based catalysts are listed in Table 5.3. The highest enantioselectivity along with good conversion was obtained with the *N*,*N*-dimethyl substituted catalyst **2** (Entry 1). The exchange of the dimethylamino group with a pyrrolidine in catalyst **4** resulted in slightly higher conversion and lower enantioselectivity (Entry 2). By increasing the steric demand of the substituents from methyl to ethyl, the catalytic activity was diminished significantly although somewhat less pronounced drop in enantioselectivity was observed (Entry 3). Further enhancement in steric bulk of the substituents by replacing one methyl group with a benzyl group in catalyst **5** deactivates the catalyst completely (Entry 4).

Table 5.3 Catalyst screening to optimize the *Brønsted* basic part of the structure.

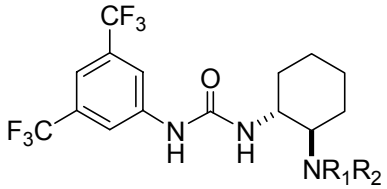

2-5

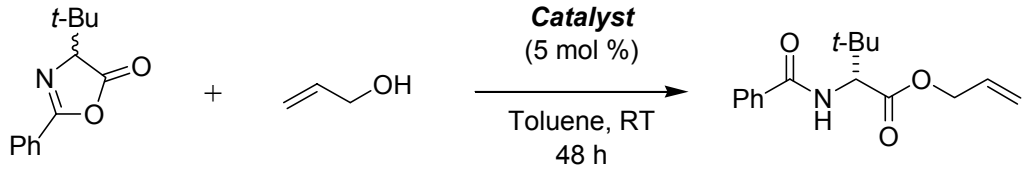

rac-**22a** **23** **24a**

Entry	Catalyst	R_1	R_2	% Conversion	% ee
1	**2**	Me	Me	67	87
2	**4**	-$(CH_2)_4$-		75	75
3	**3**	Et	Et	16	73
4	**5**	Me	Bn	<2	n.d.

Similarly, all catalysts containing a dimethylamino group as the *Brønsted* basic moiety and various substituents on the quasi-*Lewis* acidic (thio)urea functionality (Scheme 5.26) were screened for the same reaction (Scheme 5.25, page 70).

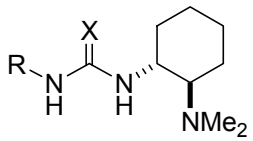

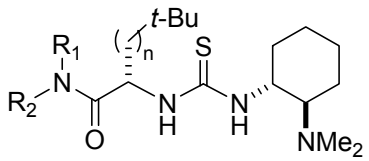

1: R = 3,5-$(CF_3)_2C_6H_3$, X = S
2: R = 3,5-$(CF_3)_2C_6H_3$, X = O
6: R = 3,5-$(NO_2)_2C_6H_3$, X = O
7: R = 2,4,6-$(CH_3)_3C_6H_2$, X = O
8: R = 3-pyridine, X = S
9: R = *c*-Hex, X = S
10: R = 1-adamantyl, X = S
12: R = (*R*)-PhCH(CH_3), X = O
13: R = (*S*)-PhCH(CH_3), X = O

15: $R_1 = R_2$ = Me, n = 0
16: $R_1 = R_2$ = Et, n = 0
17: $R_1 = R_2$ = *i*-Bu, n = 0
18: R_1 = Me, R_2 = Bn, n = 0
20: R_1 = H, R_2 = Bn, n = 0
21: R_1 = Me, R_2 = Bn, n = 1

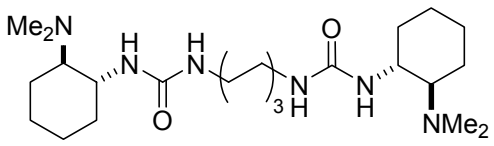

11

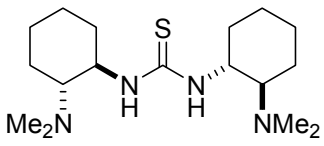

14

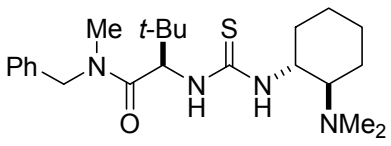

19

Scheme 5.26 Catalyst library with various (thio)urea substituents.

The results are summarized in Table 5.4.

Table 5.4 Catalyst screening to optimize the quasi-*Lewis* acidic part of the structure.

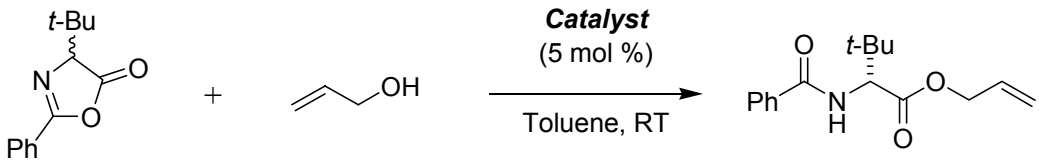

rac-**22a** **23** **24a**

Entry	Catalyst	Time (h)	% Conversion	% ee
1	**1**	48	69	83
2[a]	**1**	48	16	91
3	**2**	48	67	87
4	**6**	48	66	86
5	**7**	48	9	84
6	**8**	48	12	82
7	**9**	48	47	87
8	**10**	48	32	87
9	**11**	48	30	80
10	**12**	72	28	85
11	**13**	24	18	88
12	**14**	48	33	88
13	**15**	24	23	91
14	**16**	48	26	90
15	**17**	48	15	86
16	**18**	48	28	95
17	**19**	24	3	77
18	**20**	48	38	92
19	**21**	48	23	92

[a] Reaction was carried out at –20 °C.

From this screening, the parent catalyst **1** was found to be the most active catalyst (Entry 1) whereas the catalyst **18** containing a second element of chirality (second-generation catalyst) provided the highest enantioselectivity (Entry 16). Among simple alkyl substituted catalysts, the highest reactivity and enantioselectivity was observed with the cyclohexyl substituted catalyst **9**

(Entry 7). The enantioselectivity obtained with this catalyst was even higher than that obtained with the parent catalyst **1** at room temperature and equals with the selectivity observed with the urea-derivative **2**.

In addition to the bifunctional (thio)urea-tertiary amine catalysts, the chiral guanidine **148** and the guanidinium cation **150** (Scheme 5.27) were also tested for the same reaction (Scheme 5.25). Although in the presence of 5 mol % of the guanidine **148**, the azlactone *rac*-**22a** was completely

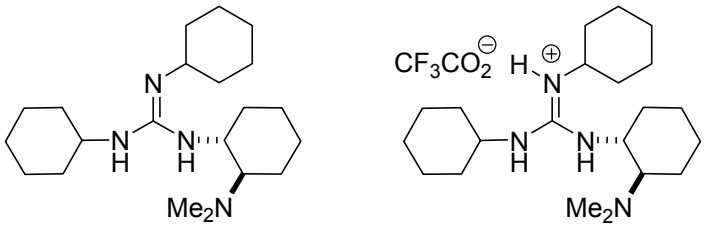

148 **150**

Scheme 5.27 Chiral guanidine **148** and the guanidinium cation **150**.

consumed after 24 hours, the product ester **24a** was obtained in only 15 % ee. On the other hand, the cation **150** did not lead to any product formation even after 48 hours.

5.2.2 Substrate scope

After optimization of the catalyst structure, a number of azlactones *rac*-**22a**-**h** derived both from natural and non-natural α-amino acids were subjected to alcoholytic ring opening in the presence of the most enantiodifferentiating catalyst **18**.

The results are summarized in Table 5.5.

Table 5.5 Substrate scope for the DKR of azlactones.

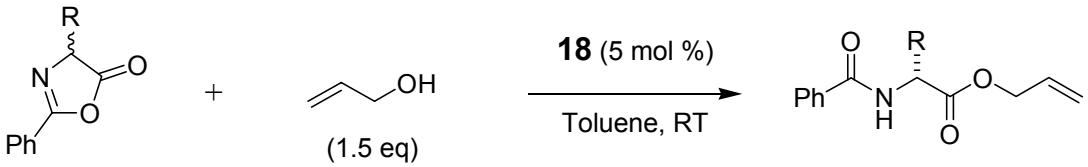

rac-**22a**-**h** **23** **24a**-**h**

Entry	Substrate	R	Time (h)	% Conversion	% ee
1	**22a**	*t*-Bu	48	28	95
2	**22b**	*i*-Bu	48	77	91
3	**22c**	*i*-Pr	48	59	92
4	**22d**	$PhCH_2$	48	77	78
5	**22e**	*t*-$BuCH_2$	48	68	90
6	**22f**	Me	24	94	80
7	**22g**	Ph	48	29	61
8	**22h**	$MeSCH_2CH_2$	48	72	80

In cases of the alkyl substituted azlactones *rac*-**22a**-**f** and the thioether functionalized azlactone *rac*-**22h**, the enantiomeric excesses obtained were higher than 75 % (Entries 1-6 and 8). A somewhat lower ee of 61 % was observed in the case of aromatic azlactone *rac*-**22g** (Entry 7). The enantioselectivities listed in the Table 5.5 are the highest achieved so far in the chemically catalyzed DKR of azlactones.[151]

In addition to the monosubstituted azlactones *rac*-**22a**-**h** listed in Table 5.5, the catalyst was also applied for the alcoholytic ring opening of the most simple (achiral) disubstituted azlactone **22i**. But, even after applying the more active catalysts like **1** and **9** over prolonged reaction time, no product was observed under the employed reaction conditions (see Table 5.5).

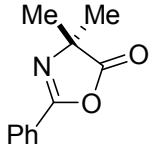

22i

5.2.3 Mechanistic investigation

To prove the involvement of only one catalyst molecule in the catalytic cycle, the alcoholytic ring opening (with allyl alcohol) of the phenylalanine-derived azlactone *rac*-**22d** (Scheme 5.28) was conducted in the presence of catalyst **9** with varying enantiomeric purities.

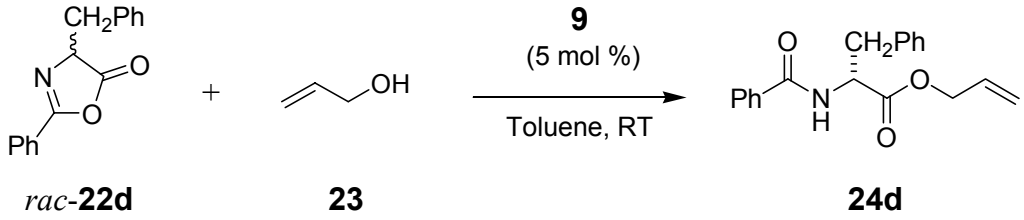

rac-**22d** **23** **24d**

Scheme 5.28 Alcoholytic DKR of phenylalanine-derived azlactone *rac*-**22d**.

A linear relationship was found between ee of the catalyst **9** and ee of the product **24d** (Figure 5.7).

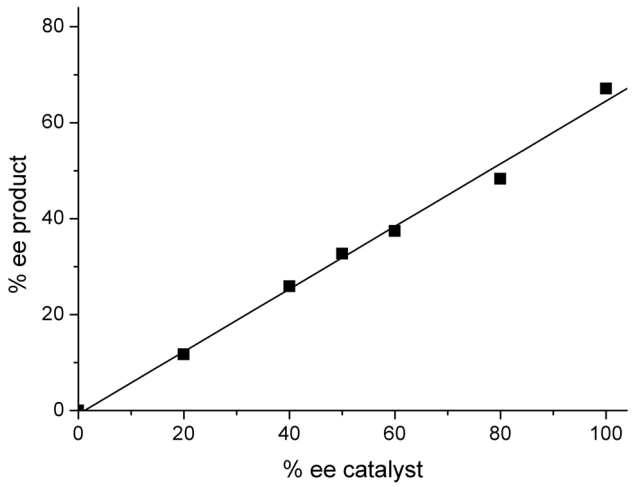

Figure 5.7 Relationship between catalyst ee and product ee in the DKR of *rac*-**22d** with **9**.

Interaction between substrate azlactone and (thio)urea moiety of the catalyst was supported by the NMR-titration of catalyst with substrate. In the ^{1}H-NMR spectrum, dramatic downfield shifts of the urea-NH protons of the catalyst **2** were observed upon addition of 1.0 equivalent of the dimethyl azlactone **22i** (Figure 5.8). In 1:1 mixture of **2** and **22i**, H_a was shifted by 3.34 ppm whereas the shift of H_b was found to be 3.66 ppm. Similar but much less pronounced shifts were also observed in case of the alanine-derived azlactone **22f** ($\Delta\delta_{Ha}$ = 0.40 ppm, $\Delta\delta_{Hb}$ = 0.19 ppm) and almost no shifts were observed in case of the phenylalanine-derived azlactone **22d** ($\Delta\delta_{Ha}$ = 0.01 ppm,

$\Delta\delta_{Hb}$ = 0.01 ppm). In addition to the urea-NH protons, other catalyst signals were also shifted downfield, particularly in the case of dimethyl azlactone **22i** (Figure 5.8).

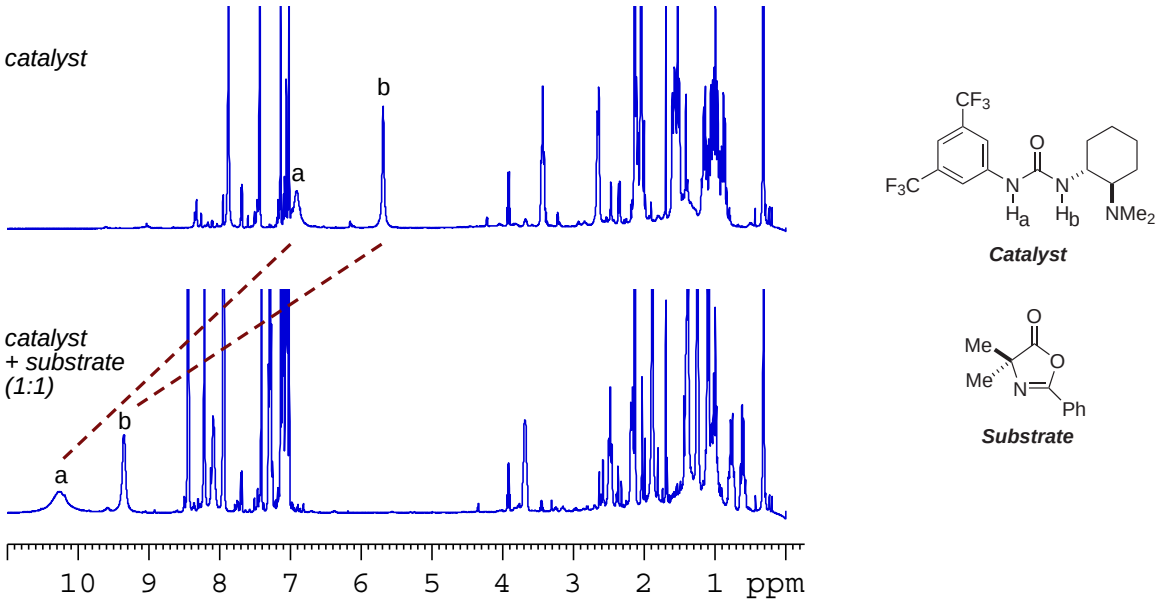

Figure 5.8 ^{1}H-NMR spectrum of the free catalyst and the 1:1 substrate-catalyst mixture.

5.3 Kinetic resolution of oxazinones

5.3.1 Catalyst screening

All catalysis experiments were conducted by *F. Cleemann* with the substrates synthesized by himself. Alcoholytic ring opening of the *β*-phenylalanine derived oxazinone *rac*-**25a** was used as

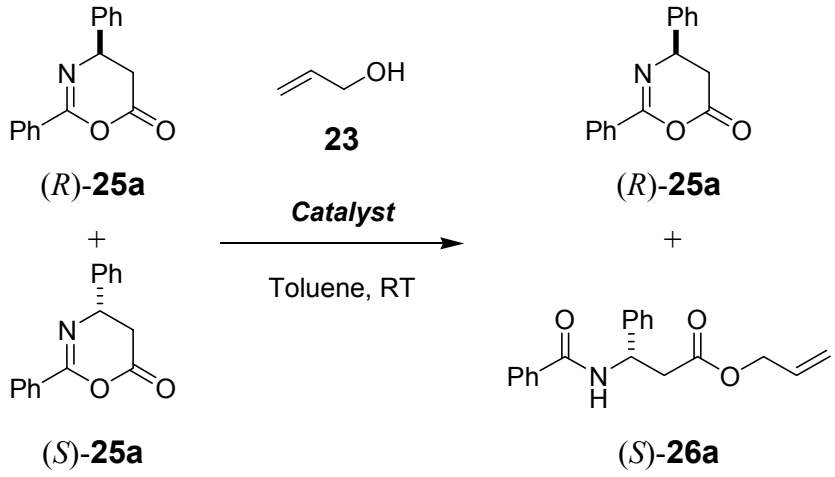

Scheme 5.29 Ring opening of *β*-phenylalanine derived oxazinone *rac*-**25a** with allyl alcohol.

the test reaction (Scheme 5.29). Allyl alcohol **23** was used as the nucleophile in all screening experiments due to its superior behaviour over all other alcohol nucleophiles studied. Similarly, toluene was found to be the optimal solvent. All catalysis experiments were carried out at room temperature using 1.0 equivalent of allyl alcohol.

Only the two most enantiodifferentiating thiourea-based bifunctional catalysts **18** and **9** for the DKR of azlactones (see Table 5.4, page 72) were screened for the ring opening of *rac*-**25a**. The results are summarized in Table 5.6.

Table 5.6 Catalyst screening for the ring opening of *rac*-**25a** with allyl alcohol.

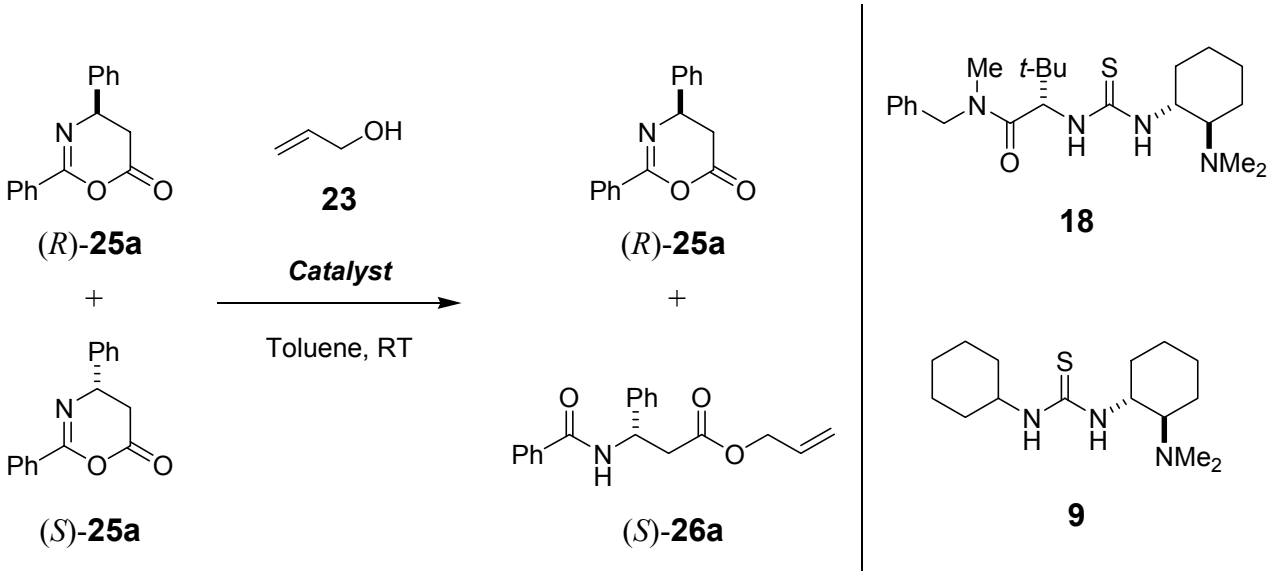

Entry	Catalyst	Loading (mol %)	Time (h)	% Conversion	% ee **25a**	% ee **26a**
1	**18**	5	6.5	57	99	86
2	**9**	5	12	59	97	81
3	**18**	10	4.5	57	>99	84
4	**18**	2.5	26	61	98	87
5[a]	**18**	1	10	61	98	85

[a] This reaction was carried out with a substrate concentration of 0.5 M; 0.1 M in all other cases.

In the presence of 5 mol % of the catalyst **18**, at 57 % conversion, the (*S*)-enantiomer of the oxazinone *rac*-**25a** was consumed almost completely (99 % ee in favor of the remaining (*R*)-enantiomer), and the enantiomeric excess of the product (*S*)-**26a** was found to be 86 % (Entry 1). From these data, the selectivity factor *S* of the reaction was calculated to be 68. Somewhat lower selectivity and activity were observed when the same amount of the cyclohexyl-

substituted bifunctional catalyst **9** was used (Entry 2). Clearly, **18** is the superior catalyst in this reaction. An increase in the catalyst loading to 10 mol % decreased the reaction time to 4.5 h, without affecting selectivity (Entry 3). At lower catalyst loading of 2.5 mol %, the reaction time was longer but the selectivity remained virtually unaffected (Entry 4). At higher substrate concentration (0.5 M instead of 0.1 M) even 1 mol % catalyst is sufficient to catalyze the reaction effectively (Entry 5). However, 5 mol % of the catalyst **18** were used for all further experiments.

5.3.2 Substrate scope

A series of oxazinones derived from *β*-substituted *β*-amino acids with different steric and electronic demand was applied for the ring opening with allyl alcohol **23** in the presence of the bifunctional organocatalyst **18** (Table 5.7). Substrates include the electron poor *p*-chloro- and *p*-nitrophenyl substituted oxazinones **25b**-**c**, electron rich *p*-methoxyphenyl substituted oxazinone **25d** as well as

Table 5.7 Substrates tested in the KR of oxazinones.

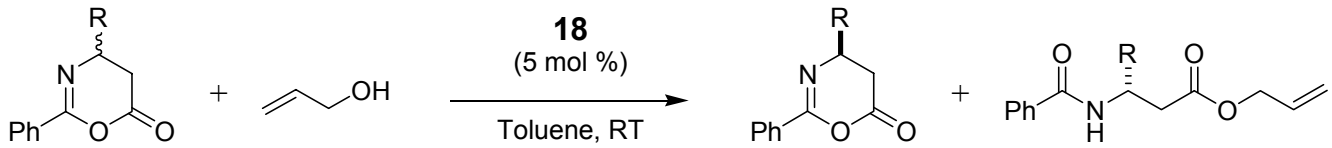

rac-**25a**-**f** **23** (*R*)-**25a**-**f** (*S*)-**26a**-**f**

Entry	Substrate	R	Time (h)	% Conversion	% ee **25**	% ee **26**
1	**25a**	Ph	6.5	57	99	86
2	**25b**	*p*-ClC_6H_4	15	59	99	83
3	**25c**	*m*-$NO_2C_6H_4$	3.0	64	99	81
4	**25d**	*p*-$OMeC_6H_4$	10.5	57	98	87
5	**25e**	*t*-Bu	48	54	97	82
6	**25f**	*i*-Pr	48	53	98	88

the alkyl substituted oxazinones **25e**-**f**. All substrates were resolved with high degree of enantioselectivities. In the presence of 5 mol % of the catalyst **18**, the oxazinones (*R*)-**25a**-**f** were generally recovered with excellent enantiomeric excess (>97 % ee) whereas the esters (*S*)-**26a**-**f** were still produced with 80-90 % ee.

5.4 Synthesis of oxazaborolidines and their precursors

The precursors for the chiral oxazaborolidines **29** are chiral *α*,*α*-diarylprolinol **97** and achiral boronic acid **98** or its dehydration product cyclic boroxine **151** (Scheme 5.30).

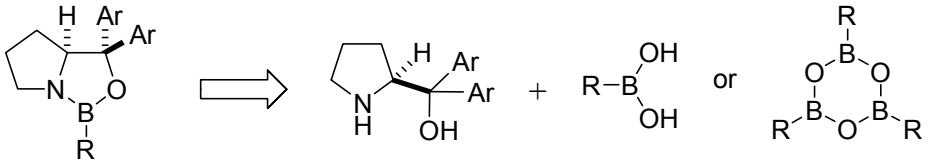

29 **97** **98** **151**

Scheme 5.30 Retrosynthesis of chiral oxazaborolidines **29**.

The chiral *α*,*α*-diarylprolinols were synthesized from the chiral pool compound L-proline **37** according to a modified literature procedure.[152] The synthesis began with the protection of both the amine as well as the acid functionality, which was achieved in one step by heating L-proline **37** with benzyl chloride **152** in DMF (Scheme 5.31). The *N*,*C*-doubly protected proline **153** was obtained in excellent yield.

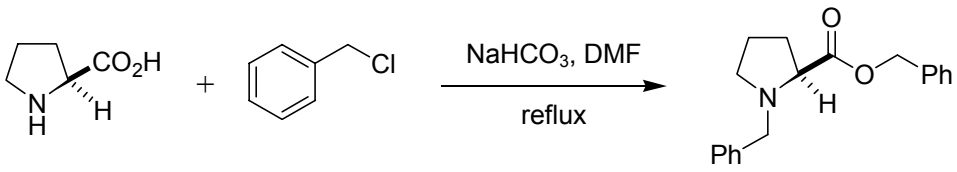

37 **152** **153**, 99 %

Scheme 5.31 Double protection of L-proline by benzylation with benzyl chloride.

Addition of the appropriate *Grignard* reagent to the ester **153** then gave *N*-benzylated *α*,*α*-diarylprolinols in moderate to excellent yields (Scheme 5.32).

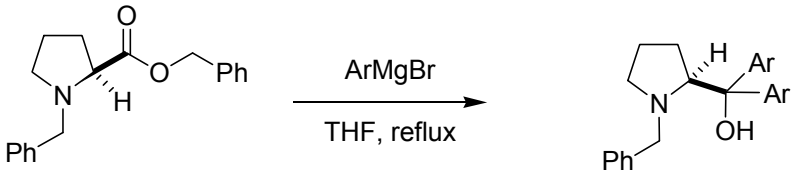

153

154a, Ar = Ph, 80 %

154b, Ar = *m*-Xyl, >99 %

154c, Ar = 2-naphthyl, 64 %

Scheme 5.32 Addition of aryl-*Grignard* to the ester **153**.

The *N*-benzyl group was then removed by hydrogenolysis to obtain the *α*,*α*-diarylprolinols in moderate to very good yields (Scheme 5.33).

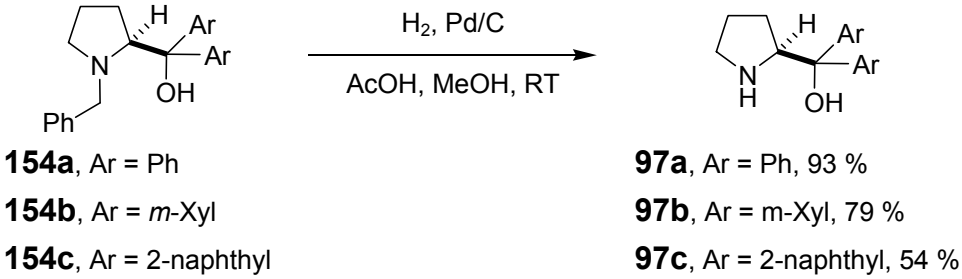

154a, Ar = Ph
154b, Ar = *m*-Xyl
154c, Ar = 2-naphthyl

97a, Ar = Ph, 93 %
97b, Ar = m-Xyl, 79 %
97c, Ar = 2-naphthyl, 54 %

Scheme 5.33 Hydrogenolysis of the *N*-benzyl groups of *N*-benzylated *α*,*α*-diarylprolinols.

The *α*,*α*-diphenylprolinol **97a** was crystallized from *n*-heptane to obtain colourless crystals which were appropriate for X-ray diffraction. The X-ray structure was determined (Figure 5.9).

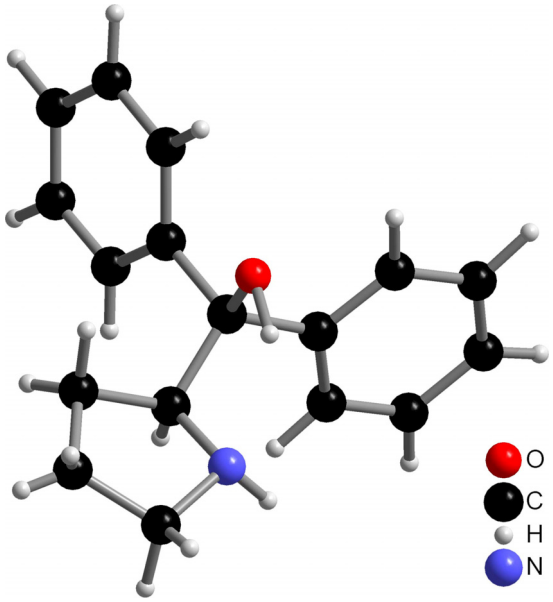

Figure 5.9 X-ray structure of (*S*)-*α*,*α*-diphenyl-2-pyrrolidin methanol **97a**.

Having synthesized the chiral *α*,*α*-diarylprolinols, the next target was the achiral boron unit. Several boronic acids are commercially available and also the oxazaborolidine **29a** (Ar = Ph, R = Me). For this work, only the boronic acids with aromatic substituents on the boron atom were employed. The cyclic boroxines **151a-b** were prepared from phenylboronic acid **98a** and *o*-tolyl boronic acid **98b** by dehydration *via* azeotropic distillation with toluene in a *Dean-Stark* apparatus (Scheme 5.34). The products were obtained in quantitative yield.

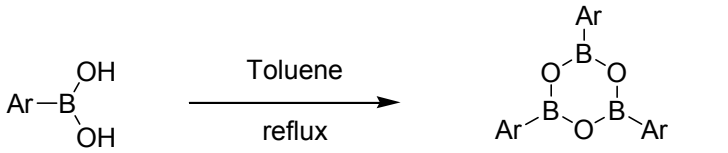

98a, Ar = Ph — **151a**, Ar = Ph, 100 %

98b, Ar = *o*-tol — **151b**, Ar = *o*-tol, 100 %

Scheme 5.34 Cyclodehydration of boronic acids to boroxines.

The triphenyl boroxine **151a** was crystallized from an *n*-hexane/toluene mixture to obtain X-ray diffraction quality crystals (Figure 5.10).

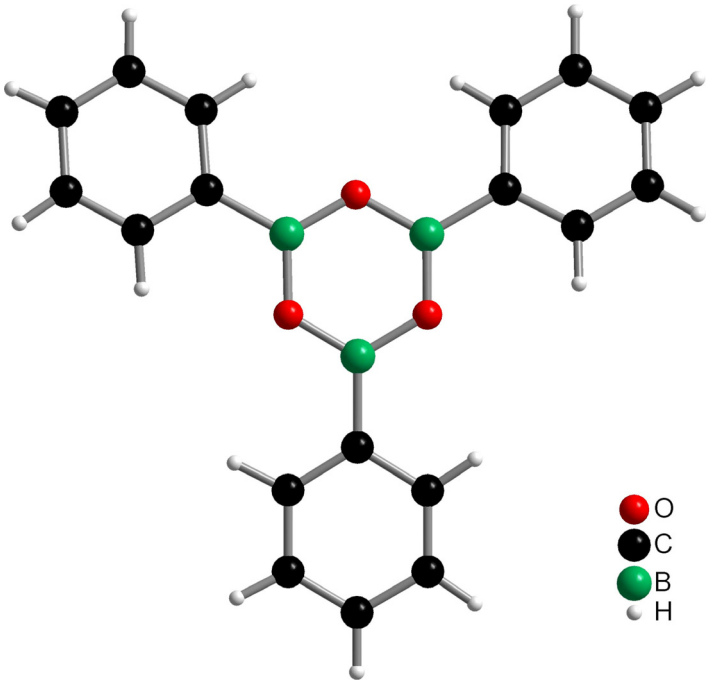

Figure 5.10 X-ray structure of triphenyl boroxine **151a**.

The oxazaborolidines **29b-c** were then prepared by condensation of *α,α*-diarylprolinols and triaryl boroxines following a literature procedure (Scheme 5.35).[138] The products were obtained in quantitative yield.

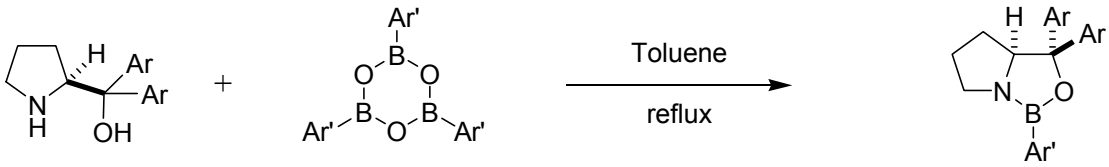

97a, Ar = Ph — **151a**, Ar′ = Ph — **29b**, Ar = Ph, Ar′ = Ph, 99 %

97b, Ar = m-Xyl — **151b**, Ar′ = *o*-tol — **29c**, Ar = *m*-Xyl, Ar′ = *o*-tol, 99 %

Scheme 5.35 Synthesis of oxazaborolidines.

In catalysis experiments where protonated oxazaborolidines (oxazaborolidinium cations) were employed as the catalysts, protonation of oxazaboroldines was conducted *in situ* with trifluoromethanesulfonic acid (TfOH = CF_3SO_3H).

5.5 Asymmetric hydrocyanation of imines

5.5.1 Preparation of imines

The imines were prepared from aldehydes and primary amines following a modified literature procedure (Scheme 5.36).[153] In most of the cases, the products were obtained in quantitative yields.

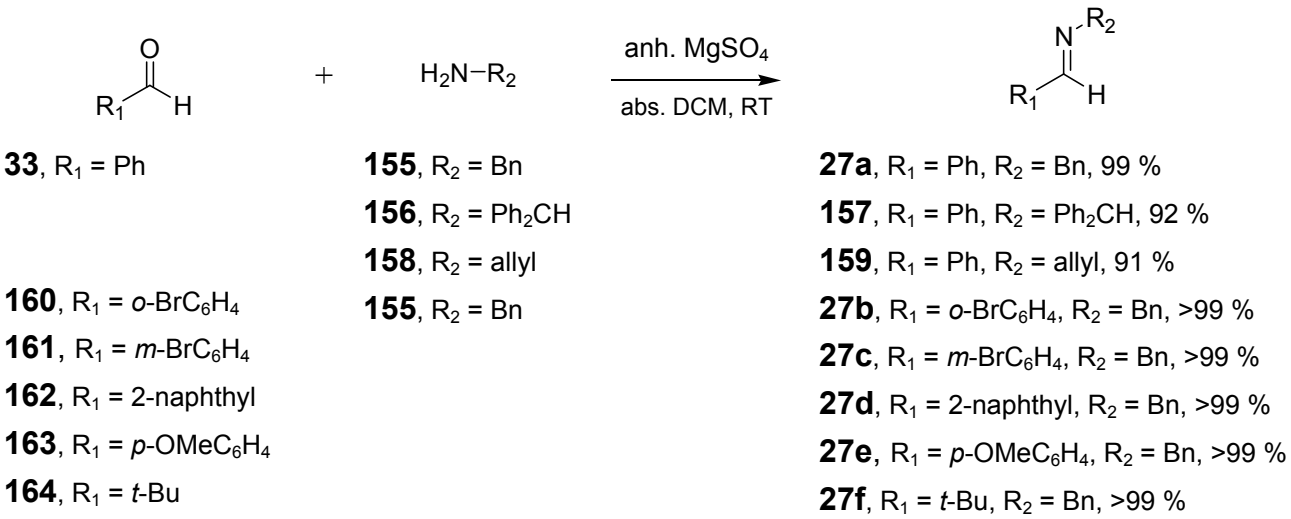

Scheme 5.36 Preparation of imines.

5.5.2 Catalyst screening and optimization of reaction conditions

The hydrocyanation of *N*-benzyl-benzylidene imine **27a** (see scheme in Table 5.8) was chosen as the test reaction. 1.5 equivalents of HCN (generated from TMSCN and MeOH) were used in each case. First, the neutral oxazaborolidines (Scheme 5.37) were used as catalysts.

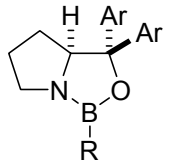

29a, Ar = Ph, R = Me
29b, Ar = Ph, R = Ph
29c, Ar = *m*-Xyl, R = *o*-tol

Scheme 5.37 Neutral oxazaborolidines **29**.

The results of the catalyst screening and the optimization of the reaction conditions are summarized in Table 5.8.

Table 5.8 Optimization of reaction conditions and screening of neutral oxazaborolidines **29**.

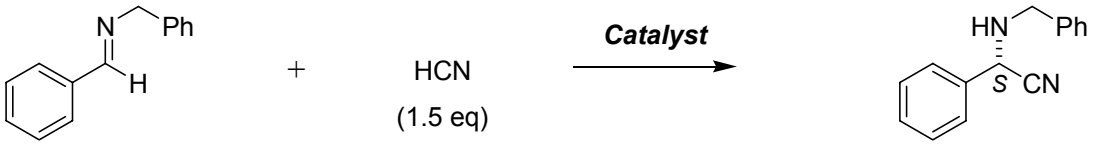

27a **28a**

Entry	Catalyst	Loading (mol %)	Solvent	Temperature (°C)	Time (h)	% Conversion	% ee
1	-	-	toluene	–25	24	28	-
2	**29a**	20	toluene	–25	24	94	71
3	**29a**	20	toluene	–78	24	<2	nd
4	**29a**	30	toluene	–25	24	99	72
5	**29a**	10	toluene	–25	24	95	62
6	**29b**	20	toluene	–25	24	98	70
7	**29c**	20	toluene	–25	24	>99	73
8	**29a**	20	CH_2Cl_2	–25	8	95	39

Initial investigations showed that in the presence of 20 mol % of oxazaborolidine **29a**, *N*-benzyl-benzylidene imine **27a** undergoes facile hydrocyanation at –25 °C in toluene to produce the *α*-amino nitrile **28a**. After 24 hours, 94 % conversion was obtained with 71 % ee in favour of the (*S*)-enantiomer (Entry 2). The absolute configuration of the product *α*-amino nitrile was determined by comparing the sense of optical rotation with literature data.[154] Interestingly, at this temperature the imine **27a** undergoes significant hydrocyanation without any catalyst (Entry 1). The background reaction was completely suppressed at –78 °C, but 20 mol % **29a** did not produce any conversion to **28a** at this temperature either, even after 24 hours (Entry 3). Little conversion was observed when TMSCN was used as the cyanide source. Increasing the amount of catalyst to

30 mol % (at –25 °C) did not increase the enantioselectivity (Entry 4), but with lowering the catalyst loading to 10 mol %, the ee dropped considerably (Entry 5). Similar conversions were obtained in both cases (Entry 4 and 5). Using 20 mol % of **29b** or **29c** as catalysts, conversions and ees similar as with **29a** were obtained (Entry 6 and 7). The solution became turbid and a white solid precipitated upon addition of HCN to a solution of imine and oxazaborolidines in toluene. In the case of oxazaborolidine **29b** the solid was isolated and crystallized from dichloromethane to obtain

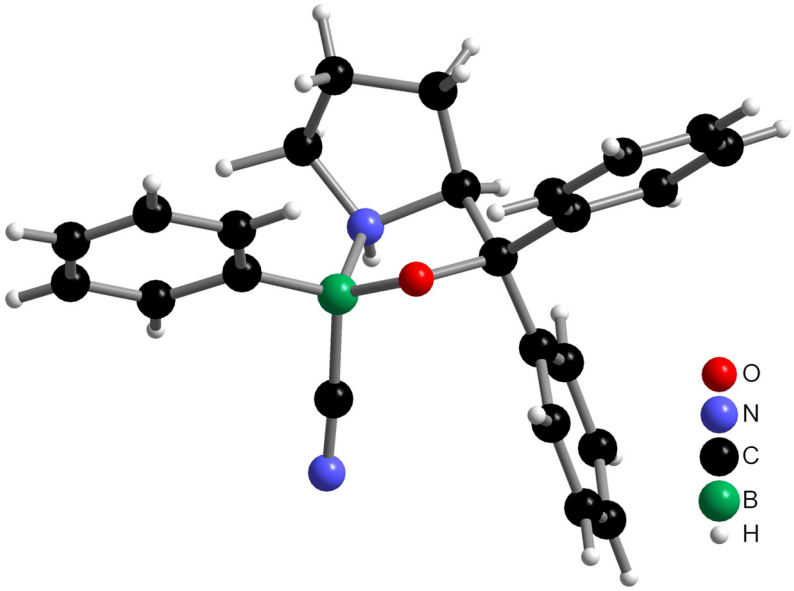

Figure 5.11 X-ray structure of the HCN-adduct **29b·HCN**.

X-ray diffraction quality crystals. The X-ray structure revealed this solid as the HCN-adduct of **29b** (Figure 5.11). When this solid was used as the catalyst in the hydrocyanation reaction, only little hydrocyanation product was detected. No such precipitation was observed when the reaction was conducted in dichloromethane; using 20 mol % of **29a**, the conversion was found to be almost complete within 8 hours (Table 5.8, Entry 8). However, the enantioselectivity obtained in this case was only 39 % ee.

The *N*-substituents of the imine were then screened using 20 mol % of **29a** at –25 °C in toluene. The results are summarized in Table 5.9.

Table 5.9 Screening of the *N*-substituents of the imines.

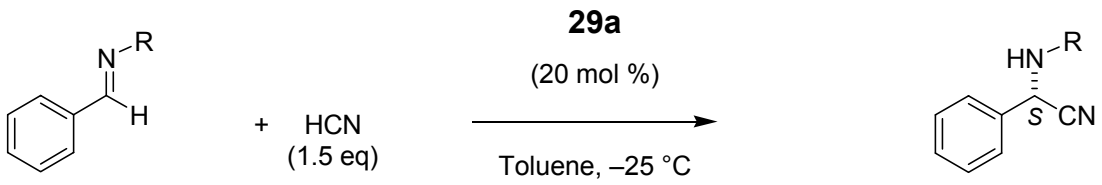

Entry	Substrate	R	Time (h)	% Conversion	% ee
1	**27a**	$PhCH_2$	24	94	71
2	**157**	Ph_2CH	24	<2	n.d.
3	**159**	Allyl	24	88	42

Clearly, the *N*-benzyl substituted imine **27a** is the best substrate for the hydrocyanation catalyzed by oxazaborolidines (Entry 1). The *N*-allyl substituted imine **159** gave fairly high conversion, but the enantioselectivity was found to be significantly lower (Entry 3). On the other hand, the *N*-benzhydryl substituted imine **157** was completely inactive in this reaction (Entry 2). Consequently, the *N*-benzyl substituted imines were used as substrates in all the following catalysis experiments.

After optimization of the substrate structure and the reaction conditions for the neutral oxazaborolidines **29**, the performance of protonated oxazaborolidines **30** i.e. oxazaborlidinium cations (Scheme 5.38) as catalyst were studied. The cationic species are known to show much higher catalytic activity than their neutral counterparts in the *Diels-Alder* reactions.[138, 139]

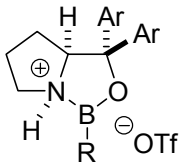

30a, Ar = Ph, R = Me
30b, Ar = Ph, R = Ph
30c, Ar = *m*-Xyl, R = *o*-tol

Scheme 5.38 Oxazaborolidinium cations **30**.

The results are summarized in Table 5.10.

Table 5.10 Optimization of reaction conditions and screening of cationic oxazaborolidines **30**.

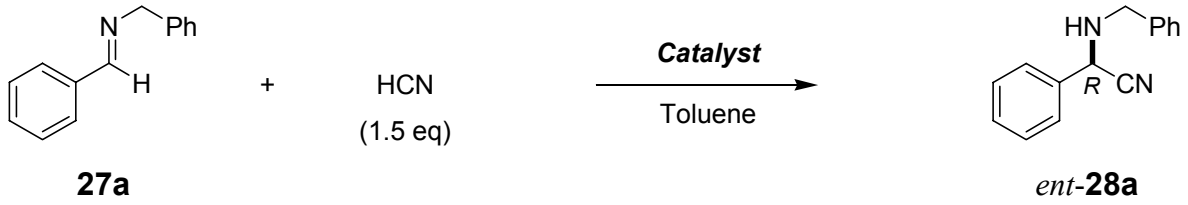

27a *ent*-**28a**

Entry	Catalyst	Loading (mol %)	Temperature (°C)	Time (h)	% Conversion	% ee
1	**30a**	20	–25	1.0	96	33
2	**30a**	20	–70	2.0	>99	38
3	**30b**	20	–70	2.0	97	35
4	**30c**	20	–70	2.0	98	39
5[a]	**30a**	20	–70	2.0	97	42
6[a]	**30a**	10	–70	2.0	95	42
7[a]	**30a**	5	–70	2.0	26	30

[a] HCN solution in toluene was added slowly *via* a syringe pump over a period of 40 mins.

Initial experiments have proven these cationic oxazaborolidines **30** to be extremely active catalysts for the hydrocyanation of imines: in the presence of 20 mol % of **30a**, the imine **27a** was completely consumed within 1 hour at –25 °C (Entry 1). The reaction time was shortened to 1 hour (cf. 24 hours with **29a**, see Table 5.8, page 83), but the enantioselectivity obtained in this case was only 33 % ee. Surprisingly, the sense of stereoinduction of the product amino nitrile obtained with catalyst **30a** was found to be opposite to the one obtained with neutral oxazaborolidine **29a** (see Table 5.8, page 83). Using the protonated catalyst **30a**, the (*R*)-enantiomer was formed in excess. Taking advantage of the short reaction time, the reaction was carried out at –70 °C. This time it took 2 hours for the reaction to reach completion and the enantioselectivity obtained in this case was slightly higher (Entry 2). With the catalysts **30b** and **30c**, not much improvement in enantioselectivity was observed (Entry 3 and 4). Enantioselectivity could be increased slightly by adding HCN slowly over a period of 40 minutes without affecting the conversion much. In the case of catalyst **30a** (20 mol %), slow addition of HCN afforded 42 % ee at –70 °C (Entry 5). Lowering the catalyst loading to 10 mol % affected neither the conversion nor the enantioselectivity (Entry 6). However, further lowering of the catalyst loading to 5 mol % decreased both the conversion and the enantioselectivity significantly (Entry 7). It is important to note that these oxazaborolidinium

cations are extremely moisture sensitive and the reactions needs to be performed under rigorous exclusion of moisture.

5.5.3 Substrate scope

Having optimized the catalyst structure for both neutral and cationic oxazaborolidines, several *N*-benzyl substituted imines were subjected to the hydrocyanation reaction under the established

Table 5.11 Substrate scope for the asymmetric hydrocyanation of imines.

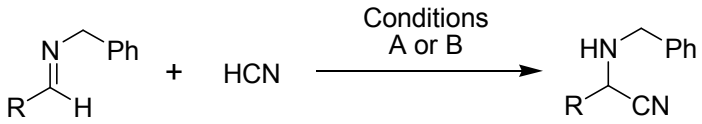

27a-f **28a-f**

Entry		Substrate	Condition[a]	Time (h)	% Conversion	% ee
1	**27a**	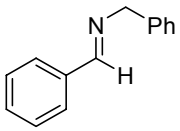	A	24	94	71 (*S*)
			B	2	95	42 (*R*)
2	**27b**	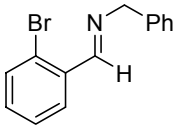	A	24	10	15 (*S*)
			B	2	97	10 (*R*)
3	**27c**	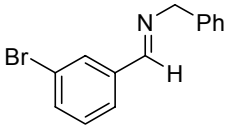	A	45	27	10 (*S*)
			B	2	98	8 (*R*)
4	**27d**	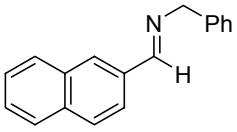	A	24	93	68 (*S*)
			B	2	95	33 (*R*)
5	**27e**	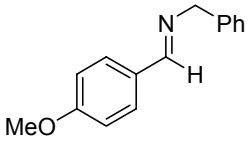	A	24	95	40 (*S*)
			B	3	75	10 (*R*)
6	**27f**	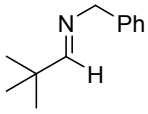	A	24	82	39 (*S*)
			B	3	76	*rac*

[a] Conditions A: 1.5 eq HCN, 20 mol % **29a**, –25 °C; Conditions B: 1.5 eq HCN, 10 mol % **30a**, –70 °C.

reaction conditions (A and B, Table 5.11) to prove the rather general substrate scope of this *protonation-induced switch of the sense of induction* process. The results are summarized in Table 5.11. Reversal of the sense of stereoinduction upon catalyst protonation was observed in all cases (A and B, Table 5.11). For example, the imine **27a** furnished 71 % ee in favour of the (*S*)-enantiomer with free oxazaborolidine **29a** (Conditions A), whereas 42 % ee in favour of (*R*)-enantiomer was obtained with protonated oxazaborolidine **30a** (Conditions B) (Entry 1). Although this trend was also observed with bromo-substituted imines **27b** and **27c**, the enantioselectivities were very low under both conditions (Entry 2 and 3). However, the difference in the catalytic activities of the neutral and the cationic oxazaborolidines are evidenced also in the conversions obtained for these two substrates. In the case of 2-naphthaldehyde derived imine **27d**, the (*S*)-enantiomer was obtained in 68 % ee under conditions A with 93 % conversion after 24 hours. Changing the reaction conditions to B produced 33 % ee in favour of the (*R*)-enantiomer (Entry 4). *p*-Methoxy benzaldehyde derived imine **27e** showed significantly lower enantiomeric excesses with both neutral and protonated catalyst, 40 % and 10 % respectively (Entry 5). A similar tendency was observed in the case of the pivalaldehyde derived imine **27f** except the fact that racemic product was obtained under conditions B (Entry 6).

5.6 Synthesis and application of a new tridentate ligand system

5.6.1 Synthesis of tridentate ligands

The precursors for the new tridentate ligands **31** are chiral α,α-diarylprolinols **97** and achiral salicylaldehyde derivatives **100** (Scheme 5.39).

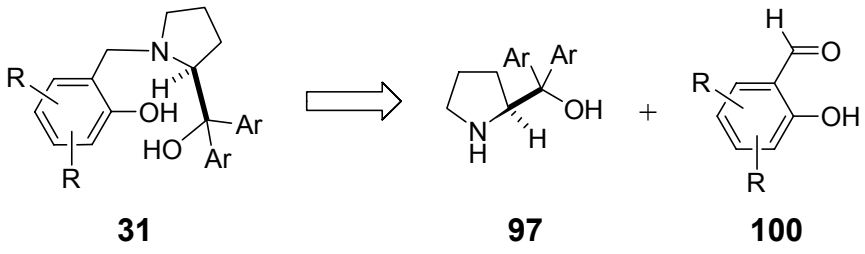

31 **97** **100**

Scheme 5.39 Retrosynthetic analysis of the new tridentate ligand **31**.

The ligands were synthesized by C–N bond formation using the reductive amination strategy. For the current study, 2,4-disubstituted salicylaldehyde derivatives **100a-c** were used as the aldehyde component and chiral *α*,*α*-diphenylprolinol **97a** was used as the secondary amine component (Scheme 5.40). The ligands were obtained in moderate to good yields.

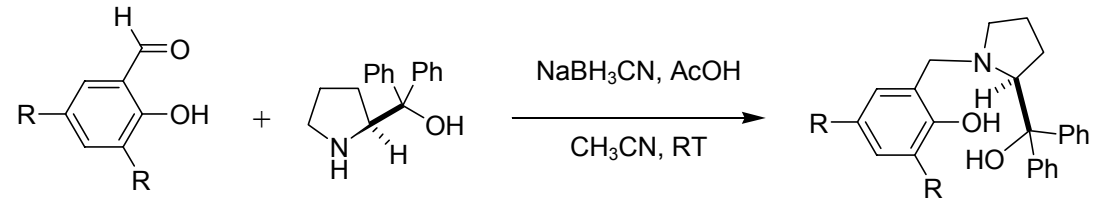

100a, R = *t*-Bu
100b, R = I
100c, R = Br

97a

31a, R = *t*-Bu, 46 %
31b, R = I, 70 %
31c, R = Br, 65 %

Scheme 5.40 Synthesis of the tridentate ligands **31**.

The *tert*-butyl substituted ligand **31a** was crystallized from ethanol to obtain X-ray diffraction quality crystals. X-ray structure of the ligand was determined (Figure 5.12).

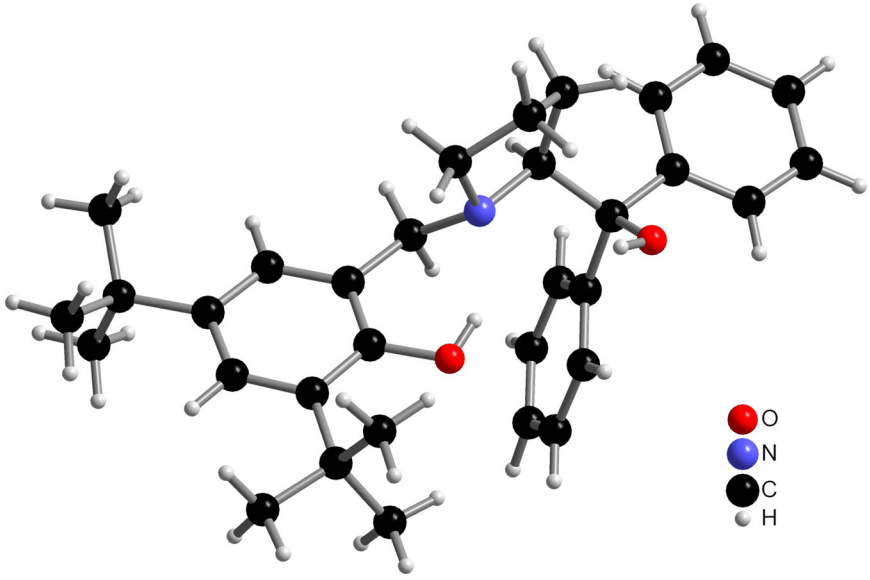

Figure 5.12 X-ray structure of the tridentate ligand 2,4-di-*tert*-butyl-6-{(*S*)-2-(hydroxydiphenyl-methyl)pyrrolidin-1-yl-methyl}phenol **31a**.

5.6.2 Preparation of an aluminium-complex and its application for the asymmetric hydrocyanation of aldehydes

To demonstrate the potential of this new ligand system, an aluminium complex of the ligand **31a** was synthesized by stirring the ligand with dimethylaluminium chloride in abs. toluene (Scheme 5.41). The aluminium-complex of a similar but C_2-symmetric ligand (see Scheme 4.11, page 52) has previously been reported by *Trost* et al. for the asymmetric cyanosilylation of aldehydes.[155]

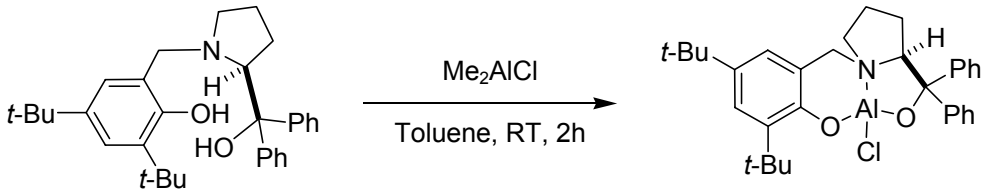

31a **32**

Scheme 5.41 Preparation of the proposed aluminium complex of the tridentage ligand **31a**.

The complex **32** was not isolated and characterized; hence the structure shown in Scheme 5.41 is only a logical speculation. The aluminium-complex in solution was applied immediately for the hydrocyanation of benzaldehyde **33** (Scheme 5.42).[156]

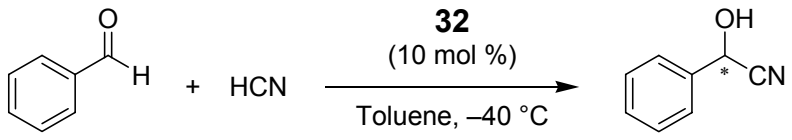

33 **34**

Scheme 5.42 Asymmetric hydrocyanation of benzaldehyde with **32**.

In the presence of 10 mol % of the complex **32** at –40 °C, benzaldehyde **33** was completely converted into the cyanohydrin **34** within 17 hours. The enantioselectivity of the product cyanohydrin **34** was found to be only moderate (50 % ee).

6 Discussion

6.1 Synthesis of bifunctional organocatalysts

The (thio)urea based bifunctional organocatalysts **1**-**21** as well as the guanidine derivatives **148** and **150** (see structure table, page 247) were synthesized using enantiomerically pure *trans*-1,2-diaminocyclohexane **102** as the chiral backbone. In most cases, the desired products were obtained in good to satisfying yields. Although the parent catalyst **1** could be synthesized *via* a shorter route by monothiourea formation followed by dimethylation (Scheme 6.1), the longer route with the

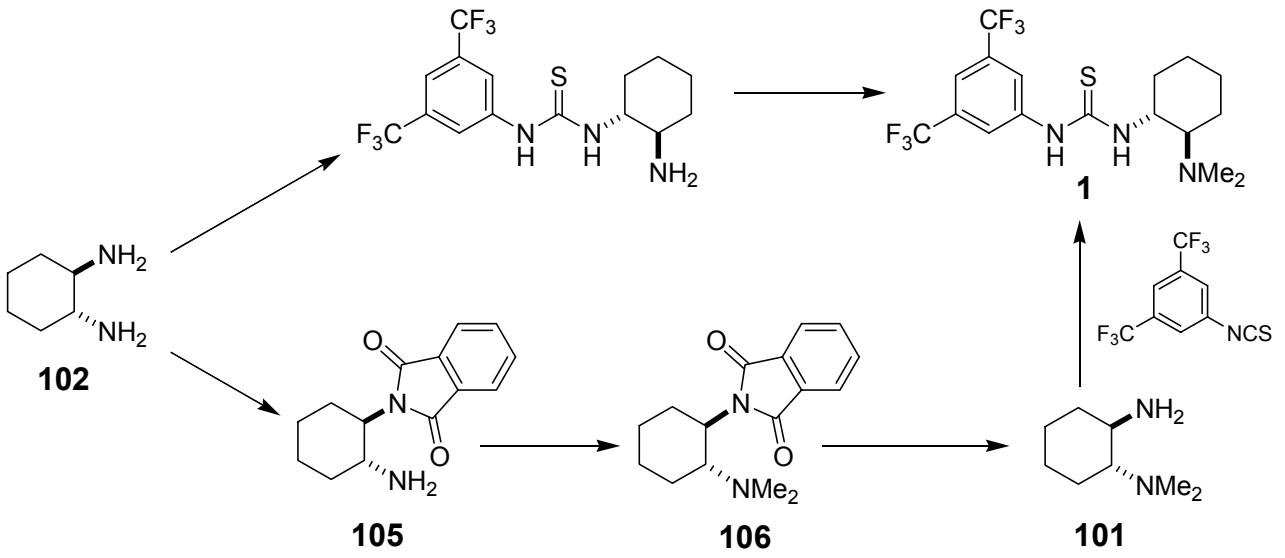

Scheme 6.1 Two different routes to the catalyst **1** from the diamine **102**.

protection-deprotection sequence was followed due to the general applicability of this route: the direct monourea formation from the diamine **102** is not possible as in most cases the bis-urea is the major, if not the exclusive product.[157] Furthermore, the selective alkylation of the amine by alkyl halides is not possible without alkylation of the thiourea NHs.

6.2 Dynamic kinetic resolution of azlactones

Highly efficient alcoholytic ring opening of azlactones was effected with the bifunctional organocatalyst **18** (see structure table). The level of enantioselectivity of the product esters obtained

is the highest ever achieved in the chemically catalyzed DKR of azlactones.[150, 151] A fairly broad range of azlactones containing both aliphatic and aromatic substituents was employed in the DKR. In these bifunctional organocatalysts, the quasi-*Lewis* acidic (thio)urea moiety is responsible for the substrate (azlactone) activation whereas the *Brønsted* basic tertiary amine activates the alcohol by hydrogen bonding. The activation of azlactones occurs by bridging hydrogen bonding from the (thio)urea hydrogens as evidenced from the similar downfield shifts of both the urea hydrogens in the NMR-titrations (see section 5.2.3, page 75). The hydrogen-bond donor ability of the (thio)ureas towards carbonyl acceptors is well-known in the literature[28] and was also observed, particularly in the case of the urea-based bifunctional organocatalysts employed in this work. For example, in the X-ray structure of **2**, intermolecular hydrogen bonds exist between the urea N–H groups of one molecule and the urea oxygen atom of a neighbouring molecule (Figure 6.1). The lengths of these two hydrogen bonds are 2.05 and 2.30 Å, respectively. The urea moiety of **2** is planar, and the

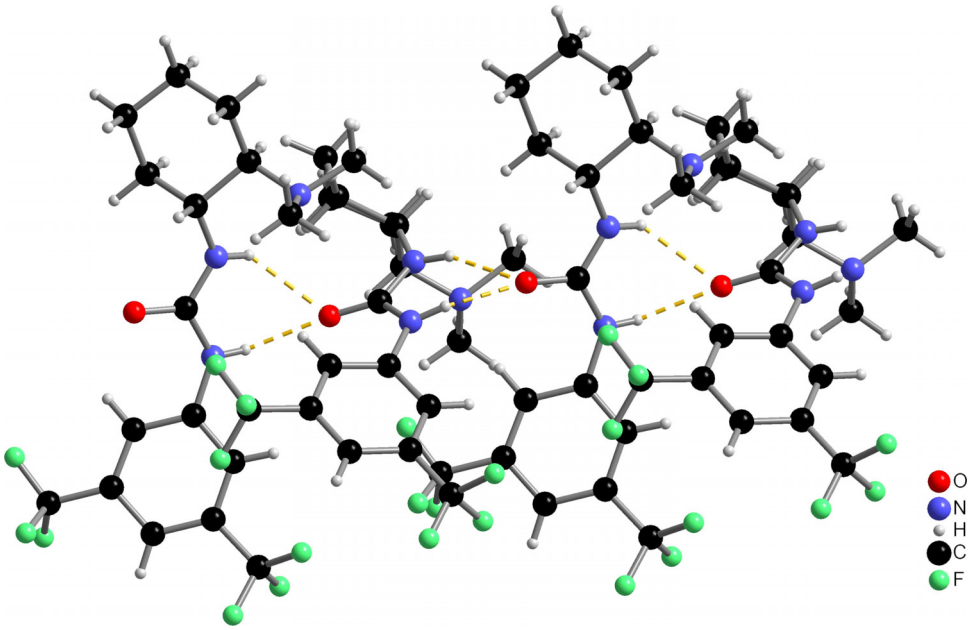

Figure 6.1 Intermolecular bifurcated hydrogen bonding in **2**.

planes of the urea moieties of neighbouring molecules intersect at an angle of about 80°. However, in contrast to the explanation (for higher solubility of such bifunctional catalysts in non-polar solvents) by *Takemoto* et al.,[53] no intra- or intermolecular H-bonds from the urea to the *Brønsted*-basic tertiary amine moietiy were observed. Such hydrogen bonding would "neutralize" the bifunctional character of the catalyst and therefore would be detrimental for the catalytic activity. Again, from the work of *Jacobsen* et al. it is known that the imine nitrogen atom could also act as hydrogen bond acceptors and do so in a bifurcated manner where the imine plane remains perpendicular to the urea plane.[39] This is in contrast to the H-bond acceptor behavior of the

carbonyls where the carbonyl plane in most cases, tends to remain coplanar with the urea plane. This kind of co-planarity is clearly seen in the X-ray structure of **7** (Figure 6.2).

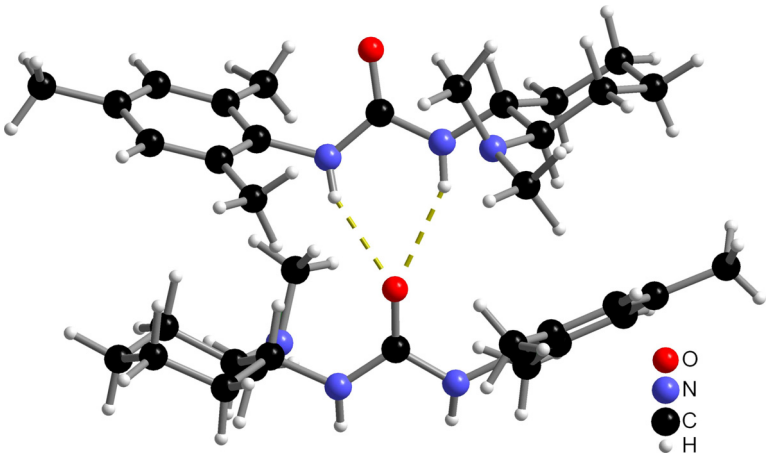

Figure 6.2 Co-planarity of the urea moieties in **7**.

Due to the presence of both a carbonyl and an imine functionality in the azlactone, its binding to the (thio)urea moiety of the catalyst can either occur *via* the carbonyl oxygen or the imine nitrogen atom. The absence of any non-linear effect (when the reaction was conducted with catalysts of varying ees) indicates the nature of the catalytically active species as monomeric.[158] Therefore, the possibility of substrate activation by more than one catalyst molecule can be ruled out. The monomeric nature of the catalyst was further supported by the molecular weight of the catalysts **1** and **2** determined by the vapour-pressure-osmometry method.[159] No evidence for the aggregated catalysts was obtained as the molecular weights of the catalysts **1** and **2** were found to be 503 (± 40) g/mol and 533 (± 30) g/mol respectively. Although the observed molecular weights are higher than those of the monomers, they are much lower than those for the dimers.

From the computational studies by *K. Etzenbach-Effers*,[160] it was found that in the absence of alcohol, the binary complex **A1** (where the binding occurs *via* the imine nitrogen) is energetically more favorable than the corresponding adduct (**A**) *via* the carbonyl oxygen (Scheme 6.2). But in the presence of alcohol, the binding mode of the substrate changes completely. In the ternary complex, the pattern of hydrogen bonding changes from bifurcated mode to the "normal" mode where both the carbonyl oxygen and the ring oxygen atom individually act as single H-bond acceptors (**B** and **B1**). In the ternary complex the alcohol is triggered by the tertiary amine towards the activated carbonyl carbon and the attack of the alcohol leads to the ring opening of azlactone to generate the zwitterion **C** and **C1**. The zwitterion **C** is energetically more favorable as compared to **C1** because **C1** suffers from severe charge separation. This also accounts for the higher stability of the ternary complex **B** and therefore the reaction proceeds via the pathway **A1** → **A** → **B** → **C**.

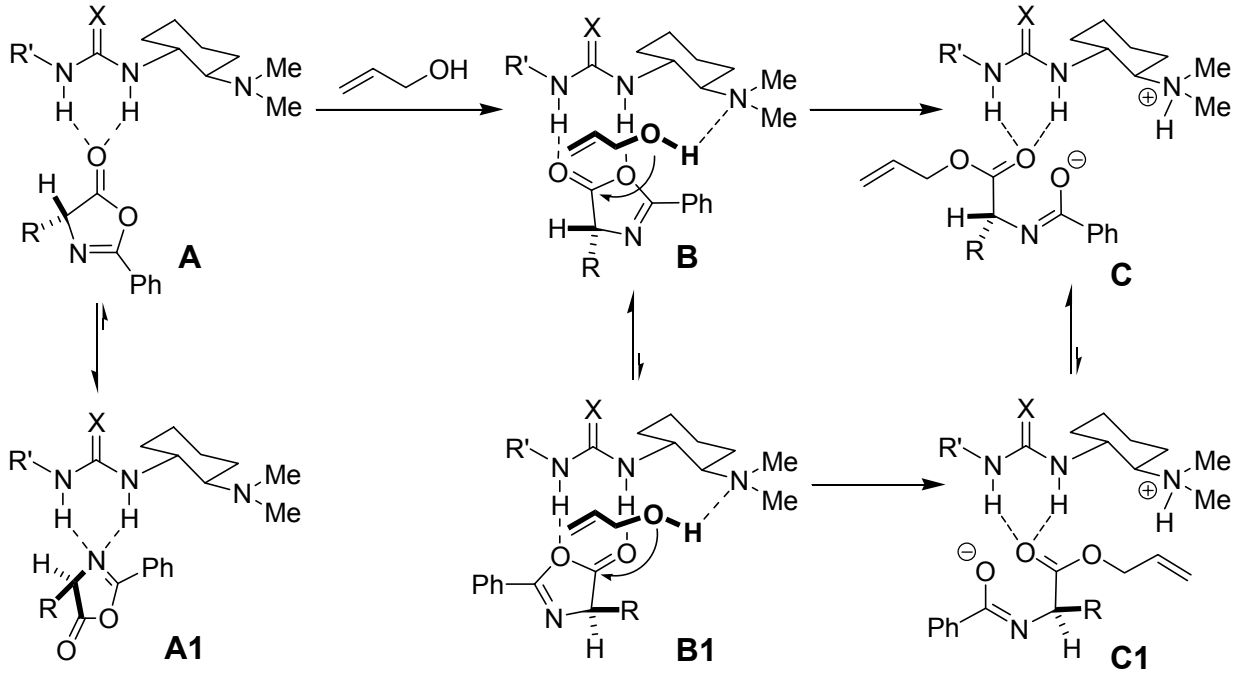

Scheme 6.2 Plausible mechanistic pathway for the DKR of azlactones.

Proton transfer from the tertiary nitrogen to the oxygen (in **C**) followed by tautomerization affords the product *N*-acyl *α*-amino acid ester **24** (Scheme 6.3).

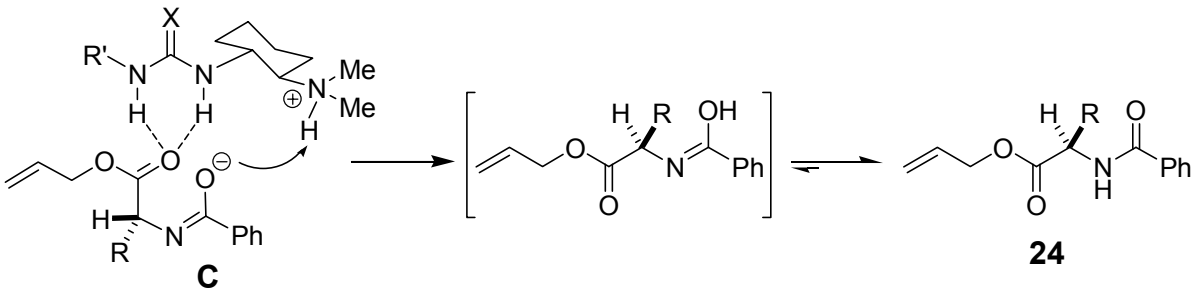

Scheme 6.3 Proton transfer in the zwitterion **C** followed by tautomerization to the product **24**.

The formation of the complex **A1** also explains the little shift of the urea hydrogens in the NMR-titration of the phenylalanine derived azlactone **22d**. Due to the steric bulk and the flexibility of the benzyl group, the binary complex (of type **A1**) of **22d** is less favorable than the binary complex of alanine derived azlactone **22f** and dimethyl azlactone **22i**. So, the binding constant of **22d** with **2** is expected to be much less than that of the other two azlactones (**22f** and **22i**).

Screening of the catalysts with different substitutents on the tertiary-amine part (Table 5.3, page 71) in the alcoholytic ring opening of the *tert*-leucine derived azlactone *rac*-**22a** (Scheme 6.4) revealed that dimethylamine is optimum for this part of the structure. An increase in steric bulk of the substituents led to a decrease in conversion and even more significantly in enantioselectivity.

Replacement of even one methyl group of the tertiary amine with a benzyl group in **5** is sufficient to deactivate the catalyst. Besides steric bulk, flexibility of the substituents is another decisive

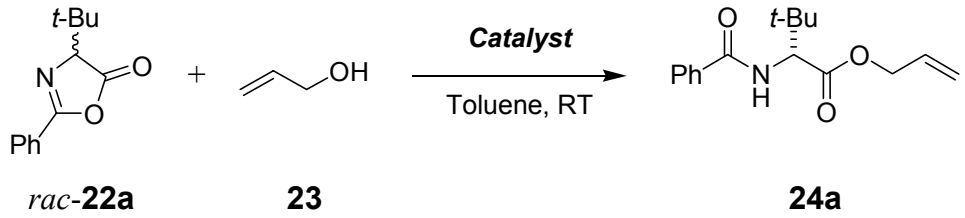

rac-**22a** **23** **24a**

Scheme 6.4 Alcoholytic DKR of tert-leucine derived azlactone *rac*-**22a**.

factor for catalytic efficiency. Although the diethylamine (in catalyst **3**) and pyrrolidine (in catalyst **4**) are expected to exert similar steric effect, the flexibility of the ethyl groups in diethyl catalyst **3** is the reason for its diminished catalytic activity. The rotation of the ethyl groups would hinder the substrate binding to the urea moiety and hence the activation. A similar steric effect of a diethylamino moiety (R' = Et) was previously demonstrated by *Wang* et al. for the *Morita-Baylis-Hillman* reaction (Scheme 6.5).[58]

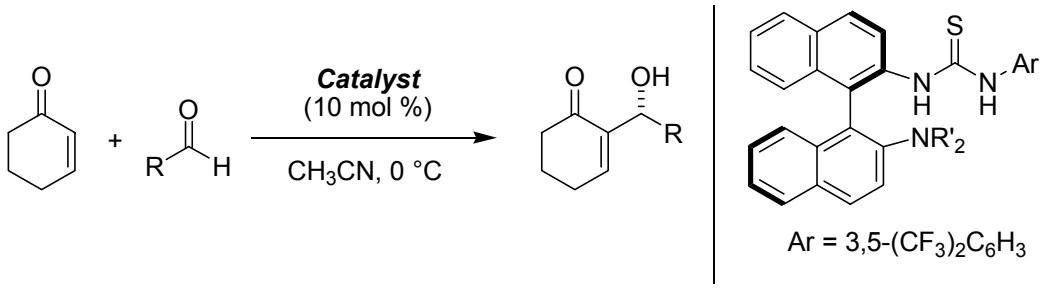

Scheme 6.5 Organocatalytic *Morita-Baylis-Hillman* reaction by *Wang* et al.[58]

The same explanation holds for the catalyst **5** with the benzyl group that needs even more space for its rotation and therefore would prevent the substrate binding completely.

The screening of the catalysts with various (thio)urea substituents (Table 5.4, page 72) in the aforementioned reaction showed the importance of the quasi-*Lewis* acidity of the (thio)urea moiety for the catalytic activity. The electron withdrawing substituents on the (thio)urea nitrogen would increase the quasi-*Lewis* acidity and would result in stronger activation. This effect was observed in the cases of the catalysts with electron-withdrawing substituents like 3,5-bis(trifluoromethyl)phenyl (in catalyst **1** and **2**) or 3,5-dinitrophenyl (in catalyst **6**). The opposite effect was observed in the cases of catalysts with electron rich substituents like mesityl (in catalyst **7**) or 3-pyridyl (in catalyst **8**). These catalysts afforded higher selectivities, but the conversions were significantly lower. In the

case of the mesityl-substituted catalyst **7**, an even lower reactivity was observed. This might be due to the methyl groups at the ortho positions of the aromatic ring that would further hinder the substrate binding. The aliphatic substituents in catalysts **9**, **10** and **11** showed an intermediate reactivity in between the two above cases. Interestingly, the C_2-symmetric catalyst **14** showed lower reactivity compared to the cyclohexyl-substituted catalyst **9**. This might be due to the presence of a bulky dimethylamino group on both sides of the thiourea moiety.

The *tert*-leucine and neopentylglycine derived catalysts in general afforded better enantioselectivities although the conversions were rather low. The diminished activity of the high enantioselective catalysts compared to the less-selective or non-selective catalysts is a common phenomenon in asymmetric catalysis. This is due to the reduction in the number of pathways that lead to the (undesired) product formation. Moreover, the presence of bulky *tert*-butyl or neopentyl groups close to the thioure moiety in these catalysts presumably hinder the H-bonding between the azlactone and the thiourea NHs. Considerably lower conversions and enantioselectivities were obtained with the catalyst **19** compared to its diastereomer **18** due to the *mismatched*-nature of the catalyst **19** (Scheme 6.6). This is the so-called *matched*-/*mismatched*-pairing of chiralities in the diastereomeric catalysts.

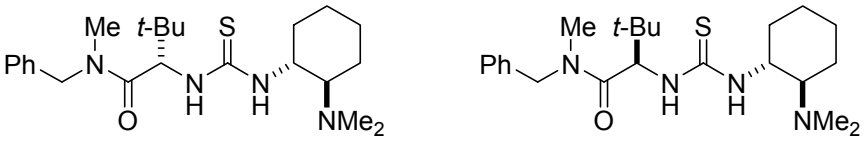

18, *matched* **19**, *mismatched*

Scheme 6.6 The *matched*- and *mismatched*-catalyst pair **18** and **19**.

The guanidine derivative **148** (see structure table, page 247) was proven to be a very active catalyst for this reaction although the enantioselectivity was found to be very low. This is not surprising, as the alcoholytic ring opening of azlactones is known to be effected by strong *Brønsted* bases like DMAP.[74] Guanidine derivatives are very strong bases (the pKa of guanidine is 13.6) and the distant positioning of the *Brønsted* basic guanidine site from the chiral center in catalyst **148** is unlikely to exhibit any stereodiscrimination between the azlactone enantiomers. Besides, the catalyst **148** does not posses any (quasi-*Lewis* acidic) binding/activation site for the substrate azlactones. In contrast, the guanidinium trifluroacetate **150** (see structure table) containing a quasi-*Lewis* acidic binding site was found to be catalytically inactive. Most likely the ion pairing between the guanidinium cation and the trifluoroactate anion prevents the binding and activation of neutral azlactone by the quasi-*Lewis* acidic NHs of the guanidinium cation. A neutral bifunctional

organocatalyst of type **148** with an electron deficient guanidine moiety should serve the purpose of double activation with efficient enantiodiscrimination (see section 7.1, page 102).

6.3 Kinetic resolution of oxazinones

The efficiency of the catalyst **18** for the alcoholytic ring opening of azlactones *via* DKR was logically extended to the alcoholytic ring opening of the *β*-amino acid analog oxazinones **25** (see section 5.3, page 76). The oxazinones are configurationally stable and therefore only one enantiomer underwent ring opening by alcohols selectively, i.e. kinetic resolution (KR) was observed. The other enantiomers of oxazinones were generally recovered with excellent enantiomeric excesses. A fairly broad range of oxazinones containing both aromatic and aliphatic substituents were employed for the KR.

Although achiral and enantiomerically pure oxazinones have been utilized in peptide chemistry for coupling to amino acid esters[161] as well as for the ring-opening polymerization reaction,[162] no catalytic ring opening reaction has been reported so far. Therefore, this is the first catalytic alcoholytic ring-opening of oxazinones with kinetic resolution.

The same sense of stereoinduction as well as similar level of enantioselectivities (as in the case of DKR of azlactones) observed for the KR of oxazinones point towards a similar mechanism for their alcholytic ring opening (Scheme 6.7). Attack of the alcohol (triggered by the *Brønsted* basic tertiary amine) to the thiourea-activated oxazinones generates the zwitterion **A**. Proton transfer from the tertiary nitrogen followed by tautomerization leads to the product *N*-acyl *β*-amino acid ester **26**.

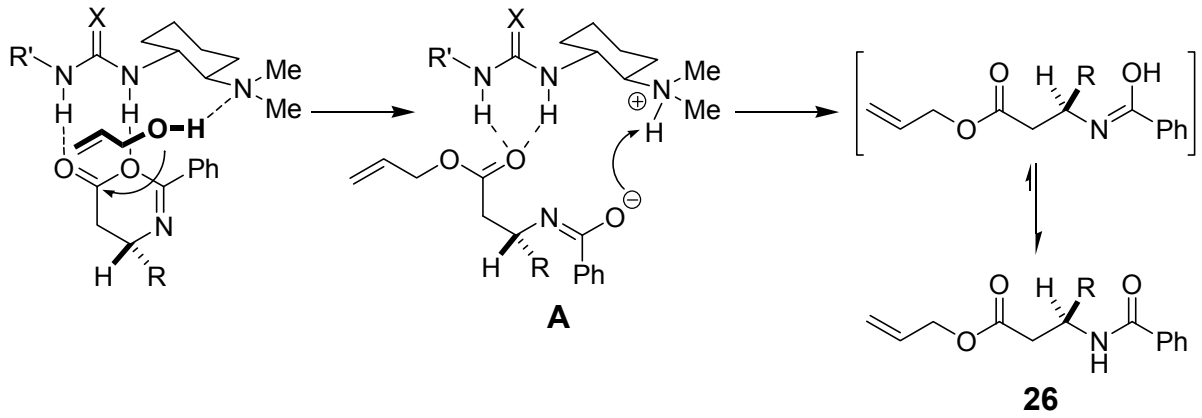

Scheme 6.7 Plausible mechanism for the alcoholytic ring opening of oxazinones.

6.4 Asymmetric hydrocyanation of imines

The asymmetric hydrocyanation of aldimines was carried out using neutral and protonated (cationic) oxazaborolidines as the catalysts **29a** and **30a** (see structure table), respectively. Low to moderate levels of enantioselectivity were obtained for a series of aromatic and aliphatic aldimines. In the case of the aromatic aldimines, the products with opposite sense of stereoinduction were obtained upon protonation of the catalyst (oxazaborolidine). This is the first successful application of oxazaborolidines and oxazaborolidinium cations for the asymmetric hydrocyanation of imines.

Although salt[163] and temperature-induced[164] reversal of stereoinductions were previously reported for different reactions, this is to the best of my knowledge the first example of protonation-induced reversal of stereoinduction.

Both in the oxazaborolidine and the oxazaborolidinium cation, the *Lewis* acidic boron atom can be regarded as the active center of the catalysts, and the activation of the imine occurs *via* coordination of the nitrogen lone pair of the imine to the *Lewis* acidic boron center. This is similar to the activation of prochiral ketones for the enantioselective reduction by borane (**I** in Scheme 6.8) as demonstrated by *Corey* et al.[45] The carbonyl and the imine group differ in the number of available

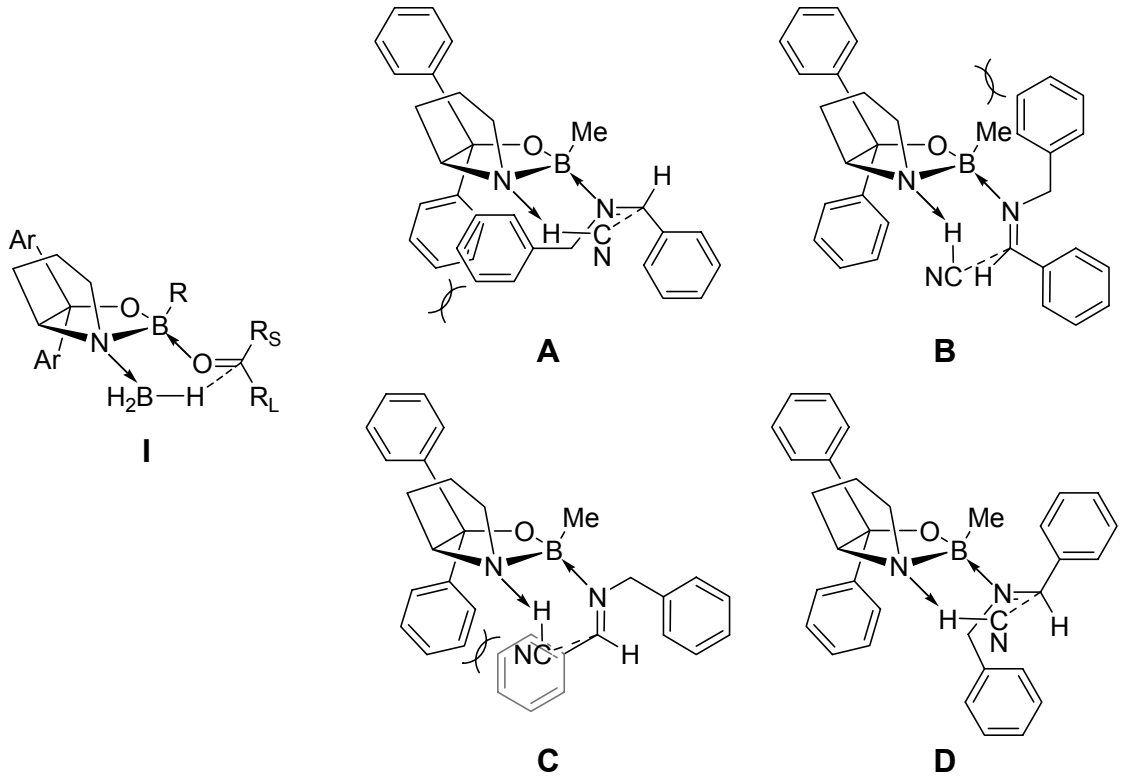

Scheme 6.8 Pre-transition-state assembly for the borane reduction of prochiral ketones (**I**) and four possible pre-transition-state assemblies for the hydrocyanation of imine by **29a**.

lone pairs for coordination: whereas the carbonyl oxygen has two lone pairs and therefore two coordination sites, the imine nitrogen atom provides only one lone pair of electrons. Moreover, imines can have two interconvertable stereoisomeric forms: *E* and *Z*.[39]

In the case of the neutral oxazaborolidine **29a**, assuming that the pre-transition-state assembly for the hydrocyanation of imine resembles that for the borane reduction of prochiral ketones, four possibilities of such an assembly exist (Scheme 6.8). In the pre-transition-state assembly **A** and **B**, the imine coordinates in the *Z*-configuration whereas in **C** and **D**, the coordination occurs in the *E*-configuration. Clearly, the most logical and likely pre-transition-state assembly is **D**, where the imine is coordinating in *E*-configuration and *cis* to the vicinal HCN. This manner of binding minimizes unfavorable steric interaction between the oxazaborolidine and the imine (like in **A**, **B** and **C**), and aligns the electrophlilic imine carbon atom and the coordinated HCN for stereoelectronically favorable, face-selective cyanide addition *via* a six-membered transition state to form the observed hydrocyanation adduct (*S*)-**28a** (Scheme 6.9).

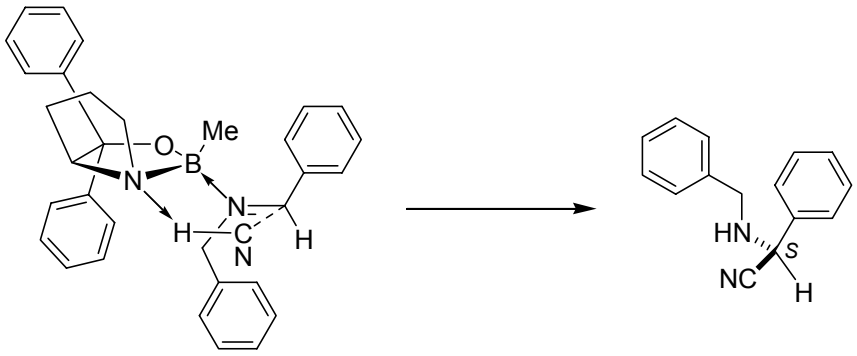

D (*S*)-**28a**

Scheme 6.9 Formation of (*S*)-**28a** from the pre-transition-state assembly **D**.

The activation of *Z*-imines by the catalyst **29a** should also be possible when the coordination of the *Z*-imine to the *Lewis* acidic boron center leads to an organized C–H···O hydrogen bonded complex

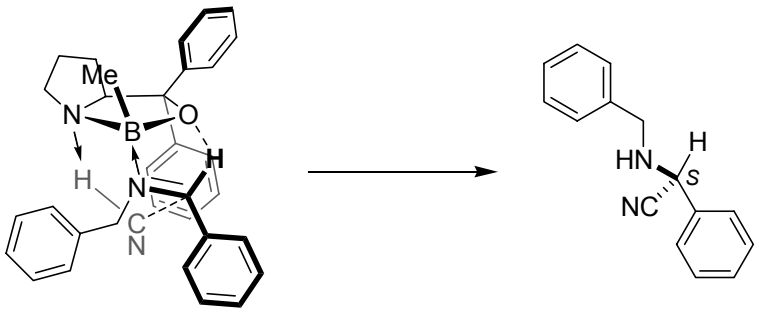

E (*S*)-**28a**

Scheme 6.10 Plausible pre-transition-state assembly **E** for the activation of *Z*-imine.

E (Scheme 6.10). Such hydrogen bonds are known to have a very important role in the enantioselective *Lewis* acid catalyzed reactions of aldehydes.[165] In this assembly **E**, tertiary nitrogen activated HCN attack should occur to the *re* face of the imine to produce (*S*)-*α*-amino nitrile (*S*)-**28a**. Neither the pre-transition-state assembly **D** nor **E** is possible for the imines with bulkier *N*-substituent. This explains the inertness of the *N*-benzhydryl substituted imine towards HCN addition in the presence of catalyst **29a** (see Table 5.9, page 85).

In the oxazaborolidinium cation **30a**, the *Lewis* acidity of the boron center is much higher than that in the neutral oxazaborolidine **29a** due to the presence of a cationic nitrogen next to boron.[138] The difference in *Lewis* acidity of the boron center in the two catalysts accounts for their reactivity difference. In the case of the catalyst **30a**, only one pre-transition-state assembly is possible where the coordination of *Z*-imine to the *Lewis* acidic boron center leads to an C–H···O hydrogen bonded complex **F** (Scheme 6.11) analogous to the pre-transition-state assembly **E**. In the complex **F**, the

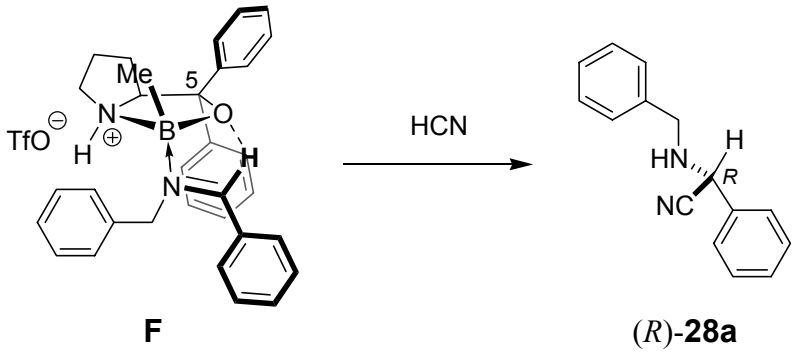

F (*R*)-**28a**

Scheme 6.11 Plausible pre-transition-state assembly for the hydrocyanation of imine by **30a** and the product formation.

electron deficient aromatic ring of the imine can attract the *cis* phenyl group on the C(5) of the oxazaborolidine ring by a π–π donor-acceptor interaction. Also, the structure **F** is fixed with regard to rotation about the coordination link between B and N by the C–H···O hydrogen bond.[140] Therefore, the cyanide attack on the imine carbon should occur at the *si* (front) face because of shielding of the *re* (rear) face by the neighboring phenyl ring of the oxazaborolidine. Cyanide addition from *si* face of the imine generates the observed (*R*)-*α*-amino nitrile (*R*)-**28a**. Interestingly, this is the same face selectivity that has been observed for the cyanosilylation of aldehydes[140] and ketones[141] reported by *Corey* et al. The importance of the π–π donor-acceptor interaction is evidenced by the formation of racemic products from the aliphatic pivalaldehyde derived imine **27f**. Since such π-stacking is not possible with this imine, the desired face selectivity was not observed.

Alternatively, in the oxazaborolidinium cation **30a**, the protonated tertiary nitrogen atom can activate the imine by N–H···N hydrogen bonding as depicted in Scheme 6.12. Undissociated HCN

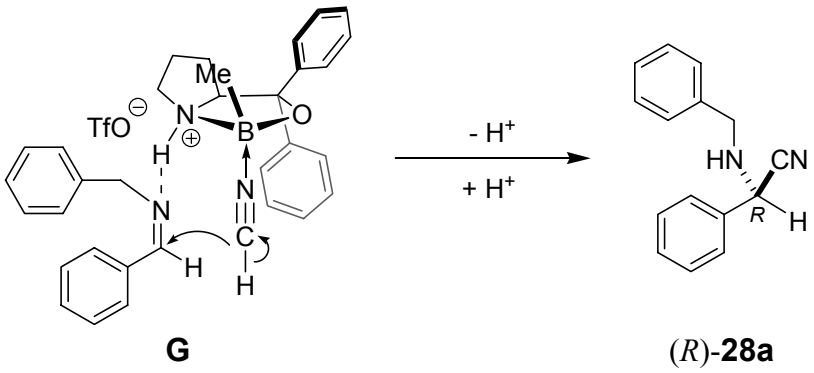

Scheme 6.12 Plausible double activation of substrates by oxazaborolidinium cation **30a**.

can then be activated by coordinating to the *Lewis* acidic boron atom *via* the available nitrogen lone pair. In this doubly activated pre-transition-state assembly **G**, the attack of HCN to the *si* face of the *Z*-imine followed by proton transfer (from HCN) generates the observed (*R*)-*α*-amino nitrile (*R*)-**28a**.

This type of activation is not favorable in the case of neutral oxazaborolidine because, protonation of the tertiary nitrogen of the catalyst by HCN generates the counter ion CN^-. The cyanide anion, due to its higher coordinating ability, binds to the *Lewis* acidic boron via the negatively charged carbon atom to produce a stable HCN-adduct as evidenced by the X-ray structure (see Figure 5.11, page 84).

7 Outlook

7.1 DKR of azlactones and KR of oxazinones

The dynamic kinetic resolution (DKR) of azlactones described herein is a versatile method that is applicable to numerous azlactones for the synthesis of a variety of α-amino acid derivatives with good to excellent enantiomeric purities. Nevertheless, only low to moderate levels of conversion in most of the cases in the presence of the optimum catalyst **18** (see structure table, page 247) is a drawback of this method. Therefore, the design and synthesis of a more active and at the same time highly enantioselective catalyst would be of practical importance. The thiourea-based bifunctional organocatalysts with a cyclohexane residue on the thiourea nitrogen were found to be quite active for the aforementioned reaction. On the other hand, the second-generation catalysts derived from α-amino acids produced high enantioselectivities. A catalyst of type **165** (Scheme 7.1) should fulfill the requirements of an active as well as a highly enantioselective catalyst. This catalyst can be synthesized from the β-amino acid *trans*-2-aminocyclohexanecarboxylic acid **166**. The β-amino acid **166** is readily accessible as its synthesis and resolution was already reported by *Berkessel* et al.[166]

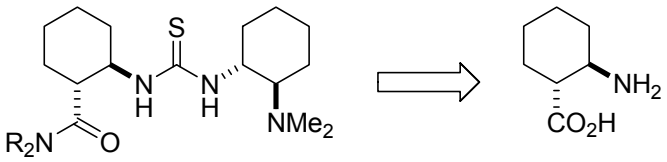

165 **166**

Scheme 7.1 Potential bifunctional organocatalyst **165** and its precursor **166**.

Furthermore, a catalyst containing a *Brønsted* basic tertiary amine and an electron-deficient guanidine moiety (which may act as a quasi-*Lewis* acid) of type **A** (EWG = electron withdrawing group; e.g. CN) should also be efficient for the ring opening of azlactones.

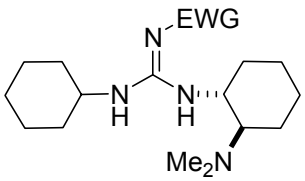

A

It was shown that the concept of DKR of azlactones can be logically extended to the KR of oxazinones. Therefore, the synthesis of enantiomerically pure higher amino acid homologs (e.g. γ-amino acids) might be possible *via* KR of their cyclic derivatives (analogous to azlactones and oxazinones).

7.2 Bifunctional organocatalysts: possible applications

The bifunctional organocatalysts described in this work have huge potential for several other applications. *Miller* et al. reported the kinetic resolution of *trans*-1,2-acetamidocyclohexanol **167** (Scheme 7.2) using small peptides as the catalysts.[167] Although high levels of enantioselectivities were reported, the main disadvantage of this method is the use of catalysts with high molecular weight. This reaction could be effected by much lower molecular weight bifunctional

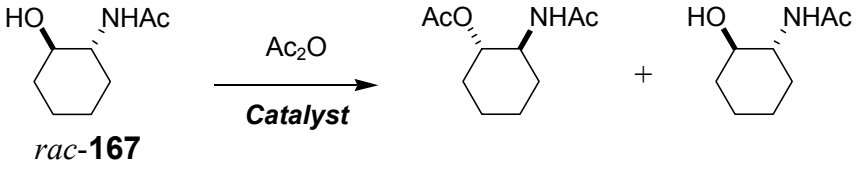

Scheme 7.2 Kinetic resolution of *trans*-1,2-acetamidocyclohexanol.

organocatalysts presented herein. The substrate binding to the (thio)urea moiety of the catalyst can be envisaged with the acetamide group whereas the tertiary amine is expected to transfer the acetyl group (*via* an acylammonium cation) to the OH-functionality of the substrate (Scheme 7.3). As can be seen in the scheme below, the OH-group in only one substrate enantiomer is in a favorable orientation in the catalyst-bound complex to undergo acetylation from the acylammonium cation. Therefore, a kinetic resolution can be expected.

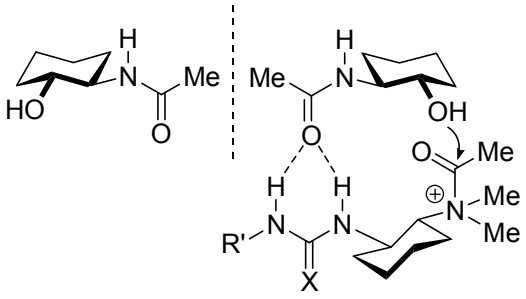

Scheme 7.3 Mechanistic model for the proposed enantioselective acylation.

The enantioselective reduction of prochiral imines to chiral amines is among the most important and challenging topics in chemistry. Recently, *Rueping* et al. reported an organocatalytic transfer hydrogenation of imines using the chiral *Brønsted* acid **39** (Scheme 7.4).[27] The *Hantzsch* dihydropyridine was used as the hydride source for this process. Using a readily available and inexpensive hydride source would be more desirable. The (thio)urea-tertiary amine bifunctional

organocatalysts might be useful for the reduction of prochiral imines using borane (BH_3) as the

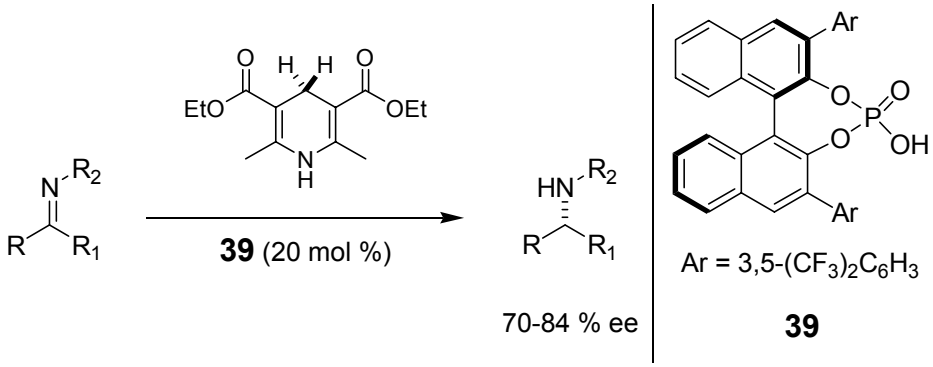

Scheme 7.4 Enantioselective transfer hydrogenation to imines by *Rueping* et al.[27]

hydride source. Activation of imine by (thio)urea moiety is well-established from the work of *Jacobsen* and co-workers[39] whereas the enhancement of hydride donor ability of borane *via* coordination to a tertiary amine is known from the work of *Corey* et al.[45] The double activation of the imine as well as the borane by the bifunctional organocatalyst can be expected and might effect the enantioselective borane reduction of imines by the face selective hydride transfer (Scheme 7.5).

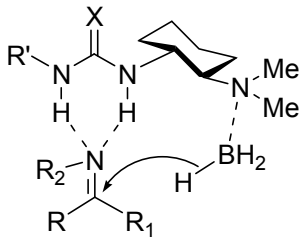

Scheme 7.5 Proposed double activation of the imine and the borane by the bifunctional organocatalysts.

7.3 New catalyst concept

The potential of (thio)urea-tertiary amine type bifunctional organocatalysts or, in general, (thio)urea-based organocatalysts has already been realized from the work of various groups. These catalysts were known to effect a wide range of different asymmetric transformations rather efficiently. However, till to date there is no report of a catalyst that combine a cyclic secondary amine and a (thio)urea functionality. The utility of cyclic secondary amines in enamine- or iminium ion-catalysis (see section 3.1, page 9) is well-established from the work of *List*, *MacMillan* and co-workers.[12] A catalyst of such (thio)urea-secondary amine type **168** (Scheme 7.6) can easily be prepared from L-proline **37**. This catalyst might be applicable for the enantioselective addition reaction of enamine or iminium ion intermediates to (thio)urea activated carbonyls, imines or nitro compounds.

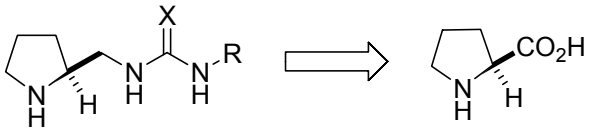

168 **37**

Scheme 7.6 L-Proline derived (thio)urea-secondary amine catalyst **168**.

8 Experimental Part

8.1 General experimental conditions

Solvents and reagents

All solvents were purified by distillation before use following standard procedures.[168] Absolute diethyl ether, tetrahydrofuran and toluene were obtained by distilling over sodium, using benzophenone as indicator. Absolute acetonitrile, chloroform and dichloromethane were obtained by distillation over calcium hydride. Absolute *tert*-butanol was obtained by distilling over calcium oxide. Ethanol, *iso*-propanol and methanol were dried by distilling over magnesium. Dimethylformamide was refluxed over calcium hydride and distilled under an inert atmosphere with reduced pressure (15 mbar, 75 °C). Commercial reagents were obtained from various commercial sources and used as received.

Inert gas atmosphere

Air and moisture-sensitive reactions were conducted under an argon atmosphere. Argon obtained from the company *Linde* with a purity of 99.998 % was dried with silical gel and phosphorous pentoxide (both with color indicator for humidity), and deoxygenated with the BTS-catalyst from *BASF* before use.

Thin layer chromatography (TLC)

Materials: *Macherey-Nagel* MN POLYGRAM Sil G/UV_{254} plates (0.25 mm thick)

The spots were visualized in UV-light (λ = 254 nm) and/or by staining with iodine, ninhydrin, vanilline or phosphomolybdic acid.

Column chromatography

Materials: *Macherey-Nagel* MN Silicagel 60, 230-400 mesh (0.04-0.063 mm)

Analytical high performance liquid chromatography (HPLC)

Apparatus: *Merck-Hitachi* L-6200A Intelligent Pump and L-4500 Diode-Array Detector.

Materials: *Daicel* Chiralpak AD column (0.46 cm × 25 cm)

Daicel Chiralcel OJ column (0.46 cm × 25 cm)

High performance liquid chromatography with mass spectrometric detector (HPLC/MS)

Apparatus: *Agilent* 1100 Series Purification Platform

Gas chromatography (GC)

Apparatus: *Hewlett Packard* GC 5890 E Series II Plus (Carrier gas: Nitrogen) with HP 6890 Series Injector

Hewlett Packard GC 5890 A Series II (Carrier gas: Nitrogen) with HP 6890 Series Injector

Hewlett Packard GC 6890 A Series Plus (Carrier gas: Nitrogen) with HP 6890 Series Injector

Materials: *Chrompak* CP-Chirasil-Dex CB (25 m, 0.25 mm ID, 0.25 μm film thickness)

Chiraldex γ-TA (20 m, 0.25 mm ID, 0.125 μm film thickness)

Gas chromatography with mass spectrometric detector (GC/MS)

Apparatus: *Hewlett Packard* GC 6890 Series and MSD 5973 (Carrier gas: Helium) with HP 6890 Series Injector

Materials: *Hewlett Packard* HP-5: Crosslinked Silicone Gum capillary column (Film thickness: 25 m × 0.25 mm × 0.33 μm)

Unless otherwise stated, all the analyses were carried out using the following temperature programs:

Standard: 100 °C (5 min), 20 °C/min → 200 °C (25 min), 20 °C/min → 280 °C (10 min).

Quick: 100 °C (5 min), 20 °C/min → 280 °C (20 min)

Nuclear magnetic resonance spectroscopy (NMR)

Apparatus: *Bruker* AC 250 (^{1}H: 250 MHz, ^{13}C: 62.5 MHz)

Bruker AC 300 (^{1}H: 300 MHz, ^{13}C: 75 MHz)

Bruker DPX 300 (^{1}H: 300 MHz, ^{13}C: 75 MHz)

Bruker DRX 500 (^{1}H: 500 MHz, ^{13}C: 125 MHz)

Spectra were recorded at room temperature (298 K) unless otherwise stated. Chemical shifts for protons and carbons were reported in parts per million (ppm) downfield from tetramethylsilane (TMS) and were referenced to residual proton in the NMR solvents (e.g. $CHCl_3$: δ 7.24) and carbon resonances of the solvents (e.g. $CDCl_3$: δ 77.0) respectively. The coupling constants (*J*) were reported in Hertz (Hz). For the fine-structure interpretation the abbre*via*tions of the signals are the

following: s = singlet, d = doublet, t = triplet, q = quartet, m = multiplet. The signal multiplicities for the ^{13}C-spectra were determined by DEPT or APT experiments.

Fourier transform infrared spectroscopy (FT-IR)

Apparatus: *Perkin Elmer* 1600 Series FT-IR spectrometer

Perkin-Elmer Paragon 1000 FT-IR spectrometer with ATR technique

The samples were measured as thin films, potassium bromide or caesium iodide discs, unless otherwise stated. The positions of the bands are reported in cm^{-1}. The intensities are reported as: s = strong, m = medium, w = weak, br = broad, sh = sharp and the kind of bands as: ν = stretching, δ = deformation (oop = out of plane).

Mass spectrometry (MS)

Apparatus: *Finnigan* MAT 900S (EB-Trap-Geometry)

Syringes pump Model 22

X-Ray structure analysis (X-RAY)

Apparatus: *Nonius* Kappa CCD diffractometer with Denzo as measurement and analysis program packet

The structures were solved by using the program SHELXS97[169] and the refinements were done by using the program SHELXL97.[170] All measurements and structure determination present in this work were performed by Dr. J. Lex and Dr. J.-M. Neudörfl, Institut für Organische Chemie, Universität zu Köln, Greinstraße 4, D-50939 Köln, Germany.

Elemental analysis (EA)

Apparatus: *Elementar Analysensysteme GmbH* Vario EL

Unless otherwise stated, the samples were recrystallized and/or dried in high vacuum ($< 10^{-4}$ mbar) before analysis. The percentages of the elements carbon, hydrogen and nitrogen in the samples were determined.

Melting point (mp)

Apparatus: *Büchi* 535 Melting Point

All the melting points were measured in open glass capillary and the values are uncorrected. In the cases where the samples were recrystallized prior to the measurements, the solvents are mentioned along with the melting point.

Specific rotation ([α])

Apparatus: *Perkin Elmer* 343plus

Optical rotations were measured using a 1 mL cell with a 1 dm path length. Measurements were carried out in different wavelengths using sample solution in chloroform at 20 °C. The sample concentrations are given in g/100 mL unit.

Bulb-to-bulb distillation (Kugelrohr)

Apparatus: Oven: Built in the Feinmechaniker-Werkstatt, Controller: *Werma* HBC 2/10 S011, Motor: *Büchi* Rotavap-R

Laboratory notebook number

All the experiments are characterized by a number within the bracket: [SMU-xx-xx]. The roman number after the three-letter-code indicates the volume number of the laboratory notebook whereas the number after the roman number indicates the page number of the corresponding notebook volume.

8.2 Synthesis of bifunctional organocatalysts

8.2.1 Preparation of (1*R*,2*R*)-*N*-phthaloyl-*N'*-ammonium-1,2-diamino-cyclohexyl-*p*-toluene sulfonate 104[146]

[SMU-III-49]

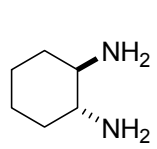

102

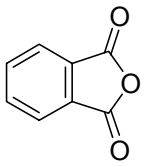

103

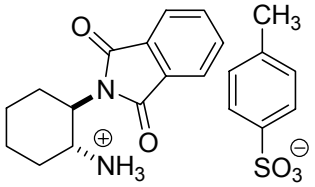

104

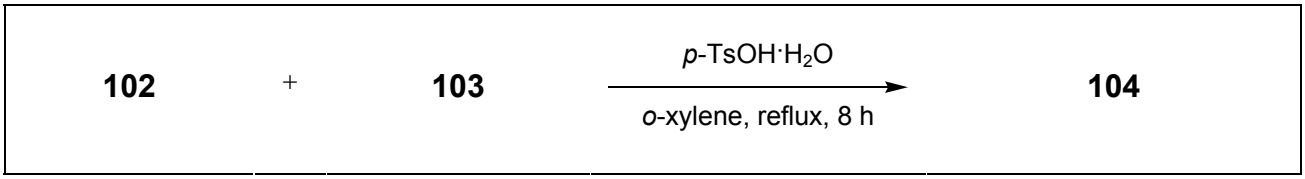

In a 500 mL round bottom flask equipped with a *Dean-Stark* apparatus and a reflux condenser, a solution of *p*-toluene sulfonic acid monohydrate (8.33 g, 43.8 mmol, 1.00 eq) in 220 mL *o*-xylene was dehydrated by azeotropic distillation for 6 hours. After cooling the resulting solution to ambient temperature, (1*R*,2*R*)-1,2-diaminocyclohexane **102** (5.00 g, 43.8 mmol, 1.00 eq) was added followed by phthalic anhydride **103** (6.48 g, 43.8 mmol, 1.00 eq). The resulting thick suspension was heated to reflux until a homogeneous solution resulted and the product begun to crystallize. The reaction mixture was cooled to room temperature and the product was collected by filtration with suction, washed with *o*-xylene/*n*-hexane (1:1) mixture and dried in vacuo to obtain an off-white amorphous solid (17.7 g, 97 %).

104 $C_{21}H_{24}N_2O_5S$ (416.49 g/mol)

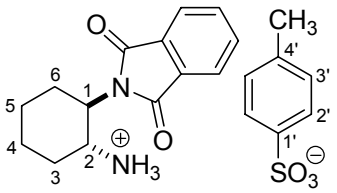

104

Yield 17.72 g (42.6 mmol, 97 %)
(Lit.[146]: 92 %)

Melting Point 250 °C (Lit.[146]: 249-252 °C)

TLC R_f = 0.82 (Silicagel, dichloromethane/methanol 3:1)

^{1}H-NMR (300 MHz, $CDCl_3$): δ = 1.20-2.11 (m; 8H, *H*-3, *H*-4, *H*-5, *H*-6), 2.32 (s; 3H, C*H*$_3$), 3.88 (dt, *J* = 3.75, 11.2 Hz; 1H, *H*-1), 4.15 (dt, *J* = 3.75, 11.4 Hz; 1H, *H*-2), 6.97 (d, *J* = 8.13 Hz; 2H, H_{ar}-3′), 7.24 (d, *J* = 8.13 Hz; 2H, H_{ar}-2′), 7.42-7.45 (m; 2H, H_{ar}), 7.55-7.58 (m; 2H, H_{ar}).
The NH_3 protons could not be detected.

^{13}C-NMR (75 MHz, $CDCl_3$): δ = 21.3 (*C*H$_3$), 23.6 (*C*H$_2$), 24.5 (*C*H$_2$), 28.9 (*C*H$_2$), 30.0 (*C*H$_2$), 50.6 (*C*-1), 52.4 (*C*-2), 122.9 (*C*H$_{ar}$), 125.9 (*C*H$_{ar}$), 128.6 (*C*H$_{ar}$), 132.1 (*C*q$_{ar}$), 133.2 (*C*H$_{ar}$), 139.8 (*C*q$_{ar}$), 141.0 (*C*q$_{ar}$), 168.5 (*C*O).
The NMR data are in agreement with the literature.[146]

FT-IR (CsI): $\tilde{\nu}$ [cm^{-1}] = 3475 (w), 3056 (w), 2948 (m), 2860 (w), 1775 (w), 1711 (s), 1606 (m), 1388 (m), 1374 (m), 1222 (s), 1193 (s), 1126 (m), 1106 (w), 1139 (m), 1013 (m), 814 (w), 718 (m), 683 (s).

8.2.2 Preparation of (1*S*,2*S*)-*N*-phthaloyl-*N'*-ammonium-1,2-diamino-cyclohexyl-*p*-toluene sulfonate *ent*-104

[SMU-VI-57]

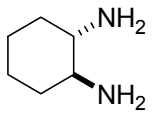

ent-**102**

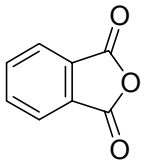

103

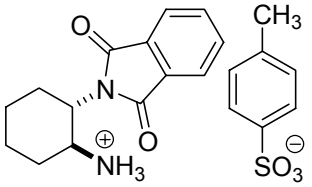

ent-**104**

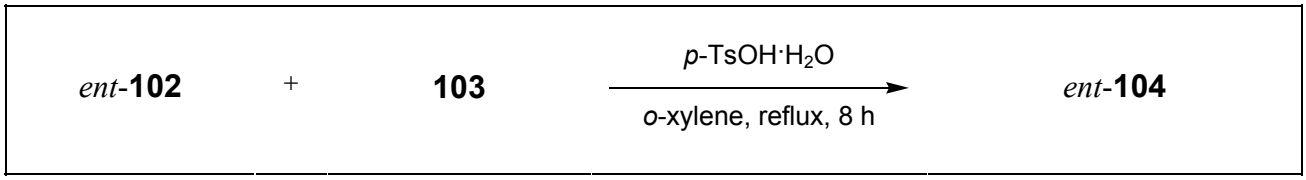

The same procedure as before (see section 8.2.1 on page 110) was followed on a 17.0 mmol scale. The product was obtained as a colorless powder (6.85 g, 97 %).

ent-**104**	$C_{21}H_{24}N_2O_5S$ (416.49 g/mol)
Yield	6.85 g (16.5 mmol, 97 %)

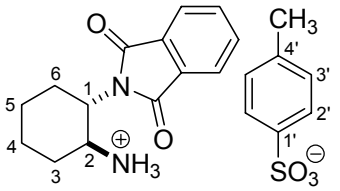

ent-**104**

Melting Point	250 °C
^{1}H-NMR	(250 MHz, $CDCl_3$): δ = 1.19-2.08 (m; 8H, *H*-3, *H*-4, *H*-5, *H*-6), 2.31 (s; 3H, C*H*$_3$), 3.87 (dt, *J* = 3.74, 11.2 Hz; 1H, *H*-1), 4.15 (dt, *J* = 3.74, 11.4 Hz; 1H, *H*-2), 6.96 (d, *J* = 8.17 Hz; 2H, H_{ar}-3′), 7.27 (d, *J* = 8.17 Hz; 2H, H_{ar}-2′), 7.38-7.44 (m; 2H, H_{ar}), 7.50-7.55 (m; 2H, H_{ar}). The NH_3 protons could not be detected.
^{13}C-NMR	(62.5 MHz, $CDCl_3$): δ = 21.3 (*C*H$_3$), 23.6 (*C*H$_2$), 24.4 (*C*H$_2$), 28.9 (*C*H$_2$), 30.0 (*C*H$_2$), 50.6 (*C*-1), 52.4 (*C*-2), 122.9 (*C*H$_{ar}$), 125.8 (*C*H$_{ar}$), 128.6 (*C*H$_{ar}$), 132.0 (*C*q$_{ar}$), 133.2 (*C*H$_{ar}$), 139.8 (*C*q$_{ar}$), 141.0 (*C*q$_{ar}$), 168.5 (*C*O).

FT-IR (ATR): $\tilde{\nu}$ [cm^{-1}] = 3465 (w), 3041(w), 2935 (m), 2863 (w), 1772 (m), 1708 (s), 1612 (m), 1528 (m), 1467 (w), 1387 (s), 1370 (s), 1331 (m), 1176 (s), 1122 (s), 1033 (s), 1009 (s), 814 (m), 719 (s), 682 (s).

8.2.3 Preparation of (1*R*,2*R*)-*N*-phthaloyl-1,2-diaminocyclohexane 105[146]

[SMU-IV-02]

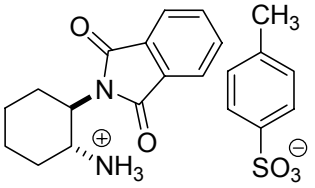

104

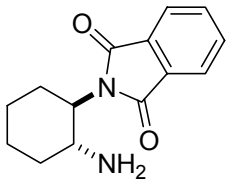

105

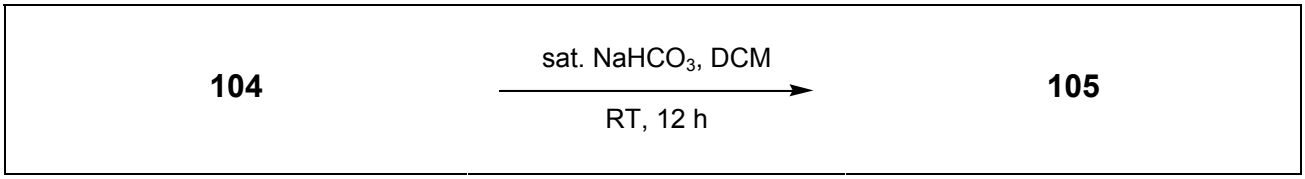

In a 1000 mL round bottom flask, a solution of **104** (10.5 g, 25.3 mmol) in 600 mL of DCM was stirred vigorously with 120 mL of saturated $NaHCO_3$ solution for 12 hours. The organic layer was separated and the aqueous layer was extracted with DCM (2 × 100 mL). The combined organic layers were the dried over anh. $MgSO_4$ and the solvent was removed in vacuo to obtain a colorless solid (5.74 g, 93 %).

105 $C_{14}H_{16}N_2O_2$ (244.29 g/mol)

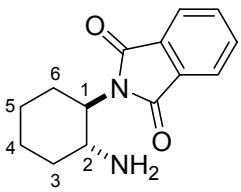

105

Yield 5.74 g (23.5 mmol, 93 %)
(Lit.[146]: 83 %)

Melting Point 125-126 °C (Lit.[146]: 123-125 °C)

^{1}H-NMR (300 MHz, $CDCl_3$): δ = 1.09 (s; 2H, NH_2), 1.11-1.44 (m; 3H, *H*-3, *H*-4, *H*-5, *H*-6), 1.69-1.79 (m; 3H, *H*-3, *H*-4, *H*-5, *H*-6), 1.95-2.19 (m; 2H, *H*-3, *H*-4, *H*-5, *H*-6), 3.34 (dt, *J* = 4.02, 10.9 Hz; 1H, *H*-2), 3.74 (dt, *J* = 4.02, 11.5 Hz; 1H, *H*-1), 7.61-7.67 (m; 2H, H_{ar}), 7.73-7.79 (m; 2H, H_{ar}).

^{13}C-NMR (75 MHz, $CDCl_3$): δ = 25.0 (*C*H_2), 25.5 (*C*H_2), 29.2 (*C*H_2), 36.6 (*C*H_2), 50.7 (*C*-2), 58.4 (*C*-1), 123.0 (*C*H_{ar}), 131.8 (*C*q_{ar}), 133.7 (*C*H_{ar}), 168.7 (*C*O).

The NMR data are in agreement with the literature.[146]

FT-IR (CsI): $\tilde{\nu}$ [cm^{-1}] = 3554 (w), 3367 (w), 3158 (br w), 2937 (m), 2864 (w), 1759 (m), 1701 (s), 1606 (m), 1472 (w), 1395 (s), 1370 (m), 1331 (w), 1067 (m), 727 (s), 714 (s), 641 (s).

8.2.4 Preparation of (1*S*,2*S*)-*N*-phthaloyl-1,2-diaminocyclohexane *ent*-105

[SMU-VI-57a]

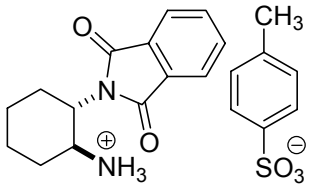

ent-**104**

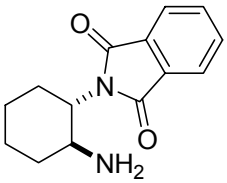

ent-**105**

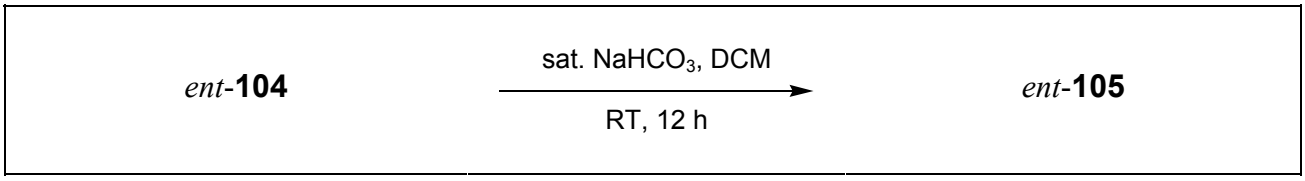

The same procedure as before (see section 8.2.3 on page 113) was followed on a 15.7 mmol scale. The product was obtained as an off-white crystalline solid (3.19 g, 83 %).

ent-**105** $C_{14}H_{16}N_2O_2$ (244.29 g/mol)

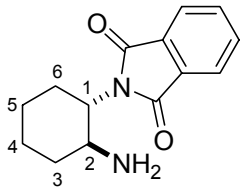

ent-**105**

Yield 5.74 g (23.5 mmol, 93 %)

Melting Point 125-126 °C

^{1}H-NMR (250 MHz, $CDCl_3$): δ = 1.10 (s; 2H, NH_2), 1.17-1.47 (m; 3H, *H*-3, *H*-4, *H*-5, *H*-6), 1.70-1.80 (m; 3H, *H*-3, *H*-4, *H*-5, *H*-6), 1.97-2.22 (m; 2H, *H*-3, *H*-4, *H*-5, *H*-6), 3.36 (dt, *J* = 4.03, 10.86 Hz; 1H, *H*-2), 3.75 (dt, *J* = 4.03, 11.41 Hz; 1H, *H*-1), 7.63-7.69 (m; 2H, H_{ar}), 7.74-7.79 (m; 2H, H_{ar}).

^{13}C-NMR (62.5 MHz, $CDCl_3$): δ = 25.0 (*C*H_2), 25.6 (*C*H_2), 29.3 (*C*H_2), 36.7 (*C*H_2), 50.8 (*C*-2), 58.5 (*C*-1), 123.1 (*C*H_{ar}), 131.8 (*C*q_{ar}), 133.8 (*C*H_{ar}), 168.7 (*C*O).

FT-IR (ATR): $\tilde{\nu}$ [cm^{-1}] = 3546 (w), 3367 (w), 3133 (br w), 2924 (s), 2853 (s), 1753 (s), 1611 (m), 1465 (m), 1389 (s), 1367 (s), 1328 (s), 1064 (s), 716 (s), 639 (sh).

8.2.5 Preparation of (1*R*,2*R*)-*N*-phthaloyl-*N'*,*N'*-dimethyl-1,2-diamino-cyclohexane **106**[146]

via Eschweiler-Clark methylation of **105**

[SMU-III-53]

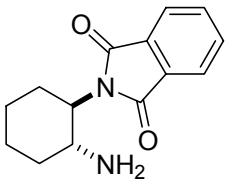

105

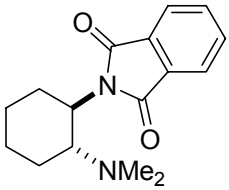

106

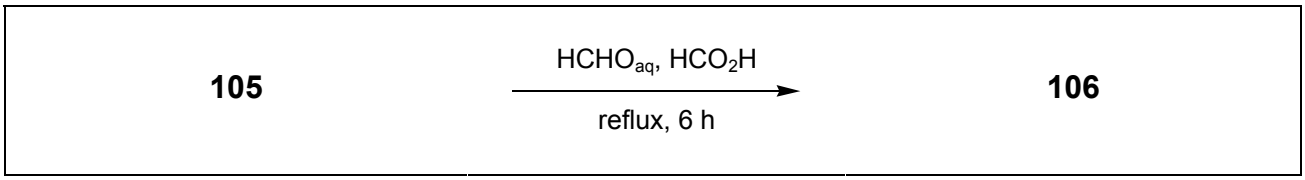

In a 50 mL round bottom flask, a solution of (1*R*,2*R*)-*N*-phthaloyl-1,2-diaminocyclohexane **105** (4.00 g, 16.4 mmol, 1.00 eq) in 37 % aqueous HCHO (3.00 mL, 36.1 mmol, 2.20 eq) and HCO_2H (6.80 mL, 180 mmol, 11.0 eq) was heated to reflux for 6 hrs. The resulting mixture was then cooled to ambient temperature and the solvent was removed in vacuo to obtain a yellow oil. It was dissolved in DCM and saturated $NaHCO_3$ solution was added to it with stirring until pH >8. The organic layer was separated and the aqueous layer was extracted with DCM (3 × 50 mL). The combined organic layer was dried over anh. $MgSO_4$ and the solvent was removed at low pressure to obtain a yellowish white solid. This was further purified by recrystallization from hexane/toluene to afford a yellowish white crystalline solid (3.32 g, 75 %).

106	$C_{16}H_{20}N_2O_2$ (272.34 g/mol)
Yield	3.32 g (12.2 mmol, 75 %) (Lit.[146]: 86 %)
Melting Point	124-126 °C (Lit.[146]: 117-120 °C)
TLC	R_f = 0.57 (Silicagel, $CHCl_3$/CH_3OH/TEA 100:5:1)

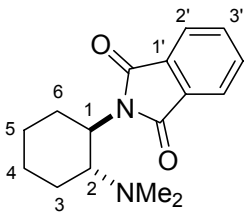

106

^{1}H-NMR (300 MHz, $CDCl_3$): δ = 1.06-1.38 (m; 3H, *H*-3, *H*-4, *H*-5), 1.73-1.91 (m; 5H, *H*-3, *H*-4, *H*-5, *H*-6), 2.12 (s; 6H, NCH_3), 3.26 (dt, *J* = 3.6, 11.4 Hz; 1H, *H*-2), 4.07 (dt, *J* = 3.6, 11.6 Hz; 1H, *H*-1), 7.60-7.66 (m; 2H, H_{ar}), 7.73-7.79 (m; 2H, H_{ar}).

^{13}C-NMR (75 MHz, $CDCl_3$): δ = 22.6 (*C*-3), 25.0 (*C*-4 or *C*-5), 25.7 (*C*-4 or *C*-5), 30.2 (*C*-6), 40.2 (NCH_3), 52.2 (*C*-1), 62.0 (*C*-2), 122.9 (*C*-2′), 132.2 (*C*-1′), 133.5 (*C*-3′), 168.6 (*C*O).

Assignments were made by 2D-NMR. The NMR data are in agreement with the literature.[146]

FT-IR (CsI): $\tilde{\nu}$ [cm^{-1}] = 3454 (w), 2932 (m), 2864 (w), 2830 (w), 2784 (w), 1763 (m), 1701 (s), 1611 (m), 1471 (m), 1453 (m), 1390 (s), 1372 (m), 1332 (w), 1273 (w), 1195 (w), 1141 (s), 1082 (s), 1067 (w), 1046 (m), 1018 (w), 956 (w), 906 (w), 872 (m), 848 (w), 826 (w), 794 (w), 719 (s), 640 (m).

HR-EI-MS Exact molecular mass for [$C_{16}H_{20}N_2O_2$] ([M]$^+$): 272.1525

Found: 272.152

8.2.6 Preparation of (1*R*,2*R*)-*N*-phthaloyl-*N*′,*N*′-dimethyl-1,2-diamino-cyclohexane 106[147]

via reductive methylation of **105**

[SMU-IV-45]

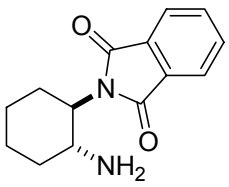

105

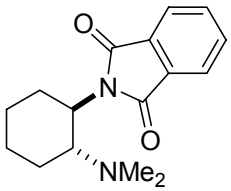

106

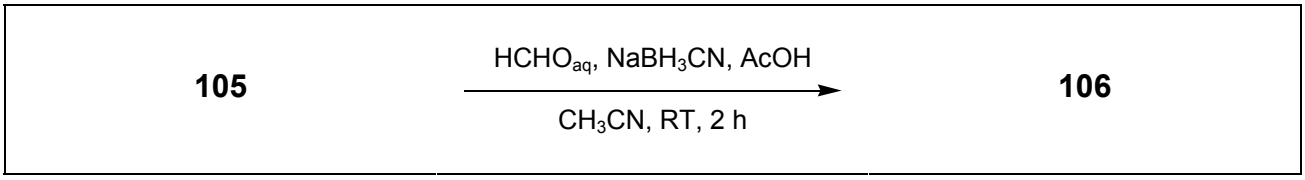

To a solution of (1*R*,2*R*)-*N*-phthaloyl-1,2-diaminocyclohexane **105** (2.0 g, 8.2 mmol, 1.00 eq) in 50 mL of acetonitrile, 37 % aqueous formaldehyde (3.32 mL, 41.0 mmol, 5.00 eq) was added and the resulting mixture was stirred for 15 minutes at room temperature. $NaBH_3CN$ (1.03 g, 16.4 mmol, 2.00 eq) was then added, followed 15 minutes later by acetic acid (2.40 mL, 41.0 mmol). After stirring 2 hours at room temperature, the reaction mixture was diluted with 2% CH_3OH-$CHCl_3$ (125 mL), washed with 1N NaOH (3 × 100 mL). The aqueous layer was re-extracted with $CHCl_3$ (70 mL), the combined organic layers were dried over anh. $MgSO_4$ and the solvent was removed in vacuo to obtain a yellowish white crystalline solid. This was dissolved in diethylether and the residue was filtered off. The filtrate was concentrated in vacuo to obtain pure (1*R*,2*R*)-*N*-phthaloyl-*N*′,*N*′-dimethyl-1,2-diaminocyclohexane **106** as a pale yellow crystalline solid (2.00 g, 90 %).

For analytical and spectral data of the compound **106**, see section 8.2.5 on page 116.

8.2.7 Preparation of (1*S*,2*S*)-*N*-phthaloyl-*N*′,*N*′-dimethyl-1,2-diaminocyclohexane *ent*-106

[SMU-VI-61]

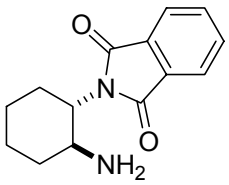

ent-**105**

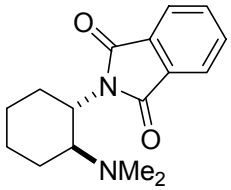

ent-**106**

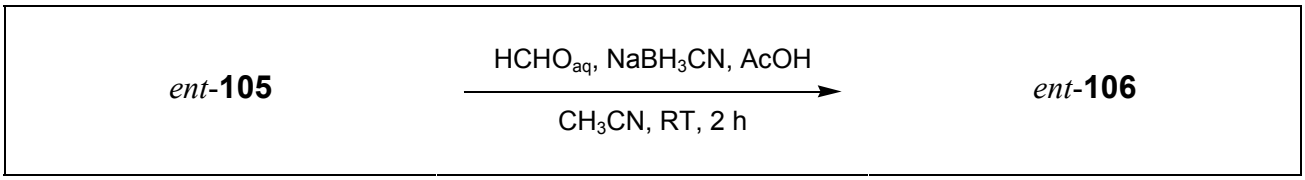

The same procedure as before (see section 8.2.6 on page 117) was followed on a 10.2 mmol scale. The product was obtained as a yellowish white crystalline solid (2.55 g, 92 %).

ent-**106** $C_{16}H_{20}N_2O_2$ (272.34 g/mol)

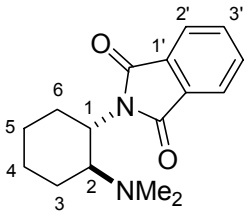

ent-**106**

Yield 2.55 g (9.36 mmol, 92 %)

Melting Point 125 °C

^{1}H-NMR (250 MHz, $CDCl_3$):δ = 1.13-1.31 (m; 3H, *H*-3, *H*-4, *H*-5, *H*-6), 1.79-1.92 (m; 5H, *H*-3, *H*-4, *H*-5, *H*-6), 2.11 (s; 6H, NCH_3), 3.27 (dt, *J* = 3.4, 11.3 Hz; 1H, *H*-2), 4.05 (dt, *J* = 3.4 , 11.5 Hz; 1H, *H*-1), 7.63-7.66 (m; 2H, H_{ar}), 7.75-7.78 (m; 2H, H_{ar}).

^{13}C-NMR (62.5 MHz, $CDCl_3$): δ = 22.7 (*C*-3), 25.1 (*C*-4 or *C*-5), 25.7 (*C*-4 or *C*-5), 30.2 (*C*-6), 40.2 (NCH_3), 52.3 (*C*-1), 62.1 (*C*-2), 122.9 (*C*-2′), 132.2 (*C*-1′), 133.5 (*C*-3′), 168.7 (*C*O).

FT-IR (ATR): $\tilde{\nu}$ [cm^{-1}] = 2928 (m), 2860 (w), 2826 (w), 2781 (w), 1760 (m), 1701 (s), 1611 (w), 1467 (m), 1450 (m), 1386 (s), 1368 (m), 1329 (w), 1272 (w), 1193 (w), 1137 (m), 1078 (m), 1064 (w), 1042 (w), 1014 (w), 953 (w), 904 (w), 870 (w), 846 (w), 823 (w), 793 (w), 716 (s), 638 (m).

HR-EI-MS Exact molecular mass for [$C_{16}H_{20}N_2O_2$] ([M]$^+$): 272.1525
Found: 272.153

8.2.8 Preparation of (1*R*,2*R*)-*N*,*N*-dimethyl-1,2-diaminocyclohexane 101[146]

[SMU-IV-65]

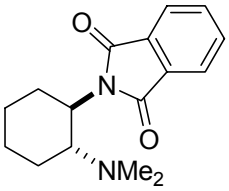

106

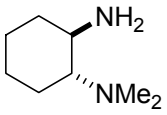

101

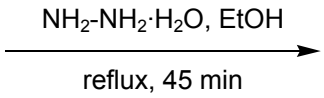

In a 100 mL round bottom flask equipped with a reflux condenser, a solution of (1*R*,2*R*)-*N*-phthaloyl-*N'*,*N'*-dimethyl-1,2-diaminocyclohexane **106** (2.25 g, 8.28 mmol, 1.00 eq) in 25 mL ethanol was refluxed with hydrazine monohydrate (1.00 mL, 20.7 mmol, 2.50 eq) for 45 minutes. The reaction mixture was then cooled to room temperature, diethyl ether was added and the white solid was filtered off. The filtrate was concentrated to afford a pale yellow oil (1.06 g, 90 %).

101 $C_8H_{18}N_2$ (142.24 g/mol)

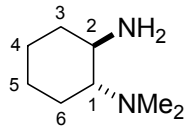

101

Yield 1.06 g (7.45 mmol, 90 %)
[Lit.[146]: 85-95 %]

^{1}H-NMR (300 MHz, $CDCl_3$): δ = 0.89-1.17 (m; 4H), 1.53-1.67 (m; 3H), 1.80-1.95 (m; 2H), 1.99 (br s; 2H, NH_2), 2.12 (s; 6H, NCH_3), 2.46 (dt, *J* = 4.1, 10.15 Hz; 1H).

^{13}C-NMR (75 MHz, $CDCl_3$): δ = 20.4 (*C*H_2), 24.9 (*C*H_2), 25.4 (*C*H_2), 35.0 (*C*H_2), 40.0 (N*C*H_3), 51.2 (*C*-2), 69.6 (*C*-1).
The NMR data are in agreement with the literature.[147]

8.2.9 Preparation of (1*S*,2*S*)-*N*,*N*-dimethyl-1,2-diaminocyclohexane *ent*-**101**

[SMU-VI-62]

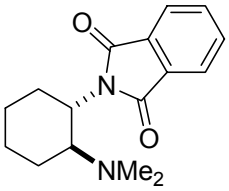

ent-**106**

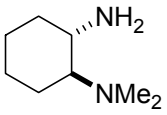

ent-**101**

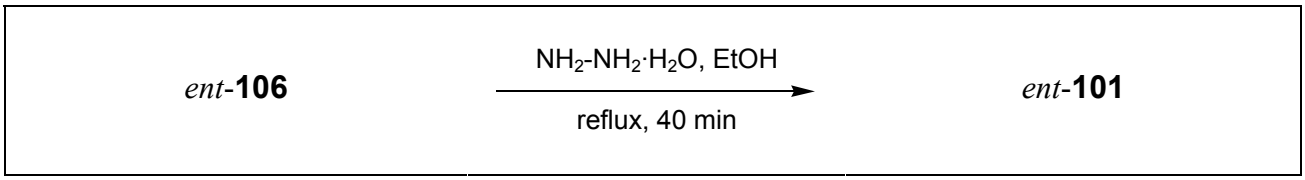

The same procedure as before (see section 8.2.8 on page 120) was followed on a 3.30 mmol scale. The product was obtained as a pale yellow oil (450 mg, 96 %).

ent-**101** $C_8H_{18}N_2$ (142.24 g/mol)

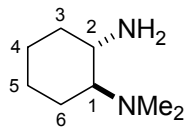

ent-**101**

Yield 450 mg (3.16 mmol, 96 %)

^{1}H-NMR (250 MHz, $CDCl_3$): δ = 0.93-1.09 (m; 2H), 1.57-1.71 (m; 5H), 1.85-2.00 (m; 2H), 2.17 (s; 6H, NC*H*$_3$), 2.50 (dt, *J* = 4.15, 10.0 Hz; 1H).
The NH_2 protons could not be detected.

^{13}C-NMR (62.5 MHz, $CDCl_3$): δ = 20.5 (*C*H_2), 25.0 (*C*H_2), 25.6 (*C*H_2), 35.2 (*C*H_2), 40.1 (N*C*H_3), 51.4 (*C*-2), 69.8 (*C*-1).

FT-IR (ATR): $\tilde{\nu}$ [cm^{-1}] = 2925 (s), 2855 (m), 2823 (w), 2776 (w), 2398 (w), 1572 (m), 1449 (s), 1377 (w), 1336 (w), 1267 (m), 1152 (w), 1097 (w), 1056 (w), 1034 (m), 942 (w), 871 (sh), 819 (w).

8.2.10 Preparation of 1-{3,5-bis(trifluoromethyl)phenyl}-3-{(1*R*,2*R*)-2-(dimethylamino)cyclohexyl}thiourea 1[51]

[SMU-IV-66]

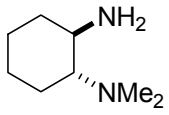

101

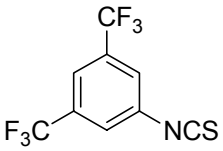

107

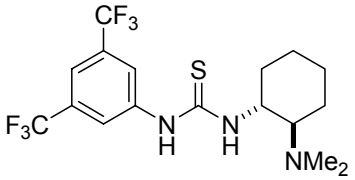

1

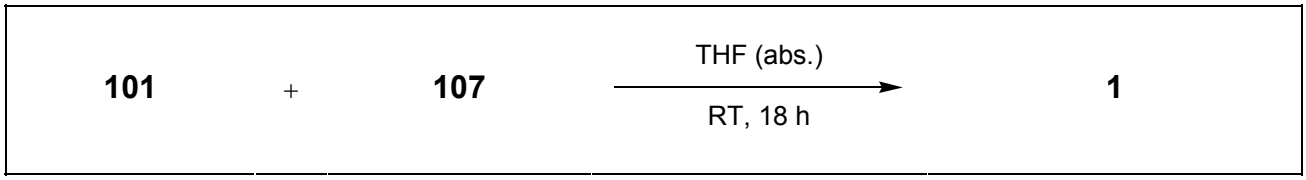

To a solution of (1*R*,2*R*)-*N*,*N*-dimethyl-1,2-diaminocyclohexane **101** (526 mg, 3.69 mmol, 1.00 eq) in absolute in 1.50 mL abs. THF, was added 3,5-bis(trifluoromethyl)phenyl isothiocyanate **107** (670 µL, 3.69 mmol, 1.00 eq) and the resulting mixture was stirred under argon for 18 hours. The reaction mixture was then concentrated in vacuo to obtain an orange foam. Purification by column chromatography on silica gel ($CHCl_3$/CH_3OH/TEA = 100:5:1 as eluant) afforded a yellowish white foam (1.28 g, 84 %).

1	$C_{17}H_{21}F_6N_3S$ (413.42 g/mol)
Yield	1.28 g (3.10 mmol, 84 %) [Lit.[51]: 65 %]
Melting Point	111-113 °C
Specific Rotation	$[\alpha]_{589}^{20}$ = -30.9°, $[\alpha]_{546}^{20}$ = -39.5°, $[\alpha]_{405}^{20}$ = -166.2° (*c* = 1.035, $CHCl_3$) [Lit.[51]: $[\alpha]_{589}^{20}$ = -32.7° (*c* = 0.99, $CHCl_3$)]
TLC	R_f = 0.25 (Silicagel, $CHCl_3$/CH_3OH/TEA 100:5:1)

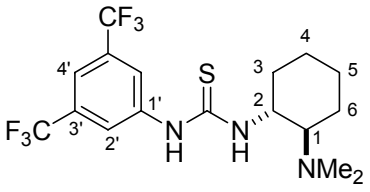

1

^{1}H-NMR (300 MHz, $CDCl_3$): δ = 1.07-1.36 (m; 4H, *H*-3, *H*-4, *H*-5, *H*-6), 1.69-1.91 (m; 3H, *H*-4, *H*-5, *H*-6), 2.26 (s; 6H, NCH_3), 2.41-2.55 (m; 2H, *H*-1, *H*-3), 3.88 (m; 1H, *H*-2), 7.58 (s; 1H, *H*-4′), 7.83 (s; 2H, *H*-2′).
The NH protons could not be detected.

^{13}C-NMR (75 MHz, $CDCl_3$): δ = 21.87 (*C*-6), 24.52 (*C*-4 or *C*-5), 24.81 (*C*-4 or *C*-5), 32.83 (*C*-3), 40.10 (NCH_3), 56.56 (*C*-2), 67.37 (*C*-1), 118.27 (*C*-4′), 122.98 (q, *J* = 271.05 Hz; CF_3), 123.26 (*C*-2′), 132.49 (q, *J* = 33.15 Hz; *C*-3′), 140.40 (*C*-1′), 178.71 (*C*S).
The assignments were made by 2D-NMR.

FT-IR (CsI): $\tilde{\nu}$ [cm^{-1}] = 3225 (br w), 2944 (m), 2867 (w), 1544 (s), 1474 (m), 1386 (s), 1280 (s), 1181 (s), 1132 (s), 885 (m), 683 (m).

HR-EI-MS Exact molecular mass for $[C_{17}H_{21}F_6N_3S]$ ($[M]^+$): 413.1360
Found: 413.138

Elemental Analysis Anal. Calcd. for $C_{17}H_{21}F_6N_3S$: C 49.39, H 5.12, N 10.16
Found: C 49.19, H 5.15, N 10.12

8.2.11 Preparation of 1-{3,5-bis(trifluoromethyl)phenyl}-3-{(1*R*,2*R*)-2-(dimethylamino)cyclohexyl}urea 2[53]

[SMU-IV-37]

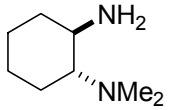

101

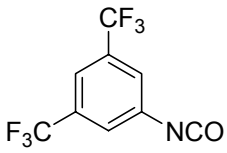

108

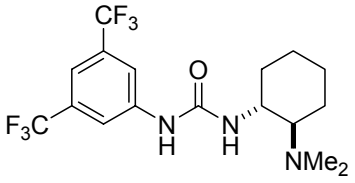

2

101	+	**108**	THF (abs.) → RT, 18 h	**2**

The same procedure as before (see section 8.2.10 on page 122) was followed on a 5.17 mmol scale. Purification in the same way afforded an off-white crystalline solid (1.79 g, 87 %). This was crystallized from chloroform to obtain colorless needles.

2 $C_{17}H_{21}F_6N_3O$ (397.36 g/mol)

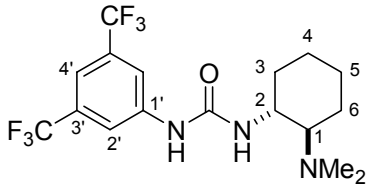

2

Yield 1.79 g (4.50 mmol, 87 %)
[Lit.[53]: 80 %]

Melting Point 163-165 °C ($CHCl_3$) (Lit.[53]: 166-167 °C)

Specific Rotation $[\alpha]_{589}^{20}$ = -35.1°, $[\alpha]_{546}^{20}$ = -41.5°, $[\alpha]_{405}^{20}$ = -83.1°, $[\alpha]_{365}^{20}$ = -106.8° (*c* = 1.00, $CHCl_3$) [Lit.[53]: $[\alpha]_{589}^{25}$ = -35.3° (*c* = 0.93, $CHCl_3$)]

TLC R_f = 0.25 (Silicagel, $CHCl_3$/CH_3OH/TEA 100:5:1)

^{1}H-NMR (300 MHz, $CDCl_3$): δ = 1.09-1.35 (m; 4H, *H*-3, *H*-4, *H*-5, *H*-6), 1.67-1.89 (m; 3H, *H*-4, *H*-5, *H*-6), 2.20-2.25 (m; 1H, *H*-1), 2.26 (s; 6H, NCH_3), 2.34-2.38 (m; 1H, *H*-3), 3.47-3.55 (m; 1H, *H*-2), 5.76 (br s; 2H, C-2-N*H*), 7.36 (s; 1H, *H*-4′), 7.76 (s; 2H, H-2′), 8.06 (br s; 1H, C-1′-N*H*).

^{13}C-NMR (75 MHz, $CDCl_3$): δ = 21.4 (*C*-6), 24.7 (*C*-4 or *C*-5), 25.0 (*C*-4 or *C*-5), 33.8 (*C*-3), 40.1 (NCH_3), 51.6 (*C*-2), 67.4 (*C*-1), 115.3 (*C*-4′), 118.5 (C-2′), 123.2 (q, *J* = 271.0 Hz; CF_3), 131.9 (q, *J* = 32.97 Hz; *C*-3′), 140.9 (C-1′), 155.6 (*C*O).
The assignments were made by 2D-NMR.

FT-IR (CsI): $\tilde{\nu}$ [cm^{-1}] = 3320 (br), 2941 (m), 2866 (w), 2787 (w), 1853 (s), 1604 (s), 1574 (s), 1516 (m), 1474 (m), 1388 (s), 1342 (m), 1279 (s), 1235 (w), 1175 (s), 1132 (s), 1067 (w), 1045 (w), 942 (w), 884 (m), 849 (w), 704 (m), 685 (m), 664 (w).

HR-EI-MS Exact molecular mass for [$C_{17}H_{21}F_6N_3O$] ([M]$^+$): 397.1588
Found: 397.159

Elemental Analysis Anal. Calcd. for $C_{17}H_{21}F_6N_3O$: C 51.38, H 5.33, N 10.57
Found: C 51.29, H 5.40, N 10.41

Crystallographic Data

For the X-ray structure see Figure 5.1 on page 55

Colourless needles from chloroform

Empirical formula:	$C_{17}H_{21}F_6N_3O$
Formula weight (M):	397.37 g/mol
Temperature (T):	100(2) K
Wavelength (λ):	0.71073 Å
Crystal system:	orthorhombic
Space group:	$P2_12_12_1$
Unit cell dimension:	a = 8.849(1) Å $\alpha = 90°$
	b = 17.212(1) Å $\beta = 90°$
	c = 24.025(1) Å $\gamma = 90°$
Unit cell volume:	3659.2(5) $Å^3$
Z:	8
Calculated density ($\rho_{calcd.}$):	1.443 g/cm^3
Absorption coefficient (μ):	0.133 mm^{-1}
F(000):	1648
Crystal size:	0.3 × 0.1 × 0.1 mm
Θ-range for data collection:	1.46° to 27.00°
Limiting indices:	$-11 \leq h \leq 8$
	$-21 \leq k \leq 20$
	$-29 \leq l \leq 30$
Reflections collected:	21188
Unique reflections:	7809 [$R_{int} = 0.1746$]
Reflections observed [I>2σ (I)]:	2669
Completeness to Θ:	99.0 %
Refinement method:	Full-matrix least-squares on F^2
Data / restraints / parameters:	7809 / 0 / 493
Goodness-of-fit on F^2:	0.961
Final *R*-indices [$I > 2\sigma(I)$]:	$R1 = 0.0979$ $\omega R2 = 0.2213$
R-indices (all data):	$R1 = 0.2931$ $\omega R2 = 0.2891$
Largest diff. peak and hole:	0.683 and -0.336 $e \cdot Å^{-3}$

8.2.12 Preparation of (1*R*,2*R*)-*N*,*N*-diethyl-*N'*-phthaloyl-1,2-diamino-cyclohexane 109

[SMU-V-11]

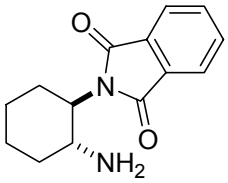

105

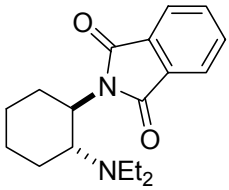

109

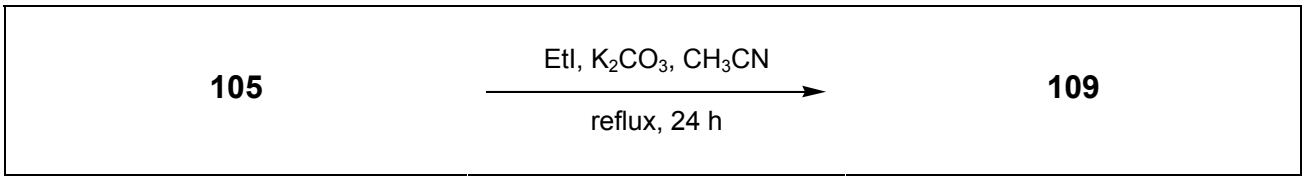

To a solution of (1*R*,2*R*)-*N*-phthaloyl-1,2-diaminocyclohexane **105** (1.00 g, 4.10 mmol, 1.00 eq) in 20 mL abs. CH_3CN and K_2CO_3 (1.30 g, 9.40 mmol, 2.30 eq) was added ethyl iodide (1.34 g, 8.60 mmol, 2.10 eq) and the resulting mixture was heated to reflux for 24 hours. The reaction mixture was cooled to ambient temperature and concentrated in vacuo. The residue was dissolved in DCM (20 mL) and water (20 mL), the organic layer was separated and the aqueous layer (pH ~10) was extracted with DCM (3 × 15 mL). The combined organic extracts were dried over anh. Na_2CO_3 and the solvent was removed in vacuo to obtain an off-white crystalline solid (1.21 g, 99 %).

109	$C_{18}H_{24}N_2O_2$ (300.4 g/mol)
Yield	1.21 g (4.03 mmol, 99 %)
Melting Point	132-133 °C
TLC	R_f = 0.77 (Silicagel, $CHCl_3$/CH_3OH/TEA 100:5:1)

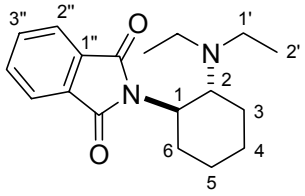

109

^{1}H-NMR (300 MHz, $CDCl_3$): δ = 0.73 (t, *J* = 7.05 Hz; 6H, *H*-2′), 1.11-1.39 (m; 3H, *H*-3, *H*-4, *H*-5), 1.75-1.91 (m; 4H, *H*-3, *H*-4, *H*-5, *H*-6), 2.17-2.38 (m; 3H, *H*-1′, *H*-6), 2.41-2.50 (m; 2H, *H*-1′), 3.27 (dt, *J* = 3.71, 11.57 Hz; 1H, *H*-2), 4.10 (dt, *J* = 3.71, 11.24 Hz; 1H, *H*-1), 7.62-7.67 (m; 2H, *H*-3″), 7.74-7.80 (m; 2H, *H*-2″).

^{13}C-NMR (75 MHz, $CDCl_3$): δ = 14.6 (*C*-2′), 24.7 (*C*-3), 25.5 (*C*-4 or *C*-5), 25.9 (*C*-4 or *C*-5), 29.8 (*C*-6), 43.0 (*C*-1′), 52.4 (*C*-1), 59.0 (*C*-2), 122.8 (*C*-2″), 132.2 (*C*-1″), 133.5 (*C*-3″), 168.8 (*C*O).

FT-IR (CsI): $\tilde{\nu}$ [cm^{-1}] = 3456 (w), 2974 (m), 2932 (m), 2870 (w), 2813 (w), 1764 (m), 1704 (s), 1614 (w), 1468 (m), 1395 (s), 1376 (s), 1335 (w), 1298 (w), 1255 (w), 1209 (w), 1144 (m), 1112 (m), 1087 (m), 1066 (w), 1024 (m), 956 (w), 904 (m), 871 (w), 844 (w), 796 (m), 718 (s).

HR-EI-MS Exact molecular mass for [$C_{18}H_{24}N_2O_2$] ([M]$^+$): 300.1838
Found: 300.183

8.2.13 Preparation of (1*R*,2*R*)-*N*,*N*-diethyl-1,2-diaminocyclohexane 114

[SMU-V-08]

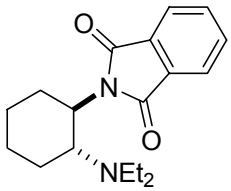

105

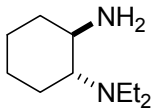

114

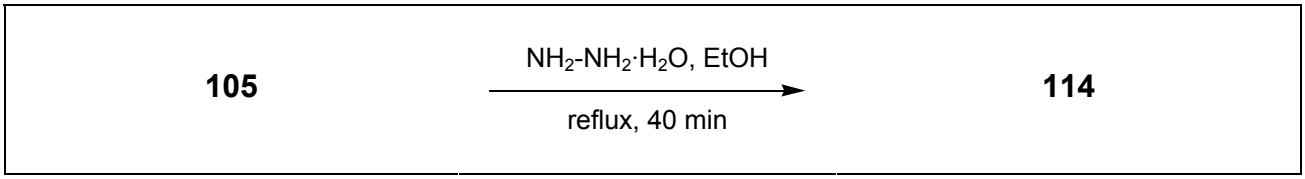

The same procedure as before (see section 8.2.8 on page 120) was followed on a 2.02 mmol scale. The product was obtained as a pale yellow oil (325 mg, 95 %).

114	$C_{10}H_{22}N_2$ (170.30 g/mol)
Yield	325 mg (1.91 mmol, 95 %)

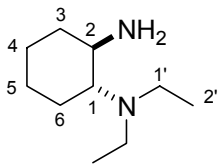

114

^{1}H-NMR	(300 MHz, $CDCl_3$): δ = 0.86 (t, *J* = 7.13 Hz; 6H, *H*-2′), 0.93-1.04 (m; 3H), 1.45-1.63 (m; 3H), 1.77-1.87 (m; 3H), 1.92-2.00 (m; 1H, *H*-2), 2.12-2.23 (m; 2H, *H*-1′), 2.36-2.50 (m; 3H, *H*-1′, *H*-1).
^{13}C-NMR	(75 MHz, $CDCl_3$): δ = 14.8 (*C*-2′), 22.9 (CH_2), 24.9 (CH_2), 25.8 (CH_2), 34.9 (CH_2), 43.1 (*C*-1′), 51.0 (*C*-2), 66.1 (*C*-1).
GC-MS	τ_R = 7.8 min (Method: Standard) m/z = 170 $[M]^+$

8.2.14 Preparation of 1-{3,5-bis(trifluoromethyl)phenyl}-3-{(1*R*,2*R*)-2-(diethylamino)cyclohexyl}urea 3

[SMU-V-09]

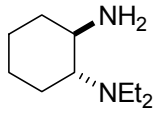

114

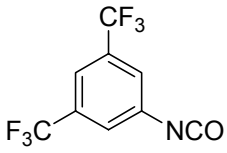

108

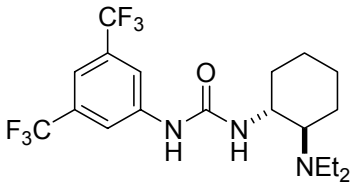

3

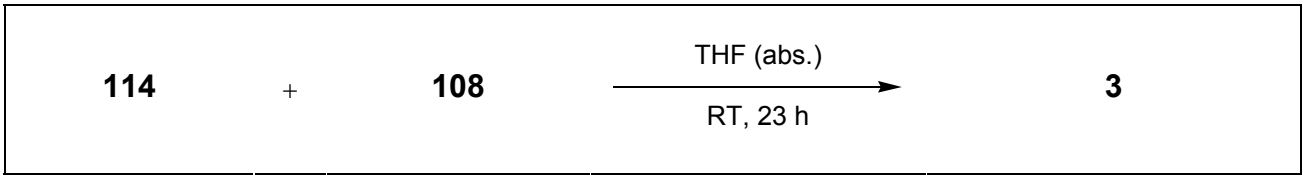

The same procedure as before (see section 8.2.10 on page 122) was followed on a 1.91 mmol scale. Purification in the same way afforded a colorless crystalline solid (580 mg, 71 %).

3 $C_{19}H_{25}F_6N_3O$ (425.41 g/mol)

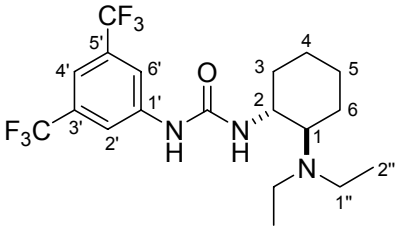

3

Yield 580 mg (1.36 mmol, 71 %)

Melting Point 195-197 °C ($CHCl_3$)

Specific Rotation $[\alpha]_{589}^{20}$ = -58.1°, $[\alpha]_{546}^{20}$ = -68.7°, $[\alpha]_{405}^{20}$ = -134.5°, $[\alpha]_{365}^{20}$ = -174.0°, $[\alpha]_{334}^{20}$ = -226.1° (*c* = 1.01, $CHCl_3$)

TLC R_f = 0.29 (Silicagel, $CHCl_3$/CH_3OH/TEA 100:5:1)

^{1}H-NMR (300 MHz, $CDCl_3$): δ = 0.98 (t, *J* = 7.13 Hz; 6H, *H*-2″), 1.04-1.31 (m; 4H, *H*-3, *H*-4, *H*-5, *H*-6), 1.63-1.81 (m; 3H, *H*-4, *H*-5, *H*-6), 2.28-2.73 (m; 6H, *H*-1, *H*-1″, *H*-3), 3.35-3.41 (m; 1H, *H*-2), 5.92 (br s; 1H, C-2-N*H*), 7.42 (s; 1H, *H*-4′), 7.86 (s; 2H, *H*-2′, *H*-6′).

^{13}C-NMR (75 MHz, $CDCl_3$): δ = 14.2 (*C*-2″), 23.5 (*C*-6), 24.5 (*C*-4 or *C*-5), 25.5 (*C*-4 or *C*-5), 33.4 (*C*-3), 43.2 (*C*-1″), 51.9 (*C*-2), 63.0 (*C*-1), 115.5 (*C*-4′), 118.6 (*C*-2′, *C*-6′), 123.2 (q, *J* = 271.1 Hz; *C*F_3), 132.1 (q, *J* = 32.97 Hz; *C*-3′, *C*-5′), 141.0 (*C*-1′), 155.8 (*C*O).
The assignments were made by 2d-NMR.

FT-IR (CsI): $\tilde{\nu}$ [cm^{-1}] = 3286 (s), 3099 (m), 2974 (m), 2937 (m), 2867 (w), 1667 (s), 1623 (w), 1581 (s), 1493 (s), 1476 (s), 1389 (s), 1338 (m), 1279 (s), 1238 (m), 1169 (s), 1140 (s), 1073 (w), 1000 (w), 957 (m), 882 (m), 734 (m).

HR-ESI-MS Exact molecular mass for [$C_{19}H_{26}F_6N_3O$] ([M+H]$^+$): 426.1975
Found: 426.199

Elemental Analysis Anal. Calcd. for $C_{19}H_{25}F_6N_3O$: C 53.64, H 5.92, N 9.88
Found: C 53.56, H 5.93, N 9.85

8.2.15 Preparation of 2-{(1*R*,2*R*)-2-(pyrrolidin-1-yl)cyclohexyl}-isoindoline-1,3-dione 111

[SMU-V-23]

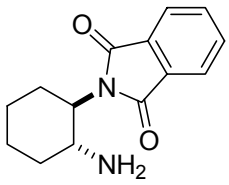

105

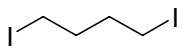

110

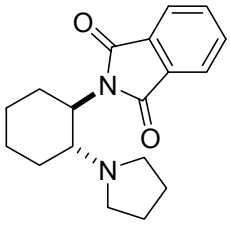

111

To a solution of (1*R*,2*R*)-*N*-phthaloyl-1,2-diaminocyclohexane **105** (1.00 g, 4.10 mmol, 1.00 eq) in 20 mL abs. CH_3CN and K_2CO_3 (1.30 g, 9.40 mmol, 2.30 eq) was added 1,4-diiodobutane **110** (1.27 g, 4.10 mmol, 1.00 eq) and the resulting mixture was heated to reflux for 6 hours. The reaction mixture was cooled to ambient temperature and concentrated in vacuo. The residue was dissolved in DCM (20 mL) and water (20 mL), the organic layer was separated and the aqueous layer (pH ~10) was extracted with DCM (2 × 20 mL). The combined organic extracts were dried over anh. Na_2CO_3 and the solvent was removed in vacuo to obtain a highly viscous yellow oil which solidified on standing at room temperature. This solid was then dried in high vacuum (10^{-5} mbar) at 60 °C to remove the unreacted 1,4-diiodobutane. The pure product was obtained as a pale yellow solid (1.21 g, 99 %).

111	$C_{18}H_{22}N_2O_2$ (298.38 g/mol)
Yield	1.21 g (4.06 mmol, 99 %)
Melting Point	93-95 °C

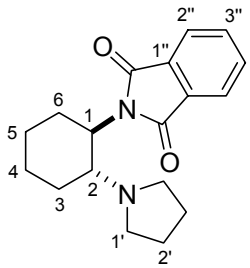

111

^{1}H-NMR (300 MHz, $CDCl_3$): δ = 1.19-1.38 (m; 3H, *H*-3, *H*-4, *H*-5), 1.42-1.55 (m; 4H, *H*-2′), 1.78-1.94 (m; 4H, *H*-3, *H*-4, *H*-5, *H*-6), 2.13-2.27 (m; 1H, *H*-6), 2.46-2.60 (m; 4H, *H*-1′), 3.50-3.57 (m; 1H, *H*-2), 4.09 (dt, *J* = 3.90, 11.72 Hz; 1H, *H*-1), 7.62-7.69 (m; 2H, *H*-3″), 7.74-7.82 (m; 2H, *H*-2″).

^{13}C-NMR (75 MHz, $CDCl_3$): δ = 23.8 (*C*-2′), 23.9 (*C*-3), 25.1 (*C*-4 or *C*-5), 25.8 (*C*-4 or *C*-5), 30.2 (*C*-6), 47.3 (*C*-1′), 53.6 (*C*-1), 57.7 (*C*-2), 122.9 (*C*-2″), 132.2 (*C*-1′), 133.5 (*C*-3″), 168.7 (*C*O).

FT-IR (KBr): $\tilde{\nu}$ [cm^{-1}] = 3452 (w), 2932 (s), 2856 (m), 2802 (w), 1764 (s), 1699 (s), 1612 (w), 1467 (m), 1389 (s), 1370 (s), 1332 (m), 1284 (w), 1116 (m), 1077 (s), 1017 (m), 1002 (w), 957 (w), 903 (m), 870 (m), 796 (w), 718 (s).

HR-EI-MS Exact molecular mass for [$C_{18}H_{22}N_2O_2$] ([M]$^+$): 298.1681
Found: 298.168

8.2.16 Preparation of (1*R*,2*R*)-2-(pyrrolidin-1-yl)cyclohexanamine 115

[SMU-V-05]

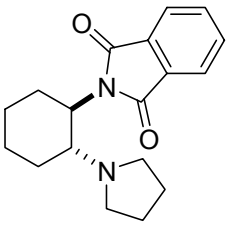

111

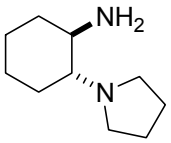

115

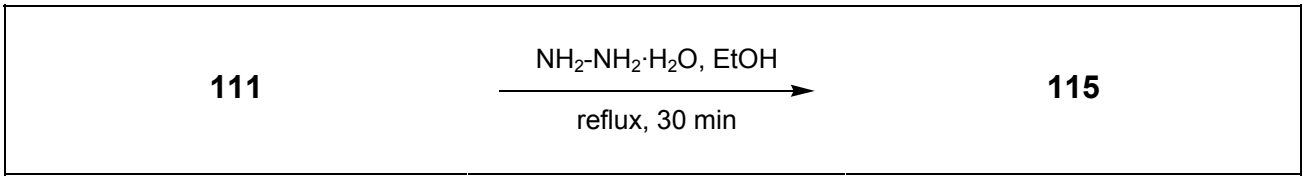

The same procedure as before (see section 8.2.8 on page 120) was followed on a 2.18 mmol scale. The product was obtained as a pale yellow oil (325 mg, 89 %).

115	$C_{10}H_{20}N_2$ (168.28 g/mol)
Yield	325 mg (1.93 mmol, 89 %)

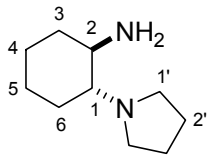

115

^{1}H-NMR	(300 MHz, $CDCl_3$): δ = 0.95-1.22 (m; 4H), 1.55-1.92 (m; 10H), 2.16-2.26 (m; 1H), 2.40-2.60 (m; 5H).
^{13}C-NMR	(75 MHz, $CDCl_3$): δ = 21.4 (*C*H_2), 23.6 (*C*-2′), 24.9 (*C*-4 or *C*-5), 25.4 (*C*-4 or *C*-5), 34.8 (*C*H_2), 47.0 (*C*-1′), 52.6 (*C*-2), 65.1 (*C*-1).
GC-MS	τ_R = 9.1 min (Method: Standard) m/z = 168 $[M]^+$

8.2.17 Preparation of 1-{3,5-bis(trifluoromethyl)phenyl}-3-{(1*R*,2*R*)-2-(pyrrolidin-1-yl)cyclohexyl}urea 4

[SMU-V-06]

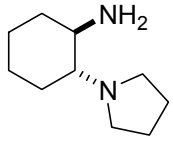

115

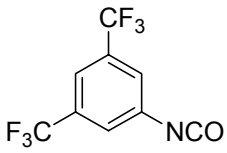

108

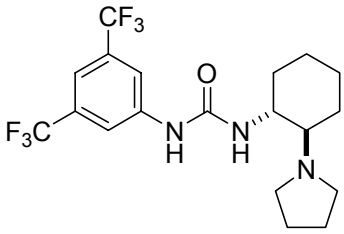

4

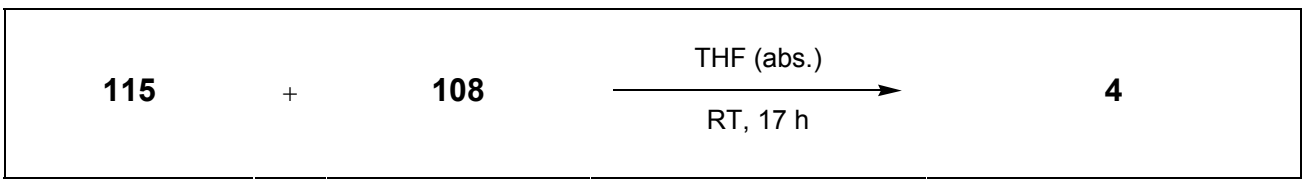

The same procedure as before (see section 8.2.10 on page 122) was followed on a 1.93 mmol scale. Purification in the same way afforded a pale yellow foam (578 mg, 71 %).

4 $C_{19}H_{23}F_6N_3O$ (423.40 g/mol)

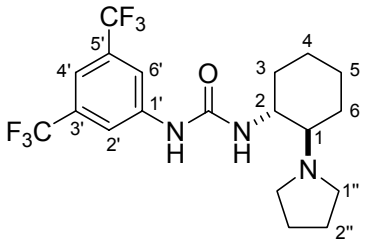

4

Yield 578 mg (1.37 mmol, 71 %)

Melting Point 98-100 °C

Specific Rotation $[\alpha]_{589}^{20}$ = -18.7°, $[\alpha]_{546}^{20}$ = -21.9°, $[\alpha]_{405}^{20}$ = -37.7° (*c* = 1.00, $CHCl_3$)

TLC R_f = 0.23 (Silicagel, $CHCl_3$/CH_3OH/TEA 100:5:1)

^{1}H-NMR (300 MHz, $CDCl_3$): δ = 1.07-1.36 (m; 4H, *H*-3, *H*-4, *H*-5, *H*-6), 1.62-1.86 (m; 7H, *H*-4, *H*-5, *H*-6, *H*-2″), 2.25-2.29 (m; 1H, *H*-3), 2.44-2.48 (m; 1H, *H*-1), 2.62-2.71 (m; 4H, *H*-1″), 3.50 (m; 1H, *H*-2), 5.87 (br s; 1H, C-2-N*H*), 7.36 (s; 1H, *H*-4′), 7.80 (s; 2H, *H*-2′, *H*-6′), 8.56 (br s; 1H, C-1′-N*H*).

^{13}C-NMR (75 MHz, $CDCl_3$): δ = 23.1 (*C*-6), 23.6 (*C*-2″), 24.3 (*C*-4 or *C*-5), 24.6 (*C*-4 or *C*-5), 33.1 (*C*-3), 48.0 (*C*-1″), 53.3 (*C*-2), 63.4 (*C*-1), 115.2 (*C*-4′), 118.2 (*C*-2′, *C*-6′), 123.0 (q, *J* = 271.1 Hz; *C*F_3), 132.0 (q, *J* = 32.97 Hz; *C*-3′, *C*-5′), 141.1 (*C*-1′), 155.9 (*C*O).

FT-IR (CsI): $\tilde{\nu}$ [cm^{-1}] = 3320 (br), 3112 (w), 2940 (m), 1863 (w), 2813 (w), 1663 (s), 1575 (s), 1508 (w), 1475 (m), 1390 (s), 1340 (w), 1278 (s), 1235 (w), 1182 (s), 1133 (s), 1040 (w), 941 (w), 881 (m), 848 (w).

HR-ESI-MS Exact molecular mass for [$C_{19}H_{24}F_6N_3O$] ([M+H]$^+$): 424.1823
Found: 424.183

Elemental Analysis Anal. Calcd. for $C_{19}H_{23}F_6N_3O$: C 53.90, H 5.48, N 9.92
Found: C 53.58, H 5.47, N 9.81

8.2.18 Preparation of 2-{(1*R*,2*R*)-2-(benzylideneamino)cyclohexyl}-isoindoline-1,3-dione 113

[SMU-V-47]

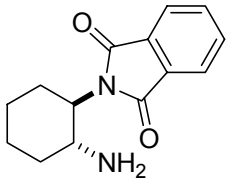

105

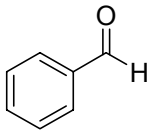

33

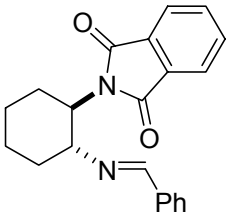

113

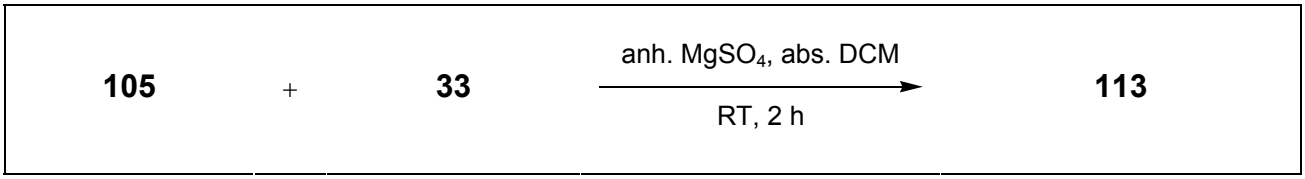

A solution of (1*R*,2*R*)-*N*-phthaloyl-1,2-diaminocyclohexane **105** (1.00 g, 4.10 mmol, 1.00 eq) in 25 mL of abs. DCM was stirred with anh. $MgSO_4$ (985 mg, 8.18 mmol, 2.00 eq) and benzaldehyde **33** (420 µL, 4.09 mmol, 1.00 eq) for 2 hours at room temperature. $MgSO_4$ was then filtered off and the solvent was removed in vacuo to obtain an off-white crystalline solid (1.32 g, 97 %).

113 $C_{21}H_{20}N_2O_2$ (332.40 g/mol)

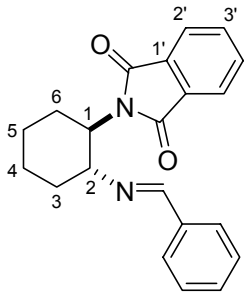

113

Yield 1.32 g (3.97 mmol, 97 %)

Melting Point 135-136 °C

^{1}H-NMR (300 MHz, $CDCl_3$): δ = 1.47-1.61 (m; 2H, *H*-4, *H*-5), 1.71-1.92 (m; 5H, 2 × *H*-3, *H*-4, *H*-5, *H*-6), 2.22-2.36 (m; 1H, *H*-6), 4.08 (dt, *J* = 4.41, 9.68 Hz; 1H, *H*-2), 4.45 (dt, *J* = 3.81, 9.68 Hz; 1H, *H*-1), 7.24-7.34 (m; 3H, H_{ar}), 7.49-7.63 (m; 4H, *H*-3′, H_{ar}), 7.70-7.80 (m; 2H, *H*-2′), 8.21 (s; 1H, N=C*H*).

^{13}C-NMR (75 MHz, $CDCl_3$): δ = 24.1 (*C*-4 or *C*-5), 25.5 (*C*-4 or *C*-5), 28.7 (*C*-6), 34.1 (*C*-3), 55.6 (*C*-1), 69.3 (*C*-2), 122.9 (*C*-2′), 128.0 (C_{ar}), 128.3 (C_{ar}), 130.4 (C_{ar}), 131.7 (*C*-1′), 133.6 (*C*-3′), 136.1 (Cq_{ar}), 160.7 (N=*C*), 168.4 (*C*O).

The assignments were made by 2D-NMR.

FT-IR (KBr): $\tilde{\nu}$ [cm^{-1}] = 3459 (w), 3063 (w), 3029 (w), 2943 (m), 2920 (s), 2851 (s), 1768 (s), 1703 (s), 1649 (s), 1582 (w), 1450 (m), 1392 (s), 1371 (s), 1330 (w), 1250 (w), 1170 (m), 1155 (m), 1098 (s), 1075 (m), 1045 (m), 1016 (m), 967 (w), 944 (w), 909 (m), 870 (m), 858 (w), 836 (m), 788 (m), 752 (s), 716 (s).

HR-EI-MS Exact molecular mass for [$C_{21}H_{20}N_2O_2$] ([M]$^+$): 332.1525

Found: 332.152

8.2.19 Preparation of 2-{(1*R*,2*R*)-2-(*N*-benzyl-*N*-methylamino)cyclohexyl} isoindoline-1,3-dione 112

[SMU-V-55]

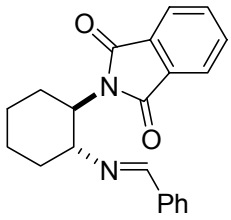

113

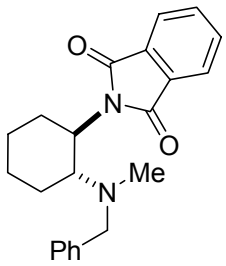

112

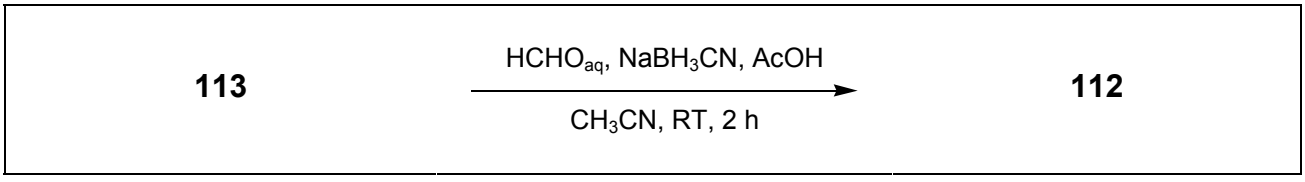

To a solution of 2-{(1*R*,2*R*)-2-(benzylideneamino)cyclohexyl}isoindoline-1,3-dione **113** (500 mg, 1.50 mmol, 1.00 eq) in 25 mL of acetonitrile, $NaBH_3CN$ (189 mg, 3.00 mmol, 2.00 eq) was added and the resulting mixture was stirred for 15 minutes at room temperature. 37 % Aqueous formaldehyde (250 µL, 3.00 mmol, 2.00 eq) was then added, followed 15 minutes later by AcOH

(350 µL, 6.00 mmol, 4.00 eq). After stirring the mixture for 2 hours at room temperature, the reaction mixture was diluted with 2% CH_3OH-$CHCl_3$ (25 mL), washed with 1N NaOH (3 × 50 mL). The aqueous layer was re-extracted with $CHCl_3$ (3 × 50 mL). The combined organic layers were dried over anh. $MgSO_4$ and the solvent was removed in vacuo to obtain a yellowish white semisolid. This was taken in diethylether and the residue was filtered off. The filtrate was concentrated in vacuo to obtain a highly viscous yellow oil (512 mg, 98 %).

112 $C_{22}H_{24}N_2O_2$ (348.44 g/mol)

Yield 512 mg (1.47 mmol, 98 %)

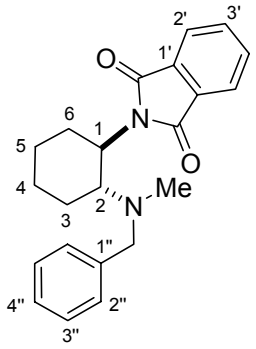

112

^{1}H-NMR (300 MHz, $CDCl_3$): δ = 1.25-1.44 (m; 3H, *H*-3, *H*-4, *H*-5), 1.78-1.89 (m; 3H, *H*-4, *H*-5, *H*-6), 1.98-2.02 (m; 1H, *H*-3), 2.04 (s; 3H, NCH_3), 2.20-2.33 (m; 1H, *H*-6), 3.38-3.47 (m; 1H, *H*-2), 3.42 (d, *J* = 13.3 Hz; 1H, NCH_2), 3.57 (d, *J* = 13.3 Hz; 1H, NCH_2), 4.20 (dt, *J* = 3.85, 11.6 Hz; 1H, *H*-1), 6.87-7.07 (m; 5H, *H*-2″, *H*-3″, *H*-4″), 7.65-7.71 (m; 2H, *H*-3′), 7.77-7.82 (m; 2H, *H*-2′).

^{13}C-NMR (75 MHz, $CDCl_3$): δ = 24.1 (*C*-3), 25.2 (*C*-4 or *C*-5), 25.7 (*C*-4 or *C*-5), 30.0 (*C*-6), 36.0 (N*C*H_3), 52.2 (*C*-1), 58.3 (N*C*H_2), 62.2 (*C*-2), 122.9 (*C*-2′), 126.3 (*C*-4″), 127.7 (*C*-2″ or *C*-3″), 128.1 (*C*-2″ or *C*-3″), 132.1 (*C*-1′), 133.5 (*C*-3′), 140.0 (*C*-1″), 168.6 (*C*O).

The assignments were made by 2D-NMR.

HR-EI-MS Exact molecular mass for [$C_{22}H_{24}N_2O_2$] ([M]$^+$): 348.1838

Found: 348.184

8.2.20 Preparation of (1*R*,2*R*)-*N*-benzyl-*N*-methylcyclohexane-1,2-diamine 116

[SMU-V-56]

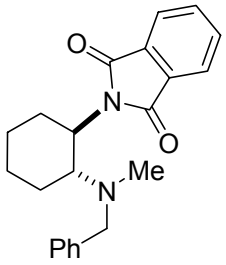

112

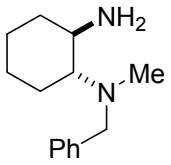

116

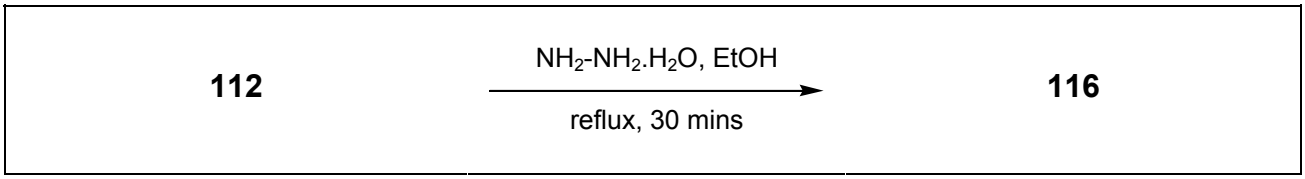

The same procedure as before (see section 8.2.8 on page 120) was followed on a 2.50 mmol scale. The product was obtained as a yellow oil (530 mg, 97 %).

116 $C_{14}H_{22}N_2$ (218.34 g/mol)

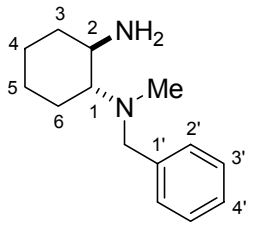

116

Yield 530 mg (2.43 mmol, 97 %)

TLC R_f = 0.47 (Silicagel, $CHCl_3$/CH_3OH/TEA 100:5:1)

^{1}H-NMR (300 MHz, $CDCl_3$): δ = 0.95-1.08 (m; 3H), 1.57-1.92 (m; 7H), 2.07 (s; 3H, CH_3), 2.10-2.15 (m; 1H, *H*-2), 2.60 (dt, *J* = 4.1, 10.13 Hz; 1H, *H*-1), 3.38 (d, *J* = 13.1 Hz; 1H, NCH_2), 3.60 (d, *J* = 13.1 Hz; 1H, NCH_2), 7.12-7.26 (m; 5H, H_{ar}).

^{13}C-NMR (75 MHz, $CDCl_3$): δ = 21.9 (*C*H_2), 24.9 (*C*-4 or *C*-5), 25.6 (*C*-4 or *C*-5), 34.9 (*C*H_2), 36.2 (*C*H_3), 51.2 (*C*-2), 57.9 (N*C*H_2), 69.3 (*C*-1), 126.6 (*C*-4′), 128.0 (*C*-2′ or *C*-3′), 128.4 (*C*-2′ or *C*-3′), 140.1 (*C*-1′).

GC-MS τ_R = 12.5 min (Method: Standard)
m/z = 218 $[M]^+$

8.2.21 Preparation of 1-{3,5-bis(trifluoromethyl)phenyl}-3-{(1*R*,2*R*)-2-(*N*-benzyl-*N*-methylamino)cyclohexyl}urea 5

[SMU-V-57]

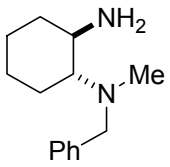

116

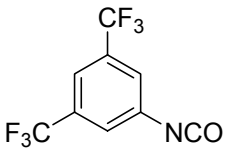

108

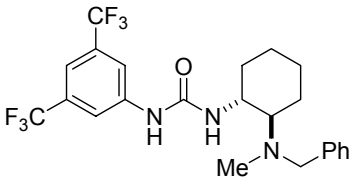

5

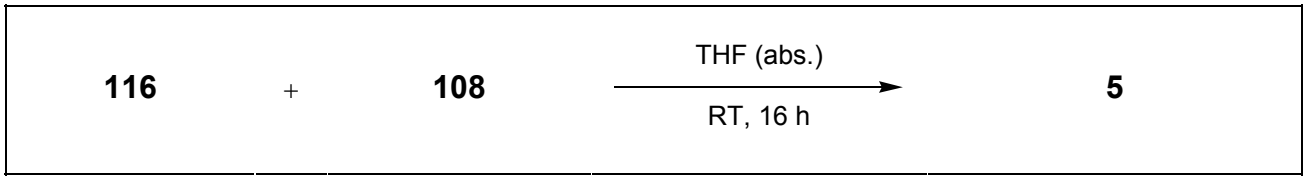

The same procedure as before (see section 8.2.10 on page 122) was followed on a 1.93 mmol scale. Purification in the same way afforded an off-white foam (980 mg, 87 %).

5 $C_{23}H_{25}F_6N_3O$ (473.45 g/mol)

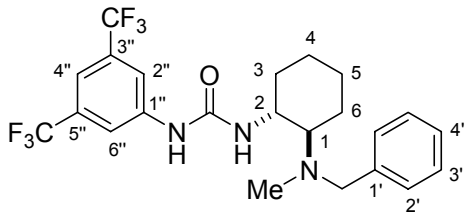

5

Yield 980 mg (2.07 mmol, 87 %)

Melting Point 63-65 °C

TLC R_f = 0.42 (Silicagel, $CHCl_3$/CH_3OH/TEA 100:5:1)

^{1}H-NMR (300 MHz, $CDCl_3$): δ = 0.99-1.25 (m; 4H, *H*-3, *H*-4, *H*-5, *H*-6), 1.57-1.89 (m; 3H, *H*-4, *H*-5, *H*-6), 2.09 (s; 3H, NCH_3), 2.26-2.37 (m; 2H, *H*-1, *H*-3), 3.34 (d, *J* = 13.1 Hz; 1H, NCH_2), 3.40-3.47 (m; 1H, *H*-2), 3.61 (d, *J* = 13.1 Hz; 1H, NCH_2), 5.71 (br s; 1H, C-2-N*H*), 7.15 (s; 5H, *H*-2′, *H*-3′, *H*-4′), 7.38

(s; 1H, *H*-4″), 7.68 (s; 2H, *H*-2″, *H*-6″), 8.18 (br s; 1H, C-1″-N*H*).

^{13}C-NMR (75 MHz, $CDCl_3$): δ = 22.7 (*C*-6), 24.5 (*C*-4 or *C*-5), 25.2 (*C*-4 or *C*-5), 33.4 (*C*-3), 36.3 (N*C*H_3), 52.0 (*C*-2), 57.9 (N*C*H_2), 66.4 (*C*-1), 115.5 (*C*-4″), 118.8 (*C*-2″, *C*-6″), 123.2 (q, *J* = 271.4 Hz; *C*F_3), 127.1 (*C*-4′), 128.3 (*C*-2′ or *C*-3′), 128.7 (*C*-2′ or *C*-3′), 132.1 (q, *J* = 32.97 Hz; *C*-3″, *C*-5″), 139.0 (*C*-1′), 140.9 (*C*-1″), 156.0 (*C*O).

The assignments were made by 2D-NMR.

FT-IR (KBr): $\tilde{\nu}$ [cm^{-1}] = 3346 (br s), 3091 (w), 2939 (s), 2861 (m), 2800 (w), 1659 (s), 1624 (m), 1571 (s), 1497 (m), 1474 (s), 1454 (m), 1388 (s), 1278 (s), 1235 (m), 1182 (s), 1132 (s), 1063 (w), 1042 (w), 1026 (m), 958 (w), 940 (m), 882 (s), 849 (m), 734 (m).

HR-EI-MS Exact molecular mass for [$C_{23}H_{25}F_6N_3O$] ([M]$^+$): 473.1902

Found: 473.190

Crystallographic Data

For the X-ray structure see Figure 5.2 on page 58

Colourless needles from ethanol

Empirical formula:	$C_{23}H_{25}N_3OF_6 \cdot CH_3CH_2OH$
Formula weight (M):	519.53 g/mol
Temperature (T):	293(2) K
Wavelength (λ):	0.71073 Å
Crystal system:	triclinic
Space group:	P_1
Unit cell dimension:	a = 8.486(1) Å α = 65.73(1)°
	b = 12.777(1) Å β = 88.64(1)°
	c = 13.460(1) Å γ = 87.43(1)°
Unit cell volume:	1329.1(2) $Å^3$
Z:	2
Calculated density ($\rho_{calcd.}$):	1.298 g/cm^3
Absorption coefficient (μ):	0.111 mm^{-1}
F(000):	544
Crystal size:	0.48 × 0.35 × 0.32 mm
Θ-range for data collection:	2.40° to 25.00°

Limiting indices:	$-8 \leq h \leq 10$
	$-15 \leq k \leq 13$
	$-15 \leq l \leq 16$
Reflections collected:	6127
Unique reflections:	6127
Reflections observed [$I>2\sigma$ (I)]:	3963
Completeness to Θ (= 27°):	99.0 %
Refinement method:	Full-matrix least-squares on F^2
Data / restraints / parameters:	6127 / 3 / 681
Goodness-of-fit on F^2:	1.341
Final *R*-indices [$I > 2\sigma(I)$]:	$R1 = 0.0981$ $\omega R2 = 0.2160$
R-indices (all data):	$R1 = 0.1455$ $\omega R2 = 0.2359$
Largest diff. peak and hole:	0.810 and -0.460 e·Å^{-3}

8.2.22 Preparation of 1-(3,5-dinitrophenyl)-3-{(1*R*,2*R*)-2-(dimethylamino)-cyclohexyl}urea 6

[SMU-IV-79]

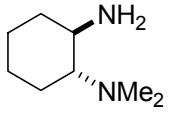

101

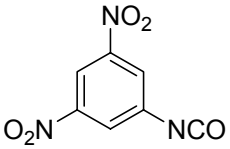

117

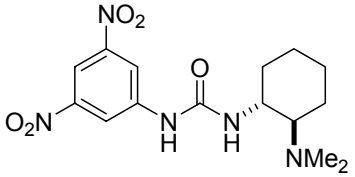

6

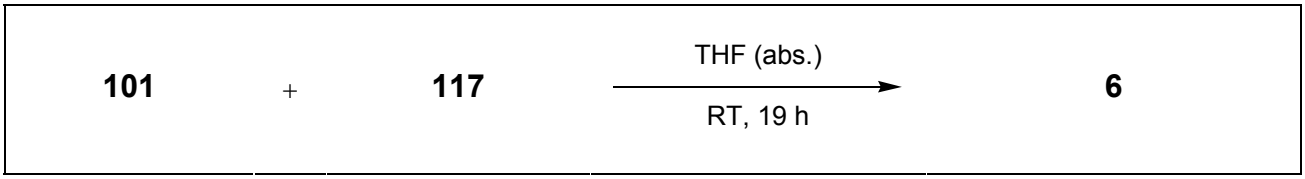

The same procedure as before (see section 8.2.10 on page 122) was followed on a 2.07 mmol scale. Purification in the same way afforded a yellow foam (584 mg, 80 %).

6 $C_{15}H_{21}N_5O_5$ (351.36 g/mol)

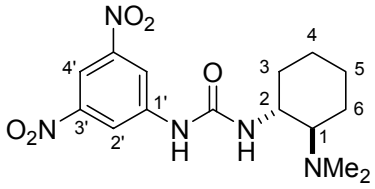

6

Yield 584 mg (1.66 mmol, 80 %)

Melting Point 97-99 °C

Specific Rotation $[\alpha]_{589}^{20}$ = -40.3°, $[\alpha]_{546}^{20}$ = -48.4° (*c* = 1.00, $CHCl_3$)

TLC R_f = 0.18 (Silicagel, $CHCl_3$/CH_3OH/TEA 100:5:1)

^{1}H-NMR (300 MHz, $CDCl_3$): δ = 1.13-1.28 (m; 4H, *H*-3, *H*-4, *H*-5, *H*-6), 1.66-1.89 (m; 3H, *H*-4, *H*-5, *H*-6), 2.28 (s; 6H, NCH_3), 2.31-2.35 (m; 2H, *H*-1, *H*-3), 3.47-3.50 (m; 1H, *H*-2), 5.87 (br s; 1H, C-2-N*H*), 8.44-8.46 (m; 1H, *H*-4′), 8.53-8.54 (m; 2H, *H*-2′).

^{13}C-NMR (75 MHz, $CDCl_3$): δ = 21.6 (*C*-6), 24.6 (*C*-4 or *C*-5), 24.9 (*C*-4 or *C*-5), 33.6 (*C*-3), 40.1 (NCH_3), 51.9 (*C*-2), 67.2 (*C*-1), 110.9 (*C*-4′), 117.8 (*C*-2′), 142.5 (*C*-1′), 148.6 (*C*-3′), 155.4 (*C*O).
The assignments were made by 2D-NMR.

FT-IR (CsI): $\tilde{\nu}$ [cm^{-1}] = 3330 (br), 3113 (w), 2940 (m), 2865 (w), 1780 (w), 1677 (s), 1601 (s), 1547 (s), 1475 (m), 1346 (s), 1261 (m), 1225 (m), 1068 (m), 1044 (w), 894 (m), 829 (w), 731 (s).

HR-ESI-MS Exact molecular mass for $[C_{15}H_{22}N_5O_5]$ ($[M+H]^+$): 352.1615
Found: 352.162

Elemental Analysis Anal. Calcd. for $C_{15}H_{21}N_5O_5$: C 51.28, H 6.02, N 19.93
Found: C 51.20, H 6.32, N 19.55

Crystallographic Data For the X-ray structure see Figure 5.3 on page 59
Colourless needles from CH_3OH/H_2O mixture
Empirical formula: $C_{15}H_{21}N_5O_5 \cdot H_2O$
Formula weight (M): 369.38 g/mol

Temperature (T):	100(2) K
Wavelength (λ):	0.71073 Å
Crystal system:	monoclinic
Space group:	$P2_1$
Unit cell dimension:	a = 8.138(1) Å α = 90.00°
	b = 22.998(2) Å β = 107.357(8)°
	c = 15.575(1) Å γ = 90.00°
Unit cell volume:	1800.0(6) $Å^3$
Z:	4
Calculated density ($\rho_{calcd.}$):	1.363 g/cm^3
Absorption coefficient (μ):	0.107 mm^{-1}
F(000):	784
Crystal size:	0.2 × 0.3 × 0.3 mm
Θ-range for data collection:	1.77° to 27.00°
Limiting indices:	$-10 \leq h \leq 10$
	$-27 \leq k \leq 26$
	$-12 \leq l \leq 12$
Reflections collected:	5944
Unique reflections:	5944
Reflections observed [I>2σ (I)]:	3042
Completeness to Θ (= 27°):	92.4 %
Refinement method:	Full-matrix least-squares on F^2
Data / restraints / parameters:	5944 / 1 / 631
Goodness-of-fit on F^2:	1.019
Final *R*-indices [$I > 2\sigma(I)$]:	$R1$ = 0.0737 $\omega R2$ = 0.1592
R-indices (all data):	$R1$ = 0.1639 $\omega R2$ = 0.1980
Largest diff. peak and hole:	0.376 and -0.345 $e \cdot Å^{-3}$

8.2.23 Preparation of 1-{(1*R*,2*R*)-2-(dimethylamino)cyclohexyl}-3-mesityl urea 7

[SMU-IV-70]

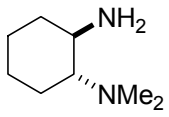

101

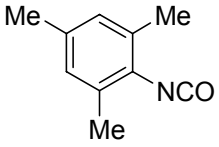

118

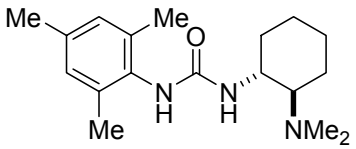

7

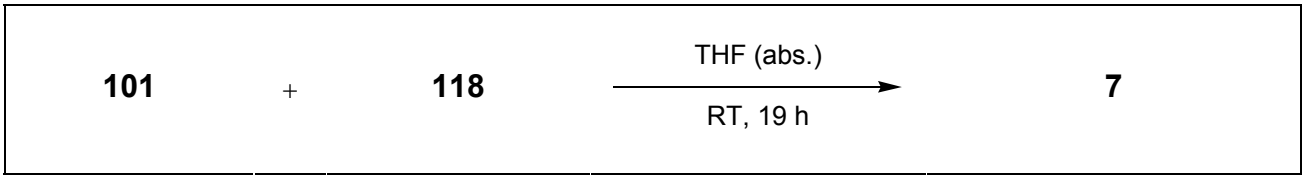

The same procedure as before (see section 8.2.10 on page 122) was followed on a 2.62 mmol scale. Purification in the same way afforded a white crystalline solid (513 mg, 65 %).

7 $C_{18}H_{29}N_3O$ (303.44 g/mol)

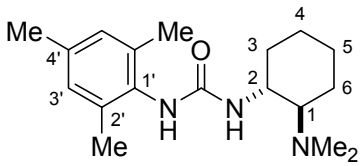

7

Yield 513 mg (1.70 mmol, 65 %)

Melting Point 168-169 °C (EtOH)

Specific Rotation $[\alpha]_{589}^{20}$ = -43.1°, $[\alpha]_{546}^{20}$ = -50.9°, $[\alpha]_{405}^{20}$ = -103.9°, $[\alpha]_{365}^{20}$ = -136.1° (*c* = 1.02, $CHCl_3$)

TLC R_f = 0.31 (Silicagel, $CHCl_3$/CH_3OH/TEA 100:5:1)

^{1}H-NMR (300 MHz, $CDCl_3$): δ = 0.89-1.32 (m; 4H, *H*-3, *H*-4, *H*-5, *H*-6), 1.55-1.74 (m; 3H, *H*-4, *H*-5, *H*-6), 1.99-2.02 (m; 1H, *H*-1), 2.08 (s; 6H, NCH_3), 2.22 (s; 6H, 2′-CH_3), 2.25 (s; 3H, 4′-CH_3), 2.30-2.38 (m; 1H, *H*-3), 3.33-3.43 (m; 1H, *H*-2), 4.97 (br s; 1H, C-2-N*H*), 5.91 (br s; 1H, C-1′-N*H*), 6.87 (s; 2H, *H*-3′).

^{13}C-NMR	(75 MHz, $CDCl_3$): δ = 18.0 (2′-*C*H$_3$), 20.9 (4′-*C*H$_3$), 21.6 (*C*-6), 24.7 (*C*-4 or *C*-5), 25.3 (*C*-4 or *C*-5), 33.8 (*C*-3), 39.8 (N*C*H$_3$), 51.5 (*C*-2), 66.5 (*C*-1), 129.0 (*C*-3′), 131.8 (*C*-4′), 137.0 (*C*-2′), 157.6 (*C*O).
FT-IR	(CsI): $\tilde{\nu}$ [cm^{-1}] = 3343 (m), 2937 (m), 2859 (w), 1638 (s), 1559 (s), 1458 (w), 1316 (w), 1264 (w), 1051 (w), 846 (m), 707 (w).
HR-ESI-MS	Exact molecular mass for [$C_{18}H_{29}N_3NaO$] ([M+Na]$^+$): 326.2208 Found: 326.221
Elemental Analysis	Anal. Calcd. for $C_{18}H_{29}N_3O$: C 71.25, H 9.63, N 13.85 Found: C 70.87, H 9.60, N 13.75
Crystallographic Data	For the X-ray structure see Figure 5.4 on page 60 Long colourless flakes from ethanol

Empirical formula:	$C_{18}H_{29}N_3O$
Formula weight (M):	303.44 g/mol
Temperature (T):	100(2) K
Wavelength (λ):	0.71073 Å
Crystal system:	orthorhombic
Space group:	$P2_12_12_1$
Unit cell dimension:	a = 11.817(1) Å α = 90°
	b = 16.662(1) Å β = 90°
	c = 18.201(1) Å γ = 90°
Unit cell volume:	3583.7(4) Å^3
Z:	8
Calculated density ($\rho_{calcd.}$):	1.125 g/cm^3
Absorption coefficient (μ):	0.071 mm^{-1}
F(000):	1328
Crystal size:	0.3 × 0.2 × 0.1 mm
Θ-range for data collection:	1.66° to 27.00°
Limiting indices:	-13 ≤ h ≤ 15
	-17 ≤ k ≤ 21
	-23 ≤ l ≤ 16
Reflections collected:	18006

Unique reflections:	7785 [R_{int} = 0.0785]
Reflections observed [I>2σ (I)]:	4125
Completeness to Θ (= 27°):	99.8 %
Refinement method:	Full-matrix least-squares on F^2
Data / restraints / parameters:	7785 / 0 / 631
Goodness-of-fit on F^2:	0.941
Final *R*-indices [$I > 2\sigma(I)$]:	$R1$ = 0.0548 $\omega R2$ = 0.0709
R-indices (all data):	$R1$ = 0.1504 $\omega R2$ = 0.0885
Largest diff. peak and hole:	0.222 and -0.193 e·Å^{-3}

8.2.24 Preparation of 1-{(1*R*,2*R*)-2-(dimethylamino)cyclohexyl}-3-(pyridine-3-yl)thiourea 8

[SMU-VII-68]

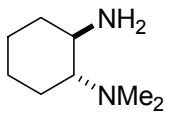

101

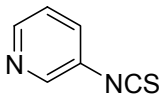

119

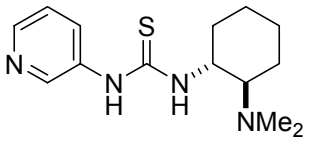

8

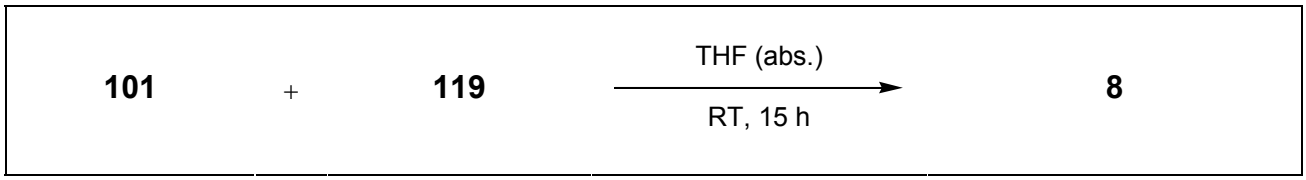

The same procedure as before (see section 8.2.10 on page 122) was followed on a 2.11 mmol scale. Purification by column chromatography on silica gel using DCM/MeOH/TEA (100:5:1 to 100:10:2) as the eluant afforded a yellow foam (415 mg, 71 %).

8 $C_{14}H_{22}N_4S$ (278.42 g/mol)

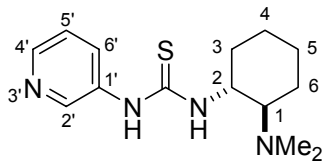

8

Yield 415 mg (1.49 mmol, 71 %)

TLC R_f = 0.20 (Silicagel, CH_2Cl_2/CH_3OH/TEA 100:5:1)

^{1}H-NMR (300 MHz, $CDCl_3$): δ = 1.14-1.27 (m; 5H), 1.65-1.92 (m; 3H), 2.31 (m; 1H), 2.45 (s; 6H, NC*H*$_3$), 2.86-2.92 (m; 1H), 4.26 (br s; 1H, C-2-N*H*), 6.14 (br s; 1H, C-1′-N*H*), 7.13-7.17(m; 1H, H_{ar}), 7.94-7.96 (m; 1H, H_{ar}), 8.23-8.24 (m; 1H, H_{ar}), 8.53 (s; 1H, *H*-2′).

^{13}C-NMR (75 MHz, $CDCl_3$): δ = 22.6 (*C*-6), 24.2 (*C*-4 or *C*-5), 24.3 (*C*-4 or *C*-5), 32.4 (*C*-3), 39.9 (N*C*H$_3$), 54.5 (*C*-2), 67.0 (*C*-1), 123.0 (C_{ar}), 131.0 (C_{ar}), 136.0 (Cq_{ar}), 144.7 (C_{ar}), 145.3 (C_{ar}), 181.5 (*C*S).
Assignments were made by 2D-NMR.

FT-IR (ATR): $\tilde{\nu}$ [cm^{-1}] = 3234 (br), 3027 (br), 2931 (s), 2857 (sh), 2783 (w), 1538 (s), 1481 (m), 1425 (m), 1316 (s), 1229 (m), 1185 (w), 1160 (sh), 1096 (m), 1062 (w), 1043 (w), 1025 (w), 991 (sh), 954 (w), 938 (w), 910 (w), 883 (m), 851 (w), 804 (s), 725 (m).

HR-EI-MS Exact molecular mass for [$C_{14}H_{23}N_4S$] ([M+H]$^+$): 279.1643
Found: 279.165

8.2.25 Preparation of 1-{(1*R*,2*R*)-2-dimethylamino-cyclohexyl}-3-cyclohexyl-thiourea 9

[SMU-VI-14]

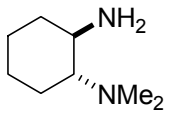

101

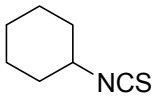

120

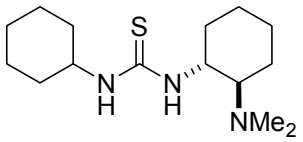

9

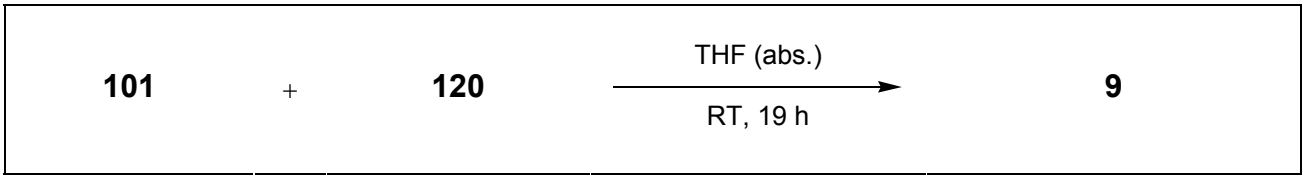

The same procedure as before (see section 8.2.10 on page 122) was followed on a 2.74 mmol scale. Purification by column chromatography on silica gel using DCM/MeOH/TEA 100:5:1 as the eluant afforded a colorless foam (600 mg, 77 %).

9	$C_{15}H_{29}N_3S$ (283.48 g/mol)
Yield	600 mg (2.12 mmol, 77 %)
Melting Point	59-60 °C
Specific Rotation	$[\alpha]_{589}^{20}$ = +23.4°, $[\alpha]_{546}^{20}$ = +27.9°, $[\alpha]_{405}^{20}$ = +45.0°, $[\alpha]_{365}^{20}$ = +29.3° (*c* = 1.01, $CHCl_3$)
TLC	R_f = 0.35 (Silicagel, CH_2Cl_2/CH_3OH/TEA 100:5:1)
^{1}H-NMR	(300 MHz, $CDCl_3$): δ = 1.01-1.41, 1.54-1.83, 1.91-2.01 (3m; 17H, *H*-3, 2×*H*-4, 2×*H*-5, 2×*H*-6, 2×*H*-2′, 2×*H*-3′, 2×*H*-4′, 2×*H*-5′, 2×*H*-6′), 2.21 (s; 6H, NCH_3), 2.28-2.43 (m; 2H, *H*-1, *H*-3), 3.50-3.55 (m; 1H, *H*-2), 3.73

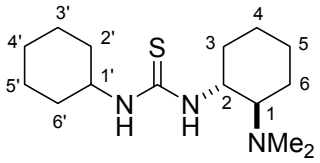

9

(br m; 1H, *H*-1′), 6.28 (s; 1H, C-2-N*H*).

^{13}C-NMR (75 MHz, $CDCl_3$): δ = 22.1 (*C*-6), 24.4, 24.7, 24.8, 24.9, 25.4 (*C*-4, *C*-5, *C*-3′, *C*-4′, *C*-5′), 32.8, 32.9, 33.1 (*C*-3, *C*-2′, *C*-6′), 40.2 (N*C*H_3), 52.8 (*C*-1′), 56.1 (*C*-2), 67.3 (*C*-1), 181.1 (*C*S).
The assignments were made by 2D-NMR.

FT-IR (ATR): $\tilde{\nu}$ [cm^{-1}] = 3259 (br), 3050 (w), 2926 (s), 2852 (s), 2783 (m), 1539 (s), 1473 (w), 1448 (m), 1360 (m), 1321 (m), 1271 (w), 1254 (m), 1239 (w), 1207 (w), 1187 (w), 1152 (w), 1081 (w), 1061 (w), 1040 (w), 978 (w), 946 (w), 889 (w), 872 (w), 847 (w), 734 (m).

HR-EI-MS Exact molecular mass for [$C_{15}H_{29}N_3S$] ([M]$^+$): 283.2082
Found: 283.209

Elemental Analysis Anal. Calcd. for $C_{15}H_{29}N_3S$: C 63.55, H 10.31, N 14.82
Found: C 63.26, H 10.22, N 14.75

8.2.26 Preparation of 1-{(1*S*,2*S*)-2-dimethylamino-cyclohexyl}-3-cyclohexyl-thiourea *ent*-**9**

[SMU-VI-63]

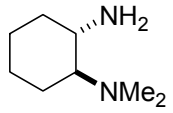

ent-**101**

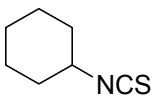

120

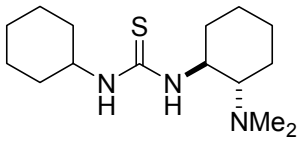

ent-**9**

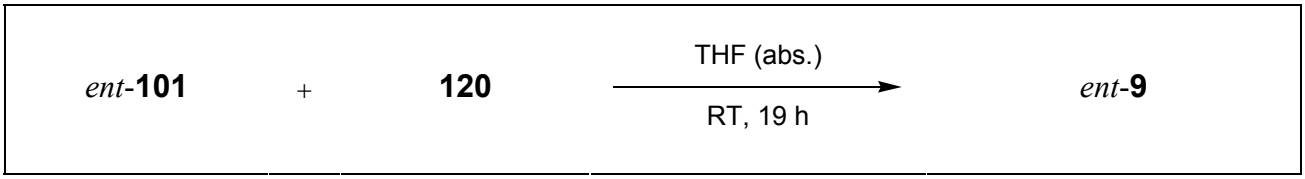

The same procedure as before (see section 8.2.10 on page 122) was followed on a 2.67 mmol scale. Purification by column chromatography on silica gel using DCM/MeOH/TEA 100:5:1 as the eluant afforded a colorless foam (585 mg, 77 %).

ent-**9**	$C_{15}H_{29}N_3S$ (283.48 g/mol)
Yield	585 mg (2.06 mmol, 77 %)
Melting Point	59-60 °C
Specific Rotation	$[\alpha]_{589}^{20}$ = -23.1°, $[\alpha]_{546}^{20}$ = -27.4°, $[\alpha]_{405}^{20}$ = -44.4°, $[\alpha]_{365}^{20}$ = -29.3° (*c* = 1.01, $CHCl_3$)
TLC	R_f = 0.36 (Silicagel, CH_2Cl_2/CH_3OH/TEA 100:5:1)
^{1}H-NMR	(300 MHz, $CDCl_3$): δ = 1.06-1.34 (m; 9H), 1.52-1.98 (m; 8H) [*H*-3, 2×*H*-4, 2×*H*-5, 2×*H*-6, 2×*H*-2′, 2×*H*-3′, 2×*H*-4′, 2×*H*-5′, 2×*H*-6′], 2.18 (s; 6H, NCH_3), 2.27-2.40 (m; 2H, *H*-1, *H*-3), 3.52 (m; 1H, *H*-2), 3.72 (m; 1H, *H*-1′), 6.33 (br s; 1H, C-2-N*H*).
^{13}C-NMR	(75 MHz, $CDCl_3$): δ = 22.1 (*C*-6), 24.4, 24.6, 24.8, 24.8, 25.4 (*C*-4, *C*-5, *C*-3′, *C*-4′, *C*-5′), 32.8, 32.9, 33.0 (*C*-3, *C*-2′, *C*-6′), 40.2 (NCH_3), 52.7 (*C*-1′), 56.0 (*C*-2), 67.2 (*C*-1), 181.0 (*C*S). The assignments were made by 2D-NMR.
FT-IR	(ATR): $\tilde{\nu}$ [cm^{-1}] = 3260 (br), 3049 (w), 2926 (s), 2852 (s), 2785 (m), 1538 (s), 1473 (w), 1448 (m), 1360 (m), 1321 (m), 1271 (w), 1254 (m), 1238 (w), 1207 (w), 1186 (w), 1151 (w), 1081 (w), 1060 (w), 1040 (w), 978 (w), 946 (w), 915 (w), 889 (w), 873 (w), 847 (w), 773 (w), 734 (s).
HR-EI-MS	Exact molecular mass for [$C_{15}H_{29}N_3S$] ([M]$^+$): 283.2082 Found: 283.208
Elemental Analysis	Anal. Calcd. for $C_{15}H_{29}N_3S$: C 63.55, H 10.31, N 14.82 Found: C 63.32, H 10.34, N 14.62

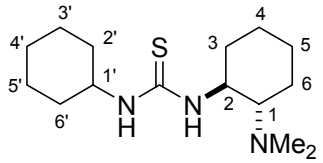

ent-**9**

8.2.27 Preparation of 1-adamantan-1-yl-3-{(1*R*,2*R*)-2-dimethylamino-cyclohexyl}-thiourea 10

[SMU-VII-65]

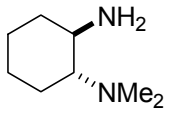

101

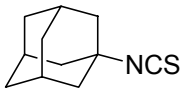

121

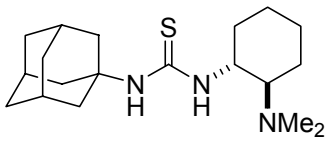

10

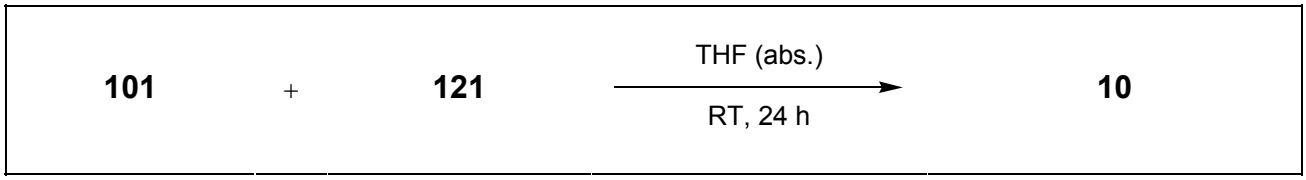

The same procedure as before (see section 8.2.10 on page 122) was followed on a 2.11 mmol scale. Purification by column chromatography on silica gel using DCM/MeOH/TEA 100:5:1 as the eluant afforded a colorless foam (550 mg, 78 %).

10	$C_{19}H_{33}N_3S$ (335.55 g/mol)	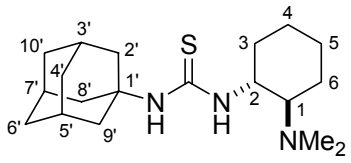 **10**
Yield	550 mg (1.64 mmol, 78 %)	
Melting Point	78-79 °C	
Specific Rotation	$[\alpha]_{589}^{20}$ = -69.0°, $[\alpha]_{546}^{20}$ = -81.8°, $[\alpha]_{405}^{20}$ = -158.6°, $[\alpha]_{365}^{20}$ = -194.8° (*c* = 1.00, $CHCl_3$)	
TLC	R_f = 0.28 (Silicagel, CH_2Cl_2/CH_3OH/TEA 100:5:1)	
^{1}H-NMR	(300 MHz, $CDCl_3$): δ = 0.93-1.35 (m; 4H), 1.55-1.66 (m; 7H), 1.80-1.82 (m; 2H), 1.94 (s; 6H), 2.05 (s; 3H), 2.17 (s; 6H, NC*H*$_3$), 2.31-2.38 (m; 1H, *H*-1), 2.93-2.97 (m; 1H), 3.45-3.55 (m; 1H, *H*-2), 6.09 (br s; 1H, C-1′-N*H*), 6.61	

(br s; 1H, C-2-N*H*).

^{13}C-NMR (75 MHz, $CDCl_3$): δ = 21.4 (*C*H_2), 24.3 (*C*H_2), 25.3 (*C*H_2), 29.3 (*C*H), 32.6 (*C*H_2), 36.0 (*C*H_2), 39.6 (N*C*H_3), 41.8 (*C*H_2), 53.4 (*C*q), 56.8 (*C*-2), 67.2 (*C*-1), 180.8 (*C*S).
The assignments were made by 2D-NMR.

FT-IR (ATR): $\tilde{\nu}$ [cm^{-1}] = 3273 (br), 2904 (s), 2849 (sh), 2784 (m), 1521(s), 1473 (w), 1450 (m), 1399 (w), 1370 (w), 1356 (sh), 1340 (w), 1306 (m), 1294 (m), 1250 (w), 1228 (w), 1203 (m), 1186 (w), 1149 (w), 1114 (w), 1088 (m), 1060 (m), 1039 (m), 979 (w), 957 (w), 914 (m), 872 (w), 836 (sh), 730 (s).

HR-EI-MS Exact molecular mass for [$C_{19}H_{34}N_3S$] ([M+H]$^+$): 336.2473
Found: 336.247

Elemental Analysis Anal. Calcd. for $C_{19}H_{33}N_3S$: C 68.01, H 9.91, N 12.52
Found: C 67.65, H 9.78, N 12.58

8.2.28 Preparation of 1,6-di-{3-(1*R*,2*R*)-2-dimethylamino-cyclohexyl}-ureado hexane 11

[SMU-VII-75]

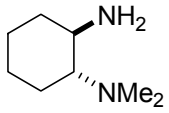

101

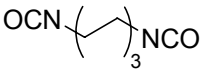

122

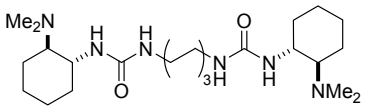

11

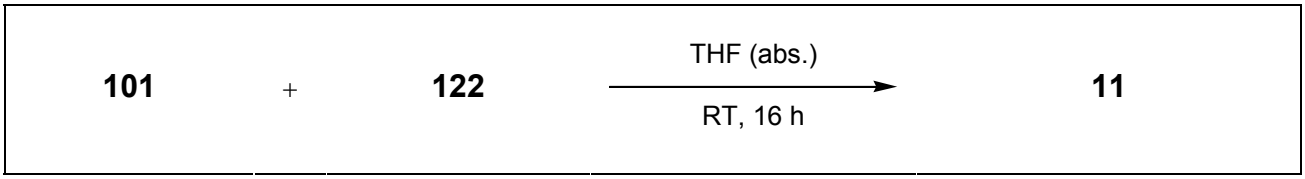

To a solution of (1*R*,2*R*)-*N*,*N*-dimethyl-1,2-diaminocyclohexane **101** (300 mg, 2.11 mmol, 2.27 eq) in absolute in 2 mL abs. THF, was added 1,6-diisocyanatohexane **122** (150 µL, 930 µmol, 1.00 eq) and the resulting mixture was stirred under argon for 16 hours at room temperature. The solvent

was removed in vacuo to yield an off-white foam. This was taken in DCM (10 mL) and washed with water (3 × 10 mL). The DCM layer was dried over anh. Na_2CO_3 and the filtrate was concentrated in vacuo to obtain a colorless foam (330 mg, 79 %).

11 $C_{24}H_{48}N_6O_2$
(452.68 g/mol)

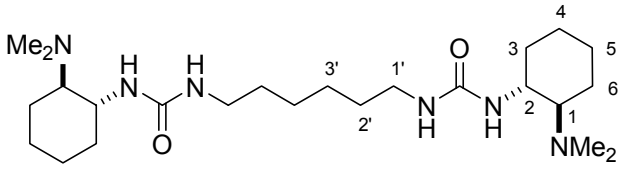

11

Yield 330 mg (730 µmol, 79 %)

Melting Point 56-58 °C

^{1}H-NMR (300 MHz, $CDCl_3$): δ = 0.92-1.78 (m; 24H), 2.15 (s; 12H, NC*H*$_3$), 2.26-2.30 (m; 2H), 3.02-3.08 (m; 4H), 3.27-3.37 (m; 2H), 4.96-4.98 (m; 2H), 5.35-5.36 (m; 2H).

^{13}C-NMR (75 MHz, $CDCl_3$): δ = 21.4 (*C*-6), 24.6 (*C*-4 or *C*-5), 25.2 (*C*-4 or *C*-5), 26.3 (*C*-3′), 29.8 (*C*-2′), 34.0 (*C*-3), 39.9 (N*C*H$_3$), 40.1 (*C*-1′), 51.3 (*C*-2), 66.7 (*C*-1), 159.1 (CO).

FT-IR (ATR): $\tilde{\nu}$ [cm^{-1}] = 3315 (br), 2926 (s), 2854 (sh), 2774 (m), 1632 (s), 1562 (s), 1453 (w), 1314 (w), 1262 (m), 1238 (m), 1188 (w), 1084 (w), 1043 (m), 871 (sh), 848 (w), 729 (m).

HR-EI-MS Exact molecular mass for [$C_{24}H_{49}N_6O_2$] ([M+H]$^+$): 453.3917
Found: 453.391

8.2.29 Preparation of 1-{(1*R*,2*R*)-2-(dimethylamino)cyclohexyl}-3-{(*R*)-1-phenylethyl}urea 12

[SMU-V-37]

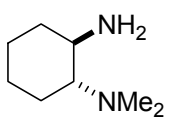

101

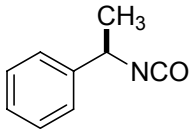

123

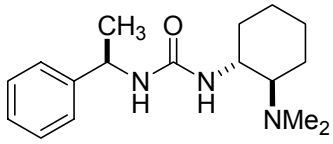

12

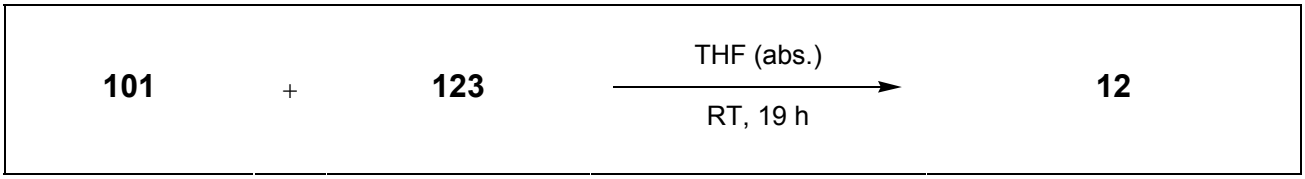

The same procedure as before (see section 8.2.10 on page 122) was followed on a 2.21 mmol scale. Purification in the same way afforded a colorless crystalline solid (445 mg, 70 %).

12 $C_{17}H_{27}N_3O$ (289.42 g/mol)

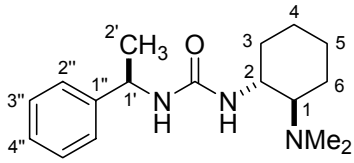

12

Yield 445 mg (1.54 mmol, 70 %)

Melting Point 137 °C ($CHCl_3$)

Specific Rotation $[\alpha]_{589}^{20}$ = -33.3°, $[\alpha]_{546}^{20}$ = -38.6°, $[\alpha]_{405}^{20}$ = -66.5°, $[\alpha]_{365}^{20}$ = -77.0°, $[\alpha]_{334}^{20}$ = -82.1° (*c* = 1.015, $CHCl_3$)

TLC R_f = 0.31 (Silicagel, $CHCl_3$/CH_3OH/TEA 100:5:1)

^{1}H-NMR (300 MHz, $CDCl_3$): δ = 0.88-1.30 (m; 4H, *H*-3, *H*-4, *H*-5, *H*-6), 1.37 (d, *J* = 6.82 Hz; 3H, *H*-2′), 1.54-1.71 (m; 3H, *H*-4, *H*-5, *H*-6), 1.91 (s; 6H, NCH_3), 2.03-2.11 (m; 1H, *H*-1), 2.37-2.43 (m; 1H, *H*-3), 3.11-3.19 (m; 1H, *H*-2), 4.64 (dq, *J* = 6.53, 6.82 Hz; 1H, *H*-1′), 5.11 (d, *J* = 6.53 Hz; 1H, C-1′-N*H*), 5.35 (br s; 1H, C-2-N*H*), 7.16-7.25 (m; 1H, *H*-4″), 7.28 (d, *J* = 4.41 Hz; 4H, *H*-2″, *H*-3″).

^{13}C-NMR (75 MHz, $CDCl_3$): δ = 21.1 (*C*-6), 23.8 (*C*-2′), 24.5 (*C*-4 or *C*-5), 25.2 (*C*-4 or *C*-5), 33.5 (*C*-3), 39.4 (NCH_3), 50.5 (*C*-1′), 51.7 (*C*-2), 66.5 (*C*-1), 125.8 (*C*-2″ or *C*-3″), 127.0 (*C*-4″), 128.5 (*C*-2″ or *C*-3″), 144.6 (*C*-1″), 158.8 (*C*O).
The assignments were made by 2D-NMR.

FT-IR (KBr): $\tilde{\nu}$ [cm^{-1}] = 3359 (s), 3298 (s), 3060 (w), 2970 (m), 2933 (s), 2858 (s), 2820 (m), 2778 (m), 1670 (w), 1622 (s), 1570 (s), 1449 (m), 1375 (w), 1321 (w), 1262 (m), 1239 (m), 1190 (w), 1095 (m), 1027 (w), 872 (m), 764 (m).

HR-ESI-MS Exact molecular mass for $[C_{17}H_{28}N_3O]$ ($[M+H]^+$): 290.2227
Found: 290.223

Elemental Analysis Anal. Calcd. for $C_{17}H_{27}N_3O$: C 70.55, H 9.40, N 14.52
Found: C 70.05, H 9.22, N 14.45

Crystallographic Data For the X-ray structure see Figure 5.5 on page 63
Colourless needles from chloroform

Empirical formula:	$C_{17}H_{27}N_3O$
Formula weight (M):	289.42 g/mol
Temperature (T):	100(2) K
Wavelength (λ):	0.71073 Å
Crystal system:	monoclinic
Space group:	$P2_1$
Unit cell dimension:	a = 8.727(1) Å α = 90°
	b = 22.143(1) Å β = 101.78(1)°
	c = 9.924(1) Å γ = 90°
Unit cell volume:	1877.3(3) $Å^3$
Z:	4
Calculated density ($\rho_{calcd.}$):	1.024 g/cm^3
Absorption coefficient (μ):	0.065 mm^{-1}
F(000):	632
Crystal size:	0.20 × 0.15 × 0.15 mm
Θ-range for data collection:	2.10° to 27.00°
Limiting indices:	$-11 \leq h \leq 11$
	$-26 \leq k \leq 28$

	$-11 \leq l \leq 11$
Reflections collected:	9720
Unique reflections:	6657 [R_{int} = 0.0405]
Reflections observed [I>2σ (I)]:	4339
Completeness to Θ:	91.7 %
Refinement method:	Full-matrix least-squares on F^2
Data / restraints / parameters:	6657 / 1 / 597
Goodness-of-fit on F^2:	1.032
Final *R*-indices [$I > 2\sigma(I)$]:	$R1$ = 0.0553 $\omega R2$ = 0.0914
R-indices (all data):	$R1$ = 0.1076 $\omega R2$ = 0.1076
Largest diff. peak and hole:	0.189 and -0.219 e·Å^{-3}

8.2.30 Preparation of 1-{(1*R*,2*R*)-2-(dimethylamino)cyclohexyl)-3-{(*S*)-1-phenylethyl)urea 13

[SMU-V-49]

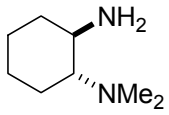

101

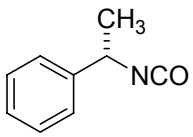

ent-**123**

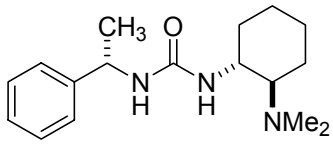

13

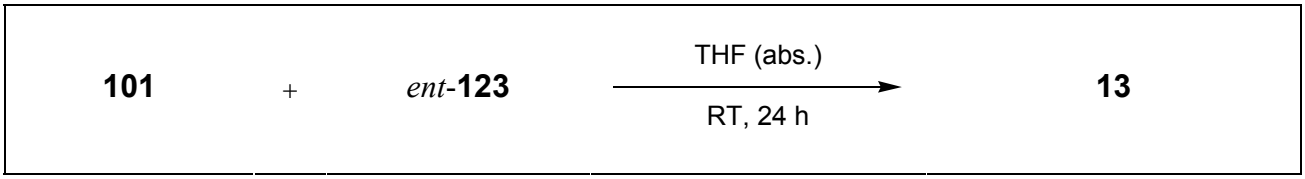

The same procedure as before (see section 8.2.10 on page 122) was followed on a 1.58 mmol scale. Purification in the same way afforded a colorless crystalline solid (345 mg, 75 %).

13 $C_{17}H_{27}N_3O$ (289.42 g/mol)

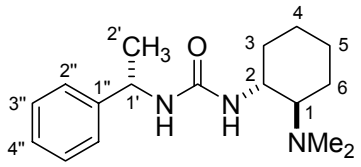

13

Yield 345 mg (1.19 mmol, 75 %)

Melting Point 146 °C ($CHCl_3$)

Specific Rotation $[\alpha]_{589}^{20}$ = -57.2°, $[\alpha]_{546}^{20}$ = -67.7°, $[\alpha]_{405}^{20}$ = -137.1°, $[\alpha]_{365}^{20}$ = -179.5°, $[\alpha]_{334}^{20}$ = -230.2° (*c* =1.00, $CHCl_3$)

TLC R_f = 0.31 (Silicagel, $CHCl_3$/CH_3OH/TEA 100:5:1)

^{1}H-NMR (300 MHz, $CDCl_3$): δ = 0.88-1.29 (m; 4H, *H*-3, *H*-4, *H*-5, *H*-6), 1.42 (d, *J* = 6.93 Hz; 3H, *H*-2′), 1.56-1.77 (m; 3H, *H*-4, *H*-5, *H*-6), 2.09-2.14 (m, 1H, *H*-1), 2.16 (s; 6H, N*CH*$_3$), 2.36-2.42 (m; 1H, *H*-3), 3.19-3.28 (m; 1H, *H*-2), 4.79 (dq, *J* = 6.93, 6.85 Hz; 1H, *H*-1′), 4.98 (br s; 1H, C-1′-N*H*), 5.18 (br s; 1H, C-2-N*H*), 7.17-7.31 (m; 5H, H_{ar}).

^{13}C-NMR (75 MHz, $CDCl_3$): δ = 21.4 (*C*-6), 23.1 (*C*-2′), 24.5 (*C*-4 or *C*-5), 25.2 (*C*-4 or *C*-5), 33.6 (*C*-3), 39.9 (N*C*H$_3$), 50.0 (*C*-1′), 51.9 (*C*-2), 66.8 (*C*-1), 126.0 (*C*-2″ or *C*-3″), 127.0 (*C*-4″), 128.5 (*C*-2″ or *C*-3″), 144.6 (*C*-1″), 158.4 (*C*O).
The assignments were made by 2D-NMR.

FT-IR (KBr): $\tilde{\nu}$ [cm^{-1}] = 3335 (s), 3302 (s), 2976 (m), 2921 (s), 2859 (m), 2821 (m), 2777 (m), 1674 (w), 1622 (s), 1559 (s), 1456 (m), 1372 (w), 1330 (m), 1255 (m), 1235 (m), 1208 (m), 1106 (m), 1074 (m), 1052 (w), 1020 (m), 873 (w), 830 (w), 745 (w).

HR-ESI-MS Exact molecular mass for [$C_{17}H_{27}N_3NaO$] ([M+Na]$^+$): 312.2052
Found: 312.206

Elemental Analysis Anal. Calcd. for $C_{17}H_{27}N_3O$: C 70.55, H 9.40, N 14.52
Found: C 70.32, H 9.34, N 14.47

Crystallographic Data For the X-ray structure see Figure 5.5 on page 63
Colourless needles from chloroform

Empirical formula:	$C_{17}H_{27}N_3O$
Formula weight (M):	289.42 g/mol
Temperature (T):	100(2) K
Wavelength (λ):	0.71073 Å
Crystal system:	orthorhombic
Space group:	$P2_12_12_1$
Unit cell dimension:	a = 9.1661(4) Å $\alpha = 90°$
	b = 11.3191(6) Å $\beta = 90°$
	c = 15.5757(8) Å $\gamma = 90°$
Unit cell volume:	1616.01(14) $Å^3$
Z:	4
Calculated density ($\rho_{calcd.}$):	1.190 g/cm^3
Absorption coefficient (μ):	0.075 mm^{-1}
F(000):	632
Crystal size:	0.1 × 0.2 × 0.3 mm
Θ-range for data collection:	2.22° to 26.99°
Limiting indices:	$-11 \leq h \leq 11$
	$-14 \leq k \leq 11$
	$-18 \leq l \leq 19$
Reflections collected:	7841
Unique reflections:	2021 [$R_{int} = 0.0444$]
Reflections observed [I>2σ (I)]:	1677
Completeness to Θ:	100.0 %
Refinement method:	Full-matrix least-squares on F^2
Data / restraints / parameters:	2021 / 0 / 298
Goodness-of-fit on F^2:	1.004
Final *R*-indices [$I > 2\sigma(I)$]:	$R1 = 0.0339$ $\omega R2 = 0.0678$
R-indices (all data):	$R1 = 0.0475$ $\omega R2 = 0.0718$
Largest diff. peak and hole:	0.132 and -0.187 $e \cdot Å^{-3}$

8.2.31 Preparation of 1,3-bis{(1*R*,2*R*)-2-(dimethylamino)cyclohexyl} thiourea 14

[SMU-V-85]

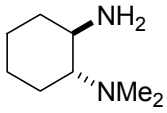

101

124

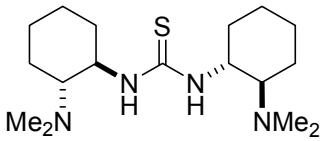

14

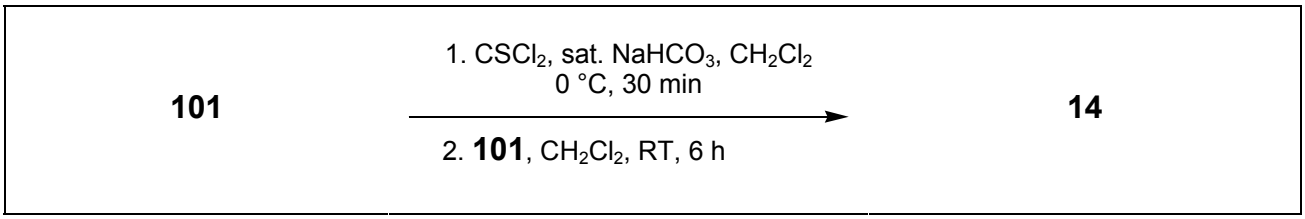

Saturated aqueous sodium bicarbonate solution (10 mL) was added to a solution of (1*R*,2*R*)-*N*,*N*-dimethyl-1,2-diaminocyclohexane **101** (240 mg, 1.69 mmol, 1.00 eq) in 10 mL of DCM and the resulting biphasic mixture was cooled to 0 °C. Thiophosgene (140 µL, 1.86 mmol, 1.10 eq) was added to the organic (lower) phase by a syringe. The resulting mixture was then vigorously stirred at 0°C for 30 minutes. The mixture was then diluted with dichloromethane (20 mL) and the organic phase was separated. The aqueous phase was extracted with DCM (5 × 15 mL). The combined organic layers were dried over anh. Na_2SO_4 and concentrated under reduced pressure to afford (1*R*,2*R*)-2-isothiocyanato-*N*,*N*-dimethylcyclohexanamine **124** as an brown semisolid which was used immediately in the following step without purification. The crude isothiocyanate **124** was dissolved in 3 mL of abs. DCM and a solution of **101** (250 mg, 1.76 mmol, 1.04 eq) in 7 mL abs. DCM was added in one portion. The resulting mixture was then stirred at room temperature for 6 hours and then concentrated in vacuo. The crude product was purified by column chromatography on silica gel (CH_2Cl_2/MeOH/TEA = 100:5:1 to 25:25:1 as eluant) to obtain an off-white foam (330 mg, 60 %).

14 $C_{17}H_{34}N_4S$ (326.54 g/mol)

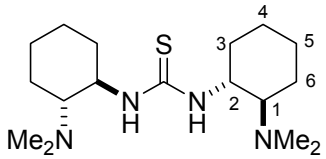

14

Yield 330 mg (1.01 mmol, 60 %)

TLC R_f = 0.18 (Silicagel, CH_2Cl_2/CH_3OH/TEA 100:5:1)

^{1}H-NMR (300 MHz, $CDCl_3$): δ = 0.99-1.33 (m; 8H, *H*-3, *H*-4, *H*-5, *H*-6), 1.61-1.84 (m; 6H, *H*-4, *H*-5, *H*-6), 2.21 (s; 12H, NC*H*$_3$), 2.33-2.41 (m; 4H, *H*-1, *H*-3), 3.60-3.69 (m; 2H, *H*-2), 7.17 (br s; 2H, N*H*).

^{13}C-NMR (75 MHz, $CDCl_3$): δ = 21.9 (*C*-6), 24.5 (*C*-4 or *C*-5), 25.0 (*C*-4 or *C*-5), 33.0 (*C*-3), 39.1 (N*C*H$_3$), 55.7 (*C*-2), 66.7 (*C*-1), 182.6 (*C*S).
The assignments were made by 2D-NMR.

FT-IR (KBr): $\tilde{\nu}$ [cm^{-1}] = 3265 (br), 2931 (s), 2857 (s), 2783 (m), 1540 (s), 1457 (m), 1362 (m), 1323 (m), 1270 (m), 1240 (w), 1187 (w), 1165 (w), 1085 (w), 1038 (m), 957 (w), 871 (m), 739 (m).

HR-EI-MS Exact molecular mass for [$C_{17}H_{34}N_4S$] ([M]$^+$): 326.2504
Found: 326.251

8.2.32 Preparation of (*S*)-2-*tert*-butoxycarbonylamino-3,3-dimethyl-butanoic acid 128

[SMU-V-92]

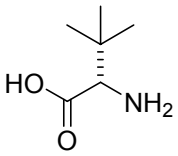

126

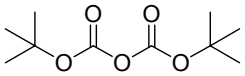

125

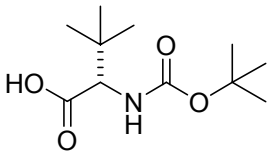

128

To a solution of L-*tert*-leucine **126** (1.00 g, 7.62 mmol, 1.00 eq) and Na_2CO_3 (888 mg, 8.38 mmol, 1.10 eq) in 30 mL MeOH/H_2O (1:1), was added di-*tert*-butyl dicarbonate **125** (1.83 g, 8.38 mmol, 1.10 eq) and the resulting mixture was stirred at room temperature for 18 hours. Methanol was removed completely; the aqueous solution was acidified with sat. citric acid solution (pH ~4) and extracted with DCM (4 × 25 mL) and Et_2O (2 × 25 mL). The combined organic layers were dried over anh. Na_2CO_3 and the solvent was removed in vacuo to obtain a colorless amorphous solid (1.61 g, 91 %).

128 $C_{11}H_{21}NO_4$ (231.29 g/mol)

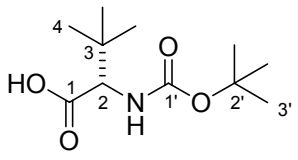

128

Yield 1.61 g (6.96 mmol, 91 %)

Melting Point 99-100 °C [Lit.[171]: 100-101 °C]

^{1}H-NMR (300 MHz, CD_3OD): δ = 0.96 (s; 9H, *H*-4), 1.42 (s; 9H, *H*-3′), 3.78 (s; 1H, *H*-2).
The OH and NH protons could not be detected.

^{13}C-NMR (75 MHz, CD_3OD): δ = 27.5 (*C*-4), 28.8 (*C*-3′), 35.0 (*C*-3), 65.7 (*C*-2), 79.8 (*C*-2′), 157.6 (*C*-1′), 178.4 (*C*-1).

FT-IR (KBr): $\tilde{\nu}$ [cm^{-1}] = 3422 (br), 2976 (s), 1690 (s), 1590 (s), 1501 (s), 1392 (s), 1366 (s), 1334 (w), 1250 (m), 1175 (s), 1059 (m), 1013 (m), 914 (w), 862 (w), 818 (w), 772 (w).

8.2.33 Preparation of (*R*)-2-*tert*-butoxycarbonylamino-3,3-dimethyl-butanoic acid *ent*-128

[SMU-VI-22]

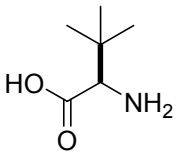

ent-**126**

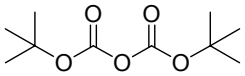

125

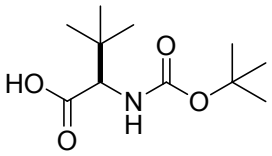

ent-**128**

The same procedure as before (see section 8.2.32 on page 160) was followed on a 15.3 mmol scale. Pure product was obtained as a colorless crystalline solid (3.44 g, 98 %).

ent-**128** $C_{11}H_{21}NO_4$ (231.29 g/mol)

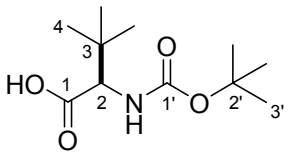

ent-**128**

Yield 3.44 g (14.9 mmol, 98 %)

Melting Point 100 °C [Lit.[171]: 100-101 °C]

^{1}H-NMR (300 MHz, $CDCl_3$): δ = 0.99 (s; 9H, *H*-4), 1.41 (s; 9H, *H*-3′), 4.09 (d, *J* = 9.35 Hz; 1H, *H*-2), 5.11 (d, *J* = 9.35 Hz; 1H, N*H*), 9.71 (br s; 1H, O*H*).

^{13}C-NMR (75 MHz, $CDCl_3$): δ = 26.5 (*C*-4), 28.3 (*C*-3′), 34.5 (*C*-3), 61.6 (*C*-2), 80.0 (*C*-2′), 155.6 (*C*-1′), 176.7 (*C*-1).

FT-IR (ATR): $\tilde{\nu}$ [cm^{-1}] = 3318 (br), 2967 (m), 2671 (w), 1710 (s), 1658 (s), 1506 (m), 1478 (w), 1454 (w), 1394 (s), 1367 (s), 1329 (m), 1233 (m), 1159 (s), 1059 (m), 1034 (w), 1011 (m), 909 (w), 854 (w), 776 (w), 732 (w).

8.2.34 Preparation of (*S*)-2-*tert*-butoxycarbonylamino-4,4-dimethyl-pentanoic acid 129

[SMU-VI-59]

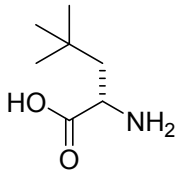

127

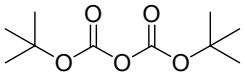

125

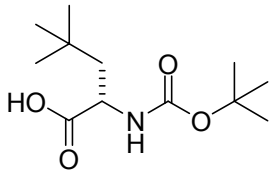

129

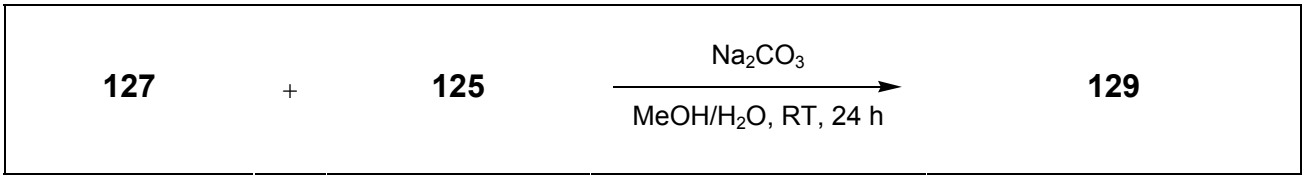

The same procedure as before (see section 8.2.32 on page 160) was followed on a 20.7 mmol scale. Pure product was obtained as a colorless solid (4.64 g, 92 %).

129 $C_{12}H_{23}NO_4$ (245.32 g/mol)

Yield 4.64 g (18.9 mmol, 92 %)

Melting Point 102 °C [Lit.[172]: 102-103 °C]

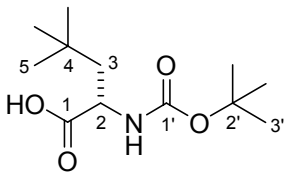

129

^{1}H-NMR (300 MHz, $CDCl_3$): δ = 0.96 (s; 9H, *H*-5), 1.42 (s; 9H, *H*-3′), 1.76-1.81 (m; 1H, *H*-3), 4.29-4.34 (m; 1H, *H*-2), 4.81-4.84 (m; 1H, *H*-3), 10.66 (br s; 1H, O*H*).

^{13}C-NMR (75 MHz, $CDCl_3$): δ = 28.3 (*C*-5), 29.5 (*C*-3′), 30.7 (*C*-4), 46.0 (*C*-3), 51.3 (*C*-2), 80.2 (*C*-2′), 155.4 (*C*-1′), 178.9 (*C*-1).

FT-IR (ATR): $\tilde{\nu}$ [cm^{-1}] = 3321 (br), 2955 (m), 1714 (s), 1663 (s), 1518 (m), 1477 (w), 1454 (w), 1392 (s), 1366 (sh), 1300 (w), 1243 (m), 1164 (s), 1051 (m), 1022 (w), 909 (w), 868 (w), 778 (w), 733(w).

8.2.35 Preparation of (*S*)-(1-dimethylcarbamoyl-2,2-dimethyl-propyl) carbamic acid-*tert*-butyl ester 130

[SMU-VIII-15]

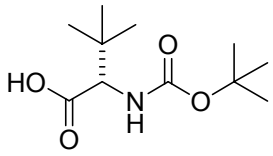

128

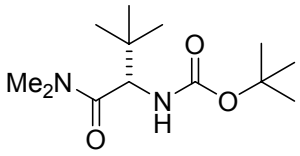

130

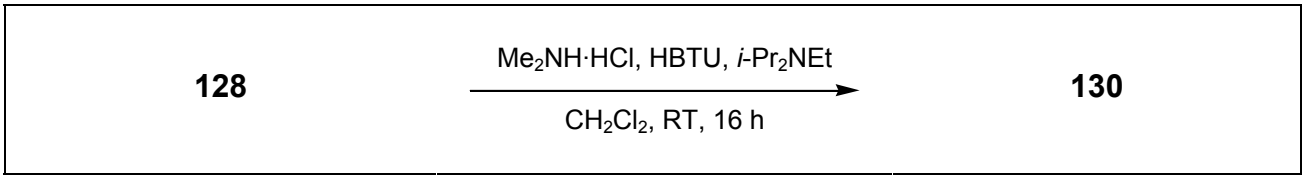

To a suspension of (*S*)-2-*tert*-butoxycarbonylamino-3,3-dimethylbutyric acid **128** (578 mg, 2.50 mmol, 1.00 eq) and *O*-benzotriazol-1-yl-*N*,*N*,*N*′,*N*′-tetramethyluronium hexafluorophosphate (HBTU) (1.04 g, 2.75 mmol, 1.10 eq) in 30 mL DCM, was added diisopropyl ethylamine (0.94 mL, 5.5 mmol, 2.20 eq) followed by dimethylamine hydrochloride (224 mg, 2.75 mmol, 1.10 eq) at room temperature. The resulting mixture was then stirred at room temperature for 16 hours. The reaction mixture was then diluted with diethylether (50 mL), washed with 1 M hydrochloric acid (2 × 50 mL), sat. $NaHCO_3$ solution (2 × 50 mL) and finally with brine (50 mL). The organic layer was dried over anh. Na_2SO_4 and concentrated in vacuo to obtain a pale yellow oil (643 mg, >99 %). It was used in the following step (see section 8.2.42 on page 171) without further purification.

130 $C_{13}H_{26}N_2O_3$ (258.36 g/mol)

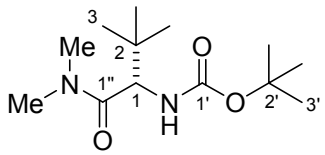

130

Yield 643 mg (2.49 mmol, >99 %)

^{1}H-NMR (300 MHz, $CDCl_3$): δ = 0.86 (s; 9H, *H*-3), 1.31 (s; 9H, *H*-3′), 2.85 (s; 3H, NC*H*$_3$), 3.02 (s; 3H, NC*H*$_3$), 4.41 (d, *J* = 9.47 Hz; 1H, *H*-1), 5.24 (d, *J* = 9.47 Hz; 1H, N*H*).

^{13}C-NMR (75 MHz, $CDCl_3$): δ = 26.2 (*C*-3), 28.2 (*C*-3′), 35.3 (N*C*H$_3$), 35.6 (*C*-2), 38.2 (N*C*H$_3$), 55.6 (*C*-1), 79.1 (*C*-2′), 155.5 (*C*-1′), 171.73 (*C*-1″).

FT-IR (Film): $\tilde{\nu}$ [cm^{-1}] = 3435 (m), 3315 (br), 2961 (s), 1707 (s), 1636 (s), 1490 (s), 1392 (s), 1364 (sh), 1327 (m), 1244 (s), 1167 (s), 1128 (w), 1054 (sh), 1032 (w), 1008 (sh), 969 (m), 933 (w), 909 (w), 873 (sh), 847 (w), 779 (w), 744 (w).

8.2.36 Preparation of (*S*)-(1-diethylcarbamoyl-2,2-dimethyl-propyl)-carbamic acid-*tert*-butyl ester 131

[SMU-V-76]

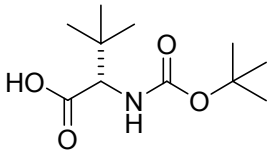

128

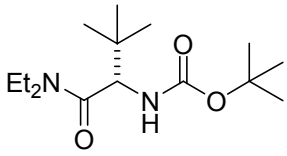

131

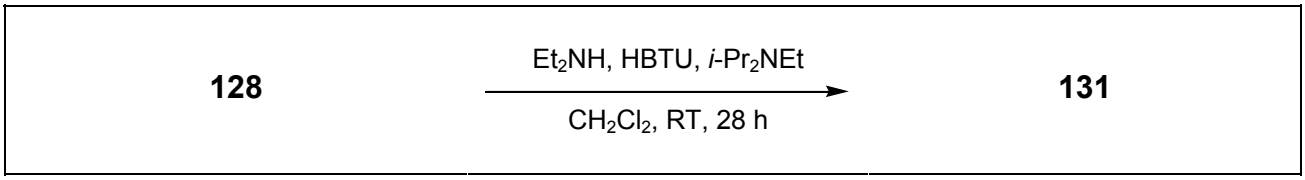

The same procedure as before (see section 8.2.35 on page 163) was followed to obtain a thick oil (611 mg, 85 %). It was used in the following step (see section 8.2.43 on page 173) without further purification.

131 $C_{15}H_{30}N_2O_3$ (286.41 g/mol)

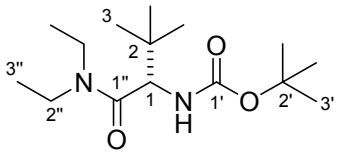

131

Yield 611 mg (2.13 mmol, 85 %)

^{1}H-NMR (300 MHz, $CDCl_3$): δ = 0.92 (s; 9H, *H*-3), 1.06 (t, *J* = 7.17 Hz; 3H, *H*-3′), 1.15 (t, *J* = 7.17 Hz; 3H, *H*-3″), 1.37 (s; 9H, *H*-3′), 2.90-3.02 (m; 1H, *H*-2″), 3.13-3.25 (m; 1H, *H*-2″), 3.53-3.76 (m; 2H, *H*-2″), 4.40 (d, *J* = 10.0 Hz; 1H, *H*-1*)*, 5.24 (d, *J* = 10.0 Hz; 1H, N*H*).

^{13}C-NMR (75 MHz, $CDCl_3$): δ = 12.9 (*C*-3″), 14.4 (*C*-3″), 26.4 (*C*-3), 28.2 (*C*-3′), 35.6 (*C*-2), 40.1 (*C*-2″), 42.7 (*C*-2″), 55.7 (*C*-1), 79.2 (*C*-2′), 155.5 (*C*-1′), 170.9 (*C*-1″).

FT-IR (Film): $\tilde{\nu}$ [cm^{-1}] = 3439 (w), 3316 (br), 2970 (s), 1716 (s), 1636 (s), 1497 (s), 1458 (m), 1433 (m), 1365 (s), 1335 (w), 1244 (m), 1173 (s), 1058 (m), 1009 (w), 906 (w), 863 (w), 835 (w).

8.2.37 Preparation of (*S*)-(1-diisobutylcarbamoyl-2,2-dimethyl-propyl)-carbamic acid-*tert*-butyl ester 132

[SMU-VI-20]

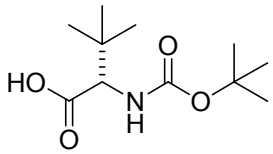

128

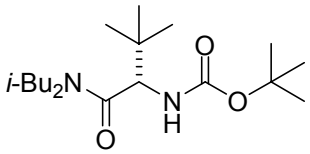

132

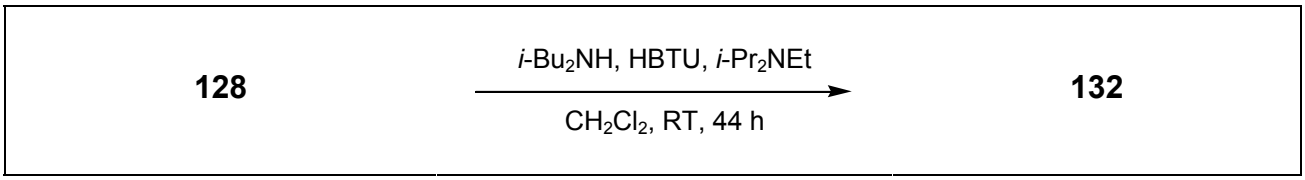

The same procedure as before (see section 8.2.35 on page 163) was followed to obtain a pale yellow crystalline solid (865 mg, >99 %). It was used in the following step (see section 8.2.44 on page 174) without further purification.

132 $C_{19}H_{38}N_2O_3$ (342.52 g/mol)

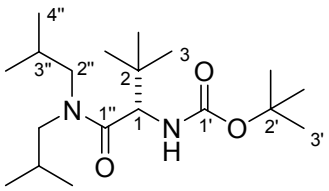

132

Yield 865 mg (2.53 mmol, >99 %)

^{1}H-NMR (250 MHz, $CDCl_3$): δ = 0.78-0.88 (m; 12H, *H*-4″), 0.92 (s; 9H, *H*-3), 1.34 (s; 9H, *H*-3′), 1.84-2.00 (m; 2H, *H*-3″), 2.49 (dd, *J* = 7.8, 13.2 Hz; 1H, *H*-2″), 2.96 (dd, *J* = 6.1, 14.7 Hz; 1H, *H*-2″), 3.38 (dd, *J* = 9.3, 14.7 Hz; 1H, *H*-2″), 3.73 (dd, *J* = 6.7, 13.3 Hz; 1H, *H*-2″), 4.47 (d, *J* = 9.7 Hz; 1H, *H*-1), 5.31 (d, *J* = 9.7 Hz; 1H, N*H*).

^{13}C-NMR (62.5 MHz, $CDCl_3$): δ = 18.7 (*C*-4″), 20.0 (*C*-4″), 20.3 (*C*-4″), 20.5 (*C*-4″), 26.4 (*C*-3), 26.5 (*C*-3″), 27.3 (*C*-3″), 28.1 (*C*-3′), 36.0 (*C*-2), 53.4 (*C*-2″), 56.0 (*C*-1), 56.3 (*C*-2″), 78.8 (*C*-2′), 155.1 (*C*-1′), 171.9 (*C*-1″).
The assignments were made by 2D-NMR.

FT-IR (ATR): $\tilde{\nu}$ [cm^{-1}] = 3344 (s), 2959 (s), 2871 (m), 1689 (s), 1626 (s), 1521 (s), 1444 (m), 1420 (w), 1386 (w), 1367 (m), 1348 (w), 1241 (s), 1173 (s), 1133 (w), 1101 (w), 1057 (s), 1035 (w), 1012 (m), 938 (w), 898 (w).

8.2.38 Preparation of {(*S*)-1-(benzyl-methyl-carbamoyl)-2,2-dimethyl-propyl}-carbamic acid-*tert*-butyl ester 133

[SMU-V-93]

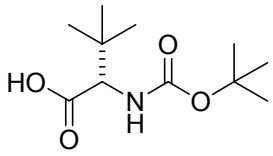

128

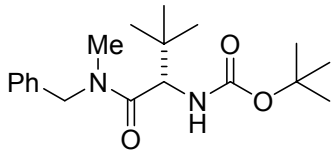

133

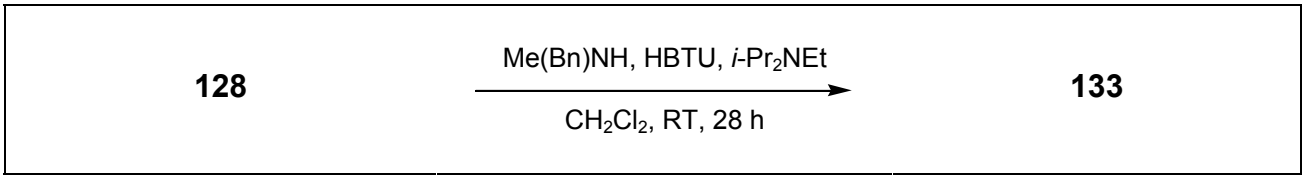

The same procedure as before (see section 8.2.35 on page 163) was followed to obtain **133** contaminated with tetramethyl urea as a thick yellowish oil (760 mg, 91 %). It was used in the following step (see section 8.2.45 on page 175) without further purification.

133 $C_{19}H_{30}N_2O_3$ (334.45 g/mol)

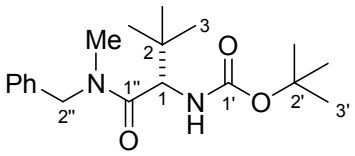

133

Yield 760 mg (2.27 mmol, 91 %)

^{1}H-NMR (250 MHz, $CDCl_3$): δ = 0.95 (s; 9H, *H*-3), 1.39 (s; 9H, *H*-3′), 3.00 (s; 3H, NCH_3), 4.44-4.51 (m; 2H, *H*-1, *H*-2″), 4.62-4.67 (m; 1H, *H*-2″), 5.32-5.33 (m; 1H, N*H*), 7.14-7.28 (m; 5H, H_{ar}).

^{13}C-NMR (62.5 MHz, $CDCl_3$): δ = 26.3 (*C*-3), 28.2 (*C*-3′), 35.5 (*C*-2), 35.7 (N*C*H_3),

51.0 (*C*-2″), 56.0 (*C*-1), 79.3 (*C*-2′), 127.3 (C_{ar}), 128.0 (C_{ar}), 128.5 (C_{ar}), 136.8 (Cq_{ar}), 155.8 (*C*-1′), 172.1 (*C*-1″).

The assignments were made by 2D-NMR.

8.2.39 Preparation of {(*R*)-1-(benzyl-methyl-carbamoyl)-2,2-dimethyl-propyl}-carbamic acid-*tert*-butyl ester *ent*-133

[SMU-VI-23]

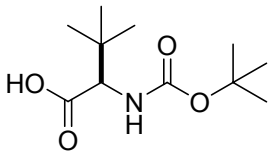

ent-**128**

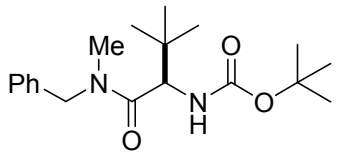

ent-**133**

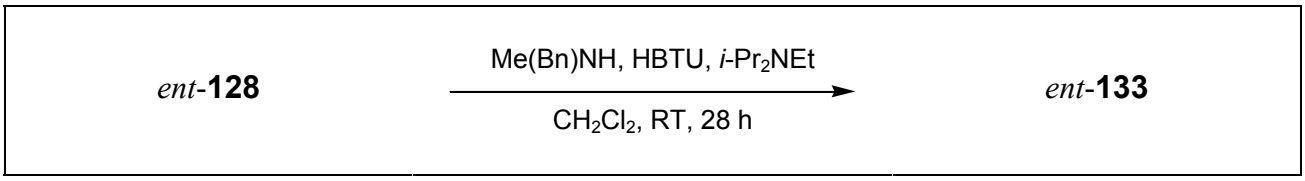

The same procedure as before (see section 8.2.35 on page 163) was followed to obtain a thick yellowish oil (880 mg, >99 %). It was used in the following step (see section 8.2.46 on page 176) without further purification.

ent-**133**	$C_{19}H_{30}N_2O_3$ (334.45 g/mol)
Yield	880 mg (2.63 mmol, >99 %)
^{1}H-NMR	(250 MHz, $CDCl_3$): δ = 0.97 (s; 9H, *H*-3), 1.41 (s; 9H, *H*-3′), 3.02 (s; 3H, NCH_3), 4.45-4.53 (m; 2H, *H*-1, *H*-2″), 4.64-4.70 (m; 1H, *H*-2″), 5.31-5.35 (m; 1H, N*H*), 7.16-7.31 (m; 5H, H_{ar}).
^{13}C-NMR	(62.5 MHz, $CDCl_3$): δ = 26.4 (*C*-3), 28.3 (*C*-3′), 35.5 (*C*-2), 35.8 (N*C*H_3), 51.0 (*C*-2″), 56.0 (*C*-1), 79.4 (*C*-2′), 127.3 (C_{ar}), 128.0 (C_{ar}), 128.5 (C_{ar}),

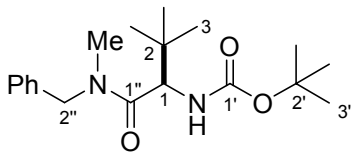

ent-**133**

136.9 (*C*q_{ar}), 155.8 (*C*-1′), 172.2 (*C*-1″).

The assignments were made by 2D-NMR.

FT-IR (Film): $\tilde{\nu}$ [cm^{-1}] = 3436 (w), 3327 (br), 2968 (s), 1714 (s), 1646 (s), 1496 (s), 1456 (w), 1401 (w), 1394 (w), 1366 (sh), 1339 (w), 1246 (m), 1171 (s), 1111 (w), 1056 (m), 1031 (w), 1010 (m), 909 (w), 875 (w), 736 (w).

8.2.40 Preparation of (*S*)-(1-benzylcarbamoyl-2,2-dimethyl-propyl)-carbamic acid-*tert*-butyl ester 134

[SMU-VIII-40]

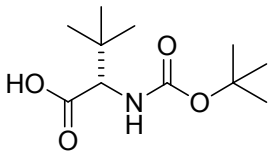

128

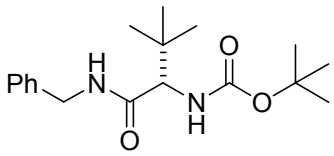

134

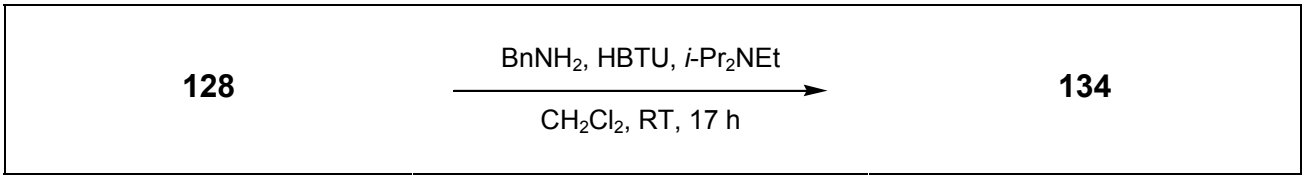

The same procedure as before (see section 8.2.35 on page 163) was followed on a 2.00 mmol scale to obtain a colourless oil (667 mg, >99 %). It was used in the following step (see section 8.2.47 on page 177) without further purification.

134 $C_{18}H_{28}N_2O_3$ (320.43 g/mol)

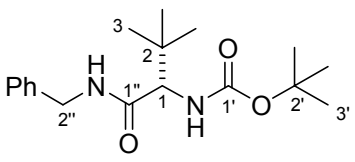

134

Yield 667 mg (2.08 mmol, >99 %)

^{1}H-NMR (300 MHz, $CDCl_3$): δ = 0.93 (s; 9H, *H*-3), 1.29 (s; 9H, *H*-3′), 4.04-4.17 (m; 2H, *H*-2″), 4.34-4.43 (m; 1H, *H*-1), 5.60 (d, *J* = 9.3 Hz; 1H, C-1-N*H*),

7.10-7.23 (m; 5H, H_{ar}), 7.50 (br s; 1H, C-1″-N*H*).

^{13}C-NMR ($CDCl_3$): δ = 26.4 (*C*-3), 28.1 (*C*-3′), 34.2 (*C*-2), 42.9 (*C*-2″), 61.9 (*C*-1), 79.1 (*C*-2′), 126.8 (C_{ar}), 127.3 (C_{ar}), 128.1 (C_{ar}), 138.1 (Cq_{ar}), 155.9 (*C*-1′), 171.1 (*C*-1″).

The assignments were made by 2D-NMR.

FT-IR (ATR): $\tilde{\nu}$ [cm^{-1}] = 3307 (br), 2965 (m), 1697 (s), 1649 (s), 1536 (m), 1518 (s), 1503 (s), 1453 (sh), 1391 (w), 1365 (s), 1243 (s), 1169 (s), 1069 (sh), 1028 (w), 1006 (m), 908 (m), 859 (m), 729 (m).

8.2.41 Preparation of {(*S*)-1-(benzyl-methyl-carbamoyl)-3,3-dimethyl-butyl}-carbamic acid-*tert*-butyl ester 135

[SMU-VI-72]

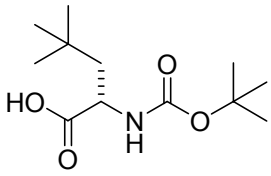

129

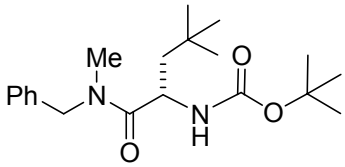

135

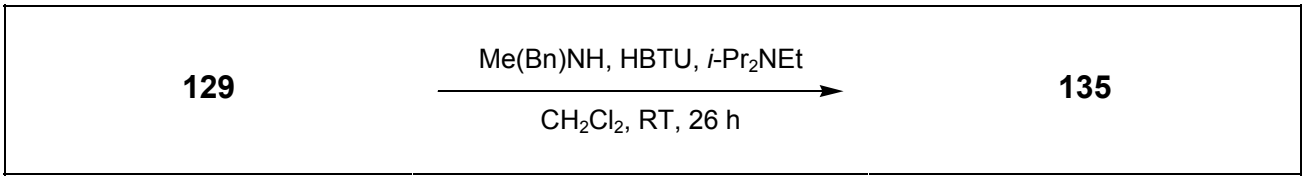

The same procedure as before (see section 8.2.35 on page 163) was followed on a 2.50 mmol scale to obtain a thick yellowish oil (940 mg, >99 %). It was used in the following step (see section 8.2.48 on page 178) without further purification.

135 $C_{20}H_{32}N_2O_3$ (348.48 g/mol)

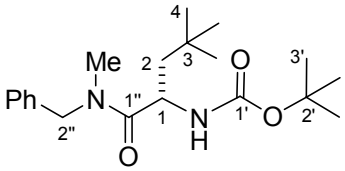

135

Yield 940 mg (2.70 mmol, >99 %)

^{1}H-NMR (300 MHz, $CDCl_3$): δ = 0.83, 0.96 (2s; 9H, *H*-4), 1.39, 1.41 (2s; 9H, *H*-3′), 1.49-1.51 (m; 2H), 2.90, 2.98 (2s; 3H, NC*H*$_3$), 4.47-4.63 (m; 2H), 4.70-4.82 (m; 1H), 5.13-5.22 (m; 1H), 7.17-7.34 (m; 5H, H_{ar}).

^{13}C-NMR (75 MHz, $CDCl_3$): δ = 28.35, 29.60, 29.76, 30.47, 30.67, 34.07, 34.54, 38.56, 46.40, 46.74, 47.51, 47.87, 51.16, 53.10, 79.50, 126.80, 127.37, 127.66, 127.88, 128.59, 128.79, 136.23, 136.82, 155.02, 155.39, 173.79, 174.09.

Two sets of signals were obtained due to dynamic NMR.

8.2.42 Preparation of (*S*)-2-amino-*N*,*N*-dimethyl-3,3-dimethyl-butanamide **136**

[SMU-VIII-16]

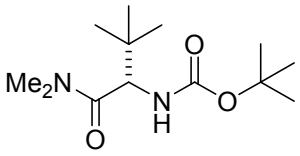

130

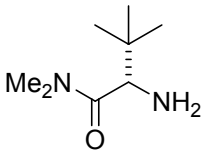

136

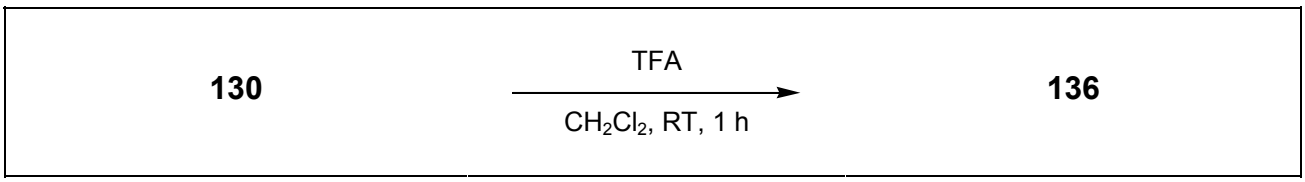

To a solution of (*S*)-(1-dimethylcarbamoyl-2,2-dimethyl-propyl)-carbamic acid-*tert*-butyl ester **130** (635 mg, 2.46 mmol, 1.00 eq) in 10 mL of DCM, trifluoroacetic acid (1.89 mL, 24.6 mmol, 10.0 eq) was added in one portion and the resulting solution was stirred at room temperature for 1 hour. The reaction mixture was cooled to 0 °C and a 20 % aqueous Na_2CO_3 solution was added slowly until pH ~ 10. The biphasic mixture was then diluted with chloroform (20 mL). The organic layer

was separated and washed with 20 % aqueous Na_2CO_3 solution (3 × 10 mL). The combined aqueous layers were extracted with chloroform (3 × 20 mL). Combined organic extracts were washed with brine (20 mL) and dried over anh. Na_2SO_4. The solvent was removed in vacuo to obtain a pale yellow oil (300 mg, 77 %). This was used in the following step (see section 8.2.49 on page 179) without any further purification.

136	$C_8H_{18}N_2O$ (158.14 g/mol)
Yield	300 mg (1.90 mmol, 77 %)

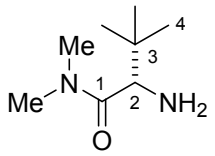

136

^{1}H-NMR	(300 MHz, $CDCl_3$): δ = 0.82 (s; 9H, *H*-4), 1.62 (s; 2H, NH_2), 2.81 (s; 3H, NCH_3), 2.93 (s; 3H, NCH_3), 3.39 (*H*-2).
^{13}C-NMR	(75 MHz, $CDCl_3$): δ = 26.0 (*C*-4), 35.1 (*C*-3), 35.3 (N*C*H$_3$), 38.3 (N*C*H$_3$), 57.3 (*C*-2), 174.3 (*C*-1).
FT-IR	(ATR): $\tilde{\nu}$ [cm^{-1}] = 3373 (br), 2950 (s), 2868 (m), 1626 (s), 1504 (w), 1478 (w), 1419 (w), 1395 (m), 1360 (sh), 1255 (sh), 1230 (w), 1137 (s), 1088 (m), 1056 (w), 1032 (m), 970 (m), 913 (m), 866 (w), 812 (m), 781 (w).

8.2.43 Preparation of (*S*)-2-amino-*N*,*N*-diethyl-3,3-dimethyl-butanamide 137

[SMU-V-77]

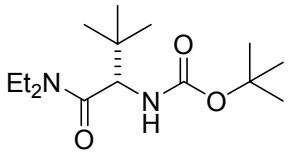

131

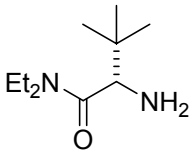

137

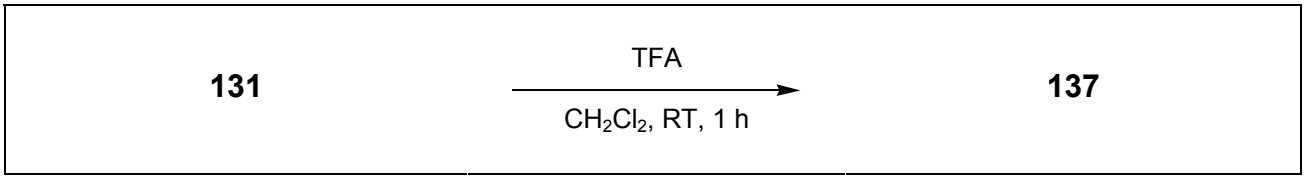

The same procedure as before (see section 8.2.42 on page 171) was followed on a 2.13 mmol scale to obtain a clear oil (394 mg, 99 %). This was used in the following step (see section 8.2.50 on page 180) without further purification.

137 $C_{10}H_{22}N_2O$ (186.29 g/mol)

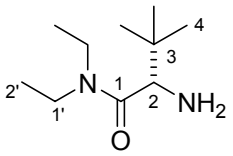

137

Yield 394 mg (2.11 mmol, 99 %)

^{1}H-NMR (300 MHz, $CDCl_3$): δ = 0.85 (s; 9H, *H*-4), 0.99 (t, *J* = 7.17 Hz; 3H, *H*-2′), 1.06 (t, *J* = 7.17 Hz; 3H, *H*-2′), 1.48 (s; 2H, N*H*$_2$), 2.89-3.00 (m; 1H, *H*-1′), 3.00-3.13 (m; 1H, *H*-1′), 3.26 (s; 1H, *H*-2), 3.40-3.62 (m; 2H, *H*-1′).

^{13}C-NMR (75 MHz, $CDCl_3$): δ = 12.8 (C-2′), 14.5 (C-2′), 26.2 (C-4), 34.9 (C-3), 40.1 (C-1′), 42.2 (C-1′), 57.5 (C-2), 173.6 (C-1).

FT-IR (Film): $\tilde{\nu}$ [cm^{-1}] = 3384 (br), 2961 (s), 2871 (w), 2241 (m), 1630 (s), 1464 (m), 1380 (w), 1360 (m), 1268 (m), 1218 (w), 1137 (m), 1097 (w), 1034 (w), 925 (m), 732 (m).

HR-ESI-MS Exact molecular mass for $[C_{10}H_{23}N_2O]$ ($[M+H]^+$): 187.1810
Found: 187.181

8.2.44 Preparation of (*S*)-2-amino-*N*,*N*-diisobutyl-3,3-dimethyl-butanamide 138

[SMU-VI-21]

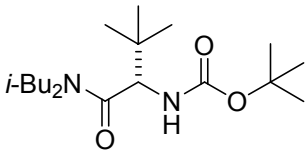

132

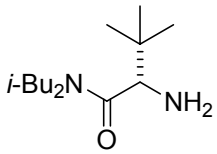

138

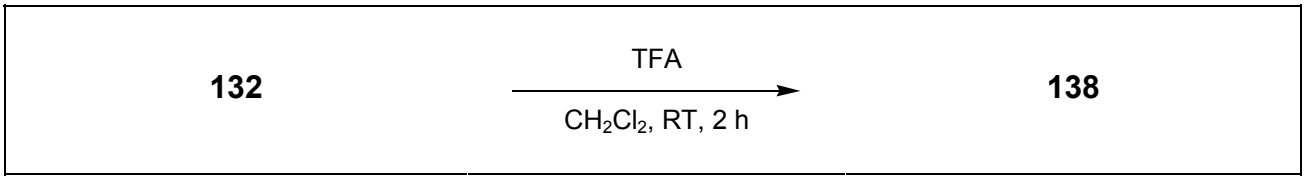

The same procedure as before (see section 8.2.42 on page 171) was followed on a 2.24 mmol scale to obtain a pale yellow oil (557 mg, >99 %). This was used in the following step (see section 8.2.51 on page 181) without further purification.

138 $C_{14}H_{30}N_2O$ (242.4 g/mol)

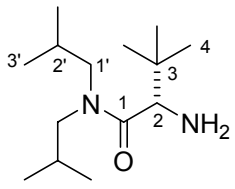

138

Yield 557 mg (2.30 mmol, >99 %)

^{1}H-NMR (250 MHz, $CDCl_3$): δ = 0.75-0.85 (m; 12H, *H*-3′), 0.87 (s; 9H, *H*-4), 1.49 (br s; 2H, N*H*$_2$), 1.72-1.99 (m; 2H, *H*-2′), 2.42 (dd, *J* = 8.2, 13.3 Hz; 1H, *H*-1′), 2.81 (dd, *J* = 6.8, 14.7 Hz; 1H, *H*-1′), 3.31 (s; 1H, *H*-2), 3.32 (dd, *J* = 8.5, 14.7 Hz; 1H, *H*-1′), 3.70 (dd, *J* = 6.4, 13.4 Hz; 1H, *H*-1′).

^{13}C-NMR (62.5 MHz, $CDCl_3$): δ = 19.6 (*C*-3′), 20.2 (*C*-3′), 20.3 (*C*-3′), 20.5 (*C*-3′), 26.4 (*C*-4), 26.7 (*C*-2′), 28.1 (*C*-2′), 35.1 (*C*-3), 54.3 (*C*-1′), 56.5 (*C*-1′), 57.8

(*C*-2), 175.0 (*C*-1).

The assignments were made by 2D-NMR.

FT-IR (Film): $\tilde{\nu}$ [cm^{-1}] = 3385 (br), 2959 (s), 2871 (m), 1638 (s), 1500 (w), 1467 (m), 1426 (w), 1387 (w), 1367 (m), 1340 (w), 1259 (m), 1206 (w), 1141 (m), 1099 (m), 1031 (w), 913 (w), 870 (w), 806 (w), 756 (w).

8.2.45 Preparation of (*S*)-2-amino-*N*-benzyl-3,3,*N*-trimethyl-butanamide 139

[SMU-V-94]

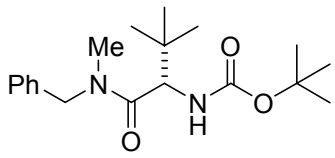

133

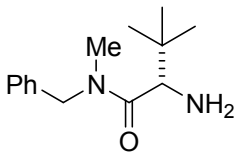

139

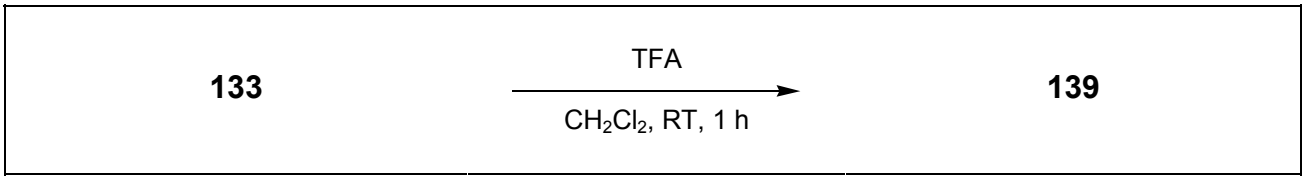

The same procedure as before (see section 8.2.42 on page 171) was followed on a 2.27 mmol scale to obtain a pale yellow oil (531 mg, 100 %). This was used in the following step (see section 8.2.52 on page 181) without further purification.

139 $C_{14}H_{22}N_2O$ (234.34 g/mol)

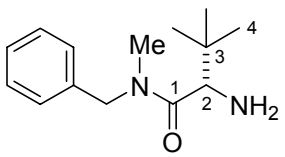

139

Yield 531 mg (2.27 mmol, 100 %)

^{1}H-NMR (300 MHz, $CDCl_3$): δ = 0.99 (s; 9H, *H*-4), 1.59 (s; 2H, NH_2), 2.97 (s; 3H, NCH_3), 3.54 (s; 1H, *H*-2), 4.48 (d, *J* = 14.37 Hz; 1H, NCH_2), 4.73 (d, *J* = 14.37 Hz; 1H, NCH_2), 7.17-7.30 (m; 5H, H_{ar}).

^{13}C-NMR (75 MHz, $CDCl_3$): δ = 26.2 (*C*-4), 35.1 (*C*-3), 35.3 (N*C*H$_3$), 50.9 (N*C*H$_2$), 57.8 (*C*-2), 126.3 (C_{ar}), 128.1 (C_{ar}), 128.4 (C_{ar}), 137.2 (Cq_{ar}), 174.6 (*C*O).
The assignments were made by 2D-NMR.

FT-IR (Film): $\tilde{\nu}$ [cm^{-1}] = 3384 (br), 2954 (s), 2869 (w), 1636 (s), 1496 (w), 1456 (w), 1363 (m), 1260 (w), 1179 (w), 1082 (w), 1029 (w), 953 (w), 915 (w), 820 (w), 736 (w).

8.2.46 Preparation of (*R*)-2-amino-*N*-benzyl-3,3,*N*-trimethyl-butanamide *ent*-**139**

[SMU-VI-28]

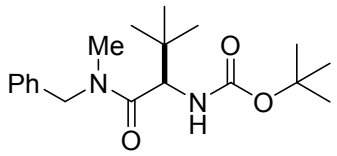

ent-**133**

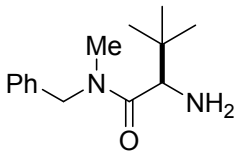

ent-**139**

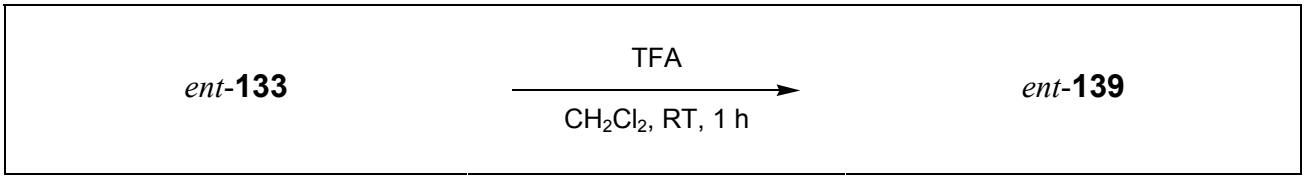

The same procedure as before (see section 8.2.42 on page 171) was followed on a 2.50 mmol scale to obtain a pale yellow oil (588 mg, >99 %). This was used in the following step (see section 8.2.53 on page 182) without further purification.

ent-**139** $C_{14}H_{22}N_2O$ (234.34 g/mol)

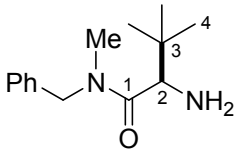

ent-**139**

Yield 588 mg (2.51 mmol, >99 %)

^{1}H-NMR (250 MHz, $CDCl_3$): δ = 0.93 (s; 9H, *H*-4), 1.66 (s; 2H, N*H*$_2$), 2.90 (s; 3H,

NCH_3), 3.49 (s; 1H, *H*-2), 4.40 (d, *J* = 14.37 Hz; 1H, NCH_2), 4.67 (d, *J* = 14.37 Hz; 1H, NCH_2), 7.10-7.32 (m; 5H, H_{ar}).

^{13}C-NMR (62.5 MHz, $CDCl_3$): δ = 26.2 (*C*-4), 35.0 (*C*-3), 35.3 (N*C*H_3), 50.9 (N*C*H_2), 57.7 (*C*-2), 126.2 (C_{ar}), 128.1 (C_{ar}), 128.4 (C_{ar}), 137.1 (Cq_{ar}), 174.5 (*C*O).
The assignments were made by 2D-NMR.

FT-IR (Film): $\tilde{\nu}$ [cm^{-1}] = 3376 (br), 2953 (s), 2868 (w), 1637 (s), 1496 (w), 1473 (w), 1454 (w), 1418 (w), 1362 (m), 1259 (w), 1180 (w), 1112 (w), 1083 (w), 1030 (w), 986 (w), 951 (w), 914 (w), 860 (w), 816 (w), 736 (m).

8.2.47 Preparation of (*S*)-2-amino-*N*-benzyl-3,3-dimethyl-butanamide 140

[SMU-VIII-41]

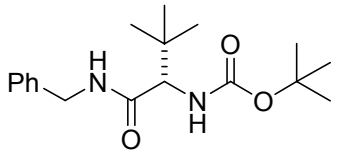

134

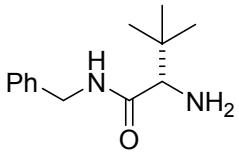

140

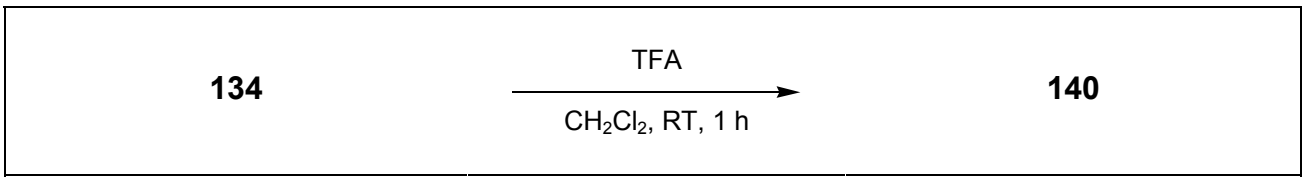

The same procedure as before (see section 8.2.42 on page 171) was followed on a 2.00 mmol scale to obtain a pale yellow oil (370 mg, 84 %). This was used in the following step (see section 8.2.54 on page 183) without further purification.

140 $C_{13}H_{20}N_2O$ (220.31 g/mol)

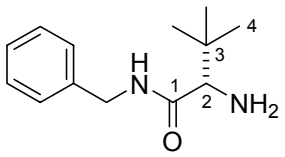

140

Yield 370 mg (1.68 mmol, 84 %)

^{1}H-NMR (250 MHz, $CDCl_3$): δ = 0.91 (*H*-4), 1.57 (br s; 2H, N*H*$_2$), 3.02 (s; 1H, *H*-2), 4.32 (d, *J* = 5.88 Hz; 2H, PhC*H*$_2$), 7.13-7.26 (m; 6H, *H*$_{ar}$, N*H*).

^{13}C-NMR (62.5 MHz, $CDCl_3$): δ = 26.5 (*C*-4), 33.9 (*C*-3), 42.8 (Ph*C*H$_2$), 64.0 (*C*-2), 127.0 (*C*$_{ar}$), 127.5 (*C*$_{ar}$), 128.3 (*C*$_{ar}$), 138.4 (*C*q$_{ar}$), 173.4 (*C*-1).

FT-IR (Film): $\tilde{\nu}$ [cm^{-1}] = 3307 (br), 3063 (w), 3028 (w), 2951 (sh), 2866 (w), 1650 (s), 1538 (m), 1496 (w), 1476 (w), 1453 (sh), 1394 (w), 1364 (m), 1327 (w), 1264 (m), 1205 (w), 1079 (w), 1028 (sh), 928 (w), 744 (m).

8.2.48 Preparation of (*S*)-2-amino-*N*-benzyl-4,4,*N*-trimethyl-pentanamide 141

[SMU-VI-76]

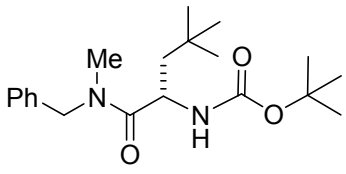

135

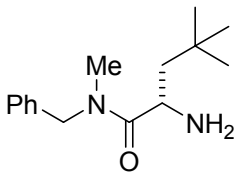

141

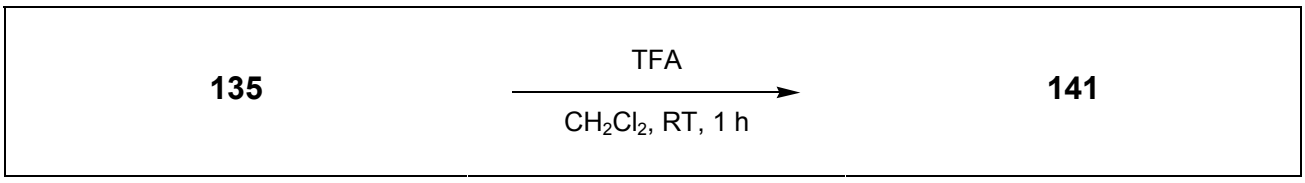

The same procedure as before (see section 8.2.42 on page 171) was followed on a 2.50 mmol scale to obtain a pale yellow oil (670 mg, >99 %). This was used in the following step (see section 8.2.55 on page 183) without further purification.

141 $C_{15}H_{24}N_2O$ (248.36 g/mol)

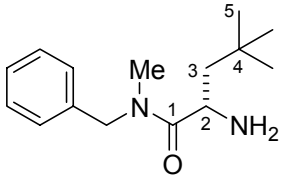

141

Yield 670 mg (2.70 mmol, >99 %)

^{1}H-NMR (300 MHz, $CDCl_3$): δ = 0.88, 0.95 (2s; 9H, *H*-5), 1.31-1.38, 1.61-1.67 (2m; 4H, *H*-3, NH_2), 2.90, 2.93 (2s; 3H, NCH_3), 3.69-3.80 (m; 1H, *H*-2), 4.40-4.68 (m; 2H, PhCH_2), 7.13-7.35 (m; 5H, H_{ar}).

^{13}C-NMR (75 MHz, $CDCl_3$): δ = 30.0, 30.1, 30.5, 30.6, 34.2, 34.5, 38.5, 48.8, 48.9, 49.2, 51.2, 52.7, 126.2, 127.3, 128.0, 128.5, 128.9, 136.6, 137.1, 176.3, 176.9.

Two sets of signals were obtained because of dynamic NMR.

FT-IR (ATR): $\tilde{\nu}$ [cm^{-1}] = 3359 (br), 2949 (s), 2863 (w), 1640 (s), 1494 (m), 1475 (m), 1451 (m), 1411 (w), 1363 (m), 1251 (m), 1202 (w), 1094 (w), 1028 (w), 943 (w), 916 (w), 848 (w), 816 (w), 731 (m).

8.2.49 Preparation of (*S*)-*N*,*N*-dimethyl-2-isothiocyanato-3,3-dimethyl-butanamide 142

[SMU-VIII-20]

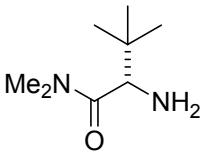

136

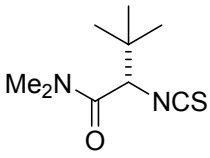

142

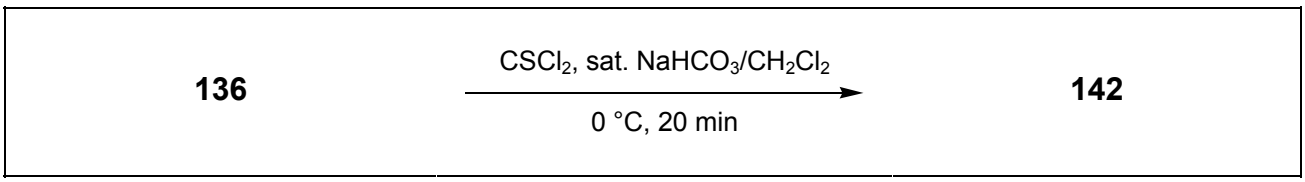

Saturated aqueous sodium bicarbonate solution (10 mL) was added to an ice-cold solution of (*S*)-2-amino-*N*,*N*-dimetheyl-3,3-dimethyl-butyramide **136** (275 mg, 1.74 mmol, 1.00 eq) in 10 mL

of DCM and the mixture was stirred for 5 minutes. The stirring was stopped and thiophosgene (150 µL, 1.91 mmol, 1.10 eq) was added to the organic (lower) phase by a syringe. The resulting orange mixture was vigorously stirred at 0 °C for 20 mins. The reaction mixture was then diluted with DCM (20 mL) and the organic phase was separated. The aqueous phase was extracted with DCM (2 × 20 mL). The combined organic layers were dried over anh. Na_2SO_4 and concentrated in vacuo to obtain a pale yellow oil which became crystalline solid (337 mg, 1.68 mmol, 97 %) on standing in the refrigerator. This was used immediately for the thiourea formation (see section 8.2.56 on page 184) without further purification and characterization.

8.2.50 Preparation of (*S*)-*N*,*N*-diethyl-2-isothiocyanato-3,3-dimethyl-butanamide 143

[SMU-V-78]

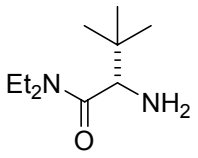

137

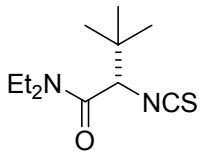

143

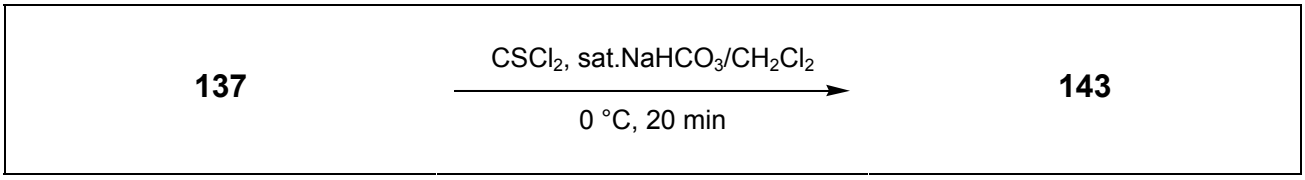

The same procedure as before (see section 8.2.49 on page 179) was followed on a 2.11 mmol scale to obtain a pale yellow oil which became crystalline solid (440 mg, 1.93 mmol, 92 %) on standing in the refrigerator. This was used immediately for the thiourea formation (see section 8.2.57 on page 186) without any purification or characterization.

8.2.51 Preparation of (*S*)-*N*,*N*-diisobutyl-2-isothiocyanato-3,3-dimethyl-butanamide 144

[SMU-VI-33]

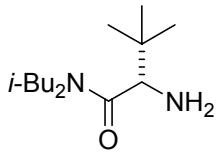

138

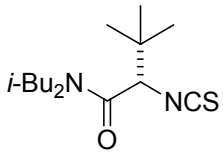

144

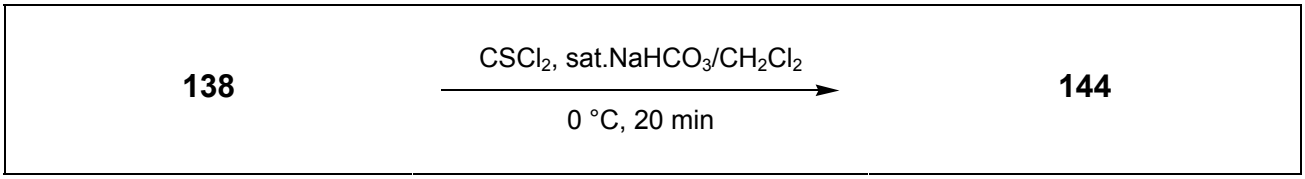

The same procedure as before (see section 8.2.49 on page 179) was followed on a 2.17 mmol scale to obtain a pale yellow crystalline solid (598 mg, 2.10 mmol, 97 %). This was used immediately for the thiourea formation (see section 8.2.58 on page 188) without any purification or characterization.

8.2.52 Preparation of (*S*)-*N*-benzyl-2-isothiocyanato-3,3,*N*-trimethyl-butanamide 145

[SMU-VI-02]

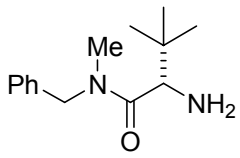

139

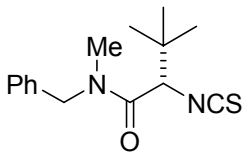

145

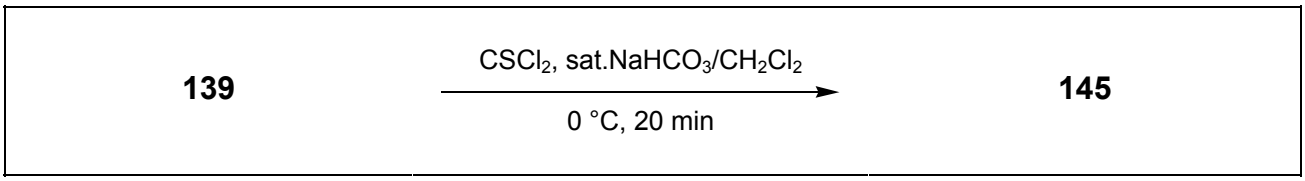

The same procedure as before (see section 8.2.49 on page 179) was followed on a 1.62 mmol scale to obtain a thick oil (430 mg, 1.56 mmol, 96 %). This was used immediately for the thiourea formation (see section 8.2.59 on page 190) without any purification or characterization.

8.2.53 Preparation of (*R*)-*N*-benzyl-2-isothiocyanato-3,3,*N*-trimethyl-butanamide *ent*-145

[SMU-VI-29]

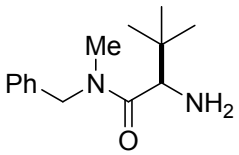

ent-**139**

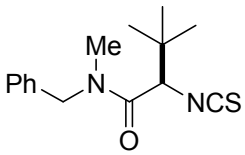

ent-**145**

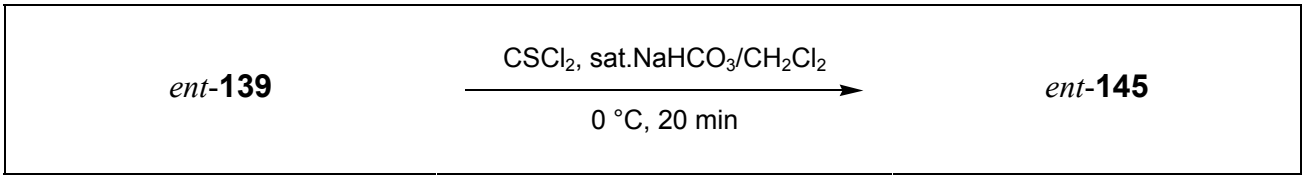

The same procedure as before (see section 8.2.49 on page 179) was followed on a 2.10 mmol scale to obtain a yellow oil (552 mg, 2.00 mmol, 95 %). This was used immediately for the thiourea formation (see section 8.2.60 on page 192) without any purification or characterization.

8.2.54 Preparation of (*S*)-*N*-benzyl-2-isothiocyanato-3,3-dimethyl-butanamide 146

[SMU-VIII-42]

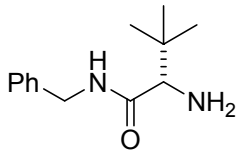

140

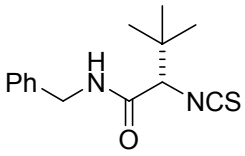

146

140	$CSCl_2$, sat.$NaHCO_3$/CH_2Cl_2 0 °C, 20 min	**146**

The same procedure as before (see section 8.2.49 on page 179) was followed on a 1.66 mmol scale to obtain a thick yellow oil (430 mg, 1.64 mmol, 99 %). This was used immediately for the thiourea formation (see section 8.2.61 on page 193) without any purification or characterization.

8.2.55 Preparation of (*S*)-*N*-benzyl-2-isothiocyanato-4,4,*N*-trimethyl-pentanamide 147

[SMU-VI-82]

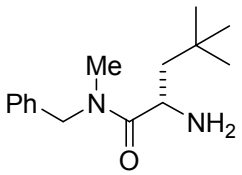

141

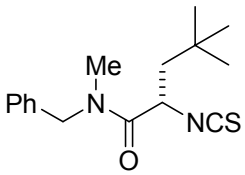

147

141	$CSCl_2$, sat.$NaHCO_3$/CH_2Cl_2 0 °C, 20 min	**147**

The same procedure as before (see section 8.2.49 on page 179) was followed on a 2.68 mmol scale to obtain a yellowish oil (747 mg, 2.57 mmol, 96 %). This was used immediately for the thiourea formation (see section 8.2.62 on page 195) without any purification or characterization.

8.2.56 Preparation of 1-{(*S*)-1-(dimethylcarbamoyl)-2,2-dimethyl-propyl}-3-{(1*R*,2*R*)-2-(dimethylamino)cyclohexyl}thiourea 15

[SMU-VIII-22]

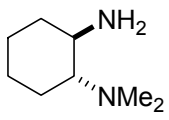

101

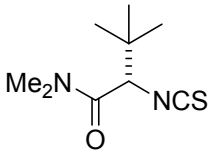

142

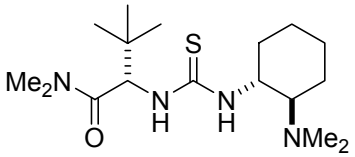

15

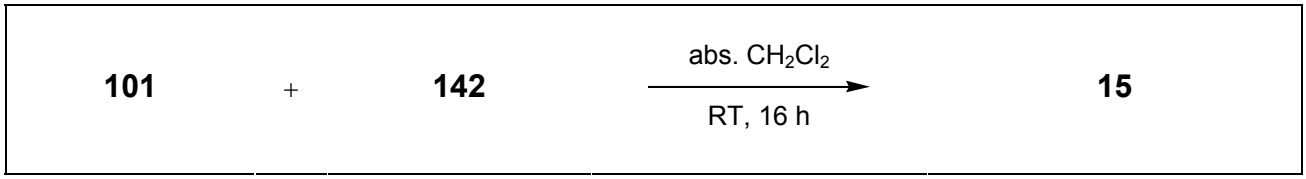

A solution of (*S*)-*N*,*N*-dimethyl-2-isothiocyanato-3,3-dimethyl-butyramide **142** (337 mg, 1.68 mmol, 1.00 eq) in 3 mL abs. DCM was added to a solution of (1*R*,2*R*)-*N*,*N*-dimethyl-1,2-diaminocyclohexane **101** (275 mg, 1.93 mmol, 1.15 eq) in DCM (1 mL). The resulting mixture was stirred at room temperature under argon for 16 hours. The reaction mixture was then concentrated in vacuo and the residue was purified by column chromatography on silicagel (CH_2Cl_2/MeOH/TEA = 100:5:1 as the eluant) to afford a colorless foam (350 mg, 61 %).

15	$C_{17}H_{34}N_4OS$ (342.54 g/mol)
Yield	350 mg (1.02 mmol, 61 %)
Melting Point	146 °C
Specific Rotation	$[\alpha]_{589}^{20} = +7.3°$, $[\alpha]_{546}^{20} = +8.9°$, $[\alpha]_{405}^{20} = +10.6°$, $[\alpha]_{365}^{20} = -2.9°$ (c =0.71, $CHCl_3$)

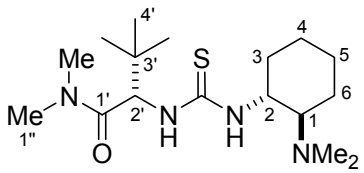

15

TLC R_f = 0.22 (Silicagel, CH_2Cl_2/CH_3OH/TEA 100:5:1)

^{1}H-NMR (300 MHz, $CDCl_3$): δ = 0.93 (s; 9H, *H*-4′), 1.02-1.12 (m; 4H, *H*-3, *H*-4, *H*-5, *H*-6), 1.58-1.76 (m; 3H, *H*-4, *H*-5, *H*-6), 2.13 (s; 6H, NC*H*$_3$), 2.21-2.29 (m; 2H, *H*-1, *H*-3), 2.85 (s; 3H, *H*-1″), 3.15 (s; 3H, *H*-1″), 3.50 (m; 1H, *H*-2), 5.50 (d, *J* = 8.97 Hz; 1H, *H*-2′), 6.66 (br s; 1H, C-2-N*H*), 7.03 (d, *J* = 8.97 Hz; 1H, C-2′-N*H*).

^{13}C-NMR (75 MHz, $CDCl_3$): δ = 21.9 (*C*-6), 24.5 (*C*-4 or *C*-5), 24.9 (*C*-4 or *C*-5), 26.6 (*C*-4′), 32.9 (*C*-3), 35.4 (*C*-1″), 35.9 (*C*-3′), 38.4 (*C*-1″), 40.1 (N*C*H$_3$), 55.4 (*C*-2), 59.9 (*C*-2′), 66.5 (*C*-1), 171.9 (*C*-1′), 182.3 (*C*S).
The assignments were made by 2D-NMR.

FT-IR (ATR): $\tilde{\nu}$ [cm^{-1}] = 3307 (br), 2928 (s), 2857 (sh), 2781 (w), 1624 (s), 1536 (s), 1477 (w), 1416 (w), 1396 (m), 1364 (m), 1319 (w), 1253 (w), 1238 (w), 1188 (w), 1139 (m), 1118 (w), 1083 (m), 1062 (w), 1036 (m), 947 (m), 914 (m), 872 (sh), 825 (w), 730 (s).

HR-ESI-MS Exact molecular mass for [$C_{17}H_{35}N_4OS$] ([M+H]$^+$): 343.2531
Found: 343.253

Elemental Analysis Anal. Calcd. for $C_{17}H_{34}N_4OS$: C 59.61, H 10.00, N 16.36
Found: C 59.20, H 9.88, N 16.19

8.2.57 Preparation of 1-{(*S*)-1-(diethylcarbamoyl)-2,2-dimethyl-propyl}-3-{(1*R*,2*R*)-2-(dimethylamino)cyclohexyl}thiourea 16

[SMU-V-80]

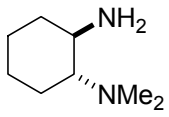

101

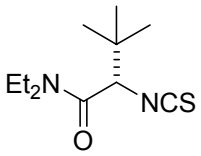

143

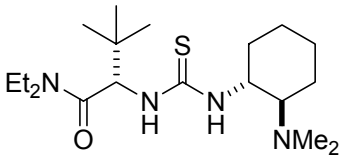

16

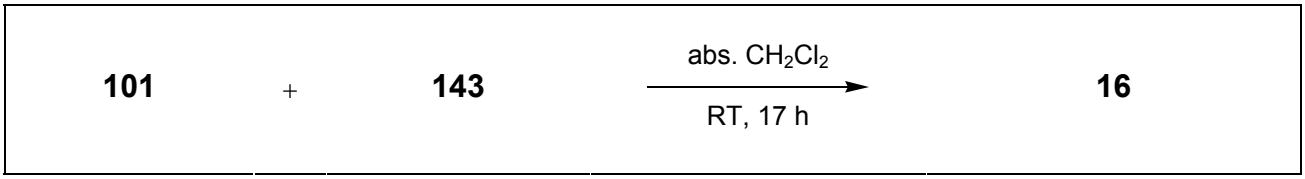

The same procedure as before (see section 8.2.56 on page 184) was followed on a 1.93 mmol scale. Purification in the same way afforded a colorless foam (515 mg, 72 %).

16 $C_{19}H_{38}N_4OS$ (370.6 g/mol)

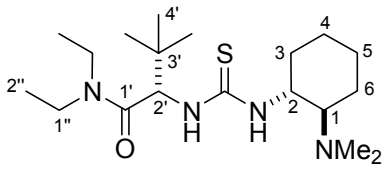

16

Yield 515 mg (1.39 mmol, 72 %)

Melting Point 120-121 °C

Specific Rotation $[\alpha]_{589}^{20}$ = -46.4°, $[\alpha]_{546}^{20}$ = -55.9°, $[\alpha]_{405}^{20}$ = -135.9°, $[\alpha]_{365}^{20}$ = -209.7° (*c* =1.01, $CHCl_3$)

TLC R_f = 0.37 (Silicagel, CH_2Cl_2/CH_3OH/TEA 100:5:1)

^{1}H-NMR (300 MHz, $CDCl_3$): δ = 0.94 (s; 9H, *H*-4′), 1.02 (t, *J* = 7.13 Hz; 3H, *H*-2″), 1.09-1.12 (m; 4H, *H*-3, *H*-4, *H*-5, *H*-6), 1.20 (t, *J* = 7.13 Hz; 3H, *H*-2″), 1.58-1.78 (m; 3H, *H*-4, *H*-5, *H*-6), 2.14 (s; 6H, NC*H*$_3$), 2.25-2.33 (m; 2H, *H*-1, *H*-3), 2.91-3.03 (m; 1H, *H*-1″), 3.25-3.34 (m; 1H, *H*-1″), 3.45-3.49 (m; 1H, *H*-2), 3.54-3.67 (m; 2H, *H*-1″), 5.44 (d, *J* = 8.96 Hz; 1H, *H*-2′), 6.60 (br

s; 1H, C-2-N*H*), 6.95 (d, *J* = 8.96 Hz; 1H, C-2′-N*H*).

^{13}C-NMR (75 MHz, $CDCl_3$): δ = 12.7 (*C*-2″), 14.5 (*C*-2″), 21.8 (*C*-6), 24.5 (*C*-4 or *C*-5), 24.8 (*C*-4 or *C*-5), 26.7 (*C*-4′), 32.9 (*C*-3), 36.1 (*C*-3′), 39.8 (*C*-1″), 40.0 (N*C*H_3), 42.7 (*C*-1″), 55.2 (*C*-2), 59.7 (*C*-2′), 66.5 (*C*-1), 170.6 (*C*-1′), 182.2 (*C*S).

The assignments were made by 2D-NMR.

FT-IR (KBr): $\tilde{\nu}$ [cm^{-1}] = 3320 (br), 2934 (s), 2861 (m), 2788 (w), 1622 (s), 1540 (s), 1458 (s), 1364 (s), 1321 (m), 1265 (m), 1216 (w), 1187 (w), 1138 (w), 1084 (w), 1035 (w), 949 (m), 873 (m), 840 (m), 787 (w), 747 (m).

HR-ESI-MS Exact molecular mass for [$C_{19}H_{39}N_4OS$] ([M+H]$^+$): 371.2839
Found: 371.284

Elemental Analysis Anal. Calcd. for $C_{19}H_{38}N_4OS$: C 61.58, H 10.34, N 15.12
Found: C 61.28, H 10.30, N 15.01

Crystallographic Data For the X-ray structure see Figure 5.6 on page 68

Colorless needles from acetone

Empirical formula:	$C_{19}H_{38}N_4OS$
Formula weight (M):	370.59 g/mol
Temperature (T):	100(2) K
Wavelength (λ):	0.71073 Å
Crystal system:	monoclinic
Space group:	$P2_1$
Unit cell dimension:	a = 11.702(1) Å α = 90°
	b = 13.351(1) Å β = 100.81(1)°
	c = 14.156(1) Å γ = 90°
Unit cell volume:	2172.4(3) $Å^3$
Z:	4
Calculated density ($\rho_{calcd.}$):	1.133 g/cm^3
Absorption coefficient (μ):	0.163 mm^{-1}
F(000):	816
Crystal size:	0.30 × 0.30 × 0.25 mm
Θ-range for data collection:	2.08° to 27.00°

Limiting indices:	$-14 \leq h \leq 14$
	$-14 \leq k \leq 17$
	$-12 \leq l \leq 18$
Reflections collected:	10636
Unique reflections:	8211 [$R_{int} = 0.0387$]
Reflections observed [I>2σ (I)]:	6520
Completeness to Θ:	99.9 %
Refinement method:	Full-matrix least-squares on F^2
Data / restraints / parameters:	8211 / 1 / 756
Goodness-of-fit on F^2:	1.023
Final *R*-indices [$I > 2\sigma(I)$]:	$R1 = 0.0439$ $\omega R2 = 0.0887$
R-indices (all data):	$R1 = 0.0655$ $\omega R2 = 0.0973$
Largest diff. peak and hole:	0.308 and -0.277 e·Å^{-3}

8.2.58 Preparation of 1-{(*S*)-1-(diisobutylcarbamoyl)-2,2-dimethyl-propyl}-3-{(1*R*,2*R*)-2-(dimethylamino)cyclohexyl}thiourea 17

[SMU-VI-35]

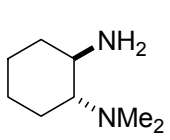

101

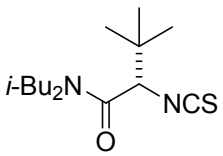

144

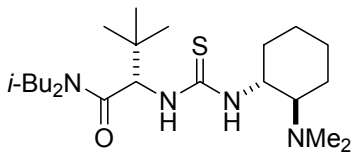

17

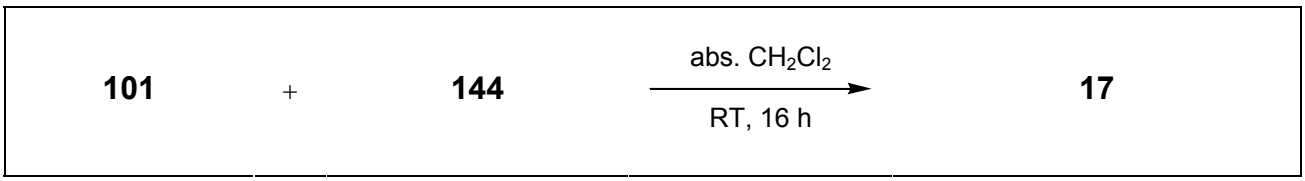

The same procedure as before (see section 8.2.56 on page 184) was followed on a 2.10 mmol scale. Purification in the same way afforded a colorless foam (600 mg, 67 %).

17 $C_{23}H_{46}N_4OS$ (426.7 g/mol)

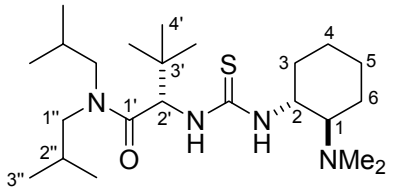

17

Yield 600 mg (1.41 mmol, 67 %)

Melting Point 59-61 °C

Specific Rotation $[\alpha]_{589}^{20}$ = -34.9°, $[\alpha]_{546}^{20}$ = -42.6°, $[\alpha]_{405}^{20}$ = -107.3°, $[\alpha]_{365}^{20}$ = -174.3° (*c* = 1.03, $CHCl_3$)

TLC R_f = 0.33 (Silicagel, CH_2Cl_2/CH_3OH/TEA 100:5:1)

^{1}H-NMR (300 MHz, $CDCl_3$): δ = 0.80-0.88 (m; 12H, *H*-3″), 0.97 (s; 9H, *H*-4′), 1.03-1.24 (m; 4H, *H*-3, *H*-4, *H*-5, *H*-6), 1.59-1.79 (m; 3H, *H*-4, *H*-5, *H*-6), 1.85-2.05 (m; 2H, *H*-2″), 2.13 (s; 6H, NC*H*$_3$), 2.19-2.35 (m; 2H, *H*-1, *H*-3), 2.58-2.65 (m; 1H, *H*-1″), 3.05-3.12 (m; 1H, *H*-1″), 3.37-3.65 (m; 3H, *H*-1″, *H*-2), 5.53 (br m; 1H, *H*-2′), 6.43 (s; 1H, C-2-N*H*), 6.92 (d, *J* = 8.6 Hz; 1H, C-2′-N*H*).

^{13}C-NMR (75 MHz, $CDCl_3$): δ = 19.3 (*C*-3″), 20.2 (*C*-3″), 20.4 (*C*-3″), 20.5 (*C*-3″), 21.7 (*C*-6), 24.5 (*C*-4 or *C*-5), 25.0 (*C*-4 or *C*-5), 26.5 (*C*-2″), 26.9 (*C*-4′), 27.9 (*C*-2″), 32.9 (*C*-3), 36.9 (*C*-3′), 39.9 (N*C*H$_3$), 53.5 (*C*-1″), 55.3 (*C*-2″), 56.2 (*C*-1″), 59.8 (*C*-2′), 66.6 (*C*-1), 172.2 (*C*-1′), 182.1 (*C*S).
The assignments were made by 2D-NMR.

FT-IR (ATR): $\tilde{\nu}$ [cm^{-1}] = 3315 (br), 3054 (br), 2954 (s), 2928 (s), 2865 (m), 2825 (w), 2782 (w), 1617 (s), 1527 (s), 1465 (s), 1445 (s), 1385 (m), 1363 (s), 1338 (w), 1320 (w), 1301 (w), 1268 (w), 1238 (m), 1207 (m), 1188 (w), 1140 (m), 1119 (w), 1096 (m), 1085 (m), 1062 (w), 1035 (m), 946 (sh), 900 (w), 872 (sh), 848 (w), 821 (m), 753 (sh).

HR-EI-MS Exact molecular mass for [$C_{23}H_{46}N_4OS$] ([M]$^+$): 426.3392
Found: 426.339

Elemental Analysis	Anal. Calcd. for $C_{23}H_{46}N_4OS$: C 64.74, H 10.87, N 13.13 Found: C 64.34, H 10.84, N 13.09

8.2.59 Preparation of 1-{(*S*)-1-(*N*-benzyl-*N*-methylcarbamoyl)-2,2-dimethylpropyl}-3-{(1*R*,2*R*)-2-(dimethylamino)cyclohexyl}thiourea 18

[SMU-VI-04]

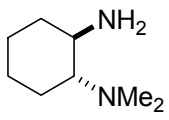

101

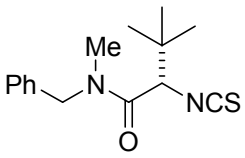

145

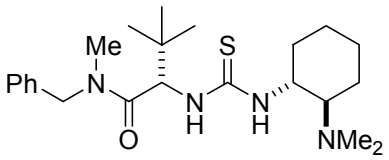

18

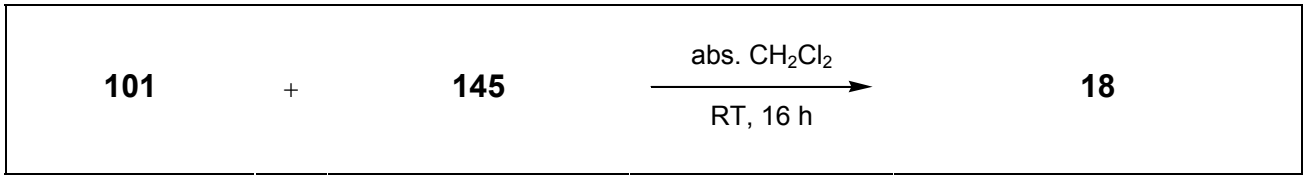

The same procedure as before (see section 8.2.56 on page 184) was followed on a 1.56 mmol scale. Purification in the same way afforded a colorless foam (483 mg, 74 %).

18	$C_{23}H_{38}N_4OS$ (418.64 g/mol)
Yield	483 mg (1.15 mmol, 73.7 %)
Melting Point	58-59 °C
Specific Rotation	$[\alpha]_{589}^{20}$ = -17.5°, $[\alpha]_{546}^{20}$ = -21.8°, $[\alpha]_{405}^{20}$ = -60.2°, $[\alpha]_{365}^{20}$ = -99.2° (*c* =1.01, $CHCl_3$)
TLC	R_f = 0.33 (Silicagel, CH_2Cl_2/CH_3OH/TEA 100:5:1)

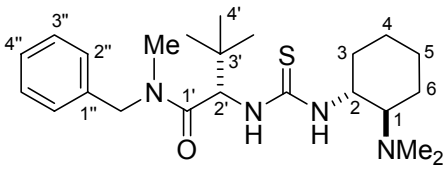

18

^{1}H-NMR (500 MHz, $CDCl_3$): δ = 1.06 (s; 9H, *H*-4′), 1.18-1.32 (m; 4H, *H*-3, *H*-4, *H*-5, *H*-6), 1.69-1.87 (m; 3H, *H*-4, *H*-5, *H*-6), 2.28 (s; 6H, NMe_2), 2.36-2.42 (m; 1H, *H*-3), 2.56-2.58 (m; 1H, *H*-1), 3.19 (s; 3H, NCH_3), 3,84 (m; 1H, *H*-2), 4.50 (d, *J* = 14.6 Hz; 1H, $PhCH_2$), 4.69 (d, *J* = 14.6 Hz; 1H, $PhCH_2$), 5.48 (d, *J* = 8.5 Hz; 1H, *H*-2′), 7.11 (br s; 1H, C-2-N*H*), 7.20 (br d, *J* = 8.5 Hz; 1H, C-2′-N*H*), 7.22-7.34 (m; 5H, H_{ar}).

^{13}C-NMR (125 MHz, $CDCl_3$): δ = 21.8 (*C*-6), 24.5 (*C*-4 or *C*-5), 24.8 (*C*-4 or *C*-5), 26.8 (*C*-4′), 32.9 (*C*-3), 35.7 (*C*-3′), 36.0 (NCH_3), 39.9 (NMe_2), 51.2 ($PhCH_2$), 55.2 (*C*-2), 60.3 (*C*-2′), 66.5 (*C*-1′), 127.2 (*C*-4″), 127.9 (*C*-2″ or *C*-3″), 128.4 (*C*-2″ or *C*-3″), 136.8 (*C*-1″), 172.5 (*C*O), 182.5 (*C*S).
The assignments were made by 2D-NMR.

FT-IR (ATR): $\tilde{\nu}$ [cm^{-1}] = 3308 (br), 3060 (w), 2930 (s), 2857 (m), 2782 (w), 1626 (s), 1535 (s), 1494 (w), 1477 (w), 1450 (m), 1413 (m), 1364 (m), 1320 (m), 1267 (w), 1237 (w), 1186 (w), 1081 (m), 1030 (w), 950 (w), 873 (w), 733 (m), 701 (s).

HR-ESI-MS Exact molecular mass for $[C_{23}H_{39}N_4OS]$ ($[M+H]^+$): 419.2845
Found: 419.284

Elemental Analysis Anal. Calcd. for $C_{23}H_{38}N_4OS$: C 65.99, H 9.15, N 13.38
Found: C 65.60, H 9.15, N 13.15

8.2.60 Preparation of 1-{(*R*)-1-(*N*-benzyl-*N*-methylcarbamoyl)-2,2-dimethylpropyl}-3-{(1*R*,2*R*)-2-(dimethylamino)cyclohexyl}thiourea 19

[SMU-VI-31]

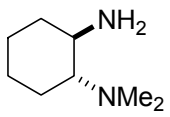

101

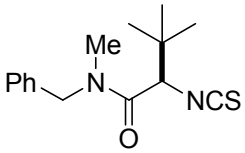

ent-**145**

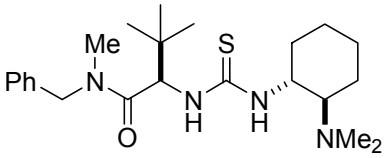

19

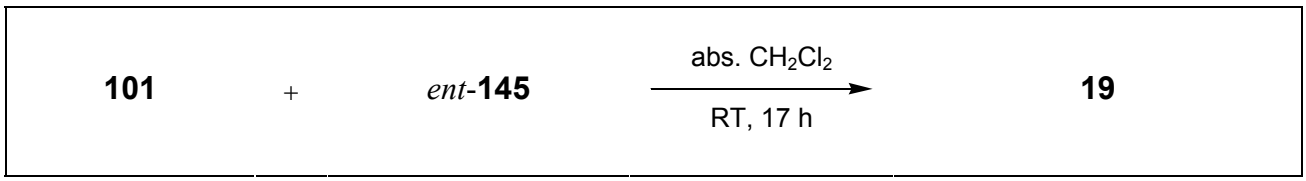

The same procedure as before (see section 8.2.56 on page 184) was followed on a 2.00 mmol scale. Purification in the same way afforded a colorless foam (530 mg, 64 %).

19 $C_{23}H_{38}N_4OS$ (418.64 g/mol)

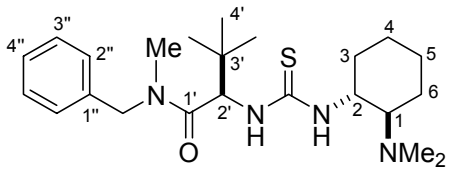

19

Yield 530 mg (1.27 mmol, 64 %)

Melting Point 64-65 °C

Specific Rotation $[\alpha]_{589}^{20} = +47.7°$, $[\alpha]_{546}^{20} = +58.9°$, $[\alpha]_{405}^{20} = +149.1°$, $[\alpha]_{365}^{20} = +216.7°$ (*c* = 1.00, $CHCl_3$)

TLC $R_f = 0.36$ (Silicagel, CH_2Cl_2/CH_3OH/TEA 100:5:1)

^{1}H-NMR (300 MHz, $CDCl_3$): δ = 1.02 (s; 9H, *H*-4′), 1.09-1.26 (m; 4H, *H*-3, *H*-4, *H*-5, *H*-6), 1.64-1.85 (m; 3H, *H*-4, *H*-5, *H*-6), 2.19-2.31 (m; 2H, *H*-1, *H*-3), 2.24 (s; 6H, NMe_2), 3.17 (s; 3H, NCH_3), 3.48 (br m; 1H, *H*-2), 4.36 (d,

J = 14.6 Hz; 1H, PhCH_2), 4.76 (d, J = 14.6 Hz; 1H, PhCH_2), 5.60 (d, J = 9.3 Hz; 1H, H-2′), 6.45 (br s; 1H, C-2-NH), 7.19-7.34 (m; 5H, H_{ar}), 8.28 (br s; 1H, C-2′-NH).

^{13}C-NMR (75 MHz, $CDCl_3$): δ = 23.3 (*C*-6), 24.5 (*C*-4 or *C*-5), 24.9 (*C*-4 or *C*-5), 26.8 (*C*-4′), 33.0 (*C*-3), 36.1 (*C*-3′), 36.2 (N*C*H$_3$), 40.8 (NMe$_2$), 51.1 (Ph*C*H$_2$), 56.7 (*C*-2), 60.8 (*C*-2′), 67.5 (*C*-1), 127.3 (*C*-4″), 128.0 (*C*-2″ or *C*-3″), 128.5 (*C*-2″ or *C*-3″), 136.9 (*C*-1″), 172.1 (*C*-1′), 183.3 (*C*S).
The assignments were made by 2D-NMR.

FT-IR (ATR): $\tilde{\nu}$ [cm^{-1}] = 3324 (br), 3059 (w), 3027 (w), 2929 (s), 2857 (m), 2823 (w), 2782 (m), 1620 (s), 1530 (s), 1494 (w), 1477 (w), 1448 (m), 1413 (m), 1363 (m), 1319 (m), 1268 (m), 1253 (w), 1234 (m), 1207 (w), 1189 (w), 1153 (w), 1108 (w), 1082 (m), 1028 (w), 947 (m), 910 (m), 873 (sh), 849 (w), 822 (w), 730 (s).

HR-ESI-MS Exact molecular mass for [$C_{23}H_{39}N_4OS$] ([M+H]$^+$): 419.2845
Found: 419.284

Elemental Analysis Anal. Calcd. for $C_{23}H_{38}N_4OS$: C 65.99, H 9.15, N 13.38
Found: C 65.55, H 9.08, N 13.38

8.2.61 Preparation of 1-{(*S*)-1-(benzylcarbamoyl)-2,2-dimethyl-propyl}-3-{(1*R*,2*R*)-2-(dimethylamino)cyclohexyl}thiourea 20

[SMU-VIII-44]

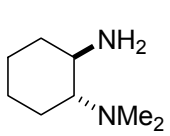

101

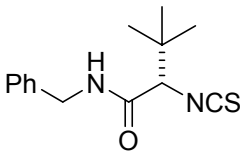

146

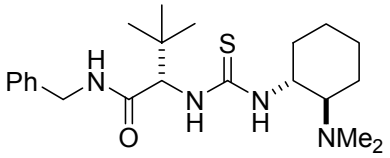

20

101	+	**146**	abs. CH_2Cl_2, RT, 16 h	**20**

The same procedure as before (see section 8.2.56 on page 184) was followed on a 1.64 mmol scale. Purification in the same way afforded an off-white foam (490 mg, 74 %).

20 $C_{22}H_{36}N_4OS$ (404.61 g/mol)

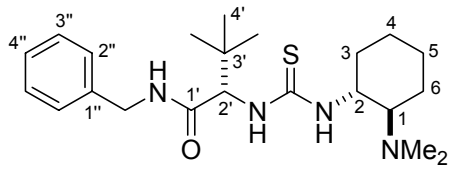

20

Yield 490 mg (1.21 mmol, 74 %)

Melting Point 89-91 °C

TLC R_f = 0.36 (Silicagel, CH_2Cl_2/CH_3OH/TEA 100:5:1)

^{1}H-NMR (300 MHz, $CDCl_3$): δ = 1.00 (s; 9H, *H*-4′), 1.09-1.85 (m; 4H, *H*-3, *H*-4, *H*-5, *H*-6), 1.61-1.76 (m; 3H, *H*-4, *H*-5, *H*-6), 2.16 (s; 6H, NC*H*$_3$), 2.22-2.24 (m; 1H, *H*-3), 2.54 (m; 1H, *H*-1), 3.98 (m; 1H, *H*-2), 4.20 (dd, *J* = 5.38, 14.88 Hz; 1H, PhC*H*$_2$), 4.42 (dd, *J* = 6.10, 14.88 Hz; 1H, PhC*H*$_2$), 4.70 (m; 1H, *H*-2′), 4.86 (br m; 1H, N*H*), 7.17-7.24 (m; 7H, H_{ar}, 2N*H*s).

^{13}C-NMR (75 MHz, $CDCl_3$): δ = 22.0 (*C*-6), 24.5 (*C*-4 or *C*-5), 24.6 (*C*-4 or *C*-5), 27.0 (*C*-4′), 32.9 (*C*-3), 34.4 (*C*-3′), 39.8 (N*C*H$_3$), 43.1 (Ph*C*H$_2$), 54.9 (*C*-2), 66.5 (*C*-1, *C*-2′), 127.0 (*C*-4″), 127.6 (*C*-2″ or *C*-3″), 128.3 (*C*-2″ or *C*-3″), 138.1 (*C*-1″), 171.3 (*C*-1′), 182.2 (*C*S).
The assignments were made by 2D-NMR.

FT-IR (ATR): $\tilde{\nu}$ [cm^{-1}] = 3264 (br), 3061 (m), 2933 (s), 2862 (m), 2793 (w), 1644 (s), 1537 (s), 1474 (w), 1452 (m), 1399 (w), 1359 (m), 1309 (m), 1232 (w), 1182 (w), 1088 (m), 1028 (sh), 991 (w), 949 (w), 909 (m), 873 (sh), 851 (w), 824 (w), 728 (s).

HR-ESI-MS Exact molecular mass for [$C_{22}H_{37}N_4OS$] ([M+H]$^+$): 405.2688
Found: 405.269

8.2.62 Preparation of 1-{(*S*)-1-(*N*-benzyl-*N*-methylcarbamoyl)-3,3-dimethylbutyl}-3-{(1*R*,2*R*)-2-(dimethylamino)cyclohexyl}thiourea 21

[SMU-VI-84]

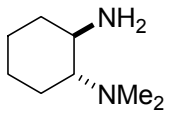

101

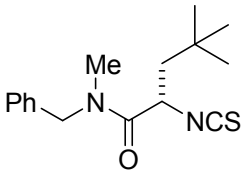

147

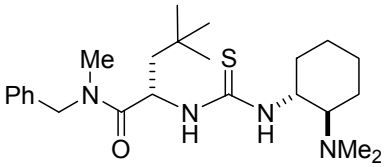

21

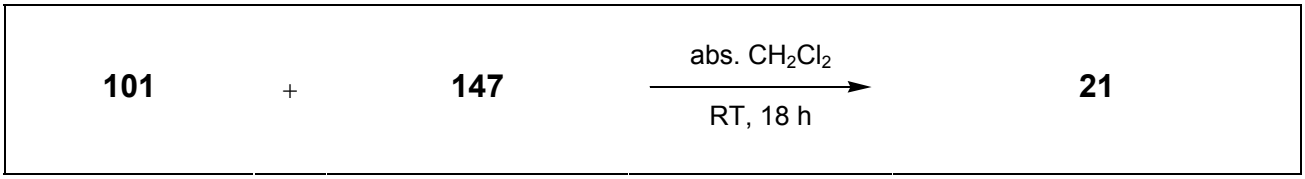

The same procedure as before (see section 8.2.56 on page 184) was followed on a 2.57 mmol scale. Purification in the same way afforded a colorless foam (832 mg, 75 %).

21 $C_{24}H_{40}N_4OS$ (432.67 g/mol)

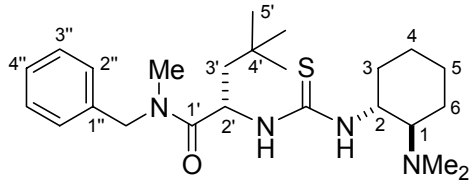

21

Yield 832 mg (1.92 mmol, 75 %)

Melting Point 67-68 °C

TLC R_f = 0.38 (Silicagel, CH_2Cl_2/CH_3OH/TEA 100:5:1)

^{1}H-NMR (300 MHz, $CDCl_3$): δ = 0.82, 0.99 (2s; 9H, *H*-5′), 1.06-1.27 (m; 5H), 1.53-1.77 (m; 5H), 2.24, 2.26 (2s; 6H, NMe_2), 2.34-2.41 (m; 2H), 2.92, 3.11 (2s; 3H, NCH_3), 3.64-3.71 (br m; 1H), 4.42 (d, *J* = 14.84 Hz; 0.7H, $PhCH_2$), 4.60 (d, *J* = 16.50 Hz; 0.3H, $PhCH_2$), 4.68 (d, *J* = 14.84 Hz; 0.7H, $PhCH_2$), 5.06 (d, *J* = 16.50 Hz; 0.3H, $PhCH_2$), 5.69 (br m; 1H), 6.66 (br m; 1H), 7.18-7.35 (m; 5H, H_{ar}), 7.91 (br s; 1H).

^{13}C-NMR (75 MHz, $CDCl_3$): δ = 22.0 (CH_2), 22.3 (CH_2), 24.5 (CH_2), 24.8 (CH_2),

29.7 (*C*H$_3$), 30.0 (*C*H$_3$), 30.7 (*C*q), 30.9 (*C*q), 33.2 (*C*H$_2$), 34.4 (*C*H$_2$), 35.0 (*C*H$_2$), 40.2 (*C*H$_3$), 46.2 (*C*H$_2$), 46.8 (*C*H$_2$), 51.3 (*C*H$_2$), 52.4 (*C*H), 53.5 (*C*H$_2$), 55.1 (*C*H), 55.3 (*C*H), 67.0 (*C*H), 127.1 (*C*$_{ar}$), 127.4 (*C*$_{ar}$), 127.6 (*C*$_{ar}$), 127.7 (*C*$_{ar}$), 128.6 (*C*$_{ar}$), 128.7 (*C*$_{ar}$), 136.5 (*C*q$_{ar}$), 136.7 (Cq$_{ar}$), 174.2 (*C*O), 181.7 (*C*S), 182.0 (*C*S).

Two sets of signals were obtained due to dynamic NMR.

FT-IR (ATR): $\tilde{\nu}$ [cm^{-1}] = 3318 (br s), 2931 (s), 2858 (m), 2823 (w), 2779 (m), 1629 (s), 1543 (s), 1494 (w), 1475 (w), 1450 (m), 1419 (w), 1362 (m), 1318 (w), 1270 (w), 1253 (w), 1206 (w), 1150 (w), 1084 (m), 1038 (w), 945 (w), 911 (m), 875 (w), 851 (w), 730 (s).

HR-EI-MS Exact molecular mass for [$C_{24}H_{41}N_4OS$] ([M+H]$^+$): 433.3001

Found: 433.300

8.2.63 Preparation of 1,2-dicyclohexyl-3-{(1*R*,2*R*)-2-(dimethylamino)-cyclohexyl}guanidine 148

[SMU-VIII-33]

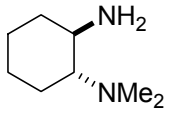

101

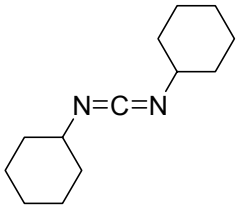

149

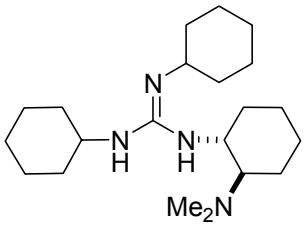

148

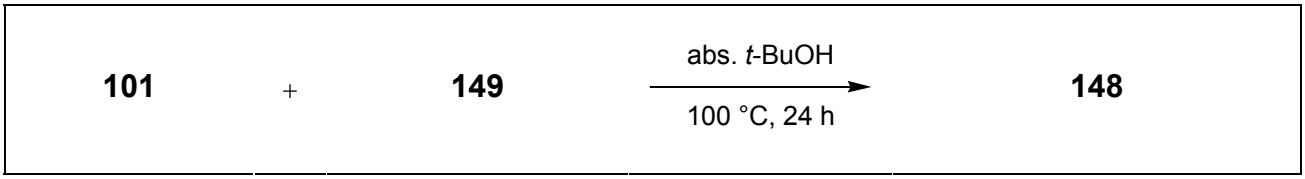

To a solution of (1*R*,2*R*)-*N*,*N*-dimethyl-1,2-diaminocyclohexane **101** (250 mg, 1.76 mmol, 2.00 eq) in 4 mL of abs. *t*-BuOH, was added *N*,*N*-dicyclohexyl carbodiimide **149** (182 mg, 880 µmol, 1.00 eq) and the resulting solution was heated to reflux under argon for 24 hours. The reaction mixture was then cooled to ambient temperature and the solvent was removed in vacuo to obtain a highly

viscous yellow oil. Purification by bulb-to-bulb distillation (175 °C, <1 mbar) afforded a pale yellow oil (230 mg, 75 %).

148 $C_{21}H_{40}N_4$ (348.57 g/mol)

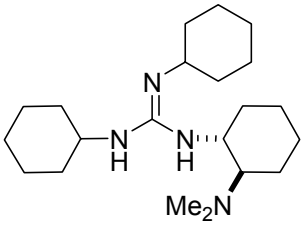

148

Yield 230 mg (660 µmol, 75 %)

^{1}H-NMR (250 MHz, $CDCl_3$): δ = 1.07-1.31 (m; 15 H), 1.54-1.67 (m; 15 H), 2.16 (s; 6H, NC*H*$_3$), 3.03 (br m; 2H).
The NH protons could not be detected.

FT-IR (ATR): $\tilde{\nu}$ [cm^{-1}] = 3247 (br), 2923 (s), 2849 (s), 2778 (m), 2117 (sh s), 1637 (s), 1447 (s), 1337 (w), 1267 (w), 1207 (w), 1188 (m), 1150 (m), 1095 (w), 1042 (m), 951 (w), 889 (sh m), 871 (sh m), 846 (w), 819 (w), 726 (br m).

HR-EI-MS Exact molecular mass for $[C_{21}H_{41}N_4]$ ($[M+H]^+$): 349.3326
Found: 349.333

8.2.64 Preparation of 1,2-dicyclohexyl-3-{(1*R*,2*R*)-2-(dimethylamino)-cyclohexyl}guanidinidinium trifluoroacetate 150

[SMU-VIII-38]

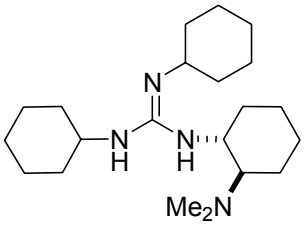

148

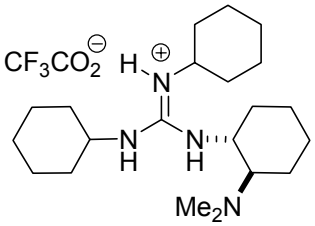

150

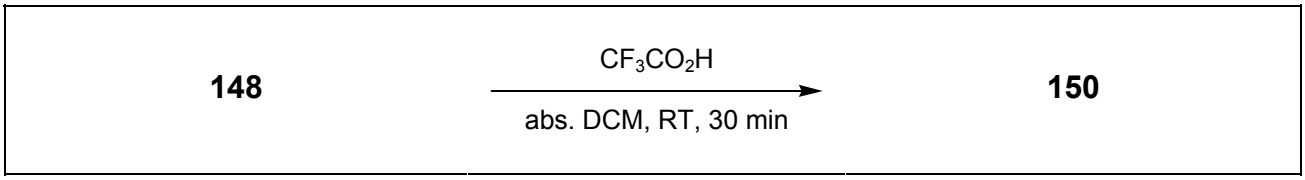

To a solution of **148** (215 mg, 620 µmol, 1.00 eq) in 3 mL of abs. DCM was added a solution of CF_3CO_2H (48 µL, 620 µmol, 1.00 eq) in 1 mL abs. DCM and the solution was stirred at room temperature for 30 minutes. The reaction mixture was then concentrated in vacuo to obtain a pale yellow foam (285 mg, 100 %).

150 $C_{23}H_{41}F_3N_4O_2$ (462.59 g/mol)

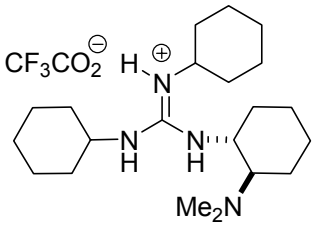

150

Yield 285 mg (620 µmol, 100 %)

^{1}H-NMR (250 MHz, $CDCl_3$): δ = 1.17-1.43 (m; 15H), 1.60-2.04 (m; 15H), 2.34 (s; 6H, NC*H*$_3$), 3.18-3.21 (m; 2H), 8.39 (br s; 1H).
Two NH protons could not be detected.

FT-IR (ATR): $\tilde{\nu}$ [cm^{-1}] = 3254 (br), 3090 (br), 2929 (s), 2855 (s), 2116 (sh m), 1685 (s), 1621 (s), 1450 (m), 1365 (w), 1348 (w), 1246 (w), 1198 (s), 1168 (w), 1124 (s), 1042 (w), 890 (sh), 872 (w), 825 (s), 797 (s), 717 (sh s).

HR-EI-MS Exact molecular mass for $[C_{21}H_{41}N_4]$ ($[M–CF_3CO_2]^+$): 349.3326
Found: 349.333

8.3 Synthesis of oxazaborolidines and its precursors

8.3.1 Preparation of *N*-benzyl-(*S*)-pyrrolidin-2-carboxylic acid benzyl ester 153

[SMU-III-77]

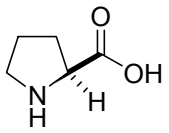

37

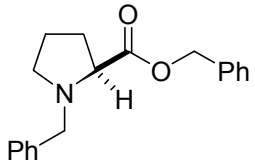

153

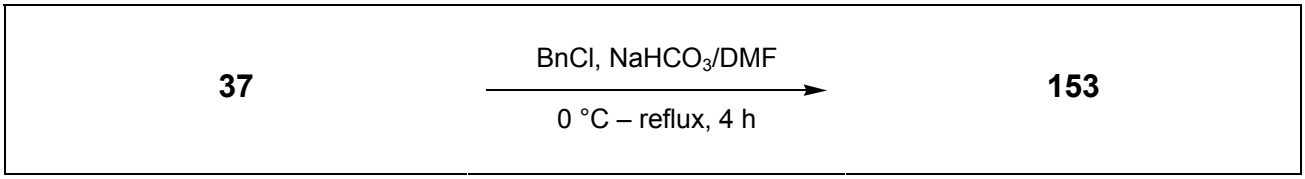

To an ice-cold suspension of L-proline **37** (10.0 g, 86.9 mmol, 1.00 eq) and $NaHCO_3$ (18.2 g, 217.2 mmol, 2.50 eq) in 150 mL of absolute DMF, benzyl chloride (24.2 g, 191.1 mmol, 2.20 eq) was added dropwise over a period of 40 mins. After complete addition, the resulting mixture was stirred for 30 mins at room temperature and then refluxed for 4 hrs under argon atmosphere. The reaction mixture was then cooled to room temperature and stirred overnight at that temperature. 150 mL of water was added to it and stirred for 5 mins to obtain a homogeneous solution. This was then extracted with toluene (3 × 100 mL). The combined organic extract was washed with sat. NaCl solution and water (100 mL each) and dried over anh. $MgSO_4$. Solvent was removed in vacuo to obtain a pale yellow oil which was dried overnight in vacuo at 60 °C. This oil (25.4 g, 99 %) was used in the following step without further purification.

153	$C_{19}H_{21}NO_2$ (295.38 g/mol)
Yield	25.4 g (85.8 mmol, 99 %)

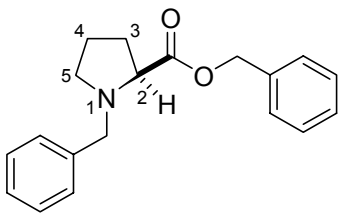

153

^{1}H-NMR (300 MHz, $CDCl_3$): δ = 1.78-2.21 (m; 4H, *H*-3, *H*-4), 2.39-2.48 (m; 1H, *H*-5), 3.02-3.09 (m; 1H, *H*-5), 3.32-3.37 (m; 1H, *H*-2), 3.58 (d, *J* = 12.9 Hz; 1H, NCH_2), 3.95 (d, *J* = 12.9 Hz; 1H, NCH_2), 5.11 (d, *J* = 12.3 Hz; 1H, OCH_2), 5.16 (d, *J* = 12.3 Hz; 1H, OCH_2), 7.23-7.41 (m; 10H, H_{ar}).

FT-IR (Film): $\tilde{\nu}$ [cm^{-1}] = 2956 (m), 2877 (w), 2801 (m), 2360 (s), 2341 (m), 1729 (s), 1495 (m), 1454 (s), 1371 (w), 1269 (m), 1167 (s), 1028 (w), 911 (w), 738 (m).

8.3.2 Preparation of *N*-benzyl-(*S*)-diphenyl(pyrrolidin-2-yl)methanol 154a[173]

[SMU-III-11]

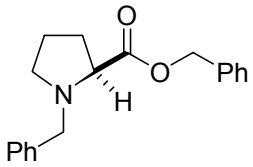

153

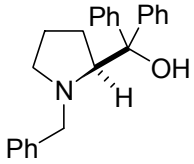

154a

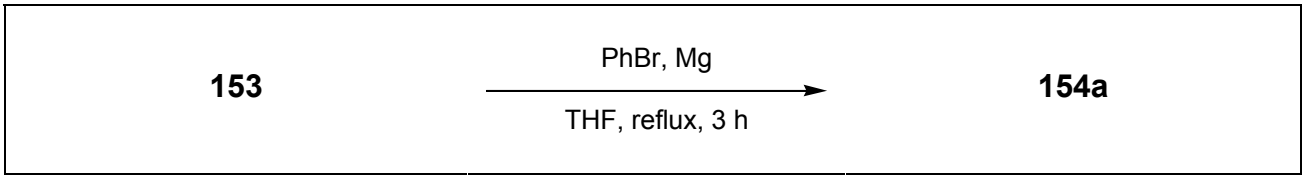

An oven-dried 250 mL two-necked flask fitted with an argon inlet and a 50 mL pressure-equalized addition funnel containing a solution of bromobenzene (3.91 g, 24.9 mmol, 2.80 eq) in 15 mL abs. THF was charged with magnesium turnings (606 mg, 24.9 mmol, 2.80 eq; activated with iodine) in 10 mL of abs. THF. A small portion (2 mL) of the solution of bromobenzene was added with stirring at room temperature. After the exothermic reaction started, the reaction flask was cooled with a water bath. The remaining bromobenzene was added dropwise over a period of 30 min. After the addition was complete, the reaction mixture was stirred at room temperature for 30 min until all the magnesium turnings consumed. This solution was then cooled to 0 °C and a solution of *N*-benzyl-(*S*)-pyrrolidin-2-carboxylic acid benzyl ester **153** (2.63 g, 8.90 mmol, 1.00 eq) in 15 mL abs. THF was added dropwise over a period of 1 hr. The resulting mixture was then refluxed for 3 hrs. The reaction mixture was then cooled to room temperature and an ice-cold saturated NH_4Cl-

solution (12 mL) was added to it followed by 2 mL of 2N hydrochloric acid. 2N KOH solution was added to it until pH ~ 7.5. The organic layer was separated and the aqueous layer was extracted with ethyl acetate (2 × 200 mL). The combined organic layer was washed with sat. NaCl solution (100 mL), dried over anh. Na_2CO_3 and the solvent was removed in vacuo to obtain a pale yellow solid. Recrystallization from ethanol afforded a white crystalline solid (2.45 g, 80 %).

154a $C_{24}H_{25}NO$ (343.46 g/mol)

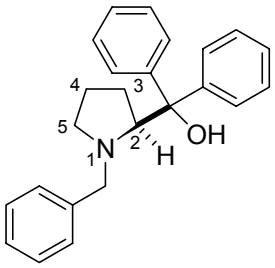

154a

Yield 2.45 g (7.13 mmol, 80 %)
[Lit.[173]: 76 %]

Melting Point 115 °C (EtOH)
[Lit[173]: 116 °C (Et_2O)]

TLC R_f = 0.65 (Silicagel, *n*-Hex/EtOAc 5:1)

^{1}H-NMR (300 MHz, $CDCl_3$): δ = 1.68-1.91 (m; 3H, *H*-3, *H*-4), 1.99-2.13 (m; 1H, *H*-3), 2.41-2.50 (m; 1H, *H*-5), 2.99-3.05 (m; 1H, *H*-5), 3.13 (d, *J* = 12.63 Hz; 1H, NC*H*$_2$), 3.33 (d, *J* = 12.63 Hz; 1H, NC*H*$_2$), 4.08 (2d, *J* = 4.64 Hz; 1H, *H*-2), 5.03 (br s; 1H, O*H*), 7.13-7.42 (m; 11H, H_{ar}), 7.67-7.70 (m; 2H, H_{ar}), 7.81-7.84 (m; 2H, H_{ar}).

^{13}C-NMR (75 MHz, $CDCl_3$): δ = 24.2 (*C*-4), 29.8 (*C*-3), 55.5 (*C*-5), 60.6 (N*C*H$_2$), 70.6 (*C*-2), 77.9 (*C*OH), 125.5 (C_{ar}), 125.6 (C_{ar}), 126.2 (C_{ar}), 126.4 (C_{ar}), 126.8 (C_{ar}), 128.0 (C_{ar}), 128.1 (C_{ar}), 128.2 (C_{ar}), 128.6 (C_{ar}), 139.7 (Cq_{ar}), 146.7 (Cq_{ar}), 148.0 (Cq_{ar}).
The NMR data are in agreement with the literature.[173]

FT-IR (CsI): $\tilde{\nu}$ [cm^{-1}] = 3440 (s), 3052 (m), 1962 (m), 2804 (s), 2357 (m), 2335 (w), 1604 (s), 1495 (s), 1448 (s), 1375 (s), 1358 (s), 1311 (m), 1252 (m), 1202 (w), 1162 (w), 1130 (s), 1102 (s), 1040 (s), 866 (m), 766 (s), 705 (s).

8.3.3 Preparation of *N*-benzyl-(*S*)-bis(3,5-dimethylphenyl)-pyrrolidin-2-methanol 154b[174]

[SMU-III-78]

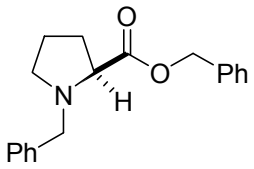

153

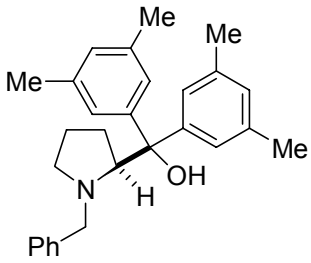

154b

153	*m*-Xyl-5-Br, Mg THF, reflux, 3 h	**154b**

The same procedure as before (see section 8.3.2 on page 200) was followed on a 10.2 mmol scale. The crude product was obtained as a yellowish orange oil (4.10 g, >99 %). This was used in the subsequent step (see section 8.3.6 on page 207) without further purification.

154b $C_{28}H_{33}NO$ (399.57 g/mol)

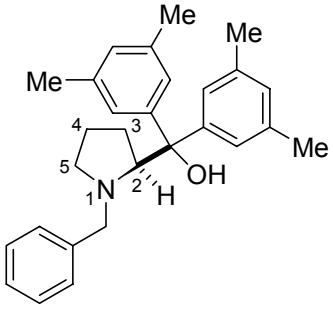

154b

Yield 4.10 g (10.3 mmol, >99 %)

^{1}H-NMR (300 MHz, $CDCl_3$): δ = 1.56-1.82 (m; 2H), 1.90-2.03 (m; 1H), 2.24 (s; 6H, C*H*$_3$), 2.29 (s; 6H, C*H*$_3$), 2.21-2.37 (m; 2H), 2.87-2.93 (m; 1H), 2.99 (d, *J* = 12.62 Hz; 1H, NC*H*$_2$), 3.15 (d, *J* = 12.62 Hz; 1H, NC*H*$_2$), 3.87-3.91 (m; 1H, *H*-2), 4.60 (s; 1H, O*H*), 6.70 (s; 1H, *H*$_{ar}$), 6.80 (s; 1H, *H*$_{ar}$), 7.03-7.05 (m; 2H, *H*$_{ar}$), 7.17-7.32 (m; 7H, *H*$_{ar}$).

^{13}C-NMR (75 MHz, $CDCl_3$): δ = 21.4 (*C*H_3), 21.5 (*C*H_3), 24.2 (*C*-4), 29.8 (*C*-3), 55.6 (*C*-5), 60.5 (N*C*H_2), 70.7 (*C*-2), 78.0 (*C*OH), 123.4 (C_{ar}), 126.6 (C_{ar}), 126.8 (C_{ar}), 127.4 (C_{ar}), 128.4 (C_{ar}), 128.5 (C_{ar}), 128.9 (C_{ar}), 137.17 (Cq_{ar}), 137.23 (Cq_{ar}), 139.8 (Cq_{ar}), 146.3 (Cq_{ar}), 147.7 (Cq_{ar}).

8.3.4 Preparation of *N*-benzyl-(*S*)-2-(di-*β*-naphthylhydroxymethyl)-pyrrolidine 154c[175]

[ILO-I-04]

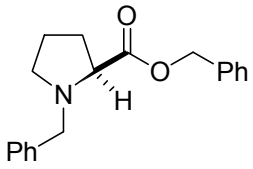

153

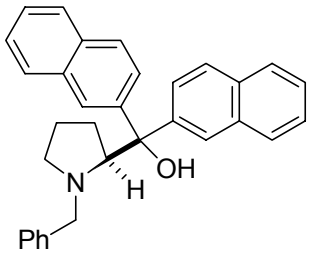

154c

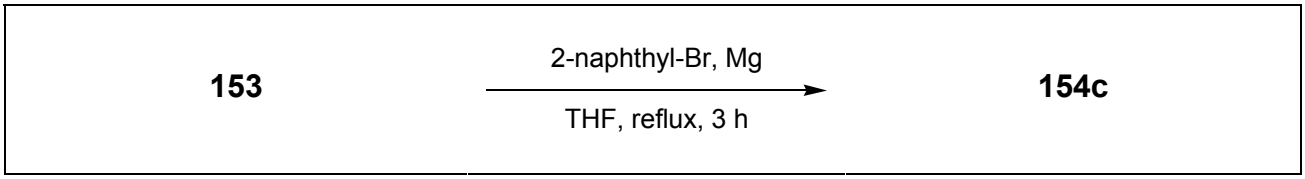

The same procedure as before (see section 8.3.2 on page 200) was followed on an 8.46 mmol scale. The crude product was purified by column chromatography on silica gel (10:1 *n*-hexane/EtOAc as the eluant) to obtain an off-white solid (2.40 g, 64 %).

$nbndnaphproh $C_{32}H_{29}NO$ (443.58 g/mol)

Yield 2.40 g (5.41 mmol, 64 %)
[Lit.[175]: 83 %]

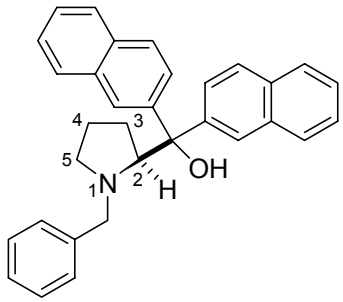

154c

Melting Point 78 °C [Lit.[175]: 78-79 °C (hexane/*tert*-butyl methyl ether)]

TLC R_f = 0.19 (Silicagel, *n*-hexane/EtOAc 10:1)

^{1}H-NMR (300 MHz, $CDCl_3$): δ = 1.62-2.13 (m; 4H, *H*-3, *H*-4), 2.37-2.46 (m; 1H, *H*-5), 2.94-3.09 (m; 1H, *H*-5), 3.06 (d, *J* = 12.5 Hz; 1H, NCH_2), 3.29 (d, *J* = 12.5 Hz; 1H, NCH_2), 4.23 (dd, *J* = 4.8, 9.2 Hz; 1H, *H*-2), 6.98-7.01 (m; 2H, H_{ar}), 7.11-7.20 (m; 3H, H_{ar}), 7.33-7.47 (m; 4H, H_{ar}), 7.67-7.88 (m; 8H, H_{ar}), 8.11 (s; 1H, H_{ar}), 8.35 (s; 1H, H_{ar}).

^{13}C-NMR (75 MHz, $CDCl_3$): δ = 24.2 (*C*-4), 29.9 (*C*-3), 55.6 (*C*-5), 60.6 (NCH_2), 70.0 (*C*-2), 78.3 (*C*-OH), 123.9 (C_{ar}), 124.1 (C_{ar}), 124.3 (C_{ar}), 124.4 (C_{ar}), 125.6 (C_{ar}), 125.7 (C_{ar}), 125.9 (C_{ar}), 126.0 (C_{ar}), 126.8 (C_{ar}), 127.38 (C_{ar}), 127.42 (C_{ar}), 127.8 (C_{ar}), 127.9 (C_{ar}), 128.06 (C_{ar}), 128.16 (C_{ar}), 128.19 (C_{ar}), 128.6 (C_{ar}), 132.0 (Cq_{ar}), 133.2 (Cq_{ar}), 133.3 (Cq_{ar}), 139.4 (Cq_{ar}), 143.8 (Cq_{ar}), 145.2 (Cq_{ar}).

The NMR data are in agreement with the literature.[175]

8.3.5 Preparation of (*S*)-*α*,*α*-diphenyl-2-pyrrolidin-methanol 97a[174]

[SMU-III-19]

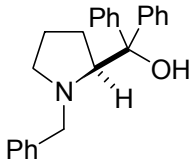

154a

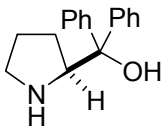

97a

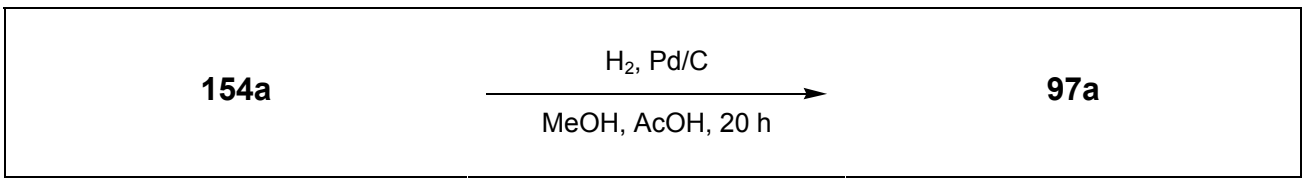

In a 100 mL round bottom flask *N*-benzyl-(*S*)-diphenyl(pyrrolidin-2-yl)methanol **154a** (1.96 g, 5.71 mmol, 1.00 eq) and palladium (10 % on charcoal, 60.7 mg, 57 µmol, 0.01 eq) was suspended in 35 mL methanol along with 0.5 mL of glacial acetic acid. This suspension was then stirred at room temperature under hydrogen atmosphere (p = 1 bar) for 20 hrs. The reaction mixture was then filtered through a Celite® pad with suction and concentrated in vacuo to obtain a white crystalline

solid (1.78 g) which was dissolved in chloroform (35 mL) and washed with saturated $NaHCO_3$ solution (40 mL). The aqueous layer was extracted with chloroform (2 × 10 mL) and the combined organic layer was washed with sat. NaCl solution (25 mL). The organic layer was dried over anh. $MgSO_4$ and the solvent was removed in vacuo to obtain a thick colourless oil. This oil was refluxed with *n*-heptane (15 mL) and cooled to afford a colorless crystalline solid (1.35 g, 93 %).

97a	$C_{17}H_{19}NO$ (253.34 g/mol)
Yield	1.35 g (5.33 mmol, 93 %) [Lit.[174]: 95 %]
Melting Point	76-78 °C (*n*-heptane) [Lit.[174]: 79-79.5 °C]

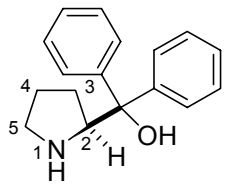

97a

^{1}H-NMR	(300 MHz, $CDCl_3$): δ = 1.47-1.77 (m; 4H, *H*-3, *H*-4), 2.86-3.03 (m; 2H, *H*-5), 4.22 (t, *J* = 7.5 Hz; 1H, *H*-2), 7.10-7.16 (m; 2H, H_{ar}), 7.21-7.99 (m; 4H, H_{ar}), 7.44-7.48 (m, 2H, H_{ar}), 7.52-7.55 (m; 1H, H_{ar}).
^{13}C-NMR	(75 MHz, $CDCl_3$): δ = 25.5 (*C*-4), 26.2 (*C*-3), 46.7 (*C*-5), 64.4 (*C*-2), 77.1 (*C*OH), 125.5 (C_{ar}), 125.8 (C_{ar}), 126.3 (C_{ar}), 126.4 (C_{ar}), 127.9 (C_{ar}), 128.2 (C_{ar}), 145.3 (Cq_{ar}), 148.1 (Cq_{ar}). The NMR data are in agreement with the literature.[174]
FT-IR	(CsI): $\tilde{\nu}$ [cm^{-1}] = 3373 (br s), 3061 (w), 2964 (m), 2354 (m), 1606 (s), 1492 (m), 1452 (m), 1397 (m), 1343 (m), 1189 (m), 1128 (w), 1068 (m), 993 (m), 754 (s), 708 (s).
Crystallographic Data	For the X-ray structure see Figure 5.9 on page 80 Colorless needles from *n*-heptane

Empirical formula:	$C_{17}H_{19}NO$
Formula weight (M):	253.34 g/mol
Temperature (T):	100(2) K
Wavelength (λ):	0.71073 Å
Crystal system:	orthorhombic
Space group:	$P2_12_12_1$

Unit cell dimension:	a = 9.0190(2) Å α = 90°
	b = 9.2900(2) Å β = 90°
	c = 16.8057(4) Å γ = 90°
Unit cell volume:	1408.09(5) Å^3
Z:	4
Calculated density ($\rho_{calcd.}$):	1.195 g/cm^3
Absorption coefficient (μ):	0.074 mm^{-1}
F(000):	544
Crystal size:	0.28 × 0.22 × 0.20 mm
Θ-range for data collection:	2.56° to 27.00°
Limiting indices:	-11 ≤ h ≤ 10
	-11 ≤ k ≤ 11
	-20 ≤ l ≤ 21
Reflections collected:	9650
Unique reflections:	3070 [R_{int} = 0.0380]
Reflections observed [I>2σ (I)]:	2117
Completeness to Θ:	99.7 %
Refinement method:	Full-matrix least-squares on F^2
Data / restraints / parameters:	3070 / 0 / 250
Goodness-of-fit on F^2:	0.987
Final *R*-indices [$I > 2\sigma(I)$]:	$R1$ = 0.0419 $\omega R2$ = 0.0952
R-indices (all data):	$R1$ = 0.0694 $\omega R2$ = 0.1076
Largest diff. peak and hole:	0.120 and -0.104 e·Å^{-3}

8.3.6 Preparation of (*S*)-*α*,*α*-bis(3,5-dimethylphenyl)-pyrrolidin-2-yl-methanol 97b[174]

[SMU-III-82]

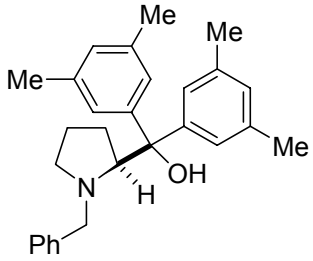

154b

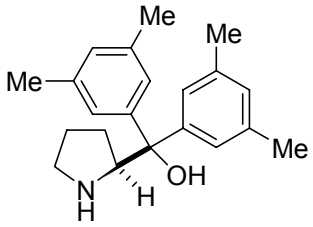

97b

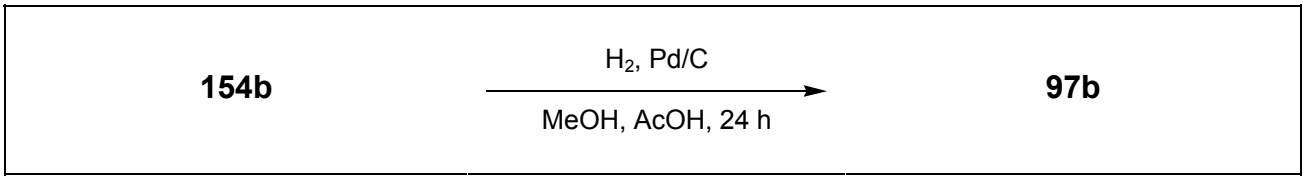

The same procedure as before (see section 8.3.5 on page 204) was followed on a 10.3 mmol scale to obtain the crude product as a thick oil. This was purified by column chromatography on silica gel (*n*-Hex/EtOAc 5:1 to 1:10 as eluant) to afford a clear oil which was then crystallized from *n*-heptane to obtain colorless crystals (2.49 g, 79 %).

97b $C_{21}H_{27}NO$ (309.45 g/mol)

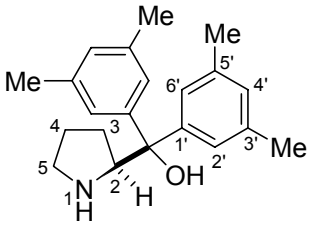

97b

Yield 2.49 g (8.05 mmol, 79 %)
[Lit.[174]: 75 %]

Melting Point 98 °C (*n*-heptane)
[Lit.[174]: 97.5-98 °C]

^{1}H-NMR (300 MHz, $CDCl_3$): δ = 1.53-1.85 (m; 5H, *H*-3, *H*-4, N*H*), 2.30 (s; 6H, CH_3), 2.31 (s; 6H, CH_3), 2.90-3.07 (m; 2H, *H*-5), 4.23 (t, *J* = 7.58 Hz; 1H, *H*-2), 6.82 (s; 2H, *H*-4′), 7.14 (s; 2H, *H*-2′), 7.20 (s; 2H, *H*-6′).

^{13}C-NMR (75 MHz, $CDCl_3$): δ = 21.51 (*C*H_3), 21.53 (*C*H_3), 25.4 (*C*-4), 26.2 (*C*-3), 46.7 (*C*-5), 64.4 (*C*-2), 76.9 (*C*OH), 123.1 (C_{ar}), 123.5 (C_{ar}), 127.9 (C_{ar}),

128.0 (C_{ar}), 137.1 (Cq_{ar}), 137.4 (Cq_{ar}), 145.3 (Cq_{ar}), 148.1 (Cq_{ar}).
The NMR data are in agreement with the literature.[174]

FT-IR (ATR): $\tilde{\nu}$ [cm^{-1}] = 3348 (br), 2943 (s), 2912 (s), 2864 (m), 1602 (s), 1456 (s), 1394 (m), 1373 (m), 1281 (m), 1151 (s), 1108 (s), 1033 (s), 981 (w), 941 (w), 919 (w), 901 (m), 847 (s), 795 (w), 740 (s), 689 (w).

8.3.7 Preparation of (*S*)-2-(di-*β*-naphthylhydroxymethyl)-pyrrolidine 97c[175]

[ILO-I-07]

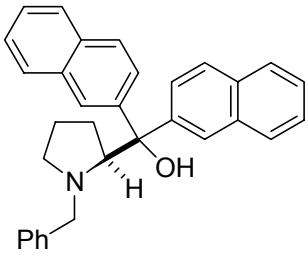

154c

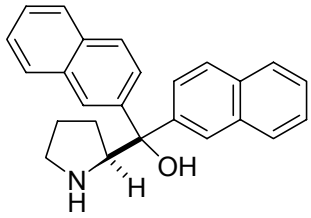

97c

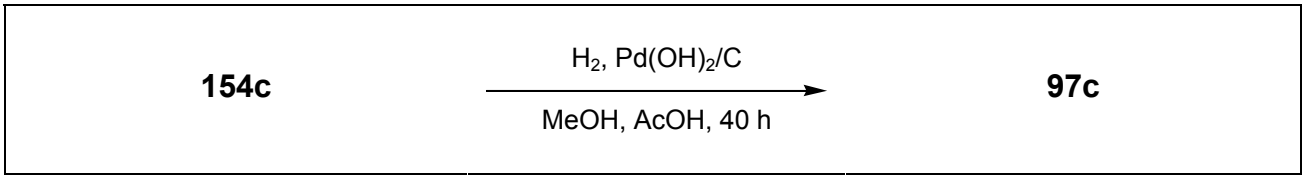

The same procedure as before (see section 8.3.5 on page 204) was followed on a 5.37 mmol scale to obtain a clear oil (1.03 g, 54 %). Recrystallization from *n*-heptane afforded a white amorphous solid.

97c $C_{25}H_{23}NO$ (353.46 g/mol)

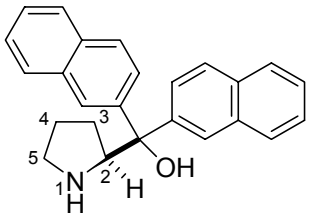

97c

Yield 1.03 g (2.91 mmol, 54 %)
[Lit.[175]: 87 %]

Melting Point 138 °C (*n*-heptane)
[Lit.[175]: 137-138 °C (*n*-hexane/ethyl acetate)]

TLC R_f = 0.04 (Silicagel, *n*-hexane/EtOAc 1:1)

^{1}H-NMR (300 MHz, $CDCl_3$): δ = 1.56-1.84 (m; 4H, *H*-3, *H*-4), 2.95-3.10 (m; 2H, *H*-5), 4.48-4.52 (m; 1H, *H*-2), 7.37-7.48 (m; 4H, H_{ar}), 7.56-7.60 (m; 1H, H_{ar}), 7.66-7.76 (m; 5H, H_{ar}), 7.82-7.87 (m; 2H, H_{ar}), 8.10 (s; 2H, H_{ar}).

^{13}C-NMR (75 MHz, $CDCl_3$): δ = 25.6 (C-4), 26.5 (C-3), 46.8 (C-5), 64.0 (C-2), 77.5 (C-OH), 123.7 (C_{ar}), 124.0 (C_{ar}), 124.4 (C_{ar}), 125.2 (C_{ar}), 125.6 (C_{ar}), 125.75 (C_{ar}), 125.85 (C_{ar}), 126.0 (C_{ar}), 127.4 (C_{ar}), 127.6 (C_{ar}), 128.0 (C_{ar}), 128.17 (C_{ar}), 128.23 (C_{ar}), 132.19 (Cq_{ar}), 132.22 (Cq_{ar}), 133.09 (Cq_{ar}), 133.17 (Cq_{ar}), 142.6 (Cq_{ar}), 145.3 (Cq_{ar}).
The NMR data are in agreement with the literature.[175]

FT-IR (ATR): $\tilde{\nu}$ [cm^{-1}] = 3349 (br), 3053 (sh), 2965 (m), 2867 (m), 1916 (w), 1628 (m), 1597 (s), 1504 (sh s), 1457 (w), 1432 (w), 1398 (s), 1268 (s), 1245 (w), 1156 (s), 1121 (s), 1017 (sh), 998 (m), 946 (w), 892 (m), 857 (s), 819 (s), 786 (s), 743 (s), 701 (w).

8.3.8 Preparation of 2,4,6-triphenyl-1,3,5-trioxa-2,4,6-triborinane 151a

[SMU-II-54]

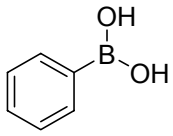

98a

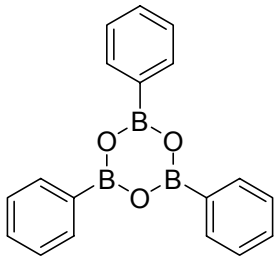

151a

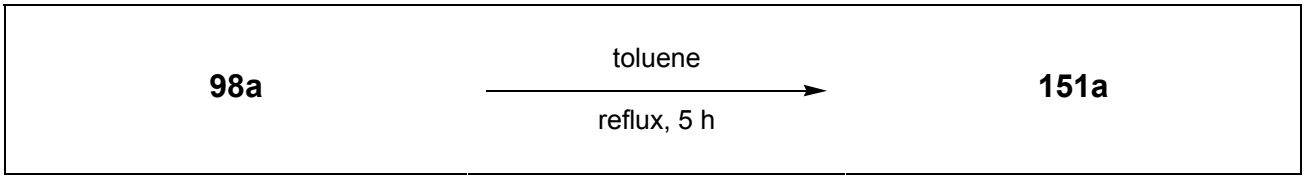

In a 50 mL round-bottomed flask equipped with a magnetic stir-bar and a *Dean-Stark* apparatus, phenylboronic acid **98a** (500 mg, 4.1 mmol) was dissolved in 40 mL of freshly dried toluene. **98a**

was then dehydrated by azeotropic distillation for 5 hrs. The reaction mixture was then cooled to ambient temperature and the solvent was removed in vacuo to afford a colorless crystalline solid (426 mg, quant.).

151a $C_{18}H_{15}B_3O_3$ (311.74 g/mol)

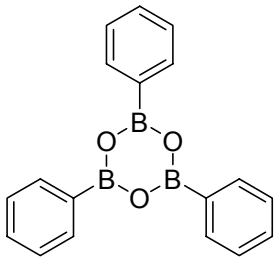

151a

Yield 426 mg (1.37 mmol, quant.)

^{1}H-NMR (300 MHz, $CDCl_3$): δ = 7.46-7.62 (m; 9H, H_{ar}), 8.22-8.25 (m; 6H, H_{ar}).

^{13}C-NMR (75 MHz, $CDCl_3$): δ = 127.9 (CH_{ar}), 132.7 (CH_{ar}), 135.6 (CH_{ar}).

FT-IR (CsI): $\tilde{\nu}$ [cm^{-1}] = 1604 (s), 1494 (m), 1444 (s), 1370 (s), 1344 (br s), 1306 (s), 1261 (s), 1180 (w), 1126 (m), 1088 (s), 1025 (s), 844 (w), 804 (s), 760 (w), 700 (s).

Crystallographic Data

For X-ray structure see Figure 5.10 on page 81

Colorless needles from *n*-hexane/toluene mixture

Empirical formula:	$C_{18}H_{15}B_3O_3$	
Formula weight (M):	311.74 g/mol	
Temperature (T):	293(2) K	
Wavelength (λ):	0.71073 Å	
Crystal system:	monoclinic	
Space group:	$P2_1/c$	
Unit cell dimension:	a = 10.7077(6) Å	α = 90°
	b = 13.6285(7) Å	β = 100.38°
	c = 11.7104(9) Å	γ = 90°
Unit cell volume:	1680.94(18) $Å^3$	
Z:	2	
Calculated density ($\rho_{calcd.}$):	1.232 mg/m^3	
Absorption coefficient (μ):	0.079 mm^{-1}	
F(000):	648	

Crystal size:	0.20 × 0.20 × 0.30 mm
Θ-range for data collection:	1.93° to 26.99°
Limiting indices:	-9 ≤ h ≤ 13
	-15 ≤ k ≤ 17
	-14 ≤ l ≤ 14
Reflections collected:	7138
Unique reflections:	3528 [R_{int} = 0.0539]
Reflections observed [I>2σ (I)]:	1397
Completeness to Θ:	96.0 %
Refinement method:	Full-matrix least-squares on F^2
Data / restraints / parameters:	3528 / 0 / 277
Goodness-of-fit on F^2:	1.014
Final *R*-indices [$I > 2\sigma(I)$]:	$R1$ = 0.0617 $\omega R2$ = 0.1446
R-indices (all data):	$R1$ = 0.1876 $\omega R2$ = 0.1853
Largest diff. peak and hole:	0.148 and -0.161 e·Å^{-3}

8.3.9 Preparation of 2,4,6-tri(*o*-tolyl)-1,3,5-trioxa-2,4,6-triborinane 151b[138]

[SMU-II-81]

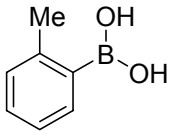

98b

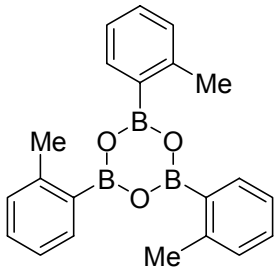

151b

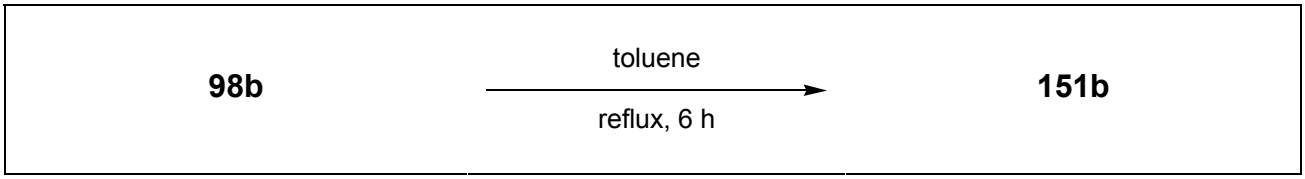

The same procedure as before (see section 8.3.8 on page 209) was followed on a 3.68 mmol scale to obtain a colorless crystalline solid (435 mg, quant.).

151b	$C_{21}H_{21}B_3O_3$ (353.82 g/mol)
Yield	435 mg (1.23 mmol, quant.)
Melting Point	165 ºC [Lit.[138]: 165-166 °C]

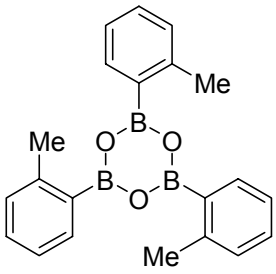

151b

^{1}H-NMR (300 MHz, $CDCl_3$): δ = 2.80 (s; 9H, CH_3), 7.25-7.32 (m; 3H, H_{ar}), 7.44 (app. dt, J = 1.5, 7.5 Hz; 3H, H_{ar}), 8.20 (dd, J = 1.5, 7.4 Hz; 3H, H_{ar}).

^{13}C-NMR (75 MHz, $CDCl_3$): δ = 23.1 (CH_3), 125.2 (CH_{ar}), 130.6 (CH_{ar}), 132.2 (CH_{ar}), 137.2 (CH_{ar}), 146.3 (Cq_{ar}).
The NMR data are in agreement with the literature.[138]

FT-IR (CsI): $\tilde{\nu}$ [cm^{-1}] = 1601 (s), 1486 (m), 1442 (s), 1342 (br s), 1301 (s), 1200 (m), 1164 (w), 1067 (m), 736 (s).

8.3.10 Preparation of (*S*)-hexahydro-1,3,3-triphenylpyrrolo[1,2-*c*][1,3,2]-oxazaborole 29b[174]

[SMU-II-79]

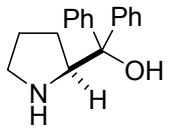

97a

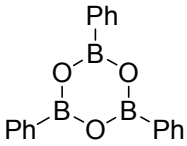

151a

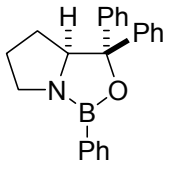

29b

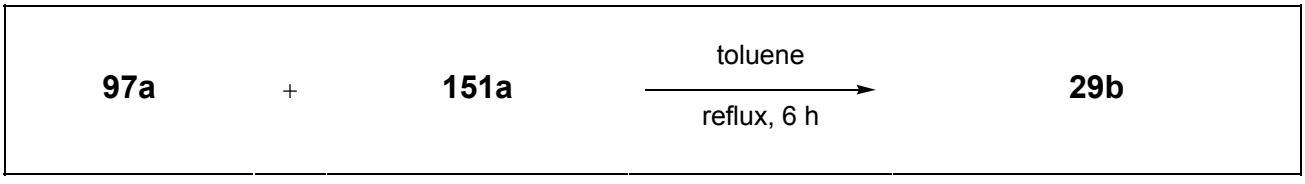

A 100 mL oven-dried round bottom flask equipped with a magnetic stirring bar, a dropping funnel (filled with 4Å MS) and a reflux condenser was charged with (*S*)-*α*,*α*-diphenyl-2-pyrrolidin methanol **97a** (200 mg, 0.79 mmol, 1.00 eq) and 2,4,6-triphenyl-1,3,5-trioxa-2,4,6-triborinane

151a (81 mg, 0.26 mmol, 0.33 eq). 30 mL of abs. toluene was then added and the resulting solution was heated to reflux under positive pressure of argon for 6 hours. The reaction mixture was then cooled to ambient temperature under argon, and the dropping funnel and reflux condenser was quickly replaced by a short-path distillation set-up. The solvent was then distilled off to a small volume under argon atmosphere. The distillation was repeated three times after adding 3 × 5 mL toluene. The residual solution was then cooled to room temperature and the distillation head was quickly replaced by an argon inlet adapter. It was then concentrated in vacuo to obtain a colourless semisolid (263 mg, 99 %). This semisolid was then dissolved in abs. toluene and the solution was used for the catalysis experiments.

8.3.11 Preparation of (*S*)-hexahydro-3,3-bis(3,5-dimethylphenyl)-1-*o*-tolylpyrrolo[1,2-c][1,3,2]oxazaborole 29c[138]

[SMU-VII-32]

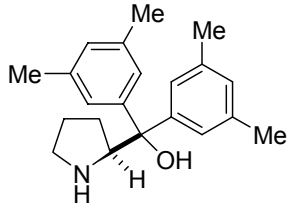

97b

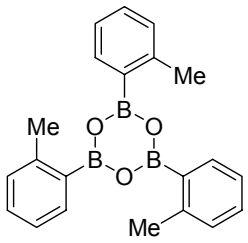

151b

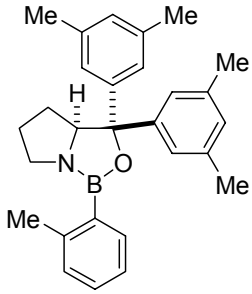

29c

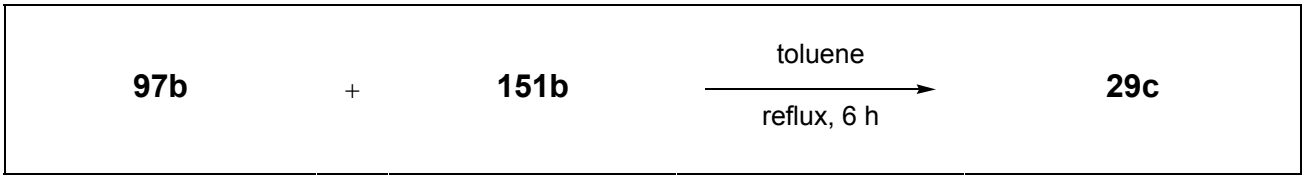

The same procedure as before (see section 8.3.10 on page 212) was followed on a 0.61 mmol scale to obtain a colourless semisolid (249 mg, 99 %). This was dissolved in abs. toluene and the solution was used in the catalysis experiments.

8.4 Asymmetric hydrocyanation of imines

8.4.1 Preparation of *N*-benzylidene-1-phenyl-methanamine 27a[36]

[SMU-I-77]

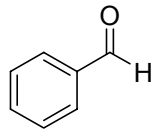

33

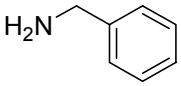

155

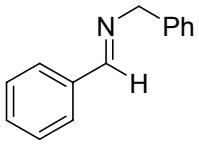

27a

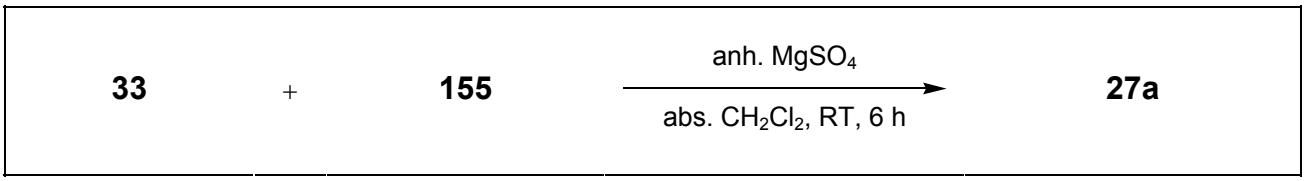

In a 50 mL oven-dried round bottom flask charged with magnetic stirring bar and anh. $MgSO_4$ (3.0 g, 24.9 mmol, 1.26 eq) 10 ml of abs. DCM was added. To this suspension benzaldehyde **33** (2.00 mL, 19.7 mmol, 1.00 eq) was added followed by benzyl amine **155** (2.15 mL, 19.7 mmol, 1.00 eq). The resulting mixture was then stirred at room temperature under argon atmosphere for 6 hours. $MgSO_4$ was filtered off and the solvent was removed in vacuo to obtain a highly viscous oil (3.83 g, 99 %).

27a $C_{14}H_{13}N$ (195.26 g/mol)

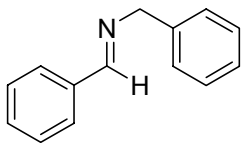

27a

Yield 3.83 g (19.6 mmol, 99 %)

^{1}H-NMR (300 MHz, $CDCl_3$): δ = 4.87 (s; 2H, CH_2), 7.28-7.48 (m; 8H, H_{ar}), 7.82-7.86 (m; 2H, H_{ar}), 8.42 (s; 1H, N=C*H*).

^{13}C-NMR (75 MHz, $CDCl_3$): δ = 64.9 (*C*H_2), 126.9 (C_{ar}), 127.9 (C_{ar}), 128.2 (C_{ar}), 128.4 (C_{ar}), 128.5 (C_{ar}), 130.6 (C_{ar}), 136.1 (Cq_{ar}), 139.2 (Cq_{ar}), 161.8 (N=*C*H).

FT-IR (Film): $\tilde{\nu}$ [cm^{-1}] = 3273 (w), 3085 (w), 3061 (m), 3028 (m), 2871 (m), 2841 (m), 1959 (w), 1813 (w), 1701 (s), 1643 (s), 1600 (m), 1580 (m),

1496 (m), 1452 (s), 1379 (m), 1343 (w), 1311 (w), 1292 (w), 1219 (w), 1204 (w), 1169 (w), 1157 (w), 1073 (w), 1039 (w), 1026 (m), 1002 (w), 960 (w), 916 (w), 858 (w), 827 (w), 753 (s), 734 (s), 697 (s).

HR-EI-MS Exact molecular mass for $[C_{14}H_{13}N]$ ($[M]^+$): 195.1048
Found: 195.105

HPLC τ_R = 8.1 min (Chiralcel OJ, *n*-hexane/*i*-PrOH 90:10, 1.0 mL/min)

8.4.2 Preparation of *N*-benzylidene-1,1-diphenylmethanamine 157[100]

[SMU-I-20]

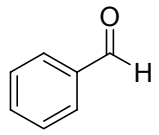

33

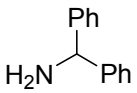

156

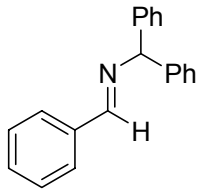

157

The same procedure as before (see section 8.4.1 on page 214) was followed on a 49.2 mmol scale to obtain as a colorless solid (12.3 g, 92 %). This was recrystallized from diethylether to obtain colorless crystals.

157 $C_{20}H_{17}N$ (271.36 g/mol)

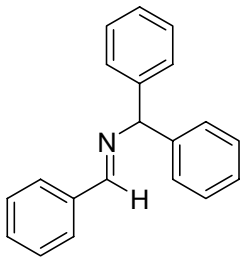

157

Yield 12.28 g (45.3 mmol, 92 %)
[Lit.[100]: 93 %]

Melting Point 100 ºC (Et_2O)
[Lit.[176]: 98-100 ºC (pentane)]

^{1}H-NMR (300 MHz, $CDCl_3$): δ = 5.60 (s; 1H, C*H*Ph_2), 7.20-4.42 (m; 13H, H_{ar}), 7.83-7.86 (m; 2H, H_{ar}), 8.42 (s; 1H, N=C*H*).

^{13}C-NMR (75 MHz, $CDCl_3$): δ = 77.9 (*C*HPh_2), 127.0 (C_{ar}), 127.7 (C_{ar}), 128.42 (C_{ar}), 128.46 (C_{ar}), 128.51 (C_{ar}), 130.8 (C_{ar}), 136.3 (Cq_{ar}), 143.9 (Cq_{ar}), 160.8 (N=*C*H).

FT-IR (CsI): $\tilde{\nu}$ [cm^{-1}] = 3264 (w), 3060 (m), 3032 (m), 3083 (m), 2871 (m), 2851 (m), 1954 (w), 1896 (w), 1880 (w), 1814 (w), 1700 (w), 1685 (w), 1639 (s), 1599 (m), 1579 (m), 1540 (w), 1493 (s), 1457 (s), 1450 (s), 1445 (s), 1380 (s), 1341 (s), 1312 (m), 1285 (s), 1277 (s), 1251 (w), 1217 (s), 1195 (w), 1178 (w), 1160 (w), 1084 (m), 1076 (m), 1034 (s), 1025 (s), 1001 (m), 981 (m), 920 (m), 911 (m), 881 (m), 855 (m), 819 (m), 758 (s), 743 (s), 738 (s), 700 (s).

HPLC τ_R = 5.5 min (Chiralpak AD, *n*-hexane/*i*-PrOH 90:10, 1.0 mL/min)

8.4.3 Preparation of *N*-benzylidene-prop-2-en-1-amine 159[177]

[SMU-IV-15]

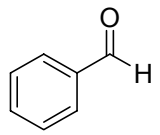

33

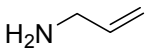

158

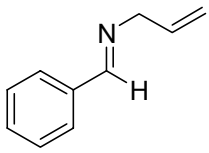

159

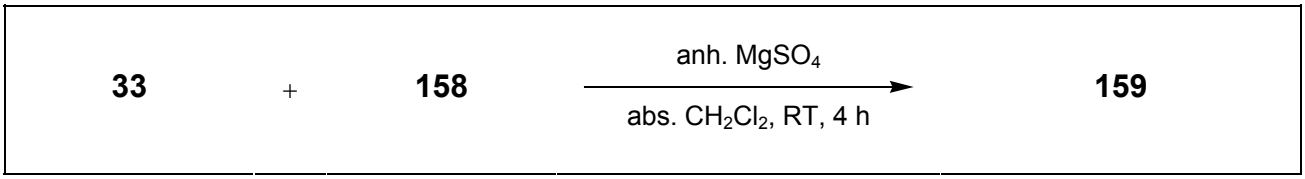

The same procedure as before (see section 8.4.1 on page 214) was followed on a 29.5 mmol scale. The product was obtained as a pale yellow oil (3.90 g, 91 %).

159 $C_{10}H_{11}N$ (145.20 g/mol)

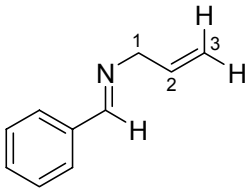

159

Yield 3.90 g (26.86 mmol, 91 %)

^{1}H-NMR (300 MHz, $CDCl_3$): δ = 4.23-4.26 (m; 2H, *H*-1), 5.13-5.14 (m; 0.5 H, *H*-1), 5.16-5.18 (m; 0.5 H, *H*-1), 5.20-5.22 (m; 0.5 H, *H*-1), 5.26-5.27 (m; 0.5 H, *H*-1), 6.00-6.13 (m; 1H, *H*-2), 7.38-7.42 (m; 3 H, H_{ar}), 7.72-7.77 (m; 2H, H_{ar}), 8.26 (s; 1H, N=C*H*).

^{13}C-NMR (75 MHz, $CDCl_3$): δ = 63.4 (*C*-1), 115.9 (*C*-3), 128.0 (C_{ar}), 128.4 (C_{ar}), 130.5 (C_{ar}), 135.8 (*C*-2), 136.0 (Cq_{ar}), 168.8 (*C*=N).

FT-IR (Film): $\tilde{\nu}$ [cm^{-1}] = 3062 (w), 3026 (w), 2981 (w), 2874 (w), 2842 (m), 2360 (m), 2342 (w), 1960 (w), 1648 (s), 1580 (m), 1490 (w), 1451 (m), 1375 (w), 1308 (m), 1219 (w), 1025 (m), 993 (m), 920 (s), 846 (w), 755 (s), 694 (s).

HPLC τ_R = 4.5 min (Chiralcel OJ, *n*-hexane/*i*-PrOH 90:10, 1.0 mL/min)

8.4.4 Preparation of *N*-(2-bromobenzylidene)(phenyl)methanamine 27b

[SMU-III-27]

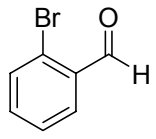

160

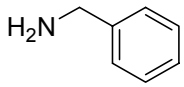

155

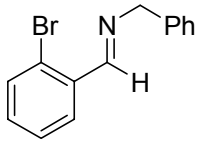

27b

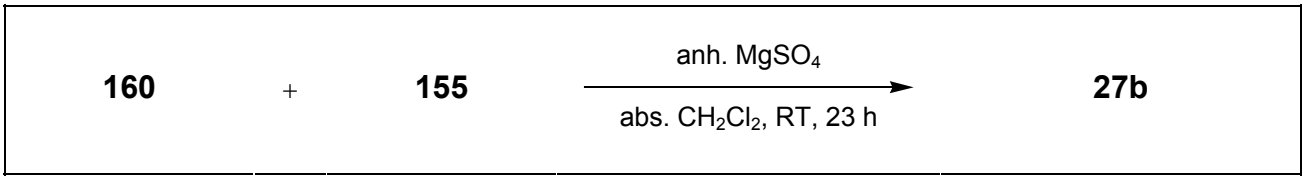

The same procedure as before (see section 8.4.1 on page 214) was followed on a 17.1 mmol scale to obtain a highly viscous oil (4.67 g, >99 %).

27b	$C_{14}H_{12}BrN$ (274.16 g/mol)
Yield	4.67 g (17.0 mmol, >99 %)
^{1}H-NMR	(300 MHz, $CDCl_3$): δ = 4.75 (s; 2H, CH_2), 7.11-7.25 (m; 7H, H_{ar}), 7.45 (d, J = 8.1 Hz; 1H, H_{ar}), 7.98 (dd, J = 1.8, 7.7 Hz; 1H, H_{ar}), 8.67 (s; 1H, N=CH).
^{13}C-NMR	(75 MHz, $CDCl_3$): δ = 65.1 (CH_2), 125.0 (Cq_{ar}), 127.0 (CH_{ar}), 127.5 (CH_{ar}), 127.9 (CH_{ar}), 128.5 (CH_{ar}), 128.9 (CH_{ar}), 131.8 (CH_{ar}), 132.9 (CH_{ar}), 134.4 (Cq_{ar}), 138.9 (Cq_{ar}), 160.9 (N=CH).
FT-IR	(Film): $\tilde{\nu}$ [cm^{-1}] = 3085 (w), 3062 (s), 3028 (s), 2888 (s), 2833 (m), 2360 (w), 2341 (w), 1945 (w), 1697 (s), 1635 (s), 1601 (w), 1588 (s), 1563 (s), 1495 (s), 1465 (s), 1439 (s), 1373 (s), 1341 (m), 1272 (s), 1213 (w), 1044 (m), 1028 (s), 959 (w), 754 (s), 734 (s), 697 (s), 682 (m).
HR-EI-MS	Exact molecular mass for [$C_{14}H_{12}BrN$] ([M]$^+$): 273.0153 Found: 273.015
HPLC	τ_R = 14.1 min (Chiralcel OJ, *n*-hexane/*i*-PrOH 90:10, 0.5 mL/min)

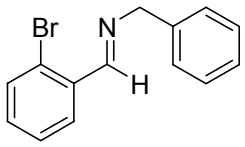

27b

8.4.5 Preparation of *N*-(3-bromobenzylidene)(phenyl)methanamine 27c

[SMU-VII-34]

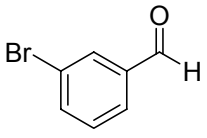

161

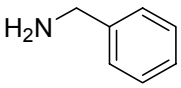

155

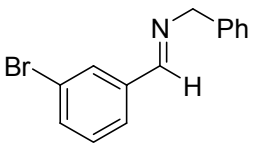

27c

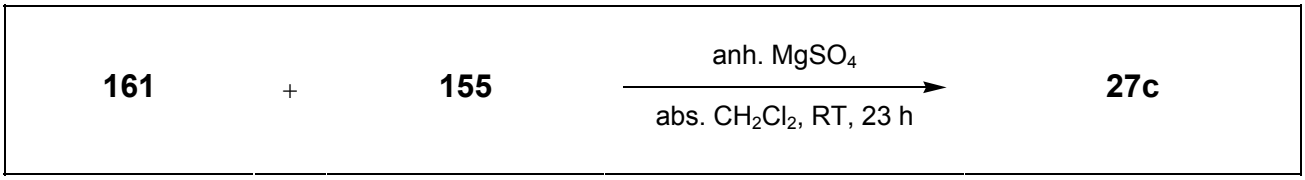

The same procedure as before (see section 8.4.1 on page 214) was followed on an 8.58 mmol scale to obtain a clear oil (2.35 g, >99 %) which became yellowish white crystalline solid on standing in the refrigerator.

27c $C_{14}H_{12}BrN$ (274.16 g/mol)

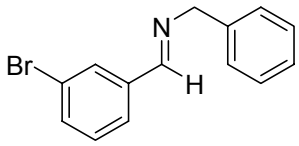

27c

Yield 2.35 g (8.57 mmol, >99 %)

^{1}H-NMR (300 MHz, $CDCl_3$): δ = 4.79 (s; 2H, CH_2), 7.21-7.64 (m; 6H, H_{ar}), 7.51 (d, J = 7.93 Hz; 1H, H_{ar}), 7.63 (d, J = 7.55 Hz; 1H, H_{ar}), 7.94 (s; 1H, H_{ar}), 8.28 (s; 1H, N=CH).

^{13}C-NMR (75 MHz, $CDCl_3$): δ = 64.9 (CH$_2$), 122.9 (Cq$_{ar}$), 127.0 (C_{ar}), 127.1 (C_{ar}), 128.0 (C_{ar}), 128.5 (C_{ar}), 130.1 (C_{ar}), 130.8 (C_{ar}), 133.6 (C_{ar}), 138.1 (Cq$_{ar}$), 138.9 (Cq$_{ar}$), 160.2 (N=CH).

FT-IR (ATR): $\tilde{\nu}$ [cm^{-1}] = 3060 (sh), 3025 (sh), 2836 (m), 1643 (s), 1563 (s), 1494 (sh), 1467 (m), 1451 (sh), 1424 (m), 1371 (m), 1340 (m), 1279 (w), 1262 (w), 1210 (m), 1092 (w), 1064 (sh), 1027 (w), 995 (sh), 956 (w), 896 (w), 781 (s), 733 (s), 697 (s), 682 (s).

HR-EI-MS Exact molecular mass for [$C_{14}H_{12}BrN$] ([M]$^+$): 273.0153
Found: 273.015

HPLC τ_R = 8.9 min (Chiralcel OJ, *n*-hexane/*i*-PrOH 95:5, 1.0 mL/min)

8.4.6 Preparation of *N*-{(naphthalene-3-yl)methylene}(phenyl)methanamine 27d[153]

[SMU-III-13]

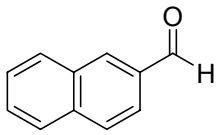

162

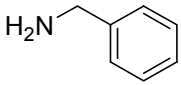

155

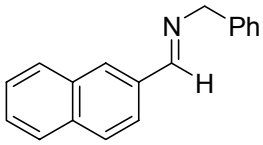

27d

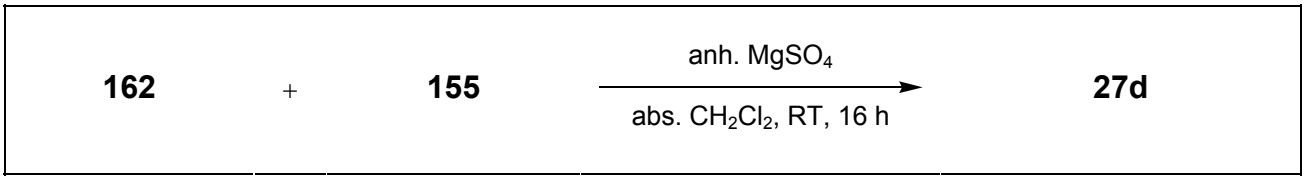

The same procedure as before (see section 8.4.1 on page 214) was followed on a 6.40 mmol scale to obtain a pale yellow solid (1.56 g, >99 %).

27d $C_{18}H_{15}N$ (245.32 g/mol)

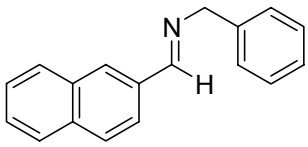

27d

Yield 1.56 g (6.36 mmol, >99 %)

^{1}H-NMR (300 MHz, $CDCl_3$): δ = 4.74 (s; 2H, CH_2), 7.09-7.46 (m; 7H, H_{ar}), 7.69-7.76 (m; 3H, H_{ar}), 7.89-7.93 (m; 2H, H_{ar}), 8.39 (s; 1H, N=CH).

^{13}C-NMR (75 MHz, $CDCl_3$): δ = 65.1 (CH_2), 123.9 (C_{ar}), 126.4 (C_{ar}), 126.9 (C_{ar}), 127.1 (C_{ar}), 127.8 (C_{ar}), 128.0 (C_{ar}), 128.4 (C_{ar}), 128.5 (C_{ar}), 128.6 (C_{ar}), 130.1 (C_{ar}), 133.0 (Cq_{ar}), 133.8 (Cq_{ar}), 134.7 (Cq_{ar}), 139.2 (Cq_{ar}), 162.0 (N=CH).

FT-IR (CsI): $\tilde{\nu}$ [cm^{-1}] = 3055 (m), 3030 (w), 2866 (m), 2360 (m), 2355 (w), 1638 (s), 1604 (s), 1496 (m), 1453 (m), 1422 (w), 1350 (m), 1297 (w), 1174 (w), 1122 (w), 1047 (m), 992 (w), 956 (m), 903 (m), 867 (s), 833 (s), 751 (s), 731 (s), 697 (s).

HR-EI-MS Exact molecular mass for $[C_{18}H_{15}N]$ ($[M]^+$): 245.1204
Found: 245.120

HPLC τ_R = 14.2 min (Chiralcel OJ, *n*-hexane/*i*-PrOH 80:20, 1.0 mL/min)

8.4.7 Preparation of *N*-(4-methoxybenzylidene)(phenyl)methanamine 27e

[SMU-VII-30]

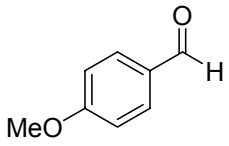

163

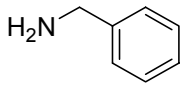

155

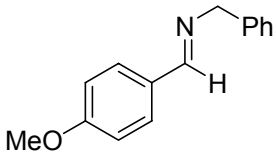

27e

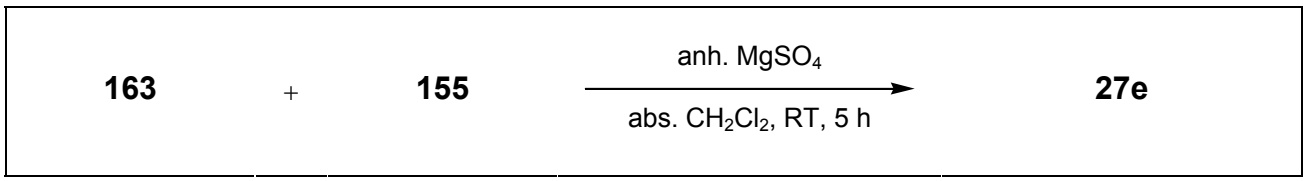

The same procedure as before (see section 8.4.1 on page 214) was followed on an 8.23 mmol scale to obtain a highly viscous oil (1.85 g, >99 %).

27e $C_{15}H_{15}NO$ (225.29 g/mol)

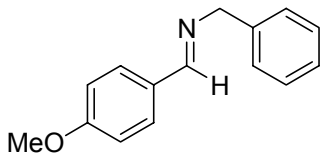

27e

Yield 1.85 g (8.22 mmol, >99 %)

^{1}H-NMR (300 MHz, $CDCl_3$): δ = 3.83 (s; 3H, OC*H*$_3$), 4.80 (s; 2H, C*H*$_2$), 6.94 (d, *J* = 8.80 Hz; 2H, *H*$_{ar}$), 7.24-7.37 (m; 5H, *H*$_{ar}$), 7.75 (d, *J* = 8.80 Hz; 2H, *H*$_{ar}$), 8.33 (s; 1H, N=C*H*).

^{13}C-NMR (75 MHz, $CDCl_3$): δ = 55.2 (O*C*H$_3$), 64.9 (*C*H$_2$), 113.9 (*C*$_{ar}$), 126.8 (*C*$_{ar}$), 127.9 (*C*$_{ar}$), 128.4 (*C*$_{ar}$), 129.1 (*C*q$_{ar}$), 129.8 (*C*$_{ar}$), 139.5 (*C*q$_{ar}$), 161.2 (N=*C*H), 161.6 (*C*q$_{ar}$).

FT-IR (ATR): $\tilde{\nu}$ [cm^{-1}] = 3060 (w), 3026 (w), 2834 (m), 1645 (s), 1604 (s), 1576 (sh), 1510 (s), 1494 (sh), 1451 (sh), 1440 (w), 1420 (sh), 1377 (w), 1341 (w), 1305 (s), 1249 (s), 1178 (w), 1164 (sh), 1106 (w), 1078 (w), 1028 (s), 962 (w), 905 (w), 866 (w), 832 (s), 733 (s), 697 (s).

HR-EI-MS Exact molecular mass for [$C_{15}H_{15}NO$] ([$M]^+$): 225.1154
Found: 225.115

HPLC τ_R = 22.6 min (Chiralcel OJ, *n*-hexane/*i*-PrOH 97:3, 1.0 mL/min)

8.4.8 Preparation of *N*-(2,2-dimethylpropylidene)(phenyl)methanamine 27f[37]

[SMU-VII-10]

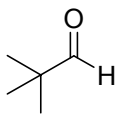

164

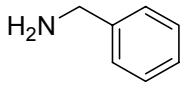

155

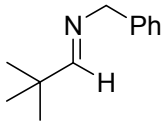

27f

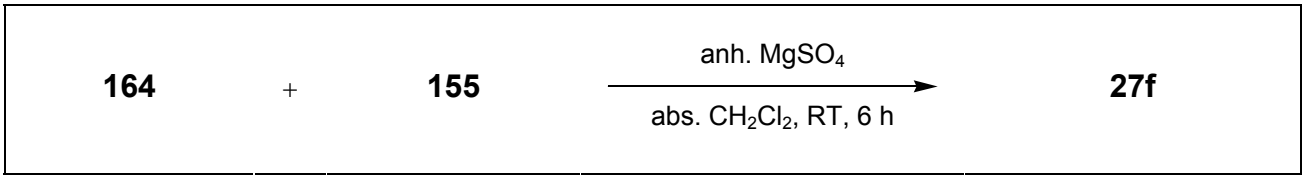

The same procedure as before (see section 8.4.1 on page 214) was followed on a 13.6 mmol scale to obtain a clear oil (2.38 g, >99 %).

27f $C_{12}H_{17}N$ (175.27 g/mol)

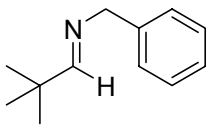

27f

Yield 2.38 g (13.6 mmol, >99 %)

^{1}H-NMR (300 MHz, $CDCl_3$): δ = 1.15 (s; 9H, C*H*$_3$), 4.61 (s; 2H, C*H*$_2$), 7.23-7.39 (m; 5H, *H*$_{ar}$), 7.70 (s; 1H, N=C*H*).

^{13}C-NMR (75 MHz, $CDCl_3$): δ = 26.9 (*C*H_3), 36.2 (*C*me_3), 64.5 (*C*H_2), 126.7 (C_{ar}), 127.5 (C_{ar}), 128.3 (C_{ar}), 139.6 (*C*q_{ar}), 173.3 (N=*C*H).

FT-IR (ATR): $\tilde{\nu}$ [cm^{-1}] = 3061 (w), 3026 (w), 2958 (s), 1898 (w), 2865 (m), 2813 (m), 1665 (s), 1603 (w), 1495 (sh), 1474 (m), 1451 (sh), 1393 (w), 1363 (s), 1340 (w), 1297 (w), 1204 (w), 1051 (m), 1029 (sh), 914 (w), 818 (w), 776 (w), 731 (s), 696 (s).

HR-EI-MS Exact molecular mass for [$C_{12}H_{17}N$] ([$M]^+$): 175.1361
Found: 175.136

GC τ_R = 2.0 min (Chiraldex γ-TA, Isothermal 120 °C, 1.0 mL/min)

8.4.9 General procedure for the preparation of racemic *α*-amino nitriles

To an ice-cold solution of the imine (1.00 eq) in DCM was added TMSCN (2.00 eq), followed by methanol (2.00 eq), and the resulting mixture was stirred at 0 °C for 1 hour and then at room temperature. After the imine was consumed completely (the reaction was monitored by HPLC), the reaction mixture was concentrated in vacuo to obtain the pure *α*-amino nitrile.

Analytical data of the racemic *α*-amino nitriles are given below.

8.4.9.1 2-(Benzylamino)-2-phenylacetonitrile *rac*-28a

[SMU-I-91]

rac-**28a** $C_{15}H_{14}N_2$ (222.29 g/mol)

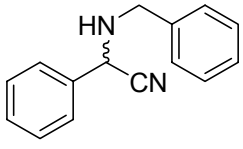

rac-**28a**

^{1}H-NMR (300 MHz, $CDCl_3$): δ = 1.89 (s; 1H, N*H*), 3.95 (d, *J* = 13.1 Hz; 2H, CH_2), 4.06 (d, *J* = 13.1 Hz; 2H, CH_2), 4.74 (s; 1H, C*H*CN), 7.27-7.45 (m; 8H, H_{ar}), 7.52-7.56 (m; 2H, H_{ar}).

^{13}C-NMR (75 MHz, $CDCl_3$): δ = 51.1 (*C*HCN), 53.3 (*C*H_2), 118.7 (*C*N), 127.2 (C_{ar}),

127.5 (C_{ar}), 128.3 (C_{ar}), 128.5 (C_{ar}), 128.8 (C_{ar}), 128.9 (C_{ar}), 134.7 (Cq_{ar}), 138.0 (Cq_{ar}).

HPLC τ_R = 16.8 min [(*R*)-**28a**], 20.4 min [(*S*)-**28a**] (Chiralcel OJ, *n*-hexane/*i*-PrOH 90:10, 1.0 mL/min)

8.4.9.2 2-(Benzhydrylamino)-2-phenylacetonitrile *rac*-169

[SMU-I-30]

rac-**169** $C_{21}H_{18}N_2$ (298.38 g/mol)

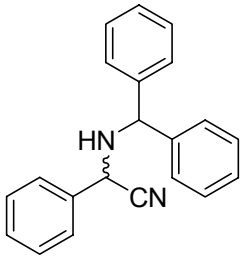

rac-**169**

^{1}H-NMR (300 MHz, $CDCl_3$): δ = 2.08 (s; 1H, N*H*), 4.54 (s; 1H, C*H*Ph_2), 5.18 (s; 1H, C*H*CN), 7.14-7.51 (m; 15 H, H_{ar}).

^{13}C-NMR (75 MHz, $CDCl_3$): δ = 52.4 (*C*HPh_2), 65.6 (*C*HCN), 118.7 (*C*N), 127.1 (C_{ar}), 127.2 (C_{ar}), 127.4 (C_{ar}), 127.7 (C_{ar}), 127.9 (C_{ar}), 128.8 (C_{ar}), 129.0 (C_{ar}), 134.9 (Cq_{ar}), 141.0 (Cq_{ar}), 142.7 (Cq_{ar}).

FT-IR (CsI): $\tilde{\nu}$ [cm^{-1}] = 3304 (s), 3083 (m), 3061 (m), 3038 (m), 3022 (m), 2847 (m), 2229 (m), 1596 (m), 1494 (s), 1472 (m), 1456 (s), 1354 (m), 1343 (w), 1311 (m), 1269 (m), 1199 (m), 1188 (w), 1158 (w), 1098 (s), 1079 (m), 1029 (m), 918 (s), 910 (m), 887 (w), 836 (w), 771 (s), 745 (s), 699 (s).

HPLC τ_R = 10.6 min [(*R*)-**169**], 19.5 min [(*S*)-**169**] (Chiralpak AD, *n*-hexane/*i*-PrOH 90:10, 1.00 mL/min)

8.4.9.3 2-(Allylamino)-2-phenylacetonitrile *rac*-170

[SMU-IV-16]

rac-**170** $C_{11}H_{12}N_2$ (172.23 g/mol)

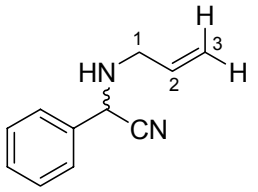

rac-**170**

^{1}H-NMR (300 MHz, $CDCl_3$): δ = 1.70 (N*H*), 3.36-3.53 (m; 2H, *H*-1), 4.78 (s; 1H, C*H*CN), 5.16-5.18 (m; 0.5 H, *H*-3), 5.20-5.21 (m; 0.5 H, *H*-3), 5.27-5.29 (m; 0.5 H, *H*-3), 5.33-5.34 (m; 0.5 H, *H*-3), 5.82-5.95 (m; 1H, *H*-2), 7.33-7.42 (m; 3H, H_{ar}), 7.49-7.53 (m; 2H, H_{ar}).

^{13}C-NMR (75 MHz, $CDCl_3$): δ = 49.8 (*C*-1), 53.4 (*C*HCN), 117.7 (*C*-3), 118.7 (*C*N), 127.2 (C_{ar}), 128.8 (C_{ar}), 128.9 (C_{ar}), 134.7 (*C*-2).

FT-IR (Film): $\tilde{\nu}$ [cm^{-1}] = 3322 (m), 3066 (m), 2840 (m), 2227 (w), 1644 (s), 1601 (w), 1494 (s), 1453 (s), 1419 (m), 1305 (w), 1191 (w), 1104 (s), 1028 (m), 994 (s), 925 (s), 832 (w), 754 (s), 698 (s).

HPLC τ_R = 9.3 min [(*R*)-**170**], 11.4 min [(*S*)-**170**] (Chiralcel OJ, *n*-hexane/*i*-PrOH 90:10, 1.0 mL/min)

8.4.9.4 2-(Benzylamino)-2-(2-bromophenyl)acetonitrile *rac*-28b

[SMU-III-30]

rac-**28b** $C_{15}H_{13}BrN_2$ (301.18 g/mol)

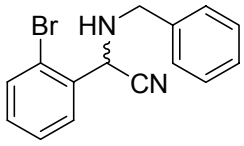

rac-**28b**

^{1}H-NMR (300 MHz, $CDCl_3$): δ = 1.89 (br s; 1H, N*H*), 3.81 (d, *J* = 12.7 Hz; 2H, CH_2), 3.92 (d, *J* = 12.7 Hz; 2H, CH_2), 4.89 (s; 1H, C*H*CN), 7.07-7.27 (m;

7H, H_{ar}), 7.46 (dd, J = 1.3, 7.9 Hz; 1H, H_{ar}), 7.51 (dd, J = 1.7, 7.8 Hz; 1H, H_{ar}).

^{13}C-NMR (75 MHz, $CDCl_3$): δ = 51.7 (CH_2), 53.5 (CHNH), 118.23 (CN), 123.4 (Cq_{ar}), 127.7 (C_{ar}), 128.1 (C_{ar}), 128.5 (C_{ar}), 128.6 (C_{ar}), 129.2 (C_{ar}), 130.7 (C_{ar}), 133.6 (C_{ar}), 134.2 (Cq_{ar}), 137.7 (Cq_{ar}).

HPLC τ_R = 37.0 min [(*R*)-**28b**], 42.8 min [(*S*)-**28b**] (Chiralcel OJ, *n*-hexane/*i*-PrOH 90:10, 0.5 mL/min)

8.4.9.5 2-(Benzylamino)-2-(3-bromophenyl)acetonitrile *rac*-28c

[SMU-VII-35]

rac-**28c** $C_{15}H_{13}BrN_2$ (301.18 g/mol)

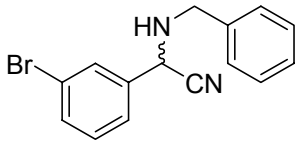

rac-**28c**

^{1}H-NMR (300 MHz, $CDCl_3$): δ = 1.92 (s; 1H, NH), 3.90 (d, J = 12.93 Hz; 1H, CH_2), 4.02 (d, J = 12.93 Hz; 1H, CH_2), 4.69 (s; 1H, CHCN), 7.12-7.38 (m; 6H, H_{ar}), 7.44-7.54 (m; 2H, H_{ar}), 7.67 (s; 1H, H_{ar}).

^{13}C-NMR (75 MHz, $CDCl_3$): δ = 51.2 (CH_2), 52.7 (CHCN), 118.1 (CN), 122.9 (Cq_{ar}), 125.9 (C_{ar}), 127.7 (C_{ar}), 128.4 (C_{ar}), 128.7 (C_{ar}), 130.35 (C_{ar}), 130.4 (C_{ar}), 132.2 (C_{ar}), 136.9 (Cq_{ar}), 137.7 (Cq_{ar}).

FT-IR (ATR): $\tilde{\nu}$ [cm^{-1}] = 3321 (br), 3061 (w), 3027 (w), 2845 (w), 2226 (w), 1594 (m), 1570 (s), 1494 (m), 1472 (s), 1452 (s), 1422 (m), 1362 (w), 1299 (w), 1260 (w), 1185 (s), 1106 (w), 1072 (s), 1027 (w), 997 (w), 967 (w), 928 (w), 885 (w), 858 (w), 781 (s), 738 (s), 698 (s).

HPLC τ_R = 23.7 min [(*S*)-**28c**], 28.8 min [(*R*)-**28c**] (Chiralcel OJ, *n*-hexane/*i*-PrOH 95:5, 1.0 mL/min)

8.4.9.6 2-(Benzylamino)-2-(naphthalene-2-yl)acetonitrile *rac*-28d

[SMU-III-26]

rac-**28d** $C_{19}H_{16}N_2$ (272.34 g/mol)

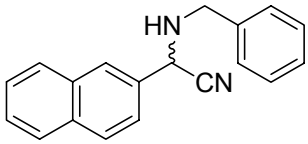

rac-**28d**

^{1}H-NMR (300 MHz, $CDCl_3$): δ = 1.93 (br s; 1H, N*H*), 3.99 (d, *J* = 13.3 Hz; 2H, CH_2), 4.08 (d, *J* = 13.3 Hz; 2H, CH_2), 4.9 (s; 1H, C*H*CN), 7.28-7.44 (m; 5H, H_{ar}), 7.50-7.61 (m; 3H, H_{ar}), 7.83-7.89 (m; 3H, H_{ar}), 8.03 (s; 1H, H_{ar}).

^{13}C-NMR (75 MHz, $CDCl_3$): δ = 51.2 (*C*H_2), 55.5 (*C*HNH), 118.7 (*C*N), 124.7 (C_{ar}), 126.4 (C_{ar}), 126.7 (C_{ar}), 126,8 (C_{ar}), 127.6 (C_{ar}), 127.7 (C_{ar}), 128.1 (C_{ar}), 128.4 (C_{ar}), 128.6 (C_{ar}), 128.9 (C_{ar}), 131.9 (Cq_{ar}), 132.9 (Cq_{ar}), 133.3 (Cq_{ar}), 138.0 (Cq_{ar}).

HPLC τ_R = 31.4 min [(*R*)-**28d**], 38.0 min [(*S*)-**28d**] (Chiralcel OJ, *n*-hexane/*i*-PrOH 80:20, 1.0 mL/min).

8.4.9.7 2-(Benzylamino)-2-(4-methoxyphenyl)acetonitrile *rac*-28e

[SMU-VII-79]

rac-**28e** $C_{16}H_{16}N_2O$ (252.31 g/mol)

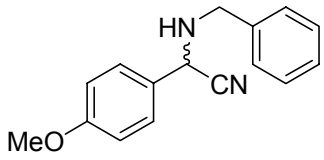

rac-**28e**

^{1}H-NMR (300 MHz, $CDCl_3$): δ = 1.77 (s; 1H, N*H*), 3.73 (s; 2H, OCH_3), 3.85 (d, *J* = 12.94 Hz; 1H, PhCH_2), 3.96 (d, *J* = 12.94 Hz; 1H, PhCH_2), 4.61 (s; 1H, C*H*CN), 6.81-6.86 (m; 2H, H_{ar}), 7.17-7.39 (m; 7H, H_{ar}).

^{13}C-NMR (75 MHz, $CDCl_3$): δ = 51.1 (*C*H_2), 52.8 (*C*HCN), 55.3 (OCH_3), 114.2 (*C*ar), 118.9 (*C*N), 126.8 (Cq_{ar}), 127.5 (C_{ar}), 128.3 (C_{ar}), 128.5 (C_{ar}), 128.6 (C_{ar}), 138.2 (Cq_{ar}), 160.0 (Cq_{ar}).

FT-IR (ATR): $\tilde{\nu}$ [cm^{-1}] = 3324 (br), 3061 (w), 3027 (w), 3001 (w), 2931 (w), 2836 (m), 2224 (w), 1719 (w), 1609 (s), 1584 (m), 1510 (s), 1495 (w), 1453 (s), 1419 (w), 1361 (w), 1305 (m), 1249 (s), 1176 (sh s), 1112 (m), 1075 (w), 1029 (s), 965 (w), 918 (w), 859 (w), 829 (s), 776 (w), 740 (s), 698 (s).

HPLC τ_R = 56.1 min [(*R*)-**28e**], 62.2 min [(*S*)-**28e**] (Chiralcel OJ, *n*-hexane/*i*-PrOH 97:3, 1.0 mL/min)

8.4.9.8 2-(Benzylamino)-3,3-dimethyl-butyronitrile *rac*-28f

[SMU-VII-18]

rac-**28f** $C_{13}H_{18}N_2$ (202.3 g/mol)

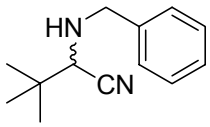

rac-**28f**

^{1}H-NMR (300 MHz, $CDCl_3$): δ = 1.06 (s; 9H, CH_3), 1.51 (br s; 1H, N*H*), 3.09 (s; 1H, C*H*CN), 3.80 (d, *J* = 13.2 Hz; 1H, CH_2), 4.13 (d, *J* = 13.2 Hz; 1H, CH_2), 7.24-7.38 (m; 5H, H_{ar}).

^{13}C-NMR (75 MHz, $CDCl_3$): δ = 26.2 (*C*H_3), 34.2 (*C*me$_3$), 52.1 (*C*H_2), 60.3 (*C*HCN), 119.6 (*C*N), 127.4 (C_{ar}), 128.3 (C_{ar}), 128.4 (C_{ar}), 138.5 (Cq_{ar}).

FT-IR (ATR): $\tilde{\nu}$ [cm^{-1}] = 3342 (br), 3026 (w), 2961 (s), 2871 (w), 2222 (w), 1603 (w), 1495 (w), 1474 (s), 1453 (s), 1397 (m), 1369 (s), 1296 (w), 1204 (w), 1119 (s), 1028 (sh), 931 (w), 880 (w), 738 (s), 698 (s).

GC After derivatization with TFAA
τ_R = 16.1 min [(*S*)-**28f**], 17.3 min [(*R*)-**28f**]
(Chiraldex γ-TA, Isothermal 120 °C, 1.0 mL/min)

8.4.10 General procedure for the asymmetric hydrocyanation of imines

Condition A: In a flame-dried *Schlenk* flask, a solution of the imine (0.51 mmol) in 1.25 mL of abs. toluene was cooled to –25 °C under positive argon pressure. To this cold solution was added 100 µL of a 1M solution of catalyst in toluene (102 µmol, 0.2 equiv.) and stirred for 5 mins. at -25 °C. In a separate flask, 1 mL abs. toluene along with 96.0 µL TMSCN (765 µmol, 1.5 equiv.) was cooled to 0 °C under argon, and 31 µL methanol (765 µmol, 1.5 equiv.) was added. This solution was stirred at 0 °C for 1 hour. and added in one portion to the reaction flask by means of a syringe. The resulting mixture was stirred at –25 °C under argon. After 24 hours, a 100 µL of sample was withdrawn, diluted with 900 µL DCM and conversion and enantiomeric excess were determined immediately by HPLC or GC using a chiral column.

Condition B: In a flame-dried Schlenk flask, a mixture of 50.0 µL of a 1M solution of catalyst in toluene (51.0 µmol, 0.1 equiv.) and 300 µL abs. toluene was cooled to –70 °C under positive pressure of argon. To this cold solution was then added a 0.2 M solution of triflic acid in toluene (250 µL, 51 µmol, 0.1 equiv.) and stirred for 5 mins. A solution of the imine (510 µmol) in 750 µL abs. toluene was added and stirred for another 5 mins. An HCN solution (765 µmol, 1.5 equiv.) in 1 mL toluene was then added by slow syringe addition of over a period of 40 mins. The resulting mixture was then stirred at –70 °C under argon. After 1, 2 or 3 hours, the reaction mixture was analyzed in the same way as described for condition A.

8.4.11 Crystallographic data for 29b·HCN

[SMU-II-52]

29b·HCN $C_{24}H_{23}BN_2O$ (366.26 g/mol)

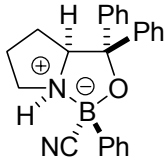

29b·HCN

Crystallographic Data	For X-ray structure see Figure 5.11 on page 84	
	Colorless needles from dichloromethane	
	Empirical formula:	$C_{24}H_{23}N_2O$
	Formula weight (M):	366.26 g/mol

Temperature (T):	293(2) K
Wavelength (λ):	0.71073 Å
Crystal system:	monoclinic
Space group:	$P2_1$
Unit cell dimension:	a = 10.588(1) Å $\alpha = 90°$
	b = 6.950(1) Å $\beta = 105.07(1)°$
	c = 14.249(2) Å $\gamma = 90°$
Unit cell volume:	1012.5(2) $Å^3$
Z:	2
Calculated density ($\rho_{calcd.}$):	1.201 g/cm^3
Absorption coefficient (μ):	0.073 mm^{-1}
F(000):	388
Crystal size:	0.18 × 0.12 × 0.08 mm
Θ-range for data collection:	1.48° to 29.91°
Limiting indices:	$-13 \leq h \leq 10$
	$-8 \leq k \leq 8$
	$-15 \leq l \leq 17$
Reflections collected:	5378
Unique reflections:	3974 [$R_{int} = 0.0612$]
Reflections observed [I>2σ (I)]:	1327
Completeness to Θ:	95.0 %
Refinement method:	Full-matrix least-squares on F^2
Data / restraints / parameters:	3974 / 1 / 259
Goodness-of-fit on F^2:	0.890
Final *R*-indices [$I > 2\sigma(I)$]:	$R1 = 0.0674$ $\omega R2 = 0.0890$
R-indices (all data):	$R1 = 0.2718$ $\omega R2 = 0.1291$
Largest diff. peak and hole:	0.136 and -0.162 $e \cdot Å^{-3}$

8.5 Synthesis of new tridentate ligands

8.5.1 Preparation of 2,4-di-*tert*-butyl-6-{(*S*)-2-(hydroxydiphenylmethyl) pyrrolidin-1-yl-methyl}phenol 31a

[SMU-IV-52]

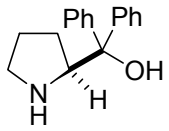

97a

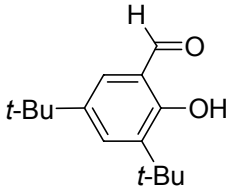

100a

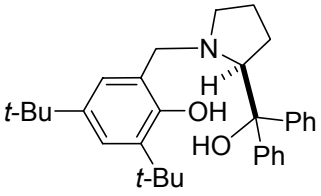

31a

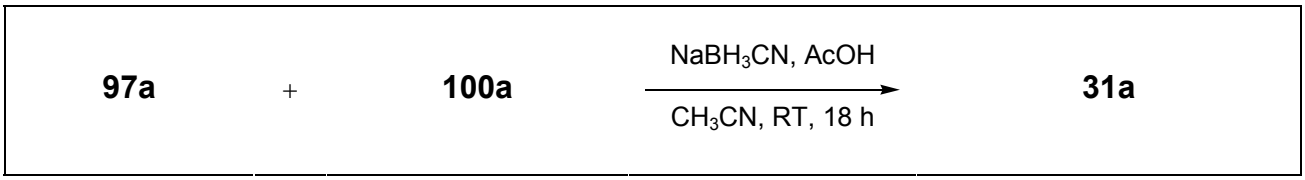

A mixture of (*S*)-*α*,*α*-diphenyl-2-pyrrolidin methanol **97a** (500 mg, 1.97 mmol, 1.02 eq) and 2,4-di-*tert*-butyl-salicylaldehyde **100a** (452 mg, 1.93 mmol, 1.00 eq) in absolute CH_3CN (22 mL) was stirred at room temperature for 1.5 hours. $NaBH_3CN$ (364 mg, 5.79 mmol, 3.00 eq) was then added followed 15 minutes later by acetic acid (580 mg, 9.65 mmol, 5.00 eq). The resulting mixture was stirred at room temperature under argon for 18 hours. The reaction mixture was then diluted with DCM (25 mL) and washed with 1N NaOH solution (20 mL). The aqueous layer was extracted with DCM (25 mL). The combined organic layer was washed with saturated NaCl solution (20 mL), dried over anh. $MgSO_4$ and the solvent was removed in vacuo to obtain a yellowish white foam. Recrystallization from ethanol afforded a colorless crystalline solid (422 mg, 46 %).

31a	$C_{32}H_{41}NO_2$ (471.67 g/mol)
Yield	422 mg (0.89 mmol, 46 %)
Melting Point	161-162 °C (EtOH)
TLC	R_f = 0.49 (Silicagel, *n*-hexane/EtOAc 11:1)

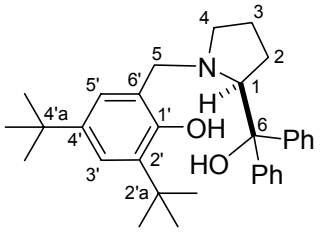

31a

^{1}H-NMR (300 MHz, $CDCl_3$): δ = 1.24 (s; 9H, 4′a-CH_3), 1.38 (s; 9H, 2′a-CH_3), 1.59-1.77 (m; 2H, *H*-3), 1.83-1.93(m; 1H, *H*-2), 2.00-2.14 (m; 1H, *H*-2), 2.38-2.46 (m; 1H, *H*-4), 2.85-2.92 (m; 1H, *H*-4), 3.26 (d, *J* = 12.93 Hz; 1H, *H*-5), 3.53 (d, *J* = 12.93 Hz; 1H, *H*-5), 3.95-3.99 (2d, *J* = 4.85 Hz; 1H, *H*-6), 6.68 (d, *J* = 2.28 Hz; 1H, *H*-5′), 7.08-7.12 (m; 1H, H_{ar}), 7.14 (d, *J* = 2.28 Hz; 1H, *H*-3′), 7.17-7.34 (m; 5H, H_{ar}), 7.54-7.63 (m; 4H, H_{ar}).

^{13}C-NMR (75 MHz, $CDCl_3$): δ = 24.2 (*C*-3), 29.4 (*C*-2), 29.5 (C-2′a-*C*H_3), 31.65 (C-4′a-*C*H_3), 34.0 (*C*-4′a), 34.8 (*C*-2′a), 55.2 (*C*-4), 61.8 (*C*-5), 72.7 (*C*-1), 79.7 (*C*-6), 122.1 (*C*-6′), 122.7 (*C*-3′), 123.2 (*C*-5′), 125.75 (C_{ar}), 125.9 (C_{ar}), 126.7 (C_{ar}), 126.9 (C_{ar}), 128.2 (C_{ar}), 128.4 (C_{ar}), 134.9 (*C*-2′), 140.1 (*C*-4′), 145.8 (Cq_{ar}), 146.0 (Cq_{ar}), 153.4 (*C*-1′).
The assignments were made by 2D-NMR.

FT-IR (ATR): $\tilde{\nu}$ [cm^{-1}] = 3544 (br w), 2951 (s), 2867 (w), 1598 (m), 1478 (sh s), 1446 (sh s), 1389 (sh), 1359 (s), 1301 (m), 1235 (s), 1201 (m), 1163 (m), 1124 (m), 1091 (w), 1059 (w), 1031 (sh), 999 (m), 938 (w), 877 (s), 822 (w), 799 (w), 766 (m), 745 (s), 701 (s).

HR-EI-MS Exact molecular mass for [$C_{32}H_{41}NO_2$] ([M]$^+$): 471.3137
Found: 471.315

Crystallographic Data For X-ray structure see Figure 5.12 on page 89
Colorless needles from ethanol

Empirical formula:	$C_{32}H_{41}NO_2$
Formula weight (M):	471.67 g/mol
Temperature (T):	100(2) K
Wavelength (λ):	0.71073 Å
Crystal system:	orthorhombic
Space group:	$P2_12_12_1$
Unit cell dimension:	a = 8.6654(1) Å $\alpha = 90°$
	b = 11.4308(2) Å $\beta = 90°$
	c = 28.3519(4) Å $\gamma = 90°$
Unit cell volume:	2808.33(7) Å^3
Z:	4

Calculated density ($\rho_{calcd.}$):	1.116 g/cm^3
Absorption coefficient (μ):	0.068 mm^{-1}
F(000):	1024
Crystal size:	0.32 × 0.28 × 0.26 mm
Θ-range for data collection:	1.92° to 27.00°
Limiting indices:	-11 ≤ h ≤ 7
	-13 ≤ k ≤ 14
	-33 ≤ l ≤ 36
Reflections collected:	16908
Unique reflections:	6109 [R_{int} = 0.0360]
Reflections observed [I>2σ (I)]:	5227
Completeness to Θ:	99.8 %
Refinement method:	Full-matrix least-squares on F^2
Data / restraints / parameters:	6109 / 0 / 454
Goodness-of-fit on F^2:	1.023
Final *R*-indices [$I > 2\sigma(I)$]:	$R1$ = 0.0407 ω$R2$ = 0.0922
R-indices (all data):	$R1$ = 0.0526 ω$R2$ = 0.0972
Largest diff. peak and hole:	0.238 and -0.221 e·Å^{-3}

8.5.2 Preparation of 2,4-diiodo-6-{(*S*)-2-(hydroxydiphenylmethyl) pyrrolidin-1-yl-methyl}phenol 31b

[SMU-IV-59]

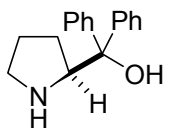

97a

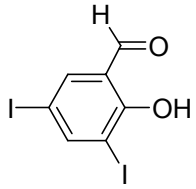

100b

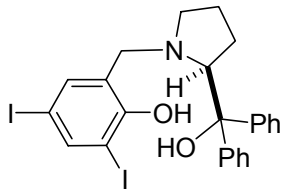

31b

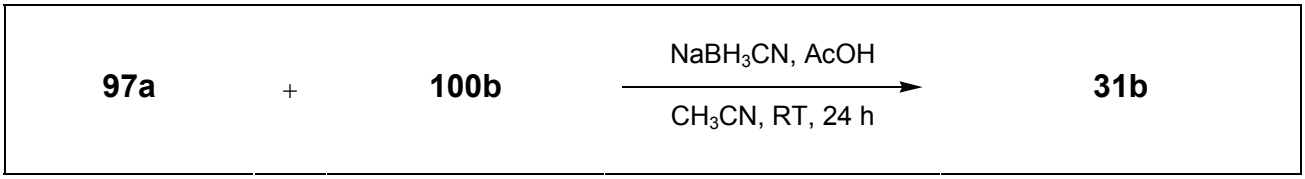

The same procedure as before (see section 8.5.1 on page 231) was followed on a 1.97 mmol scale to obtain the crude product as an off-white foam. Purification by column chromatography on silica gel (2:1 *n*-hexane/EtOAc as the eluant) afforded an off-white foam (839 mg, 70 %).

31b $C_{24}H_{23}I_2NO_2$ (611.25 g/mol)

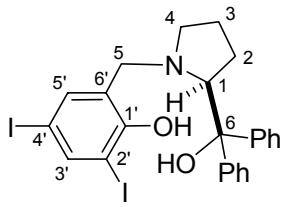

31b

Yield 839 mg (1.37 mmol, 70 %)

Melting Point 87-89 ºC

TLC R_f = 0.57 (Silicagel, *n*-hexane/EtOAc 2:1)

^{1}H-NMR (300 MHz, $CDCl_3$): δ = 1.64-1.77 (m; 2H, *H*-3), 1.83-1.93 (m; 1H, *H*-2), 2.04-2.18 (m; 1H, *H*-2), 2.29-2.38 (m; 1H, *H*-4), 2.91-2.98 (m; 1H, *H*-4), 3.16 (d, *J* = 13.8 Hz; 1H, *H*-5), 3.40 (d, *J* = 13.8 Hz; 1H, *H*-5), 3.91-3.95 (2d, *J* = 4.9 Hz; 1H, *H*-1), 7.03-7.04 (m; 1H, *H*-5′), 7.10-7.35 (m; 6H, H_{ar}), 7.49-7.57 (m; 4H, H_{ar}), 7.82-7.83 (m; 1H, *H*-3′).

^{13}C-NMR (75 MHz, $CDCl_3$): δ = 24.0 (*C*-3), 29.3 (*C*-2), 55.6 (*C*-4), 59.8 (*C*-5), 71.9 (*C*-1), 79.6 (*C*-6), 80.4 (*C*-4′), 85.6 (*C*-2′), 125.3 (*C*-6′), 125.7 (C_{ar}),125.9 (C_{ar}), 127.0 (C_{ar}), 127.1 (*C*ar), 128.3 (C_{ar}), 128.45 (C_{ar}), 136.6 (*C*-5′), 144.7 (*C*-3′), 145.3 (Cq_{ar}), 145.9 (Cq_{ar}), 156.3 (*C*-1′).
The assignments were made by 2D-NMR.

FT-IR (ATR): $\tilde{\nu}$ [cm^{-1}] = 3550 (br), 3054 (w), 2965 (m), 2876 (w), 2822 (w), 1580 (w), 1550 (w), 1490 (sh), 1445 (s), 1373 (m), 1349 (m), 1277 (m), 1259 (m), 1136 (m), 1084 (w), 1061 (w), 1031 (sh), 1000 (m), 942 (w), 863 (s), 765 (w), 735 (s), 701 (s).

HR-EI-MS Exact molecular mass for [$C_{24}H_{23}I_2NO_2$] ([M]$^+$): 610.9818
Found: 610.978

8.5.3 Preparation of 2,4-dibromo-6-{(*S*)-2-(hydroxydiphenylmethyl) pyrrolidin-1-yl-methyl}phenol 31c

[SMU-IV-61]

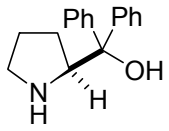

97a

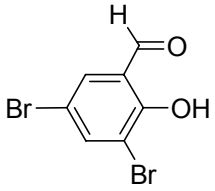

100c

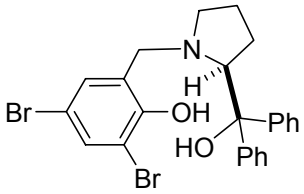

31c

97a	+	**100c**	$NaBH_3CN$, AcOH / CH_3CN, RT, 24 h	**31c**

The same procedure as before (see section 8.5.1 on page 231) was followed on a 1.97 mmol scale to obtain an off-white foam. Purification by column chromatography on silicagel (5:1 *n*-hexane/EtOAc as the eluant) afforded a pale yellow foam (660 mg, 65 %).

31c $C_{24}H_{23}Br_2NO_2$ (517.25 g/mol)

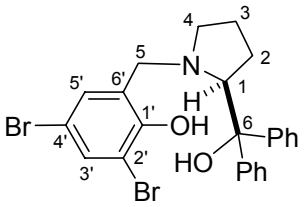

31c

Yield 660 mg (1.28 mmol, 65 %)

Melting Point 64-65 °C

TLC R_f = 0.33 (Silicagel, *n*-hexane/EtOAc 5:1)

^{1}H-NMR (300 MHz, $CDCl_3$): δ = 1.62-1.78 (m; 2H, *H*-3), 1.82-1.92 (m; 1H, *H*-2), 2.03-2.17 (m; 1H, *H*-2), 2.29-2.38 (m; 1H, *H*-4), 2.92-3.24 (m; 1H, *H*-4), 3.26 (d, *J* = 13.8 Hz; 1H, *H*-5), 3.43 (d, *J* = 13.8 Hz; 1H, *H*-5), 3.91-3.96 (2d, *J* = 4.85; 1H, *H*-1), 6.87 (d, *J* = 2.0 Hz; 1H, *H*-5′), 7.10-7.35 (m; 6H, H_{ar}), 7.46 (d, *J* = 2.0 Hz; 1H, *H*-3′), 7.49-7.59 (m; 4H, H_{ar}).

^{13}C-NMR (75 MHz, $CDCl_3$): δ = 24.0 (*C*-3), 29.3 (*C*-2), 55.6 (*C*-4), 59.6 (*C*-5), 71.8 (*C*-1), 79.6 (*C*-6), 110.3 (*C*-4′), 110.5 (*C*-2′), 125.7 (C_{ar}), 125.8 (*C*-6′),

125.9 (C_{ar}), 126.9 (C_{ar}), 127.0 (C_{ar}), 128.3 (C_{ar}), 128.4 (C_{ar}), 129.9 (*C*-5′), 133.6 (*C*-3′), 145.4 (Cq_{ar}), 146.0 (Cq_{ar}), 153.0 (*C*-1′).

The assignments were made by 2D-NMR.

FT-IR (ATR): $\tilde{\nu}$ [cm^{-1}] = 3565 (br), 3058 (w), 2966 (m), 2875 (w), 2825 (w), 1595 (m), 1559 (w), 1490 (sh), 1447 (s), 1378 (m), 1350 (w), 1262 (m), 1214 (w), 1150 (s), 1089 (w), 1061 (w), 1031 (sh), 1000 (m), 943 (w), 861 (s), 765 (w), 747 (s), 702 (s).

HR-ESI-MS Exact molecular mass for [$C_{24}H_{24}Br_2NO_2$] ([M+H]$^+$): 518.0153

Found: 518.0153

8.6 Application of metal complex of the tridentate ligand

8.6.1 Preparation of the aluminium complex 32

[SMU-IV-54]

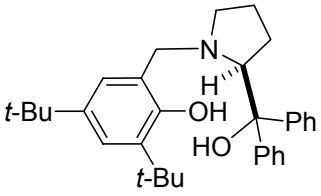

31a

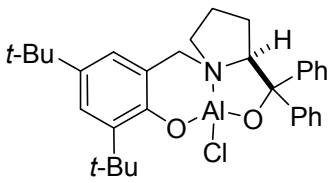

32

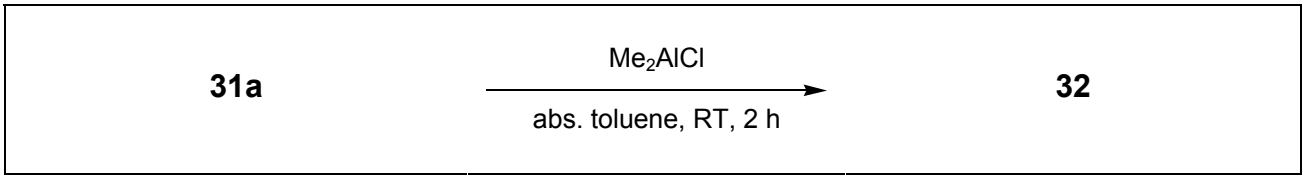

To a solution of the tridentate ligand **31a** (46 mg, 97.5 µmol, 1.0 eq) in 1 mL of abs. toluene, was added a 1M solution of dimethylaluminium chloride in *n*-hexane (98 µL, 97.5 µmol, 1.0 eq) and the resulting solution was stirred at room temperature in the glove box for 2 hours. This solution was used immediately for catalysis experiment (see section 8.6.2 on page 237).

8.6.2 Asymmetric hydrocyanation of benzaldehyde 33

[SMU-IV-56]

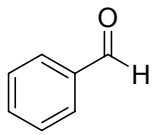

33

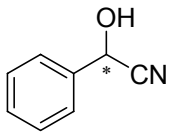

34

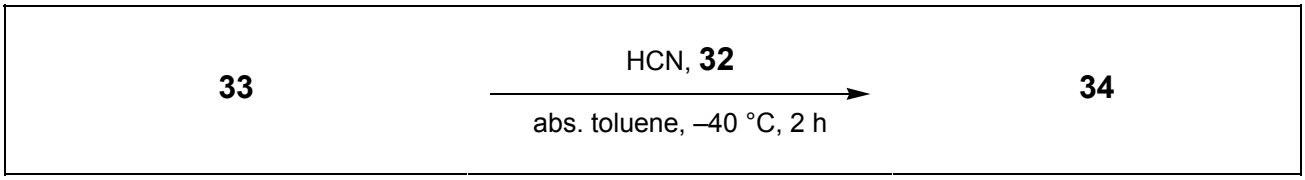

In an oven-dried *Schlenk* flask, a solution of benzaldehyde **33** (100 µL, 0.98 mmol, 1.0 eq) in 1 mL abs. toluene was cooled to –40 °C under positive pressure of argon. To this cold solution was added the solution of the aluminium-complex **32** (97.5 µmol, 0.1 eq) in 1mL abs. toluene followed by an HCN solution (generated from TMSCN and MeOH) in 1 mL toluene (1.3 eq). The resulting mixture was stirred at –40 °C under argon. After 17 hours, 100 µL of the reaction mixture was diluted with 0.9 mL of DCM and conversion and enantiomeric excess were determined immediately by HPLC using chiral column.

34 C_8H_7NO (133.15 g/mol)

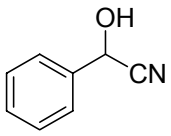

34

^{1}H-NMR (300 MHz, $CDCl_3$): δ = 3.83 (s; 1H, O*H*), 5.46 (s; 1H. C*H*CN), 7.39-7.49 (m; 5H, H_{ar}).

^{13}C-NMR (75 MHz, $CDCl_3$): δ = 63.3 (*C*HCN), 118.9 (*C*N), 126.6 (C_{ar}), 129.1 (C_{ar}), 129.7 (C_{ar}), 135.0 (Cq_{ar}).

HPLC τ_R = 5.6 min (**33**), 18.9 min (**34**), 25.3 min (*ent*-**34**)
(Chiralcel OJ, *n*-hexane/*i*-PrOH 90:10, 1.0 mL/min)

9 References

[1] K. C. Nicolaou, E. J. Sorensen, *Classics in Total Synthesis*, VCH Publisher, Weinheim, **1996**.

[2] G. M. Coppola, H. F. Schuster, *Asymmetric Synthesis: Construction of Chiral Molecules Using Amino Acids*, John Wiley & Sons, New York, **1987**.

[3] (a) G. F. Russell, J. I. Hills, *Science* **1971**, *172*, 1043-1044; (b) L. Friedman, J. G. Miller, *Science* **1971**, *172*, 1044-1046.

[4] G. W. Mellin, M. Katzenstein, *New Engl. J. Med.* **1962**, *267*, 1184.

[5] G. von Blaschke, H. P. Kraft, K. Finkentscher, F. Köhler, *Arzneim.-Forsch./Drug Res.* **1979**, *29*, 1640.

[6] R. Noyori, *Angew. Chem. Int. Ed.* **2002**, *41*, 2008-2022.

[7] E. N. Jacobsen, A. Pfaltz, H. Yamamoto, in *Comprehensive Asymmetric Catalysis, Volume I to III*, Springer, Berlin, Heidelberg, **1999**.

[8] H. U. Blaser, E. Schmidt, *Asymmetric Catalysis on Industrial Scale*, Wiley-VCH, Weinheim, **2004**.

[9] K. Drauz, H. Waldmann, in *Enzyme Catalysis in Organic Synthesis*, 2nd ed., Wiley-VCH, Weinheim, **2002**.

[10] (a) P. I. Dalko, L. Moisan, *Angew. Chem. Int. Ed.* **2001**, *40*, 3726-3748; (b) P. I. Dalko, L. Moisan, *Angew. Chem. Int. Ed.* **2004**, *43*, 5138-5175.

[11] A special issue on "Asymmetric Organocatalysis" (Ed. K. N. Houk, B. List), *Acc. Chem. Res.* **2004**, *37*, 487-631.

[12] A. Berkessel, H. Gröger, *Asymmetric Organocatalysis*, Wiley-VCH, Weinheim, **2005**.

[13] J. Saeyad, B. List, *Org. Biomol. Chem.* **2005**, *3*, 719-724.

[14] G. Bredig, W. S. Fiske, *Biochem. Z.* **1912**, 7.

[15] (a) U. Eder, G. Sauer, R. Wiechert, *Angew. Chem. Int. Ed.* **1971**, *10*, 496-497; (b) Z. G. Hajos, D. R. Parrish, *J. Org. Chem.*. **1974**, *39*, 1615-1621.

[16] (a) B. List, R. A. Lerner, C. F. Barbas III, *J. Am. Chem. Soc.* **2000**, *122*, 1395-2396; (b) W. Notz, B. List, *J. Am. Chem. Soc.* **2000**, *122*, 7386-7387.

[17] E. V. Dehmlow, S. S. Dehmlow, *Phase Transfer Catalysis*, 3rd ed., VCH, Weinheim, **1993**.

[18] R. Helder, J. C. Hummelen, R. W. P. M. Laane, J. S. Wiering, H. Wynberg, *Tetrahedron Lett.* **1976**, 1831-1834.

[19] (a) A. B. Northrup, D. W. C. MacMillan, *Science* **2004**, *305*, 1752-1755; (b) E. J. Sorensen, G. M. Sammis, *Science* **2004**, *305*, 1725-1726.

[20] (a) I. K. Mangion, D. W. C. MacMillan, *J. Am. Chem. Soc.* **2005**, *127*, 3696-3697; (b) R. M. Wilson, W. S. Jen, D. W. C. MacMillan, *J. Am. Chem. Soc.* **2005**, *127*, 11616-11617.

[21] Y. Huang, A. M. Walji, C. H. Larsen, D. W. C. MacMillan, *J. Am. Chem. Soc.* **2005**, *127*, 15051-15053.

[22] C. Bolm, T. Rantanen, I. Schiffers, L. Zani, *Angew. Chem. Int. Ed.* **2005**, *44*, 1758-1763.

[23] B. M. Nugent, R. A. Yoder, J. N. Johnston, *J. Am. Chem. Soc.* **2004**, *126*, 3418-3419.

[24] D. Uraguchi, M. Terada, *J. Am. Chem. Soc.* **2004**, *126*, 5356-5357.

[25] D. Uraguchi, K. Sorimachi, M. Terada, *J. Am. Chem. Soc.* **2004**, *126*, 11804-11805.
[26] D. Uraguchi, K. Sorimachi, M. Terada, *J. Am. Chem. Soc.* **2005**, *127*, 9360-9361.
[27] M. Rueping, E. Sugiono, C. Azap, T. Theissmann, M. Bolte, *Org. Lett.* **2005**, *7*, 3781 - 3783.
[28] P. R. Schreiner, *Chem. Soc. Rev.* **2003**, *32*, 289-296.
[29] P. M. Pikho, *Angew. Chem. Int. Ed.* **2004**, *43*, 2062-2064.
[30] (a) J. Hine, S.-M. Linden, V. M. Kanagasabapathy, *J. Org. Chem.* **1985**, *50*, 5096-5099; (b) J. Hine, K. Ahn, *J. Org. Chem.* **1987**, *52*, 2083-2086.
[31] T. R. Kelly, P. Mechani, V. S. Ekkundi, *Tetrahedron Lett.* **1990**, *31*, 3381-3384.
[32] M. C. Etter, T. W. Panunto, *J. Am. Chem. Soc.* **1988**, *110*, 5896-5897.
[33] (a) D. P. Curran, L. H. Kuo, *J. Org. Chem.* **1994**, *59*, 3259-3262; (b) D. P. Curran, L. H. Kuo, *Tetrahedron Lett.* **1995**, *39*, 6647-6650.
[34] (a) P. R. Schreiner, A. Wittkopp, *Org. Lett.* **2002**, *4*, 217-220; (b) A. Wittkopp, P. R. Schreiner, *Chem. Eur. J.* **2003**, *9*, 407-414.
[35] Y. Huang, A. K. Unni, A. N. Thadani, V. H. Rawal, *Nature* **2003**, *424*, 146.
[36] M. S. Sigman, E. N. Jacobsen, *J. Am. Chem. Soc.* **1998**, *120*, 4901-4902.
[37] M. S. Sigman, P. Vachal, E. N. Jacobsen, *Angew. Chem. Int. Ed.* **2000**, *39*, 1279-1281.
[38] (a) P. Vachal, E. N. Jacobsen, *Org. Lett.* **2000**, *2*, 867-870; (b) M. S. Taylor, E. N. Jacobsen, *J. Am. Chem. Soc.* **2004**, *126*, 10558-10559; (c) T. P. Yoon, E. N. Jacobsen, *Angew. Chem. Int. Ed.* **2005**, *44*, 466-468; (d) M. S. Taylor, N. Tokunaga, E. N. Jacobsen, *Angew. Chem. Int. Ed.* **2005**, *44*, 6700-6704.
[39] P. Vachal, E. N. Jacobsen, *J. Am. Chem. Soc.* **2002**, *124*, 10012-10014.
[40] A. G. Wenzel, M. P. Lalonde, E. N. Jacobsen, *Synlett* **2003**, 1919-1922.
[41] A. G. Wenzel, E. N. Jacobsen, *J. Am. Chem. Soc.* **2002**, *124*, 12964-12965.
[42] G. D. Joly, E. N. Jacobsen, *J. Am. Chem. Soc.* **2004**, *126*, 4102-4103.
[43] I. Ojima, in *Catalytic Asymmetric Synthesis*, 2nd ed., Wiley-VCH, Weinheim, **2000**.
[44] (a) H. Gröger, *Chem. Eur. J.* **2001**, *7*, 5246-5251; (b) M. Shibasaki, M. Kanai, K. Funabashi, *Chem. Commun.* **2002**, 1989-1999; (c) M. Kanai, N. Kato, E. Ichikawa, M. Shibasaki, *Synlett* **2005**, 1491-1508.
[45] E. J. Corey, C. J. Helal, *Angew. Chem. Int. Ed.* **1998**, *37*, 1986-2012.
[46] R. Noyori, M. Kitamura, *Angew. Chem. Int. Ed.* **1991**, *30*, 49-69.
[47] Y. Hamashima, D. Sawada, M. Kanai, M. Shibasaki, *J. Am. Chem. Soc.* **1999**, *121*, 2641-2642.
[48] J. Casas, C. Nájera, J. M. Sansano, J. M. Saá, *Org. Lett.* **2002**, *4*, 2589-2592.
[49] E. J. Corey, M. J. Grogan, *Org. Lett.* **1999**, *1*, 157-160.
[50] K. Matsui, S. Takizawa, H. Sasai, *J. Am. Chem. Soc.* **2005**, *127*, 3680-3681.
[51] T. Okino, Y. Hoashi, Y. Takemoto, *J. Am. Chem. Soc.* **2003**, *125*, 12672-12673.
[52] Y. Hoashi, T. Yabuta, Y. Takemoto, *Tetrahedron Lett.* **2004**, *45*, 9185-9188.
[53] T. Okino, Y. Hoashi, T. Furukawa, X. Xu, Y. Takemoto, *J. Am. Chem. Soc.* **2005**, *127*, 119-125.
[54] B.-J. Li, L. Jiang, M. Liu, Y.-C. Chen, L.-S. Ding, Y. Wu, *Synlett* **2005**, 603-606.
[55] Y. Hoashi, T. Okino, Y. Takemoto, *Angew. Chem. Int. Ed.* **2005**, *44*, 4032-4035.
[56] D. E. Fuerst, E. N. Jacobsen, *J. Am. Chem. Soc.* **2005**, *127*, 8964-8965.

[57] (a) B. Vakulya, S. Varga, A. Csampai, T. Soos, *Org. Lett.* **2005**, *7*, 1967-1969; (b) J. Ye, D. J. Dixon, P. S. Hynes, *Chem. Commun.* **2005**, 4481-4483; (c) S. H. McCooey, S. J. Connon, *Angew. Chem. Int. Ed.* **2005**, *44*, 6367-6370; (d) J. Wang, H. Li, W. Duan, L. Zu, W. Wang, *Org. Lett.* **2005**, *7*, 4713-4716; (e) S. B. Tsogoeva, M. J. Hateley, D. A. Yalalov, K. Meindl, C. Weckbecker, K. Hunthmacher, *Bioorg. Med. Chem.* **2005**, *13*, 5680-5685.

[58] J. Wang, H. Li, X. Yu, L. Zu, W. Wang, *Org. Lett.* **2005**, *7*, 4293-4296.

[59] (a) B. M. Trost, *Science* **1991**, *254*, 1471-1477; (b) B. M. Trost, *Angew. Chem. Int. Ed.* **1995**, *34*, 259-281.

[60] J. M. Keith, J. F. Larrow, E. N. Jacobsen, *Adv. Synth. Catal.* **2001**, *343*, 5-26.

[61] (a) H. Stecher, K. Faber, *Synthesis* **1997**, 1-16; (b) U. T. Strauss, U. Felfer, K. Faber, *Tetrahedron: Asymmetry* **1999**, *10*, 107-117.

[62] K. Faber, *Chem. Eur. J.* **2001**, *7*, 5004-5010.

[63] A. S. Bommarius, M. Schwarm, K. Drauz, *J. Mol. Catal. B: Enzymatic* **1998**, *5*, 1-11.

[64] (a) J. Seyden-Penne, *Chiral Auxiliaries and Ligands in Asymmetric Synthesis*, Wiley, New York, **1995**; (b) E. R. Jarvo, S. J. Miller, *Tetrahedron* **2002**, *58*, 2481-2495; (c) A. H. Hoveyda, A. W. Hird, M. A. Kacprzynski, *Chem. Commun.* **2004**, 1779-1785.

[65] C. Gennari, U. Piarulli, *Chem. Rev.* **2003**, *103*, 3071-3100.

[66] A. von Baeyer, *Liebigs Ann. Chem.* **1861**, *117*, 178-180.

[67] H. E. Carter, *Org. React.* **1946**, *3*, 198-239.

[68] J. de Jersey, B. Zerner, *Biochemistry* **1969**, *8*, 1967-1974.

[69] H. T. Stock, N. J. Turner, *Tetrahedron Lett.* **1996**, *37*, 6575-6578.

[70] V. Daffe, J. Fastrez, *J. Am. Chem. Soc.* **1980**, *102*, 3601-3605.

[71] (a) H. S. Bevinakatti, R. V. Newadkar, A. A. Banerji, *J. Chem. Soc., Chem. Commun.* **1990**, 1091-1092; (b) R.-L. Gu, I.-S. Lee, C. J. Sih, *Tetrahedron Lett.* **1992**, *33*, 1953-1956; (c) J. Z. Crich, R. Brieva, P. Marquart, R.-L. Gu, S. Flemming, C. J. Sih, *J. Org. Chem.* **1993**, *58*, 3252-3258; (d) N. J. Turner, J. R. Winterman, R. McCague, J. S. Parratt, S. J. C. Taylor, *Tetrahedron Lett.* **1995**, *36*, 1113-1116; (e) S. A. Brown, M.-C. Parker, N. J. Turner, *Tetrahedron: Asymmetry* **2000**, *11*, 1687-1690.

[72] (a) D. Seebach, G. Jaeschke, K. Gottwald, K. Matsuda, R. Formisano, D. A. Chaplin, *Tetrahedron* **1997**, *53*, 7539-7556; (b) K. Gottwald, D. Seebach, *Tetrahedron* **1999**, *55*, 723-738.

[73] L. Xie, W. Hua, A. S. C. Chan, Y.-C. Leung, *Tetrahedron: Asymmetry* **1999**, *10*, 4715-4728.

[74] J. Liang, J. C. Ruble, G. C. Fu, *J. Org. Chem.* **1998**, *63*, 3154-3155.

[75] R. M. Williams, *Synthesis of Optically Active Amino Acids*, Pergamon Press, Oxford, **1989**.

[76] J.-A. Ma, *Angew. Chem. Int. Ed.* **2003**, *42*, 4290-4299.

[77] M. J. Burk, F. Bienewald, in *Transition Metals for Organic Synthesis, Vol. 2* (Eds.: M. Beller, C. Bolm), Wiley-VCH, Weinheim, **1998**, 13-25.

[78] W. S. Knowles, *J. Chem. Educ.* **1986**, *63*, 222-225.

[79] J. A. Osborn, F. H. Jardine, J. F. Young, G. Wilkinson, *J. Chem. Soc. (A)* **1966**, 1711-1732.

[80] (a) W. S. Knowles, M. J. Sabacky, *J. Chem. Soc., Chem. Commun.* **1968**, 1445-1446; (b) L. Horner, H. Siegel, H. Buthe, *Angew. Chem. Int. Ed.* **1968**, *7*, 942.

[81] (a) T. P. Dang, H. B. Kagan, *J. Chem. Soc., Chem. Commun.* **1971**, 481; (b) H. B. Kagan, T. P. Dang, *J. Am. Chem. Soc.* **1972**, *94*, 6429-6433.

[82] M. J. Burk, J. E. Feaster, W. A. Nugent, R. L. Harlow, *J. Am. Chem. Soc.* **1993**, *115*, 10125-10138.
[83] M. J. Burk, M. F. Gross, J. P. Martinez, *J. Am. Chem. Soc.* **1995**, *117*, 9375-9376.
[84] T. Masquelin, E. Broger, K. Müller, R. Schmidt, D. Obrecht, *Helv. Chim. Acta* **1994**, *77*, 1395-1411.
[85] (a) M. J. O'Donnell, *Acc. Chem. Res.* **2004**, *37*, 506-517; (b) B. Lygo, B. I. Andrews, *Acc. Chem. Res.* **2004**, *37*, 518-525.
[86] M. J. O'Donnell, W. D. Bennett, S. Wu, *J. Am. Chem. Soc.* **1989**, *111*, 2353-2355.
[87] M. J. O'Donnell, S. Wu, J. C. Huffman, *Tetrahedron* **1994**, *50*, 4507-4518.
[88] B. Lygo, P. G. Wainwright, *Tetrahedron Lett.* **1997**, *38*, 8595-8598.
[89] E. J. Corey, F. Xu, M. C. Noe, *J. Am. Chem. Soc.* **1997**, *119*, 12414-12415.
[90] T. Ooi, M. Kameda, K. Maruoka, *J. Am. Chem. Soc.* **1999**, *121*, 6519-6520.
[91] K. Maruoka, T. Ooi, *Chem. Rev.* **2003**, *103*, 3013-3028.
[92] T. Shibuguchi, Y. Fukuta, Y. Akachi, A. Sekine, T. Ohshima, M. Shibasaki, *Tetrahedron Lett.* **2002**, *43*, 9539-9543.
[93] T. Kita, A. Georgieva, Y. Hashimoto, T. Nakata, K. Nagasawa, *Angew. Chem. Int. Ed.* **2002**, *41*, 2832-2834.
[94] A. Strecker, *Ann. Chem. Pharm.* **1850**, *75*, 27-51.
[95] K. Harada, *Nature* **1963**, *200*, 1201.
[96] L. Yet, *Angew. Chem. Int. Ed.* **2001**, *40*, 875-877.
[97] H. Gröger, *Chem. Rev.* **2003**, *103*, 2795-2827.
[98] M. S. Sigman, E. N. Jacobsen, *J. Am. Chem. Soc.* **1998**, *120*, 5315-5316.
[99] C. A. Krueger, K. W. Kuntz, C. D. Dzierba, W. G. Wirachun, J. D. Gleason, M. L. Snapper, A. H. Hoveyda, *J. Am. Chem. Soc.* **1999**, *121*, 4284-4285.
[100] N. S. Josephsohn, K. W. Kuntz, M. L. Snapper, A. H. Hoveyda, *J. Am. Chem. Soc.* **2001**, *123*, 11594-11599.
[101] M. Takamura, Y. Hamashima, H. Usuda, M. Kanai, M. Shibasaki, *Angew. Chem. Int. Ed.* **2000**, *39*, 1650-1652.
[102] H. Ishitani, S. Komiyama, Y. Hasegawa, S. Kobayashi, *J. Am. Chem. Soc.* **2000**, *122*, 762-766.
[103] M. Chavarot, J. J. Byrne, P. Y. Chavant, Y. Vallee, *Tetrahedron: Asymmetry* **2001**, *12*, 1147-1150.
[104] B. Liu, X. Feng, F. Chen, G. Zhang, X. Cui, Y. Jiang, *Synlett* **2001**, 1551-1554.
[105] J. Huang, E. J. Corey, *Org. Lett.* **2004**, *6*, 5027-5029.
[106] M. Johannsen, *Chem. Commun.* **1999**, 2233-2234.
[107] S. Saaby, X. Fang, N. Gathergood, K. A. Jørgensen, *Angew. Chem. Int. Ed.* **2000**, *39*, 4114-4116.
[108] B. List, *Acc. Chem. Res.* **2004**, *37*, 548-557.
[109] F. von Nussbaum, P. Spiteller, in *Highlights in Bioorganic Chemistry: Methods and Applications* (Eds.: C. Schmuck, H. Wennemers), Wiley-VCH, Weinheim, **2004**, 63-89.
[110] E. Juaristi, V. A. Soloshonok, in *Enantioselective Synthesis of ß-Amino Acids*, 2nd, Wiley-Interscience, **2005**.

[111] D. L. Steer, R. A. Law, P. Perlmutter, A. I. Smith, M.-I. Aguliar, *Curr. Med. Chem.* **2002**, *9*, 811-822.

[112] A. Pegova, H. Abe, A. Boldyrev, *Comp. Biochem. Physiol. B* **2000**, *127*, 443-446.

[113] (a) G. I. George, in *The Organic Chemistry of β-Lactams*, VCH Publishers, New York, **1992**; (b) J. Tamariz, in *Enantioselective Synthesis of β-Amino Acids* (Eds.: E. Juaristi), Wiley-VCH, New York, **1997**, 45-66.

[114] G. Cardillo, C. Tomasini, *Chem. Soc. Rev.* **1996**, 117-128.

[115] M. Liu, M. P. Sibi, *Tetrahedron* **2002**, *58*, 7991-8035.

[116] (a) J. A. Zablocki, J. G. Rico, R. B. Garland, T. E. Rogers, K. Williams, L. A. Schretzman, S. A. Rao, P. R. Bovy, F. S. Tjoeng, R. J. Lindmark, M. V. Toth, M. E. Zupec, D. E. McMackins, S. P. Adams, M. Miyano, C. S. Markos, M. N. Milton, S. Paulson, M. Herin, P. Jacqmin, N. S. Nicholson, S. G. Panzer-Knodle, N. F. Haas, J. D. Page, J. A. Szalony, B. B. Taite, A. K. Salyers, L. W. King, J. G. Campion, L. P. Feigen, *J. Med. Chem.* **1995**, *38*, 2378-2394; (b) D. Nöteberg, J. Brånalt, I. Kvarnström, B. Classon, B. Samuelsson, U. Nillroth, H. Danielson, A. Karlén, A. Hallerg, *Tetrahedron* **1997**, *53*, 7975-7984.

[117] A. F. Abdel-Magid, J. H. Cohen, C. A. Maryanoff, *Curr. Med. Chem.* **1999**, *6*, 955-970.

[118] D. O. Berbasov, T. K. Ellis, V. A. Soloshonok, in *Enantioselective Synthesis of β-Amino Acids*, 2nd ed. (Eds.: E. Juaristi, V. A. Soloshonok), Wiley-Interscience, **2005**, 397-414.

[119] H. Yang, K. Foster, C. R. J. Stephenson, W. Brown, E. Roberts, *Org. Lett.* **2000**, *2*, 2177-2179.

[120] R. Caputo, E. Cassano, L. Longobardo, G. Palumbo, *Tetrahedron* **1995**, *51*, 12337-12350.

[121] G. C. Liu, D. A. Cogan, T. D. Owens, T. P. Tang, J. A. Ellman, *J. Org. Chem.* **1999**, *64*, 1278-1284.

[122] T. P. Tang, J. A. Ellman, *J. Org. Chem.* **1999**, *64*, 12-13.

[123] T. P. Tang, J. A. Ellman, *J. Org. Chem.* **2002**, *67*, 7819-7832.

[124] D. J. Weix, J. A. Ellman, *Org. Lett.* **2003**, *5*, 1317-1320.

[125] E. Juaristi, V. M. G. García, H. L. Ruiz, in *Enantioselective Synthesis of β-Amno Acids* (Eds.: E. Juaristi, V. Soloshonok), Wiley-Interscience, **2005**, 159-179.

[126] G. Zhu, Z. Chen, X. Zhang, *J. Org. Chem.* **1999**, *64*, 6907-6910.

[127] J. You, H.-J. Drexler, S. Zhang, C. Fischer, D. Heller, *Angew. Chem. Int. Ed.* **2003**, *42*, 913-916.

[128] D. Peña, A. J. Minnaard, J. G. deVries, B. L. Feringa, *J. Am. Chem. Soc.* **2002**, *124*, 14552-14553.

[129] H. Ishitani, M. Ueno, S. Kobayashi, *J. Am. Chem. Soc.* **2000**, *122*, 8180-8186.

[130] S. Kobayashi, J. Kobayashi, H. Ishitani, M. Ueno, *Chem. Eur. J.* **2002**, *8*, 4185-4190.

[131] F. Tanaka, C. F. Barbas III, in *Enantioselective Synthesis of β-Amino Acids* (Eds.: E. Juaristi, V. Soloshonok), Wiley-Interscience, **2005**, 195-213.

[132] G. M. Sammis, E. N. Jacobsen, *J. Am. Chem. Soc.* **2003**, *125*, 4442-4443.

[133] J. K. Myers, E. N. Jacobsen, *J. Am. Chem. Soc.* **1999**, *121*, 8959-8960.

[134] (a) D. J. Guerin, T. E. Horstmann, S. J. Miller, *Org. Lett.* **1999**, *1*, 1107-1109; (b) T. E. Horstmann, D. J. Guerin, S. J. Miller, *Angew. Chem. Int. Ed.* **2000**, *39*, 3635-3638; (c) D. J. Guerin, S. J. Miller, *J. Am. Chem. Soc.* **2002**, *124*, 2134-2136.

[135] M. P. Sibi, J. J. Shay, M. Liu, C. P. Jasperse, *J. Am. Chem. Soc.* **1998**, *120*, 6615-6616.
[136] T. Okino, S. Nakamura, T. Furukawa, Y. Takemoto, *Org. Lett.* **2004**, *6*, 625-627.
[137] (a) G. Zhou, Q. Hu, E. J. Corey, *Org. Lett.* **2003**, *5*, 3979-3982; (b) D. H. Ryu, E. J. Corey, *J. Am. Chem. Soc.* **2003**, *125*, 6388-6390; (c) D. H. Ryu, G. Zhou, E. J. Corey, *J. Am. Chem. Soc.* **2004**, *126*, 4800-4802; (d) Q.-Y. Hu, G. Zhou, E. J. Corey, *J. Am. Chem. Soc.* **2004**, *126*, 13708-13713; (e) K. T. Sprott, E. J. Corey, *Org. Lett.* **2003**, *5*, 2465-2467; (f) G. Zhou, E. J. Corey, *J. Am. Chem. Soc.* **2005**, *127*, 11958-11959.
[138] E. J. Corey, T. Shibata, T. W. Lee, *J. Am. Chem. Soc.* **2002**, *124*, 3808-3809.
[139] D. H. Ryu, T. W. Lee, E. J. Corey, *J. Am. Chem. Soc.* **2002**, *124*, 9992-9993.
[140] D. H. Ryu, E. J. Corey, *J. Am. Chem. Soc.* **2004**, *126*, 8106-8107.
[141] D. H. Ryu, E. J. Corey, *J. Am. Chem. Soc.* **2005**, *127*, 5384-5387.
[142] T. Katsuki, *Synlett* **2003**, 281-297.
[143] T. R. J. Achard, L. A. Clutterbuck, M. North, *Synlett* **2005**, 1828-1847.
[144] T. P. Yoon, E. N. Jacobsen, *Science* **2003**, *299*, 1691-1693.
[145] B. M. Trost, H. Ito, *J. Am. Chem. Soc.* **2000**, *122*, 12003-12004.
[146] M. Kaik, J. Gawronski, *Tetrahedron: Asymmetry* **2003**, *14*, 1559-1563.
[147] J. M. Mitchell, N. S. Finney, *Tetrahedron Lett.* **2000**, *41*, 8431-8434.
[148] J. Christoffers, A. Mann, *Chem. Eur. J.* **2001**, *7*, 1014-1027.
[149] M. Costa, G. P. Chiusoli, D. Taffurelli, G. Dalmonego, *J. Chem. Soc., Perkin Trans. 1* **1998**, 1541-1546.
[150] A. Berkessel, F. Cleemann, S. Mukherjee, T. N. Müller, J. Lex, *Angew. Chem. Int. Ed.* **2005**, *44*, 807-811.
[151] A. Berkessel, S. Mukherjee, F. Cleemann, T. N. Müller, J. Lex, *Chem. Commun.* **2005**, 1898-1900.
[152] K. Nakano, K. Nozaki, T. Hiyama, *J. Am. Chem. Soc.* **2003**, *125*, 5501-5510.
[153] K. Hattori, H. Yamamoto, *Tetrahedron* **1993**, *49*, 1749-1760.
[154] N. A. Hassan, E. Bayer, J. C. Jochims, *J. Chem. Soc., Perkin Trans. 1* **1998**, 3747-3757.
[155] B. M. Trost, S. Martinez-Sanchez, *Synlett* **2005**, 627-630.
[156] J. -M.Brunel, I. P. Holmes, *Angew. Chem. Int. Ed.* **2004**, *43*, 2752-2778.
[157] M. Brandenburg, *Diploma Thesis* **2004**, Universität zu Köln.
[158] C. Girard, H. B. Kagan, *Angew. Chem. Int. Ed.* **1998**, *37*, 2922-2959.
[159] K.-F. Arndt, *private communication*.
[160] K. Etzenbach-Effers, *unpublished results*.
[161] (a) C. N. C. Drey, J. Lowbridge, R. J. Ridge, *J. Chem. Soc., Perkin Trans. 1* **1973**, 2001-2006; (b) C. N. C. Drey, E. Mtetwa, *J. Chem. Soc., Perkin Trans. 1* **1982**, 1587-1592.
[162] S. Kobayashi, Y. Tsukamoto, T. Saegusa, *Macromolecules* **1990**, *23*, 2609-2612.
[163] S. Arseniyadis, P. V. Subhash, A. Valleix, S. P. Mathew, D. G. Blackmond, A. Wagner, C. Mioskowski, *J. Am. Chem. Soc.* **2005**, *127*, 6138-6139.
[164] (a) C. P. Casey, S. C. Martins, M. A. Fagan, *J. Am. Chem. Soc.* **2004**, *126*, 5585-8892; (b) B. M. Trost, A. Fettes, B. T. Shireman, *J. Am. Chem. Soc.* **2004**, *126*, 2660-2661.
[165] E. J. Corey, T. W. Lee, *Chem. Commun.* **2001**, 1321-1329.
[166] A. Berkessel, K. Glaubitz, J. Lex, *Eur. J. Org. Chem.* **2002**, 2948-2952.
[167] S. J. Miller, *Acc. Chem. Res.* **2004**, *37*, 601-610.

[168] W. L. F. Armarego, C. L. L. Chai, *Purification of Laboratory Chemicals*, 5th Ed., Butterworth Heinemann, Oxford, **2003**.
[169] G. M. Sheldrick, in *SHELXS-97, Program for the Solution of Crystal Structures*, University of Göttingen, Germany, **1997**.
[170] G. M. Sheldrick, in *SHELXL-97, Program for the Refinement of Crystal Structures*, University of Göttingen, Germany, **1997**.
[171] J. Pospisek, K. Blaha, *Collect. Czech. Chem. Commun.* **1977**, *42*, 1069-1076.
[172] J. Pospisek, K. Blaha, *Collect. Czech. Chem. Commun.* **1987**, *52*, 514-521.
[173] W. A. J. Starmans, R. W. A. Walgers, L. Thijs, R. Gelder, J. M. M. Smits, B. Zwanenburg, *Tetrahedron* **1998**, *54*, 4991-5004.
[174] D. J. Mathre, T. K. Jones, L. C. Xavier, T. J. Blacklock, R. A. Reamer, J. J. Mohan, E. T. T. Jones, K. Hoogsteen, M. W. Baum, E. J. J. Grabowski, *J. Org. Chem.* **1991**, *56*, 751-762.
[175] E. J. Corey, J. O. Link, *J. Org. Chem.* **1991**, *56*, 442-444.
[176] G. Cainelli, D. Giacomini, A. Trerè, P. P. Boyl, *J. Org. Chem.* **1996**, *61*, 5134-5139.
[177] K. A. Tehrani, T. N. Van, M. Karikomi, M. Rottiers, N. D. Kimpe, *Tetrahedron* **2002**, *58*, 7145-7152.

10 Appendix

10.1 Abbreviations

abs.	absolute (distilled and dried)
Ac	Acetyl (CH_3CO)
aq.	Aqueous
ATR	Attenuated total reflection
Boc	*tert.*-Butyloxycarbonyl
Bn	Benzyl ($PhCH_2$)
CPME	Cyclopentyl methyl ether
DCC	*N*,*N*-Dicyclohexyl carbodiimide
DCM	Dichloromethane (CH_2Cl_2)
DKR	Dynamic kinetic resolution
DIPEA	Diisopropylethylamine (*Hünig* base)
DMAP	*N*,*N*-Dimethylamino pyridine
DMF	*N*,*N*-Dimethyl formamide (Me_2NCHO)
ee	enantiomeric excess
ent	Enantiomer
eq	Equivalent
Et	Ethyl (CH_3CH_2)
FT-IR	Fourier-Transform infrared spectroscopy
GC	Gas chromatography
h	hour
HBTU	*O*-benzotriazol-1-yl-*N*,*N*,*N*′,*N*′-tetramethyluronium hexafluorophosphate
HPLC	High performance liquid chromatography
HR-MS	High resolution mass spectrometry
Hz	Hertz
i-Bu	iso-butyl (Me_2CHCH_2)
KR	Kinetic resolution
Me	Methyl (CH_3)
min	minute
NMR	Nuclear magnetic resonance

n.d.	Not detected
PG	Protecting group
Ph	Phenyl
ppm	Parts per million
R_f	Retention factor
RT	Room temperature
sat.	Saturated
t-Bu	tertiary butyl (Me_3C)
TEA	Triethylamine (Et_3N)
TFA	Trifluoroacetic acid (CF_3CO_2H)
TFAA	Trifluoroacetic anhydride [$(CF_3CO)_2O$]
THF	Tetrahydrofuran

10.2 Structure table

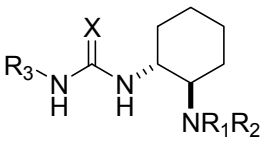

	R_1	R_2	R_3	X		R_1	R_2	R_3	X
1	Me	Me	3,5-$(CF_3)_2C_6H_3$	S	**7**	Me	Me	2,4,6-$(CH_3)_3C_6H_2$	O
2	Me	Me	3,5-$(CF_3)_2C_6H_3$	O	**8**	Me	Me	3-pyridyl	S
3	Et	Et	3,5-$(CF_3)_2C_6H_3$	O	**9**	Me	Me	*c*-hex	S
4	-$(CH_2)_4$-		3,5-$(CF_3)_2C_6H_3$	O	**10**	Me	Me	1-adamantyl	S
5	Me	Bn	3,5-$(CF_3)_2C_6H_3$	O	**12**	Me	Me	(*R*)-PhCH(CH_3)	O
6	Me	Me	3,5-$(NO_2)_2C_6H_3$	O	**13**	Me	Me	(*S*)-PhCH(CH_3)	O

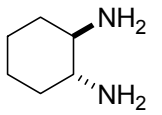

102

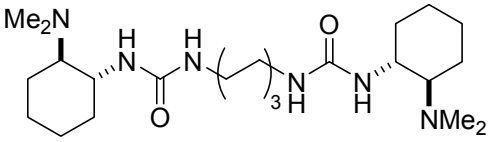

11

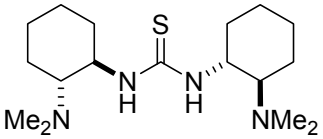

14

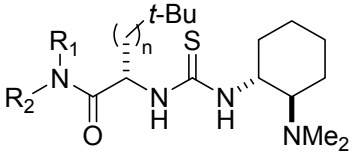

	R_1	R_2	n
15	Me	Me	0
16	Et	Et	0
17	*i*-Bu	*i*-Bu	0
18	Me	Bn	0
20	H	Bn	0
21	Me	Bn	1

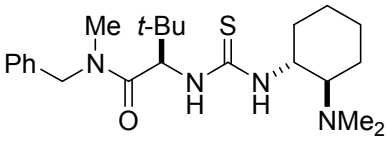

19

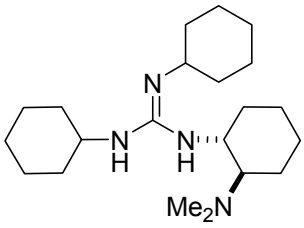

148

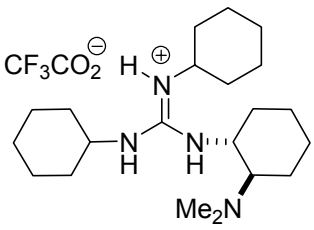

150

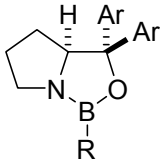

29

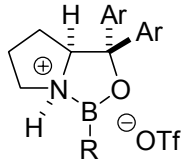

30

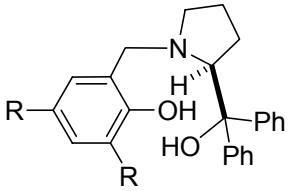

31

29a/**30a**: Ar = Ph, R = Me

29b/**30b**: Ar = Ph, R = Ph

29c/**30c**: Ar = *m*-Xyl, R = *o*-Tol

31a: R = *t*-Bu

31b: R = I

31c: R = Br

10.3 Abstract – Kurzzusammenfassung

In this work, new approaches to enantiomerically pure *α*- and *β*-amino acids *via* resolution and asymmetric synthesis were developed. First, a wide array of azlactones derived from both natural and unnatural *α*-amino acids were ring-opened with allyl alcohol under dynamic kinetic resolution (DKR) in the presence of a newly identified (thio)urea-based bifunctional organocatalyst to obtain *N*-acyl *α*-amino acid esters. The results are unprecedented in the chemically catalyzed DKR of azlactones in terms of optical purity of the product and substrate scope. Kinetic and NMR-studies indicate the formation of a 1:1 substrate-catalyst complex prior to alcoholysis.

The same bifunctional organocatalyst was then applied to the alcoholytic ring opening of oxazinones bearing aromatic as well as aliphatic substituents under kinetic resolution (KR) to afford *N*-acyl *β*-amino acid esters. This is the first time that oxazinones were subjected to a catalytic ring opening reaction.

Besides the DKR, the catalytic asymmetric hydrocyanation of imines was also revisited using chiral oxazaborolidine and oxazaborolidinium cations as the catalysts. Here a rather broad range of imines was applied. Although the resulting *α*-amino nitriles were obtained in low to moderate enantioselectivities, the catalyst afforded products with the opposite sense of stereoinduction upon protonation. This is the first successful application of neutral and cationic oxazaborolidines for the asymmetric hydrocyanation of imines.

Im Rahmen der vorliegenden Arbeit wurden neue Verfahren zur Darstellung von *α*- und *β*-Aminosäuren durch Racematspaltung bzw. asymmetrische Synthese entwickelt. Eine große Anzahl von Azlactonen, abgeleitet von natürlichen und unnatürlichen *α*-Aminosäuren wurde durch alkoholytische Ringöffnung unter dynamisch kinetischer Racemattrennung in Anwesenheit eines neuartigen bifunktionalen Organokatalysators zu *N*-Acyl *α*-Aminosäureestern umgesetzt, wobei sowohl hinsichtlich Selektivität als auch bezüglich der Breite des Substratspektrums herausragende Ergebnisse erzielt wurden. Durch kinetische Studien und NMR-Untersuchungen konnten Hinweise auf einen 1:1 Substrat-Katalysator-Komplex erhalten werden, der sich vor der Ringöffnung ausbildet.

Der gleiche bifunktionale Katalysator auf (Thio-)harnstoffbasis wurde in der alkoholytischen Ringöffnung von Oxazinonen mit aromatischen und aliphatischen Resten eingesetzt. Unter den Bedingungen einer kinetischen Racemattrennung konnten so zum ersten Mal enantiomerenreine *N*-Acyl *β*-Aminosäuren durch eine katalytische Ringöffnungsreaktion dargestellt werden.

Weiterhin wurden chirale Oxazaborolidin- und Oxazaborolidinium-Katalysatoren in der katalytischen asymmetrischen Hydrocyanierung eines breiten Spektrums von Iminen eingesetzt. Obwohl die erhaltenen α-Aminonitrile nur mit niedrigen bis moderaten Enantioselektivitäten erhalten wurden, konnten allein durch die Protonierung des Katalysators Produkte mit inverser stereochemischer Induktion erhalten werden. Hierbei handelte es sich um die erste Anwendung neutraler und kationischer Oxazaborolidine für die asymmetrische Hydrocyanierung.

10.4 Erklärung

"Ich versichere, dass ich die von mir vorgelegte Dissertation selbständig angefertigt, die benutzten Quellen und Hilfsmittel vollständig angegeben und die Stellen der Arbeit – einschließlich Tabellen, Karten und Abbildungen-, die anderen Werken im Wortlaut oder dem Sinn nach entnommen sind, in jedem Einzelfall als Entlehnung kenntlich gemacht habe; dass diese Dissertation noch keiner anderen Fakultät oder Universität zur Prüfung vorgelegen hat; dass sie noch nicht veröffentlicht worden ist, sowie, dass ich eine solche Veröffentlichung vor Abschluss des Promotionsverfahrens nicht vornehmen werde. Die Bestimmungen dieser Promotionsordnung sind mir bekannt. Die von mir vorgelegte Dissertation ist von Herrn Professor Dr. Albrecht Berkessel betreut worden."

Köln, 17. November 2005

Santanu Mukherjee

Bisher sind folgende Teilpublikationen veröffentlicht worden:

1. "*Highly Efficient Dynamic Kinetic Resolution of Azlactones by Urea-Based Bifunctional Organocatalysts*", A. Berkessel, F. Cleemann, S. Mukherjee, T. N. Müller, J. Lex, *Angew. Chem.* **2005**, *117*, 817-821; *Angew. Chem. Int. Ed.* **2005**, *44*, 807-811.
2. "*Second-Generation Organocatalysts for the Highiy Enantioselective Dynamic Kinetic Resolution of Azlactones*", A. Berkessel, S. Mukherjee, F. Cleemann, T. N. Müller, J. Lex, *Chem. Commun.* **2005**, 1898-1900.
3. "*Kinetic Resolution of Oxazinones: An Organocatalytic Approach to Enantiomerically Pure β-Amino Acids*", A. Berkessel, F. Cleemann, S. Mukherjee, *Angew. Chem.* **2005**, *117*, 7632-7635; *Angew. Chem. Int. Ed.* **2005**, *44*, 7466-7469.
4. "*Reversal of Enantioselectivity by Catalyst Protonation: Asymmetric Hydrocyanation of Imines with Oxazaborolidines*", A. Berkessel, S. Mukherjee, J. Lex, *Synlett*, **2006**, 41-44.

10.5 Curriculum Vitae

Personal Data:

Name	Santanu Mukherjee
Date of birth	April 15th, 1980
Place of birth	Hooghly (W. B.), India
Nationality	Indian
Marital status	Single

Education:

Since 7/2002	Ph. D. thesis: "*Organocatalytic Routes To Enantiomerically Pure α- And β-Amino Acids*" Under the supervision of Professor Albrecht Berkessel, Institut für Organische Chemie, Universität zu Köln, Germany
1/2002 – 4/2002	M. Sc. thesis: "*Synthesis and Characterization of Multicompartmental Aza-Thia- Cryptands and their Complexation Studies*" Under the supervision of Professor Parimal K. Bharadwaj, Indian Institute of Technology, Kanpur, India
8/2000 – 5/2002	Master of Science (M. Sc.) in Chemistry at Indian Institute of Technology, Kanpur, India
8/1997 – 6/2000	Bachelor of Science (Chemistry Honors) at Ramakrishna Mission Residential College, Narendrapur, University of Calcutta, Kolkata, India
6/1995 – 3/1997	Higher Secondary Education at Inda Krishnalal Sikshaniketan, Kharagpur, India
1991 – 1995	Secondary Education at Inda Krishnalal Sikshaniketan, Kharagpur, India
1990 – 1991	Secondary Education at Khanakul Krishnanagar Jnanada Institution, Gopalnagar, India
Up to 1990	Primary Education at Khanakul Krishnavamini Prathamik Vidyalaya, Khanakul, India